



National Library of Canada

Cataloguing Branch  
Canadian Theses Division

Ottawa, Canada  
K1A 0N4

Bibliothèque nationale du Canada

Direction du catalogage  
Division des thèses canadiennes

## NOTICE

The quality of this microfiche is heavily dependent upon the quality of the original thesis submitted for microfilming. Every effort has been made to ensure the highest quality of reproduction possible.

If pages are missing, contact the university which granted the degree.

Some pages may have indistinct print especially if the original pages were typed with a poor typewriter ribbon or if the university sent us a poor photocopy.

Previously copyrighted materials (journal articles, published tests, etc.) are not filmed.

Reproduction in full or in part of this film is governed by the Canadian Copyright Act, R.S.C. 1970, c. C-30. Please read the authorization forms which accompany this thesis.

**THIS DISSERTATION  
HAS BEEN MICROFILMED  
EXACTLY AS RECEIVED**

## AVIS

La qualité de cette microfiche dépend grandement de la qualité de la thèse soumise au microfilmage. Nous avons tout fait pour assurer une qualité supérieure de reproduction.

S'il manque des pages, veuillez communiquer avec l'université qui a conféré le grade.

La qualité d'impression de certaines pages peut laisser à désirer, surtout si les pages originales ont été dactylographiées à l'aide d'un ruban usé ou si l'université nous a fait parvenir une photocopie de mauvaise qualité.

Les documents qui font déjà l'objet d'un droit d'auteur (articles de revue, examens publiés, etc.) ne sont pas microfilmés.

La reproduction, même partielle, de ce microfilm est soumise à la Loi canadienne sur le droit d'auteur, SRC 1970, c. C-30. Veuillez prendre connaissance des formules d'autorisation qui accompagnent cette thèse.

**LA THÈSE A ÉTÉ  
MICROFILMÉE TELLE QUE  
NOUS L'AVONS REÇUE**



UNIVERSITÉ D'OTTAWA  
UNIVERSITY OF OTTAWA

DEFORMATION CHARACTERISTICS

of

SOIL

by

A.J. Hanna, B.A., B.A.I. (Dublin)

Submitted in partial fulfillment  
of the requirements for the degree of  
Master of Applied Science

Department of Civil Engineering

School of Graduate Studies

University of Ottawa

Ottawa, Canada

May, 1976

## PREFACE

The prediction of deformations of foundations is an important task in geotechnical engineering. When applied bearing pressures are less than the preconsolidation pressure, deformations are usually predicted by linear elastic analysis. Modulus values used are usually measured in the laboratory. Predictions based on laboratory moduli are generally unreliable. Sample disturbance is recognized as the main cause for non-representative laboratory modulus values. In-situ testing is preferable for modulus determination.

A full-scale footing test had been performed on Leda clay at a site in Ottawa to provide deformation data for the foundation design of a large 5 story building. Deformations were observed at various depths below the base of the footing and the observations indicated that about 92% of the total deformation occurred within a depth equal to  $1.5 \times$  width of the footing.

A research program was set up in order to study the deformation characteristics of the crust of the Leda clay at the same site. A series of plate load tests were performed, both vertical and horizontal, at different depths in the

crust of the clay. Measurements of deformations at certain depths below the plate were made.

Comparisons are made between the pressure-deformation results from the point of view of reproducibility, non-homogeneity and anisotropy. The results are analysed in the form of a function of modulus. There is a characteristic trend to the non-linear variation of this function of modulus with pressure level.

The observed deformations at depth below the plates are presented as a percentage of total deformation and compared with data from the footing test and the literature. The observed distributions of deformation with depth are in reasonably close agreement but are significantly different from the linear elastic solution.

The non-linear pressure-deformation response of the soil is studied and analysed, and a variation of modulus with depth is presented, based on the variation in stresses with depth. The linear elastic distribution of stresses with depth is used, but the analysis is illustrative. Further analysis, based on a multi-layer system representing the variation in modulus with depth, illustrates that the observed distribution of deformation with depth can be

explained by the non-linearity of the pressure-deformation response.

Some suggestions are made with regard to measuring the modulus of deformation and the non-linearity of the modulus for consideration in a non-linear analytical solution for soil deformation response. Some improvements are suggested for foundation analysis until such a solution is available.

This thesis presents a considerable amount of original data and analysis on soil deformation characteristics. This analysis represents the first attempt, to the best of the author's knowledge, to explain the observed deformation characteristics. While no general solution is presented, the method of analysis used and the suggestions for representing a non-linear medium could provide some assistance in obtaining a general solution.

## ACKNOWLEDGEMENTS

The author is grateful to all those who have contributed directly and indirectly to the completion of this study.

The permission to carry out the test program, granted by the Board of Governors of Algonquin College, is gratefully acknowledged.

Dr. G.E. Bauer, Thesis Supervisor is thanked for his interest and guidance during this research program.

Dr. J.D. Scott is thanked for his guidance, initially as Thesis Supervisor, and for his continued interest.

The assistance from Mr. Z. Tolunay during the entire field testing program is greatly appreciated.

The author is grateful to Northern Engineering Services Limited for their contribution towards the final preparation of this thesis. Individual appreciation is extended to Mrs. V. McKay for editing and Mrs. L. Geddes for the typing.

To my wife, a special appreciation for her patience understanding and assistance during the preparation of this thesis.

The financial assistance of the National Research Council of Canada through Grant No. 5105 is gratefully acknowledged.

## TABLE OF CONTENTS

	Page
TITLE PAGE	i
PREFACE	ii
ACKNOWLEDGEMENTS	v
TABLE OF CONTENTS	vii
LIST OF PLATES	xi
CONVERSION FACTORS	xviii
CHAPTER 1. INTRODUCTION	1.1
1.1 Statement of Problem	1.1
1.2 Previous Work at the Site	1.2
1.3 Extended Research Program	1.3
1.4 Objectives of the Study	1.4
1.5 Outline of the Thesis	1.5
CHAPTER 2. FOUNDATION DEFORMATIONS IN THEORY AND PRACTICE	2.1
2.1 Theoretical Introduction	2.1
2.2 Methods of Analysis in the Western Literature	2.3
2.3 Russian Practice	2.10
2.4 Comparison Between Western and Russian Practice	2.15
2.5 Proposed Method of Analysis	2.17
CHAPTER 3. DISTRIBUTION OF STRESS AND DEFORMATION BELOW A RIGID LOADED SURFACE	3.1
3.1 Introduction	3.1
3.1.1 Effect of Rigidity	3.1
3.1.2 Effect of Roughness	3.4
3.1.3 Effects of Groups of Foundations	3.4
3.1.4 Effect of Size of Loaded Area	3.5
3.1.5 Effect of Shape of Loaded Area	3.7
3.2 Ideal Homogeneous Isotropic Linear Elastic Half-Space	3.8
3.3 Non-Homogeneous Medium	3.12
3.4 Anisotropic Medium	3.20
3.5 Non-Linear Medium	3.22

## CHAPTER 4. EXPERIMENTAL INVESTIGATION

4.1	Site Description	4.1
4.1.1	Location	4.1
4.1.2	Basic Geological History of the Area	4.2
4.1.3	Geotechnical Properties of the Leda Clay in the Ottawa Area	4.5
4.1.4	Soil Conditions at the Site	4.7
4.2	Plate Load Bearing Tests	4.11
4.2.1	Experimental Setup	4.11
4.2.2	Instrumentation	4.14
4.2.3	Preparation of Test Surfaces	4.16
4.2.4	Layout of Tests	4.19
4.2.5	Testing Procedures	4.20
4.2.6	Data Recorded	4.23
4.3	Footing Test	4.24
4.3.1	Test Setup	4.24
4.3.2	Instrumentation	4.24
4.3.3	Loading Procedure	4.26
4.3.4	Observations	4.26

## CHAPTER 5. PRESENTATION AND DISCUSSION OF RESULTS

5.1	Plate Tests	5.1
5.1.1	Introduction	5.1
5.1.2	Discussion of Plate Test Results	5.4
5.1.3	Comparison of Test Procedures	5.8
5.1.4	Estimation of Failure Pressure	5.15
5.1.5	Relationship Between Recoverable and Non-Recoverable Deformations	5.17
5.1.6	Deformation at Depth	5.18
5.1.7	Comparison Between Tests Within Each Test Series	5.20
5.1.8	Comparisons Between Vertical and Horizontal Tests	5.23
5.2	Full-Scale Footing Test	5.26
5.2.1	Pressure Versus Total Deformation	5.26
5.2.2	Deformation at Depth	5.28

## CHAPTER 6. ANALYSIS AND INTERPRETATION OF RESULTS

6.1	Pressure Versus Surface Deformation	6.1
6.1.1	Introduction	6.1
6.1.2	Variation of the Average $f(M)$ with Applied Bearing Pressure for the Vertical Tests	6.4

6.1.3	Variation of $f(M)$ with Applied Bearing Pressure and Depth	6.5
6.1.4	Variation of $f(M)$ for the Vertical Plate Tests with Bearing Pressure Ratio	6.7
6.2	Distribution of Deformation with Depth Below the Loaded Surface	6.9
6.2.1	Distribution of Deformation for the Plate Tests	6.9
6.2.2	Distribution of Deformation for the Footing Test	6.12
6.2.3	Comparison Between Plate Tests and the Footing Test	6.13
6.3	Comparison with Other Work	6.15
6.4	Discussion of the Deformation Characteristics	6.17
6.4.1	General	6.17
6.4.2	Effect of Non-Linear Deformation Response	6.18
6.4.3	Distribution of Modulus of Deformation with Depth in a Non-Linear Soil	6.21
6.5	Other Factors Influencing Deformation Characteristics	6.26
6.5.1	Effect of Non-Homogeneity on the Distribution of Deformation with Depth	6.27
6.5.2	Effect of Anisotropy on the Distribution of Deformation with Depth	6.27
6.6	Modelling a Non-Linear Medium for Analytical Solutions	6.28
6.6.1	Measurement of Modulus and Its Non-Linearity	6.28
6.6.2	Representation of Non-Linearity	6.35

## CHAPTER 7. CONCLUSIONS AND RECOMMENDATIONS

7.1	Conclusions	7.1
7.1.1	Variation of Modulus of Deformation with Depth	7.1
7.1.2	Distribution of Deformation Below the Loaded Surface	7.2
7.1.3	Explanation of Deformation Characteristics	7.3
7.1.4	Suggestions for Measuring and Representing Non-Linearity	7.5

7.1.5 Some Conclusions Specifically  
Relevant to this Study

7.6

7.2 Recommendations

7.8

REFERENCES

PLATES

LIST OF PLATES

## PLATE NUMBER

- 2.1 Table 2.1 Comparison Between Observed and Predicted Settlements for Three Russian Solutions
- 2.2 Comparison Between Reported Deformation Distributions and: An Empirical Solution (SNIIP); An Elastic Solution (Giroud, 1972) and a Finite Element (Elastic) Solution (Marsland & Eason 1973).
- 3.1 Effect of Rigidity of a Foundation on Contact Pressure Distributions
- 3.2 Distribution of Vertical Stress,  $\sigma_z$ , with Depth, Comparison Between Center-line Stresses for Rigid and Flexible Loads
- 3.3 Variation of  $K_0$  with Depth
- 4.1 Map of Ottawa Region Showing Location of Test Site
- 4.2 Site Plan
- 4.3 Table 4.1 Typical Geotechnical Properties and Index Values for Leda Clay
- 4.4 Log of Soil Profile at the Test Site
- 4.5(a) Typical Photographs of Fissures on the Side of the Trench at a Depth of about 1.5 m (5 Feet)
- 4.5(b) Typical Photographs of Major Fissure Surfaces at a Depth of about 3 m (10 Feet)
- 4.6 Plan of Test Area

## PLATE NUMBER

- 4.7 Typical Photographs of Test Trench and Vertical Reaction System
- 4.8 Typical Photographs of Test and Loading Systems
- 4.9 Typical Photographs of the Instrumentation
- 4.10 Sketch of Cutting Tool Used to Prepare Parallel Vertical Faces on Sides of Trench
- 4.11 Longitudinal Section through Test Trench and the Test Footing
- 4.12 Table 4.2 List of all Tests Indicating the Level, Test Type, Loading Procedure and Duration of Each Test
- 4.13 Table 4.3 List of All Plate Tests Indicating the Number of Dial Gauges Used and the Performance Recorded
- 4.14 Table 4.4 Additional Observations Pertaining to the Performance of Individual Tests
- 4.15 Section through Test Footing and Reaction System
- 4.16 Plan View of Test Footing - Instrument Locations
- 5.1 - 5.19 Presentation of: Total Deformation, Recoverable Deformation and Function of Modulus Versus Applied Bearing Pressure
- 5.1 Test V1/1
- 5.2 Test V1/2
- 5.3 Test V1/3
- 5.4 Test H1/1A
- 5.5 Test H1/1B
- 5.6 Test H1/2A
- 5.7 Test H1/2B
- 5.8 Test H1/3A

## PLATE NUMBER

5.9	Test H1/3B
5.10	Test V2/1
5.11	Test V2/2
5.12	Test V2/3
5.13	Test H2/1A
5.14	Test H2/1B
5.15	Test H2/2A
5.16	Test H2/2B
5.17	Test V3/1
5.18	Test V3/2
5.19	Test V3/3
5.20	Table 5.1 Presentation of Tilt of Plate Tests with Respect to the Average Total Deformation and as a Percentage of Average Total Deformation
5.21(a)	Typical Photographs of some Test Failures
5.21(b)	Photographs of a Failure Wedge
5.22 - 5.26	Stepwise Pressure - Deformation Response and Time - Deformation Response
5.22	Test V1/3
5.23	Test H1/3A
5.24(a)	Test H1/3B
5.24(b)	Test H1/3B
5.25	Test V2/3
5.26	Test V3/3
5.27	Table 5.2 Actual Bearing Pressures and Bearing Pressure Ratios Separating Different Rate of Deformation Criteria (As Defined on Page 5.13)
5.28	Table 5.3 Comparison of Methods of Estimating Failure Pressure
5.29	Graphical Method of Predicting Ultimate Failure Pressure (Kondner and Krizek, 1962)

## PLATE NUMBER

5.30	Ratio of Recoverable Deformation to Total Deformation versus Pressure Ratio for the Plate Tests
5.31 - 5.36	Total Deformation and Deformation at Various Depths Below Loaded Surface
5.31	Test V2/1
5.32	Test V2/2
5.33	Test H2/1A
5.34	Test H2/2A
5.35	Test V3/1
5.36	Test V3/2
5.37 - 5.41	Comparison Between Pressure - Deformation Response for Tests within a Test Series
5.37	V1 Series
5.38	H1 Series
5.39	V2 Series
5.40	H2 Series
5.41	V3 Series
5.42 - 5.43	Comparison Between the Average Deformation Responses for Vertical and Horizontal Plate Test at the Same Depth.
5.42	V1 and H1 Series
5.43	V2 and H2 Series
5.44 - 5.45	Total Deformation and Function of Modulus versus Applied Bearing Pressure
5.44	Footing Test (center)
5.45	Footing Test (edge)
5.46	Comparison of Total Deformations and Ratios of Deformation to Radius of Loaded Area for the Footing Test and the Average Deformations of the V1 Series Plate Tests

## PLATE NUMBER

- 5.47 - 5.48 Total Deformation and Deformation at Various Depths Below Loaded Surface
- 5.47 Footing Test (center)
- 5.48 Footing Test (edge)
- 6.1 Function of Modulus versus Applied Bearing Pressure for all Plate Tests and the Footing Test
- 6.2 Function of Modulus for the Average of Each Vertical Test Series and the Footing Test Versus Applied Bearing Pressure
- 6.3 Variation of Function of Modulus with Depth for Different Pressures from the Plate Tests. Function of Modulus for Footing Test (centre) also shown.
- 6.4 Variation of Function of Modulus with Applied Bearing Pressure Ratio for some Vertical Plate Tests
- 6.5 - 6.9 Percentage of the Total Deformation which Occurs within a Certain Depth Ratio for some Vertical Plate Tests
- 6.5 Pressure Level,  $q = 0.1 q_u$
- 6.6 Pressure Level,  $q = 0.2 q_u$
- 6.7 Pressure Level,  $q = 0.3 q_u$
- 6.8 Pressure Level,  $q = 0.4 q_u$
- 6.9 Pressure Level,  $q = 0.5 q_u$
- 6.10 Comparison Between Observed and Theoretical (Giroud, 1972) Deformations Occurring within Certain Depth Ratios for the Plate Tests

## PLATE NUMBER

- 6.11 Comparison Between Observed and Theoretical (Giroud, 1972) Deformations Occuring within Certain Depth Ratios for the Footing Test
- 6.12 Comparison Between Observed and Theoretical (Giroud, 1972) Deformations Occurring within Certain Depth Ratios for the Plate Tests and the Footing Test
- 6.13 ~~Table 6.1~~ Comparison Between Observed and Theoretical (Giroud, 1972) Deformations Occurring within Certain Depth Ratios for the Plate Tests and the Footing Test
- 6.14 Presentation of Ratio of Observed to Theoretical Deformations Occurring within Certain Depth Ratios for the Plate Tests and the Footing Test
- 6.15 Comparison Between Deformation Distributions for the Plate Test and other Reported Data and: an Empirical Solution (SNiP); an Elastic Solution (Giroud, 1972); and a Finite Element (Elastic) Solution (Marsland & Eason, 1973)
- 6.16 Comparison Between Observed and Theoretical Distributions of Deformation with Depth from Various Sources
- 6.17 Distribution of Resultant Vertical Stress  $\bar{\sigma}_v$  with Depth
- 6.18 Variation of  $f(M)'$  with Resultant Vertical Stress Ratio for Test V2/2 (Considered Typical for this Soil)
- 6.19 Variation of  $f(M)'$  with Depth. Layered Profile Used to Calculate Distribution of Deformation with Depth

- 6.20 Comparison Between Observed, Linear Elastic and Calculated Distributions of Deformation with Depth
- 6.21 Graphical Method of Estimating the Limiting Depth of Deformation, H.
- 6.22 Deformation Factor for Different Values of Poisson's Ratio and Limiting Depth of Deformation, H.

CONVERSION FACTORS

$$1 \text{ cm} = 0.3937 \text{ in.}$$

$$1 \text{ m} = 3.28 \text{ ft.}$$

$$1 \text{ Newton, N} = 0.10197 \text{ kg (0.1)}^*$$

$$= 0.2248 \text{ lb.}$$

$$1 \text{ Pascal, Pa} = 1.0 \text{ N/m}^2$$

$$= 0.02088 \text{ psf}$$

$$= 1.45037 \times 10^{-4} \text{ psi}$$

$$1 \text{ kPa} = 20.88 \text{ psf}$$

$$= 0.01044 \text{ Tsf (1x10}^{-2}\text{)}$$

$$1 \text{ MPa} = 10.44 \text{ Tsf (10)}$$

\* Figures in parentheses indicate conversion factor used in calculations if different from the official value.

## CHAPTER 1

INTRODUCTION1.1 STATEMENT OF PROBLEM

The prediction of foundation deformations (settlements) has achieved varying degrees of success. Generally, the performance of foundations is predicted by performing laboratory modulus tests and using the modulus values obtained to predict deformations by means of the linear elastic theory. The values of modulus of deformation obtained in the laboratory generally result in the over-estimation of actual foundation performance. Sample disturbance has been recognized as the chief reason for low values of modulus of deformation measured in the laboratory.

The highly desiccated, fissured crust of the Leda clay in Eastern Canada presents an additional problem. Undisturbed samples of this highly fissured clay are virtually impossible to obtain, so when strength or deformation properties of this soil are required, in-situ tests are preferable. For this reason an in-situ load test was carried out recently

at a site in Ottawa, to provide deformation data for the design of foundations. This thesis discusses this test and presents and analyses additional in-situ tests carried out at the same site.

## 1.2 PREVIOUS WORK AT THE SITE

A full-scale, in-situ footing test was performed at the site of the Algonquin College of Applied Arts and Technology, in the west end of Ottawa. The chief purpose of this test was to ascertain whether shallow spread footings could be used to support a large 5-story extension to this campus, as opposed to a more expensive pile foundation system. The desiccated crust of the Leda clay at the site was expected to provide sufficient bearing capacity for the foundations and to dissipate the vertical stresses sufficiently so that the soft, underlying soil would not be over-stressed.

This full-scale footing test, which was performed at a cost of several thousands of dollars, did, in fact, indicate that spread footings would be quite feasible. By adopting a spread footing system a considerable savings in the overall foundation contract was realised.

While this full-scale test was performed primarily for the foundation engineering consultant (McRostie, Seto

and Genest Ltd.), the University of Ottawa arranged to make several additional observations during this test. Of major interest to this study was the observation of deformations at various depths below the base of the test footing. These observations showed that about 80% of the total deformation occurred within a depth equal to the width of the footing. These results are presented in detail in this thesis in support of similar observations under plate load tests performed at the site. A detailed description of the footing test and the results of laboratory modulus tests have been presented by Gaumy (1970).

### 1.3 EXTENDED RESEARCH PROGRAM

The full-scale footing test suggested two possible topics for additional study:

1. Could in-situ plate load tests, which would presumably be cheaper to perform, have been used to provide a foundation design for the structure at this site?
2. Were the observed deformations at certain depths attributable to peculiar deformation properties of a fissured clay, and in particular, to the variation in deformation properties with depth through the crust of the clay?

Considering the first topic, a detailed study of the use of plate load tests as a means of obtaining a design modulus of deformation would have required several tests for at least three different sizes of plates. For tests on a reasonable selection of plate sizes, providing a vertical reaction for the larger plates would have been too costly. Therefore, it was decided to study the second, more interesting topic of the deformation characteristics of the soil with depth through the desiccated crust. This study was carried out using plates of one size.

#### 1.4 OBJECTIVES OF THE STUDY

One of the prime objectives of this study was to determine the variation of the modulus of deformation with depth through the crust of the Leda Clay at this site. It was considered possible that the observed distribution of deformation below the test footing was due, in part, to non-homogeneity with depth through the crust.

The other prime objective was to observe the distribution of deformation with depth below loaded plates for comparison with the results from the test footing. It was expected that a characteristic deformation pattern for this soil deposit would result from this comparison.

Vertical plate tests were performed at three different levels. Horizontal tests were included to determine the degree of anisotropy in the fissured crust. Different loading procedures were chosen to illustrate various aspects of soil deformation.

Subsequent to the testing program and the analysis of the results, it became apparent that the distribution of deformation observed under the footing test was not only characteristic of the soil at this site but typical of some clays. Based on these results, the prime objective of the analysis expanded into an explanation for the observed deformation characteristics.

#### 1.5 OUTLINE OF THE THESIS

In Chapter 2 the concept of immediate settlement is introduced. The difficulties in applying this concept and the reliability of predictions is discussed. Some major limitations of this approach to predicting 'end of construction' deformations (settlements) are discussed. The Russian practice of predicting and considering the actual depth of deformation below a loaded surface is presented, with the resulting greater appreciation of and more accurate predictions of deformations. In view of the information in the literature disputing the validity of the classic linear

elastic solutions, a method of analysing deformation characteristics independent of any theory is proposed.

In Chapter 3, a systematic review of available theoretical solutions related to soil deformation characteristics is presented. The more important considerations of non-homogeneity, anisotropy and non-linearity are presented in detail.

Chapter 4 presents a description of the site and the experimental program including the geological history of the region and a detailed description of the soil at the site. The complete experimental set-up is described, including loading systems, instrumentation, layout of tests, test procedures, and data recorded.

The results of all the plate bearing tests are presented in Chapter 5. The bearing pressure versus deformation response is plotted for the nineteen tests performed. The reproduceability of the results is discussed. The time dependency of the relevant test results is presented. Various methods of predicting the ultimate failure capacity required for the final analysis are discussed. The ratio of recoverable (elastic) to total deformation is compared with bearing pressure level. The deformations at various

depths below the loaded surface are plotted. Comparisons are made between vertical and horizontal tests at the same depth. Finally, the relevant results of the full-scale footing tests are given. The total deformations and the deformations at certain depths below the loaded surface are plotted.

Chapter 6 contains the analysis and interpretation of the results. The results are analysed in the form of a function of modulus, independent of any theory. This function of modulus is plotted versus applied bearing pressure ratios (of failure pressure) in order to arrive at a characteristic form of non-linearity. The distribution of modulus with depth is plotted. The distribution of deformation with depth below the plate tests is presented in non-dimensional form and compared with the footing test and other data in the literature. The observed distributions of deformation are compared to linear elastic theories and a Russian solution. A typical form of observed non-linear deformation response is used to demonstrate that non-linearity can account for the observed distribution of deformation with depth below the loaded surface.

A summary of the pertinent discussion and analysis in this thesis is presented at the end of Chapter 6 with

regard to the measurement and representation of non-linearity for the purposes of a non-linear solution for soil deformation response. Some suggestions are made towards improving present practice until such a solution is available.

The conclusions based on this study are presented in Chapter 7. The requirements for a non-linear solution for soil deformation characteristics and more in-situ observations is emphasized.

## CHAPTER 2

FOUNDATION DEFORMATIONS - IN THEORY AND PRACTICE2.1 THEORETICAL INTRODUCTION

Until 1957, Terzaghi's theory of one-dimensional consolidation was the essential basis for all settlement analyses for structures underlain by clay soils. In 1955, MacDonald and Skempton presented a review of settlements of 20 buildings in London and pointed out that, while the conventional theory of consolidation presented reasonably accurate predictions for ultimate settlement, no recognition was given to the instantaneous deformation due to undrained shear strains in the soil. They suggested that this instantaneous deformation must be a definite component of the ultimate settlement of foundations and therefore should be considered in addition to the consolidation results from the oedometer test. Due to the rigid confinement of the oedometer test no lateral deformations could take place and the applied load is supported, initially, by the pore fluid. Later improvements to this suggestion were made by Skempton and Bjerrum (1957) who proposed that a more realistic prediction of ultimate settlements could be made by the expression:

$$\rho_{\text{total}} = \rho_i + c\rho_{\text{oed}} \quad (2.1)$$

where:

- $\rho_i$  = the immediate settlement,  
 $\rho_{\text{oed}}$  = the settlement calculated in the usual manner from oedometer test results, and  
 $c$  = a factor depending primarily on the pore pressure coefficient  $A$  (Skempton, 1954).

This factor,  $c$ , has been approximately related to overconsolidation by Skempton and Bjerrum (1957).

Hence, in 1957, the instantaneous component of deformation, known as the immediate settlement, had been recognized. The immediate settlement, by definition, is due to shear strains without dissipation of the pore pressures (constant volume). Immediate settlement can be computed by elastic theory according to the well known expression for a rigid loaded surface (based on Boussinesq's solution for the theory of elasticity):

$$\rho_i = q b \frac{1 - \mu^2}{E} I_p \quad (2.2)$$

where:

- $q$  = average bearing pressure
- $b$  = breadth or diameter of loaded area,
- $\mu$  = Poisson's ratio
- $E$  = Young's modulus from undrained tests, and
- $I_p$  = Influence value, depending on the shape of the loaded area and the depth of the clay bed.

This concept of immediate settlement was introduced to account for a limitation in the use of the oedometer test. In other tests, such as the triaxial test, the soil is not rigidly confined, and although the applied load will be initially supported by the pore water, shear strains are free to occur under that applied load. (A calculated choice of cell pressure can represent the lateral confinement in the field.) However, the immediate settlement equation (Eqn. 2.2) is fairly widely used to attempt to predict 'end of construction' deformations under foundations which apply a bearing pressure less than the preconsolidation pressure.

## 2.2 METHODS OF ANALYSIS IN THE WESTERN LITERATURE

Numerous references in Western literature discuss the use of the elastic theory in predicting the immediate or end of construction settlement under foundations which apply a bearing pressure less than the preconsolidation pressure.

The references of specific interest to this study are those which compare the predicted settlements based on a modulus of elasticity obtained in the laboratory with the actual settlements of plate tests or actual foundations. More specifically, the comparison is usually made between the laboratory modulus and the modulus inferred from the in-situ settlements, based on elastic theory, Eqn. 2.2, (Crawford and Burn, (1962); Klohn, (1965); Soderman, Kim and Milligan, (1968); DeJong and Harris (1971); Ló, Seychuck and Adams, (1971); for instance). While a complete review of these references is not presented here the major conclusions in these studies are summerized as follows:

(1) Laboratory modulus is invariably lower than inferred in-situ modulus, or predicted deformations invariably over-estimate actual performance.

(2) Obtaining realistic and consistent laboratory moduli is difficult.

The difficulties in carrying out modulus tests in the laboratory have been discussed by: Eden, (1960); Coates and McRostie (1963); Ladd, (1964); Lambe, (1964); La Rochelle and Lefebvre, (1970); D' Appolonia, Poulos and Ladd, (1970) and, Raymond, Townsend and Lojkasek, (1971). The most comprehensive study has been presented by Ladd,

(1964). Ladd has concluded that the laboratory modulus varies with:

- the stress level at which it is computed;
- the type of test;
- the direction of the applied major principal stress during loading, relative to the major principal stress in the field; and
- the degree of sample disturbance.

While some of these variables can be overcome, the general consensus among all those who have presented a comparison between laboratory modulus and the inferred in-situ modulus is that sample disturbance is the over-riding reason for disparity. However, Alderman (1957) pointed out that the laboratory modulus was very sensitive to rate of loading in strain-controlled tests. Alderman also questioned the validity of strain-controlled tests for deformation predictions and showed that stress-controlled tests provided significantly higher moduli.

Another important point was mentioned by Ladd (1964) and later by Seed (1965): even if ideal sampling and testing techniques were developed and used, the stress level and the direction of the major principal stress (i.e. the stress regime) varies in the field case throughout the soil media

and no single modulus value (such as a modulus value based on idealized center-line stress conditions) can fully represent the deformation modulus of the soil at all points. Similarly, ten years later, Krizek and Corotis (1975), stated "As is well known, the success with which a laboratory determined modulus can be used to solve a boundary value problem in soil mechanics depends to a large extent on how well the field condition corresponds to the test condition and how well the in-situ state of stress can be estimated."

In view of the generally poor success rate in obtaining a realistic modulus in the laboratory, it would appear that some justification is required for continuing to predict in-situ deformations in this manner. Even if the effects of sample disturbance could be completely overcome or evaluated, one is still faced with the following questions:

- How accurately can the in-situ stress conditions be defined?
- How accurately does the chosen test method represent the in-situ conditions?
- How representative will the results of such a test on such a small sample be in predicting the field performance?

Because of these difficulties involved in predictions based on laboratory modulus tests, the recent trend is towards

performing in-situ modulus tests and obtaining information on the actual performance of foundations. The methods of predicting foundation deformations can be arranged in order of increasing accuracy as follows:

- (1) based on laboratory moduli;
- (2) based on in-situ plate moduli;
- (3) based on moduli extrapolated from moduli for different sized plate tests;
- (4) based on full-scale footing test moduli;
- (5) based on comparison with actual similar foundation conditions.

The reason for performing tests using different sized plates is that the modulus of deformation may vary with the size of the loaded area. This will be discussed in the next chapter.

It might be assumed that a modulus obtained from a full scale footing test should be the best possible approach for predicting foundation performance. However, the direct results of such a 'quick' test do not always give a good indication of the end of construction deformations to be expected. Ideally, a full-scale footing test should observe the time dependency of the deformation under each load increment. In practice, the deformations recorded within a certain time

interval might represent the construction period for a foundation and then some additional deformation should be considered to represent the long-term, time-dependent deformations.

However, experience has shown that such a method of predicting foundation deformations can lead to an over-estimation of deformations, especially for fissured soils. Based on the full-scale footing test associated with this study (Bauer, Shields, McRostie and Scott, 1976), the immediate settlement was predicted to be 1.7 cm (0.67 inches) and the ultimate settlement 4.0 cm (1.6 inches). The actual settlements observed under an identical footing at this site, were 1.1 cm at the end of construction and 1.6 cm at the end of 5 years. The different rates of loading are likely the prime reason for the disagreement.

Lo, Seychuk and Adams (1971) have shown that for two plate tests with identical soil and pressure conditions, a 'fast' test yielded greater deformations than a 'slow' test. This soil was also a stiff fissured, glacio-lacustrine clay. The difference in the rates of loading for these two tests (fast - 0.5 tons/2 min; slow - each load increment left until settlement stopped or for 30 minutes) is not nearly as significant as between a test footing and

an actual foundation and therefore it is even more interesting that the 'fast' test settled as much as 1.6 times more than the 'slow' test.

To conclude discussion on the effect of rate of loading on the comparison between 'quick' in-situ tests and actual foundations it must be remembered that only building foundations which apply a load less than the pre-consolidation pressure are being considered. To illustrate the different rates of loading and more specifically the opportunity for dissipation of excess pore pressures, the actual foundation situation at the site being studied can be considered. The design load was applied to the test footing within about 2 hours while the same load was applied to the identical foundation, referred to above, over a period of thirteen months. Considering that the rate of loading for the foundation case is not only extremely slow, but that under normal construction sequences (say 10-hour daily shifts with no work on weekends) there is ample time for any excess pore pressures built up during a single day or week of construction activity to dissipate, especially since the loads fall below the preconsolidation pressure and the soil is fissured and has enhanced drainage properties.

Hence, with regard to the use of laboratory moduli to predict immediate settlements under foundations there appears to be a problem in justifying the use of undrained tests. The rates of loading and drainage are incompatible.

The construction of embankments can represent a much faster rate of loading, and in certain instances, the rate of construction has to be controlled in order to reduce the build-up of excess pore-pressures. However, this situation of flexible loads being applied much quicker than most rigid foundation loads is beyond the scope of this study.

### 2.3 Russian Practice

A considerable amount of research into deformation characteristics has been carried out by the Russians. In fact, their understanding of deformation characteristics has developed to the extent that they have specified methods of analysis for predicting deformations, which consider the depth of soil being deformed. These specifications are set out in the "Construction Standards and Regulations (SNiP)" (1962) which is a form of design manual. They have recognized that soil deformations are confined to a much shallower depth than the linear theory of elasticity assumes.

There appear to be three empirical methods of predicting the depth of soil that is actually deformed under foundations (Malikova, 1972). The soil is assumed to deform to:

- (1) "a depth below the lower surface of the foundation where the additional (to the natural) pressure from the structure amounts to 20% of the existing natural (soils own) pressure" (SNiP II-B.1-62).
- (2) "the depth where the total average pressure from the structure amounts to 50% of the natural pressure reckoned from the lower surface of the foundation" (SNiP II-B.3-62).
- (3) a depth, based on observed deformations of large foundations, defined by

$$H_{\text{calc}} = \sqrt[4]{\frac{b}{\alpha'}}$$

where:  $b$  = width of foundation  $\geq 1.0\text{m}$  (33' feet).  
 $\alpha'$  = coefficient having a value of  $.6 \times 10^{-4}$ ,  $1/\text{m}^3$ , for clays; and  $3 \times 10^{-3}$ ,  $1/\text{m}^3$  for sands (Malikova, 1972).

A general expression for determining the extreme depth of the "active zone of settlement," is given by Stefanoff and Krastilov (1973):

$$\sigma_{z=H_a} = \alpha \gamma H \quad (2.3)$$

where:  $\sigma_{z=H_a}$  = the induced vertical stress at the extreme depth of the zone of settlement,  $H_a$ ,  
 $\alpha$  = is a coefficient which "in the opinion of different authors and in different norms, varies in a rather wide-scale, from 0.1 to 0.5", and  
 $\gamma H$  = the in-situ effective stress at the same depth (prior to loading).

For the two SNiP solutions given on the previous page, the values of  $\alpha$  are 0.2 and 0.5 respectively. The choice of values for  $\alpha$  appears to be quite arbitrary.

Stefanoff and Krastilov (1973) have proposed an explanation for this "active zone of settlement" and have presented a method for predicting the maximum depth of deformation. This method is based on the supposition that soil deformations are negligible at stress levels less than the structural strength of the soil. At higher stress levels, the structural bond becomes broken and plastic deformations occur. Hence, if the structural strength of a soil is known, standard elastic stress distribution charts

will provide the depth below which induced vertical stresses (for a specific loading situation) become less than the structural strength. Stefanoff and Krastilov define the extreme depth of the active layer of settlement as the depth where:

$$\sigma_{z=H_a} = P_{str} \quad (2.4)$$

where:  $P_{str}$  = the structural strength of the soil.

This solution proposed by Stefanoff and Krastilov represents an approach which is sound but not necessarily very practical. Soils with the greatest structural strength are probably the most sensitive soils. Representative tests on sensitive soils are difficult to carry out in the laboratory due to their greater susceptibility to sample disturbance (Coates and McRoştie, 1963; Raymond, Townsend and Lojkasek, 1971). Hence, until sampling and testing techniques are substantially refined this structural strength approach is probably of limited practical significance.

Some observations of the distribution of deformation below rigid plates resting on various soil types have been

made by Shvets and Kul'chitskii (1970). These results were compared to the SNiP, II-B.1-62, solution. This comparison indicated that for in-situ tests on both a loam and a clay the observed deformation at any depth was less than predicted.

In addition to the two standard methods of predicting deformations (SNiP II-B.1-62 and SNiP II-B.3-62), a solution developed by Egorov given by Egorov, Kuzmin and Popov (1957) is also widely used:

$$S = 2ap \sum_{i=1}^K \frac{k_i - k_{i-1}}{E_i} \quad (2.5)$$

- where: S = settlement;
- 2a = width of foundation;
- p = average foundation pressure in kg/cm<sup>2</sup>;
- K = number of different layers of soil between the foundation bed and the lower boundary of the active zone;
- E<sub>i</sub> = Young's Modulus for layer 'i' in kg/cm<sup>2</sup>;
- k = coefficient depending on the ratios of length to width and depth to width (n = 2b/2a and m = z/a, where 2b = length of foundation and z = coordinate of depth).

Values of k for different values of m and n are given in Egorov, Kuzmin and Popov (1957).

Malikova (1972) has shown that ultimate deformation predictions based on Egorov's formula are consistently more accurate than both of the SNIIP solutions. A comparison of the accuracy of the three solutions is presented in Table 2.1, Plate 2.1 based on Table 2 from Malikova (1972).

#### 2.4. COMPARISON BETWEEN WESTERN AND RUSSIAN PRACTICE

As indicated above, the actual depth of soil being deformed has to be considered in order to arrive at a more accurate prediction of total surface deformations. This consideration has apparently been realized more fully in Russian practice. In fact, only very recently have observations of the deformation characteristics of soil been reported outside of Russia (Marsland and Eason, 1973 and Bauer, Scott and Shields 1973). Because of this, the Russian empirical solutions, based on numerous observations, seem to represent a more realistic approach to the problem. In fact, as was stated in Section 2.2, Western solutions are still largely based on the idealized theory of elasticity, which assumes an infinite depth of deformation. This depth of deformation is sometimes cut off at some arbitrary depth depending on individual practice, but there is no general solution available.

Since the basic reason for the greater accuracy of total settlement predictions in Russian practice appears to

be dependent on the more accurate prediction of the distribution of deformation with depth, it is interesting to compare the results presented by Shvets and Kul'chitskii (1970), Marsland and Eason (1973) and Bauer, Scott and Shields (1973). The observed deformations within certain depths are presented as percentages of the total deformation and plotted against depth, in Plate 2.2. The theoretical predictions presented in these references are plotted in the same manner. A linear elastic solution by Giroud (1972) is also shown in Plate 2.2 for comparison.

The predicted distribution of deformation with depth used by Marsland and Eason, based on a finite element elastic solution, is significantly different from other mathematical extensions of the elastic theory presented by Fischer (1965) and Giroud (1972), for instance. The theoretical solutions of Fischer and Giroud will be presented in the next chapter, but it is important to note at this stage that these solutions provide a better prediction of deformation characteristics than the finite element solution presented by Marsland and Eason (1973).

The obvious conclusion to be made from this presentation is that the predictions of deformation characteristics based on the Russian solution, SNiP II-B.1-62 are far superior to predictions based on linear elastic theory.

## 2.5 PROPOSED METHOD OF ANALYSIS

The purpose of the foregoing presentation has been to point out that the Western world has had generally a rather poor history of success in predicting immediate settlements of foundations which are loaded to pressures less than the preconsolidation pressure. Not only is there considerable difficulty in obtaining realistic moduli in the laboratory but relatively quick in-situ plate, and even full-scale footing tests can fail to predict accurately the 'end of construction' settlement under actual foundations. Hence, there is a need for actual foundation performance studies.

The ideal linear elastic theory assumes that deformation occurs between the loaded surface and an infinite depth. It has been shown in Sections 2.3 and 2.4, that observed deformations are confined to a finite layer, which appears to be dependent to a certain extent on soil type, strength, and density (Stefanoff and Krastilov, 1973; Shvets, et al, 1970). The footing test performed at the site of this study indicated 58% of the total deformation occurring within a depth equal to one-half the width of the footing, and 83% of total deformation occurring within a depth equal to the width of the footing (Bauer, Scott and Shields,

1973). The theoretical values for these percentages of total deformation are about 26% and 51% respectively (Giroud, 1972). Therefore the assumption, in the elastic theory, that deformations occur to an infinite depth under a constant linear modulus of deformation, does not represent the depth of soil which is deforming.

Predictions of deformations, based on analyses which consider the limiting depth of deformation and the distribution of deformation with depth (as in Russian practice), appear to be superior to Western practice. While this author has been unable to obtain the original references for the above cited Russian solutions, enough evidence has been presented to suggest detailed studies of the deformation characteristics of soil.

This author has also been unable to obtain any reference, either Russian or Western, which attempts to explain the observed distribution of deformation with depth below a loaded surface. Hence, the major portion of this thesis will be devoted to studying available solutions for soil deformations and eventually (in Chapter 6) presenting an explanation for the observed deformation characteristics.

Since the above cited references illustrate that the theoretical equation for the inference of modulus of deformation for rigid circular loads

$$E = \frac{\pi Rq}{\rho} \times \frac{1-\mu^2}{2} \quad (2.6)$$

is not valid, due to the actual depth of soil being deformed, it is proposed to analyse and interpret the results of the plate load tests and the footing test in the form of a function of the modulus,  $f(M)$ . The main reason for such an analysis is that the objective of this thesis is to illustrate that the published results presented above do not represent the reactions of an ideal linear elastic medium. Therefore, rather than analysing the deformations according to the linear elastic theory, but presenting the results in a form for discussion and interpretation, the actual basic test results will be analysed in the form:

$$f(M) = \frac{\pi Rq}{\rho} \quad (2.7)$$

This  $f(M)$  represents simply the ratio of applied bearing pressure to surface deformation for a given size of loaded area, as observed at any level of pressure. It can not be compared with the coefficient of subgrade reaction,  $k_s$ , which is by definition, a constant, independent of the bearing pressure.

## CHAPTER 3

DISTRIBUTION OF STRESS AND DEFORMATION  
BELOW A RIGID LOADED SURFACE3.1 INTRODUCTION

In order to understand the deformation characteristics of soil the solutions for stresses and deformations should be reviewed. While most of these solutions are too theoretical, they still provide a valuable insight into the possible behaviour of soil. Throughout this thesis only the stresses and deformations caused by a rigid load are considered. Since the main interest in this study is the deformation of structural foundations the effects of certain factors such as rigidity, roughness, groups of foundations, size of loaded area, and shape of loaded area are discussed briefly below. Other more important factors are discussed later.

3.1.1 Effect of Rigidity

Theoretical solutions generally consider only perfectly rigid or perfectly flexible foundations so it is pertinent to mention the difference between these two types of foundation. The degree of rigidity (or flexibility) of a

foundation has a very significant effect on the distribution of the contact pressure between the foundation and the soil. The contact pressure distribution for the two extreme cases is shown on Plate 3.1. For flexible foundations (Plate 3.1a), such as tanks, embankments, roadways, and wheel loads, the contact pressure is uniform and is equal to the average applied load. For rigid foundations (Plate 3.1b) such as heavily reinforced concrete footings and rigid steel plates, the theoretical contact pressure distribution is hyperbolic. The minimum pressure at the center is  $0.5q$  (where  $q$  is the average applied pressure), and the maximum pressure, according to elastic theory, is infinite at the edges. Clearly these infinite pressures at the edge cannot be withstood by the soil so there is a localized failure zone at the edge and the pressures are relaxed accordingly, as shown by the dotted line in Plate 3.1b.

The condition of perfect flexibility can be met more easily than the condition of perfect rigidity. However, it can be shown that a typical reinforced concrete spread footing on a soil with an 'elastic' modulus of up to about  $250 \text{ MN/m}^2$  (2500 Tsf) would not result in a significant change in the contact pressure distribution. The value of  $K_B$  (after Bgrowicka, 1936) as defined in Plate 3.1c, would

be about one for such a foundation and Plate 3.1c shows that this results in a very small change in the distribution of the contact pressure. The contact pressures on softer soils would approach the perfectly rigid case.

The difference between the contact pressure for the extreme case of complete rigidity and that of complete flexibility results in quite different distributions of the vertical stresses with depth. The vertical stress distribution below the center of the loaded area is shown on Plate 3.2 for the rigid and flexible cases. The difference in the stress distributions is very significant between depths  $z = 0$  and  $1.5R$  (where  $R$  is the radius of the foundation) and that between  $z = 1.5R$  and  $4R$  the difference is not very significant. Below a depth of  $z = 4R$  the two vertical stress distributions become almost identical. The extreme difference at the surface makes it very important that the correct stress distribution be used in analysis and design.

Raft foundations have to be considered as a special case. There may be advantages to lowering the rigidity somewhat in order to reduce the contact pressure variation and hence the bending moments in the foundation. Therefore, the objective may be to reduce the rigidity as much as possible; consistent with permissible differential movements.

that the particular structural design can accommodate. This special situation will not be considered in this study.

### 3.1.2 Effect of Roughness

For reasons of analytical simplicity most theoretical solutions for rigid loads applied to an elastic medium consider a perfectly smooth interface between the load and the medium. Carrier and Christian (1973) showed that the effect of roughness on deformations is negligible for values of Poisson's Ratio of the soil greater than 0.3. In fact if it equals 0.5 the deformations are identical. The effect of roughness can be neglected in both homogeneous and non-homogeneous (linear increase in modulus with depth) soils provided Poisson's Ratio is greater than 0.3.

### 3.1.3 Effect Of Groups of Foundations

Since a single foundation would rarely exist except as a test foundation, it is pertinent to mention a method of analysing group effects on deformations. Jumikis (1973) has presented theoretical influence values for any number of adjacent loaded areas. The only assumption made is that the depth and size of the loaded areas are the same. The spacing may be variable. The effect of adjacent foundations is to increase the deformations of a reference foundation and this

increase depends on the number, the loading conditions, and the relative spacing of the foundations in the group.

#### 3.1.4 Effect of Size of Loaded Area

A series of plate bearing tests carried out by Sudhindra and Khanna (1969), showed that, for a given applied bearing pressure on a given soil, the surface deformation increases significantly with increase in size of plate. Also, for a given amount of deformation, there is a reasonably linear relationship between applied pressure and the ratio of the perimeter to the area of the plate.

In a study of size effects on settlements of footings on a clay, Chin (1969) suggests a relationship between pressure and deformation in the form:

$$q/c = f (\Delta/d) \quad (3.1)$$

where:

- q = average applied pressure (Q/A)
- c = shear strength of the clay
- $\Delta$  = deformation
- d = diameter of loaded area

Chin has shown that for two given clays, each with constant shear strength, there is a reasonable relationship between  $q$  and  $\Delta/d$  for different sizes of loaded areas. However, the tests reported have used relatively small loaded areas (maximum diameter 24 cm (9.4 in)) and there is in fact a significant scatter in the results for the different sizes of load. The effects of edge shearing is likely a reason for the scatter for these small scale tests. Burmister (1962) recommends the use of 30 cm (12 in) diameter plates as a minimum to eliminate the effects of edge shear. The relationship in Equation 3.1 may be more valid for larger plate sizes.

It is interesting to examine the theoretical expression relating pressure and deformations for an ideally elastic half-space, for a rigid circular load:

$$E = \frac{\pi R q}{\rho} \frac{(1-\mu^2)}{2} \quad (2.6)$$

For a given applied pressure,  $q$ , and a constant modulus,  $E$ , this expression can be rewritten in the form:

$$\rho = R \cdot \frac{\pi q}{E} \frac{(1-\mu^2)}{2}$$

or  $\rho = R \cdot K$

Therefore, since all of the functions on the right hand side except  $R$  are constant, the deformation under a given applied pressure,  $q$ , is theoretically directly proportional to the size of the loaded area. The fact that this direct proportionality does not occur in practice illustrates a limitation of the ideal elastic theory in representing soil deformation performance.

### 3.1.5 Effect of Shape of Loaded Area

The effect of the shape of the loaded area will not be discussed in detail here except to compare square and circular foundations or plates. Fischer (1965) refers to a proposal by Schleicher that the classic elastic analysis for circular areas is valid for square to rectangular shapes, with length to breadth ratios up to 5:1, by means of an equivalent radius:

$$R' = \sqrt{\frac{A}{\pi}} \quad (3.2)$$

where  $A$  = area of square or rectangle.

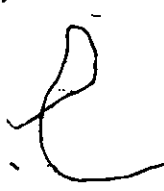
Unfortunately, very little research has been carried out to verify this proposal. Kondner and Krizek (1962) have indicated that for the same area of load, the deformation of

a square plate may be 5% greater than for a circular plate. However, the tests reported were carried out on remoulded soils, using extremely small (2 square inch) plates and only one test for each plate was performed. Therefore, these tests cannot be considered conclusive for natural clay deposits.

Charts presenting vertical stress distributions for different shapes of footings (e.g. Steinbrenner 1934, Newmark 1942) show a small difference between circles and squares. However, the equivalent radius approach (Eqn. 3.2) for the analysis of a square test footing was accepted for this study. Since only the stresses and deformations within one-half radius ( $R/2$ ) are to be used in the comparison between theoretical and experimental data, the conversion of square footings to equivalent circular footings by this method seems to be justified.

### 3.2 IDEAL HOMOGENEOUS ISOTROPIC LINEAR ELASTIC HALF-SPACE

The theoretical distribution of stresses and deformations below a loaded surface resting on a homogeneous, isotropic, linear elastic half-space have been analysed fairly extensively. While most soils do not satisfy the assumptions presentation of the analyses is necessary, since most designs are based on these analyses. In addition, the



results of this particular research program will be compared to these ideal theoretical solutions to emphasize the need for an alternative solution.

The basic equations for the stresses and deformations in an elastic medium have been integrated by Fischer (1965), to present the distribution of the 'resultant' vertical stress and deformations below the center of a circular rigid load at the surface. (The same analysis has been presented by Jumikis (1973), and is more readily available and useable.) Fischer has defined this 'resultant' vertical stress component, responsible for the vertical deformation in the ideal elastic medium as:

$$\bar{\sigma}_v = \sigma_z - 2\mu\sigma_x \quad (3.3)$$

where:  $\sigma_z$  = the vertical stress  
and  $\sigma_x$  = the horizontal stress.

By integrating this function of the resultant vertical stress, in stages, between the surface and an infinite depth, Fischer presents influence values for the distribution of deformation with depth, from the surface to infinity. The distribution of deformation with depth is defined by the expression:

$$\rho_z = \frac{\pi R q}{E} (1+\mu) \frac{1}{2\pi} \left[ 2(1-\mu) \left( \frac{\pi}{2} - \alpha \right) - \sin \alpha \cos \alpha \right] \quad (3.4)$$

$$= \frac{\pi R q}{E} \cdot f(\alpha) \quad (3.4a)$$

where:  $\alpha = \cot^{-1} z/R$ , a measure of depth.

This solution is confined to the center-line stresses and deformations but is the most practical solution available (especially as produced by Jumikis, 1973) for the theoretical center-line stress and deformation distribution in an ideally elastic medium.

In order to compare the deformation distributions measured in this research program with elastic theory, it is necessary to go to the more comprehensive analysis of stresses and deformations below a rigid loaded area, as presented by Giroud (1972). In this analysis, Giroud has integrated the basic Boussinesq elastic equations to provide influence values for the vertical stress (among others) and the vertical displacements for any point within a large range of depths and radial distances within an elastic medium. Tables and curves present these influence values for depth ranges of 0 to 10R and radial distances of 0 to 12R (where R is the radius of a rigid circular loaded area). The equations for these influence values are also given so that these values may be calculated for any other locations in the elastic medium. For the center-line case

( $r/R=0$ ), Giroud's analysis could be shown to agree exactly with the analyses presented by Fischer (1965) and Mikis (1973), for the distribution of deformation with depth.

Finite element solutions can be very useful in modelling soil deformation behaviour. A solution, based on elastic theory, by Marsland and Eason (1973) was introduced in Chapter 2. As mentioned earlier, this solution varies considerably from the elastic solutions developed by Fischer (1965) and Giroud (1972). Unfortunately, not enough is known about the theoretical basis for Marsland and Eason's solution and so the disparity with other solutions can not be investigated.

Another finite element solution has been presented by D'Appolonia and Lambe (1970). This solution appears to be quite comprehensive, in that it can consider non-homogeneity, anisotropy, and non-linearity. However, no attempt has been made to illustrate the practical significance of the solution. The solution is based on stress-path concepts (Lambe, 1964, 1967) and as such may be of research interest only. Stress-path tests are difficult to perform (Seed, 1965), though, in principle they may be more valid.

A problem of any finite element analysis is that its use in design is only as good as the input parameters.

Satisfactory representative laboratory testing of soils is very difficult to carry out, so the input parameters are not always compatible with the rigorous nature of the analysis.

### 3.3 NON-HOMOGENEOUS MEDIUM

Most soil deposits are non-homogeneous, particularly with depth. However in many cases, where a soil profile consists of the same type of soil, the non-homogeneity with depth is not very great. A possible exception to this is the situation where the surficial layer of a cohesive soil is heavily over-consolidated by desiccation.

Two extreme cases of non-homogeneity often encountered in soils engineering have been extensively analysed:

- (1) The case of a layered roadway system/in which the design results in a considerable reduction in modulus of deformation with depth, and
- (2) The case of a relatively soft soil underlain by a rigid, bedrock or till, base at a shallow depth with respect to the size of a foundation.

Studies of both of these cases are fairly extensive, especially for the road base problem. The reason for the

greater interest in road bases is primarily that such an analysis is required for the design of roadway toppings and base courses placed on softer, undesirable soils. It is generally easier to keep buildings away from undesirable sites than roadways. The extreme foundation problem can be overcome by pile foundations or can often be avoided by moving the site.

The difference between these two situations is that, when the upper layers are stiffer or stronger, there is a pronounced lateral distribution of vertical stresses, while in the other situation a relatively shallow rigid base tends to concentrate the vertical stresses in the area influenced by the foundation. This latter situation of the rigid base is more applicable to foundation engineering.

A detailed study of the effect of a rigid base at a relatively shallow depth was analysed by Burmister (1956) for the case of flexible loads. This study illustrated the effect of the rigid base on vertical stresses and surface settlements. The vertical stresses were significantly increased within the layer above the rigid base. The closer the rigid base is to the surface, relative to the width of the loaded area, the greater the concentration of stresses within the upper layer and the less the surface deformation.

Incidentally, while considering the relative depth at which a rigid base was no longer significant, Burmister recognized the relevance of the critical depth of deformation, and even proposed that values of  $\alpha$  (see Page 2.12 for definition) of 0.2 and 0.1 should be used for granular and clay soils respectively for flexible loads.

A more interesting solution to the rigid base problem has been presented by Poulos and Davis (1974), for a rigid circular foundation. This solution shows that the vertical stresses under a rigid load are even more concentrated within the upper layer, than for the flexible loading situation. Once again the surface deformations are considerably reduced as the depth of the rigid base relative to the size of loaded area decreases. In the ideal elastic solution a rigid base at a depth of  $10R$ , has a small but definite influence on the surface deformations.

The general pattern of observed distributions with depth, along with published Russian experience, indicates that in most soils, deformations are insignificant below depths of about  $6R$ . Therefore, the rigid base theory may, in practice, have no influence if the base is deeper than about  $6R$ , even though the vertical stresses are, theoretically, still affected (Milovic, 1970).

The more common forms of non-homogeneity which are encountered in foundation soils are layered systems of different soil types or consistent soil profiles with varying strength properties. The difference in the modulus of deformation in such profiles is generally considerably less than an order of magnitude, whereas, in the extreme cases discussed above, the differences can be several orders of magnitude. For this reason the extreme cases cannot be applied to the more common foundation problems.

The type of non-homogeneity encountered in more typical soil profiles does not greatly influence the stress distribution (Fischer, 1965; Jumikis, 1973; Giroud, 1972). Therefore, provided an accurate soil modulus is considered for the relevant stress level at any depth, whatever the soil at that depth may be, a realistic prediction of the soil deformation could probably be made. However, obtaining the 'accurate' value of the soil modulus is rather difficult, and the undrained soil modulus usually considered in such a prediction cannot realistically represent the field foundation situation.

With regard to the concept of a constant relationship between the modulus and shear strength of the soil,  $E/c$  (see D'Appolonia, Poulos and Ladd, 1970, for instance),

it is not uncommon for shear strengths to increase almost linearly with depth. In such cases the modulus would increase linearly with depth. A solution for rigid loads on such a soil has been presented by Carrier and Christian (1973). This analysis has shown that in extreme cases of non-homogeneity the vertical and horizontal stresses are increased considerably. Both stresses are dependent on Poisson's Ratio, especially the horizontal stresses. However, for more realistic increases in modulus (based on increasing shear strength) with depth it has been shown that these stresses and the settlement are not affected significantly. Any more extreme cases of non-homogeneity are beyond the scope and interest of this study.

In another analysis Brown and Gibson (1972) have shown that for the type of non-homogeneity being considered the effect on the surface settlement of flexible loads is negligible. Hence, it can be concluded that if both the stresses and the total settlements are not affected by a small increase in modulus with depth, the distribution of deformation with depth should not be affected.

Any discussion on non-homogeneity has to consider the fairly common situation of and desiccated, fissured crust

at the surface of a clay soil profile. A desiccated crust is heavily over-consolidated in terms of strength but the effect of desiccation, which causes fissuring, is considerably different in terms of deformability. As discussed above a reasonably constant relationship generally exists between modulus of deformation and shear strength,  $E/c$  (e.g. D'Appolonia, Poulos and Ladd, 1971). While the over-consolidation ratio does not appear to greatly influence this proposed relationship, over-consolidation due to desiccation affects soils differently.

Over-consolidation due to geological history (i.e. considerably greater compressive stresses due to 'one-time' ice or overburden pressures) results in "locked-in" horizontal stresses. As the ancestral vertical pressures are released by retreat of the ice or erosion of some of the overburden, the vertical rebound is not sufficient to fully release the original horizontal stresses. Therefore, it is quite common to find in-situ horizontal stresses greatly in excess of those which would be expected from present-day vertical overburden pressures. This represents the most common form of over-consolidation.

Another form of over-consolidation is caused by desiccation of the upper layers of a soil profile. This form of over-consolidation is greatly misunderstood. The basic effect of desiccation is to cause considerable shrinkage leading to fissuring. Fissuring results in a macrostructure of dry blocks of intact clay separated by relative openings. While the blocks of clay are highly over-consolidated, the openings (fissures) between these blocks result in low horizontal pressures within the macrostructure. There must be some contact between the desiccated blocks, but the contact pressure will be low compared to the internal pressures in each individual block of intact clay. Therefore, with respect to deformation properties, the desiccated crust is over-consolidated in terms of the microstructure (blocks of clay) but almost "under-consolidated" in terms of the macrostructure.

Laboratory determined values of  $K_0$  for this soil presented by Gaumy (1970) are shown in Plate 3.3. These values indicate very high in-situ horizontal stresses in the microstructure at the upper levels of the crust. With regard to the open fissures at the upper level of the crust these high  $K_0$  values are misleading. The fissures result in low horizontal stresses in the macrostructure and  $K_0$  becomes almost meaningless. From the point of view of deformations, Gaumy's  $K_0$  values

imply that horizontal deformations would be much smaller in the upper layers of the crust. In fact, the opposite is true, since a considerable amount of deformation will result from the closing (tightening) of fissures. Once the fissures are sufficiently compressed the soil will behave as a truly over-consolidated soil.

The state of the macrostructure obviously affects deformations. When a pressure is applied to a desiccated, fissured structure, considerable deformation will result from the closing or 'tightening' of the fissures. If the fissures are saturated (which occurs commonly in Leda clay deposits) deformations could be even greater, due to greater shear deformations, as the resulting pore pressures will tend to reduce the effective normal stresses between the blocks of clay. These stresses are probably low to start with. However, even in a 'quick' test, drainage will occur relatively easily along fissure planes, but this drainage initially will only affect the original fissure-water and not the pore-water within the blocks of clay. Hence, the rate of loading has to be extremely significant on fissured soils, especially if they are saturated. On the other hand, if a saturated, fissured soil is loaded very slowly, any excess pore pressures within the macrostructure will dissipate

very easily and shear deformations attributable to pore pressures in the fissures will be less significant. A slow test on a saturated, fissured soil will eventually close the fissures, under minimal excess pore pressure, but as soon as all the fissures are closed, the macrostructure becomes intact and excess pore pressures will build up in the intact blocks of clay. Since these blocks of clay are truly over-consolidated the shear deformations will be very much smaller than the shear deformations between the blocks of soil in the 'quick' test. Therefore the rate of loading can be particularly significant for fissured soils.

#### 3.4 ANISOTROPIC MEDIUM

Generally very little consideration is given to the effect of anisotropy on the distribution of stresses and deformation below a loaded surface. Anisotropy can be related to over-consolidation, and it is generally true that slightly over-consolidated soils are isotropic while heavily over-consolidated soils are anisotropic.

The effect of anisotropy ( $N = E_H/E_V$ ) greater than unity is to dissipate the vertical stresses such that the rate of decrease in the vertical stress with depth is greater than for the isotropic case ( $N = 1$ ), Hanna (1965). A heavily

desiccated, fissured soil deposit could have an anisotropy less than one, in which case the vertical pressures would tend to be higher in the upper layers.

The problem of an anisotropic layer underlain by a rigid base has been analysed by Milovic (1970). Considering the case where the rigid base is at a depth of 6 Radii, Milovic has shown that the vertical stresses are lower and the horizontal stresses greater than in the isotropic case, for anisotropy ( $E_H/E_V$ ) greater than unity. The net effect is a reduction in the resultant vertical stress (Eqn. 3.3). For anisotropy less than unity the vertical stresses are greater and the horizontal stresses are lower than for the isotropic case, resulting in an increase in the resultant vertical stress. However, the effect of anisotropy on the relative distribution of the resultant vertical stress is insignificant and hence the distribution of deformation should not be affected. Even though this situation considers a flexible load, the effect of anisotropy is still illustrative.

The effect of anisotropy on the total deformation has been analysed by Barden (1963) and it was shown that the

total deformation is less for anisotropy greater than one and the deformation is greater for anisotropy less than one.

There does not appear to be any analysis available for the distribution of deformation with depth in an anisotropic medium. However, it can probably be assumed that deformations will be confined within a shallower depth (due to lesser total deformations) in soils exhibiting anisotropy greater than one, based on Barden's analysis.

### 3.5 NON-LINEAR MEDIUM

In the context of this thesis a non-linear medium is a medium which exhibits a non-linear pressure versus deformation response and is not to be confused with a non-homogeneous medium which has a non-linear variation of modulus with depth. However, it will be the major contribution of this thesis to point out that the application of a pressure at the surface of an ideally homogeneous, isotropic, non-linear medium actually causes a non-linear variation of modulus with depth.

The only known complete analysis of vertical stress and deformation distributions in a non-linear medium has been presented by Huang (1968). This analysis has considered only the case of a flexible loaded area and is thus not

valid for analysing the results of this research program. However, the results of this non-linear analysis can provide an insight into the case of a rigid loaded surface. Huang has shown that for varying degrees of non-linearity the distribution of the vertical pressures varies very little from the linear case. Morgenstern and Tamuly Phukan (1968) have also shown that non-linearity has little effect on the vertical pressure distribution under a strip footing. However, Morgenstern and Tamuly Phukan show that the effect of a bi-linear deformation response is considerable on the horizontal pressure distribution. At shallow depths of  $B/2$  and  $B$ , below the loaded surface, the center-line horizontal pressures beneath the loaded surface are less (86% and 83% respectively) than in the linear case and at a depth  $2B$  the horizontal pressures are much greater (208%) than in the linear case. ( $B$  = width of strip footing).

Only Huang (1968) has analysed the deformation distribution below a flexible loaded area. The two major observations to be made from this analysis are that as the degree of non-linearity increases:

- (1) The total deformation becomes increasingly less than for the linear case, and

- (2) The depth at which deformations become negligible becomes shallower because the total deformation is less.

Another interesting observation which can be made from Huang's analysis is that the distribution of deformation is not significantly affected by non-linearity. Furthermore, it can be shown from this analysis that for increasing degrees of non-linearity, the deformations are less confined within shallower depths than the linear solution. Hence, this particular solution can not explain the observed distributions of deformation discussed in Chapter 2.

The results presented by Morgenstern and Tamuly Phukan (1968), indicating the effect of non-linearity, on the horizontal stresses, suggest a considerable effect on the resultant vertical stress. This stress is probably less than for the linear solution at depths between the surface and  $z/R = 2$ . Below this depth the resultant vertical stresses is probably much higher. Therefore, the effect on the distribution of deformations with depth could be significant in terms of non-linearity.

## CHAPTER 4

EXPERIMENTAL INVESTIGATION4.1 SITE DESCRIPTION4.1.1 Location

The research program was carried out on the west-end campus of the Algonquin College of Applied Arts and Technology in Ottawa. The location is shown on a sketch plan of the Ottawa region on Plate 4.1. A full-scale footing test, required to optimize the foundation design for a large expansion to the campus, was performed within 15 m (50 feet) of the proposed buildings, as shown on Plate 4.2. This footing test was performed in December, 1968. Four years later, after the building had been completed and the area landscaped, the plate load tests were performed adjacent to the location of the footing test. The plate load tests were set up as close as possible to the remains of the test footing but in a position that was undisturbed by the footing test. The layout of the test trench with respect to the footing test and the buildings is shown on Plate 4.2.

#### 4.1.2 Basic Geological History of the Area

7 The most recent major event in geological history which has greatly influenced the surficial geology of the Ottawa region is the Wisconsin glaciation. Under the colossal weight of the ice sheet the surface of the ground was depressed considerably. The rebound of the ground and the change in sea level since deglaciation have been determined, based on the occurrence of organic materials overlying marine clays. The age and present elevation of these organic soils gives a very good indication of the time they were deposited and their elevation when formed. Also, various features of erosion have indicated ground elevations of the period.

As deglaciation occurred in this region the ice retreated north to northeast (Kenney, 1964), and therefore the upper part of the present St. Lawrence River Valley became ice-free while the lower part remained blocked by ice. This led to the formation of a glacial lake, known as Lake Frontenac, behind this blockage. After this lake was formed, a short glacial sub-stage, the Valdres glacial sub-stage, advanced but it does not seem to have affected the upper St. Lawrence Valley or the Ottawa region (Kenney, 1964). When the ice retreated past the Quebec City region, Lake Frontenac was exposed to the open sea and the sea water eventually invaded the St. Lawrence and Ottawa River Valley regions (Prest, 1957).

This influx of sea water formed the Champlain Sea. Ottawa is situated in the northwest corner of the ancient Champlain Sea which extended to western limits around Brockville, Smith Falls and Arnprior (Karrow, 1961). The earliest date for the influx of sea water has been set at around 12,000 years B.P. (before present). Kenney (1964) reports that marine shells found at Montreal have been dated to 11,370 years B.P. ~~The occurrence of the Champlain Sea in the Ottawa Valley has been dated to 10,870 years B.P. (Dyck and Fyles, 1963).~~ Kenney also states that the waters of the Champlain Sea changed from salt water to fresh water shortly after 10,500 years B.P. Explanation for this change is either that the land rising relative to the sea level gradually cut off the supply of salt water or that the further retreat of ice unleashed vast quantities of fresh water from ancestral Lake Algonquin, which is now the Lake Huron Basin (Gadd, 1962; Kenney, 1964). Hence, it would appear that the salt water environment was relatively short-lived in the Ottawa region, possibly of the order of 500 years. However, the large volumes of material being released by the retreating ice sheet deposited up to 61 m (200 feet) of clay in the area during that period (Johnston, 1917).

The presence of fossiliferous beach deposits at present day elevations of about 206 m (675 feet) (Gadd,

1962) combined with the estimated rise in sea level of about 38 m (125 feet) since the time of the Champlain Sea (Kenney, 1964) indicates that the ground in this region was depressed about 244 m (800 feet) below its present elevation.

The initial deposit left by the retreating ice was a glacial till with a highly irregular surface. As the ice sheet retreated and the Champlain Sea formed, other deposits were laid down in the salt water environment, filling in the troughs in the till surface. These deposits, graded naturally relative to their distance from their source, were predominantly a clay (rockflour) with a large amount of silt. Later, as the source of material (the ice sheet) retreated further north the deposits became more clayey. When the Champlain Sea had changed from a salt to a fresh water environment the material being deposited was predominantly clay. As the land continued to rise, the basin of the Champlain Sea eventually rose above the water level, and the processes of erosion and deposition transformed the area into the present clearly defined St. Lawrence and Ottawa Valley system. As a result the surface features changed considerably. In most areas some of the fresh water clay and even some of the marine clay was eroded and redeposited. Also, in many areas the clay deposits were overlain by

fluvial sand deposits which originated from the fresh water Champlain Sea as it drained towards the ocean.

All the clay deposits mentioned above are referred to as Leda clay regardless of the depositional environment. The term Leda is derived from a marine fossil which was found in many locations in the marine clay (Dawson, 1893).

#### 4.1.3 Geotechnical Properties of the Leda Clay in the Ottawa Area

During and after the disappearance of the Champlain Sea, considerable erosion occurred. Eden and Crawford (1957) indicate that the original surface of the clay overlying the lower parts of the local area was probably above elevation 98 m (300 feet). If that is so, between 12 and 21 m (40 and 70 feet) of clay has been removed from the area. This explains the slight to medium over-consolidated state of the clay below the weathered crust. However, the upper material at all sites investigated by Eden and Crawford (1957) is over-consolidated much more than the underlying material. In most cases the water table is within 3.6 m (12 feet) of the surface. Above the water table the soil is truly desiccated and oxidized. However, fissures extend to depths up to 5.4 m (18 feet) and even 2.4 m (8 feet) below the present water table at one location (Eden and Crawford,

1957). The formation of this weathered, fissured crust at the surface of the clay has been reasoned by Mitchell, Sangrey and Webb (1972), who list the following natural processes as being responsible for the development of a crust:

- (1) Over-consolidation due to erosion, delayed consolidation, or ground water fluctuation;
- (2) Desiccation due to lowering of ground water table; and
- (3) Chemical changes in material due to weathering and, particularly, cementation.

Chemical weathering is believed to have produced a natural cementation (Sangrey and Townsend, 1969; Townsend, Sangrey and Walker, 1969). Strong bonds are believed to exist at the contact points of an open flocculated structure of soil particles. This phenomenon enables the soil to remain stiff and to carry large loads at moisture contents in excess of its liquid limit. Moisture content of the local Leda clay is indeed considerably higher than the liquid limit (Eden and Crawford, 1957). In general the soils in the crust have a higher shear strength and preconsolidation stress and a lower compressibility than the lower soils. The shear strength decreases from the surface to

depths up to 15 m (50 feet) and then remains almost constant or increases slightly with greater depth. The depth at which the shear strength ceases to decrease does not necessarily coincide with the depth of weathering, as depicted by the occurrence of fissures. The effect of desiccation on the  $K_0$  values and deformation characteristics has been discussed in Chapter 3.

The Leda clay is extremely sensitive and can be easily remoulded into a liquid in some cases (Crawford, 1963). Sensitivities in excess of 100 are not uncommon. The plasticity index of this clay deposit can vary considerably with depth. At greater depths where the soil has greater sand and silt contents the plasticity index can be as low as 5, whereas in the upper levels of the deposit where the soil is predominantly clay the plasticity index can be as high as 60. Typical values of various geotechnical properties of a Leda clay deposit are given on Table 4.1, Plate 4.3.

#### 4.1.4 Soil Conditions at the Site

The soil conditions at the site were fully investigated by the geotechnical consultant to Algonquin College, McRostie, Seto, and Genest Ltd. Some additional tests were

performed on samples from the site at the University of Ottawa (Gaumy, 1970). A log of the soil profile from one of the test holes at the site is presented on Plate 4.4. In addition to a description of the soil, various geotechnical properties are also presented on this plate, including moisture contents, Atterberg Limits, undisturbed and remoulded in-situ vane strengths, preconsolidation pressures, grain size analyses, and pore water salt contents. The depths shown are related to natural ground surface at the site, approximate elevation, 86.3 m (283 feet). From the variation of moisture contents, in-situ vane shear strengths, and the preconsolidation pressure with depth the depth of the crust appears to be about 4.5 m (15 feet). At the maximum depth of the test trench of 4 m (13 feet) the soil was definitely still fissured although the fissure spacing was of the order of 200 to 300 millimeters (8 to 12 inches). However, it can be expected that these large fissure surfaces could extend to a significantly greater depth. The water table was approximately 1.4 m (4.5 feet) below the ground surface at the time when the test trench was excavated to that depth. Therefore, the effect of fissuring extends to a depth of at least 3 m (10 feet) below the present water table. While the water table can be expected to fluctuate, the water table was probably lower at some time in geological history. Some photographs on Plates 4.5 (a) and (b) show

the sides of the excavation illustrating the variation in fissuring with depth in the excavation.

The fissure spacing close to the surface ranged from about 0.5 to 1cm (0.2 to 0.4 inches). The individual blocks of intact clay were extremely hard and the overall matrix appeared like a coarse granular soil. At the level of the first series of tests, 1.0 m (3.3 feet) below the surface, the fissure spacing was about 2 to 3 cm (0.8 to 1.2 inches). At this level the intact blocks of clay were hard to very stiff and were slightly columnar in form with a length to breadth ratio of about 1.5. The sides of the intact blocks were not necessarily true vertical but the minimum dip would have been about  $85^{\circ}$ . There was no characteristic orientation to these near vertical fissure surfaces and some of the blocks had up to 6 sides. The horizontal fissured surfaces appeared to be quite continuous and the maximum dip would have been about  $5^{\circ}$ .

At the level of the second series of plate tests, 2.5 m (8.2 feet) below the ground surface, the fissure spacing was significantly greater in both directions. The spacing between the vertical or near vertical fissures varied between 7.5 and 12.5cm (3 and 5 inches) however intact blocks were more columnar with length to breadth

ratios of greater than 2. At this second level of tests and lower, the horizontal fissures appeared more horizontal and may have not been real fissures. During the preparation of the vertical test surfaces for the horizontal tests at this level the blocks of intact clay appeared to break away along very thin silt layers. Due to the ever present weight of overburden on these surfaces desiccation would not likely result in true fissures in the horizontal direction, and hence these horizontal fissures are more likely bedding planes caused by variations in sedimentation.

At the maximum depth of the test trench, 4.25 m (14 feet) below the ground surface, the vertical fissure spacing was about 20 cm (8 inches). While the orientation still appeared random these fissured surfaces were definitely more continuous with dips ranging between  $90^{\circ}$  and about  $65^{\circ}$ , as shown in the Photographs on Plate 4.5(b). Major inclined fissure surfaces, as shown in these photographs, would have a very significant effect on both strength and deformation properties obtained from relatively small samples or loading tests.

At the completion of the plate bearing test program some block samples were obtained from the lower levels of

the test trench. Due to the fissures it was decided to attempt to get large blocks of intact clay. At the lowest depth, between 3.65 and 4.25 m (12 and 14 feet), the maximum size of block obtained was about 20 cm (8 inches) wide and about 76 cm (30 inches) long. While these dimensions represent the spacing between major fissures and bedding planes respectively, the soil within such a block was still definitely fissured.

The in-situ vane strength profile of the soil shows that close to the surface the shear strength is of the order of 300 kPa (3 Tsf) and that the shear strengths decrease rapidly through the crust, to an almost constant value of 40 kPa (0.4 Tsf) below the crust. It is particularly interesting to note this variation in shear strengths in the desiccated, fissured crust, with regard to the concept of a constant modulus to strength ratio,  $E/c$ , as will be discussed later.

## 4.2 PLATE LOAD BEARING TESTS

### 4.2.1 Experimental Setup

All the plate tests were carried out in a trench, 7.5 m (25 feet) long and ranging from 1.2 m (4 feet) wide at the beginning to about 2.5 m (8 feet) at the end of the test program. The trench was situated as close as possible to

the location of the footing test. A plan view of the test area, including the footing test and the test trench, is shown on Plate 4.6.

The reaction for the vertical tests was provided by a pair of 9 m (30 foot) long, 150 x 212 mm (6 x 8-1/2 inch) wide flange beams, strapped together by plates and bolts, running along the center-line of the trench. This main reaction beam rested on a pair of auxilliary beams at each end which ran perpendicular to the trench. These auxilliary beams were anchored so that when the reaction beam was securely attached to them by bolts, an estimated 80 kN (9 tons) of reaction was available. The auxilliary beams at one end were anchored by long bolts which were attached to the base of a specially constructed 1.2 x 2.4 x 1.2 m deep (4 x 8 x 4 feet deep) box. This box was placed in an excavated pit which was then backfilled. At the other end, the auxilliary beams were anchored using the auger anchors from two field vane apparatus. Some typical photographs of the trench and the reaction system are shown on Plate 4.7.

Loads were transferred from the reaction beam by means of an 89 kN (10 ton) hydraulic jack and a vertical column of 88 mm (3-1/2 inch) pipe. The points of contact of

this loading column with the reaction beam and the plate were free to rotate, so that an eccentric load could not be transmitted to the plate.

The reaction for the horizontal tests was provided by the opposite face of the excavation in each case; in fact, two tests were performed simultaneously. The same 88 mm pipe was used in conjunction with the hydraulic jack to provide the loading system. For these horizontal tests all of the loading system, including the plates, had to be suspended from the surface prior to applying the pressure on the soil. Due to the weights of the component parts it took considerable time to get everything lined up. Photographs of a vertical and a horizontal test are shown in Plate 4.8.

The actual loading plate consisted of a 457 mm (18 inch) diameter, 25 mm (1 inch) thick steel plate with two backup plates 300 and 150 mm (12 and 6 inch) in diameter to increase the rigidity. The load was applied to the 150 mm plate by means of a 50 mm (2 inch) diameter, dish-shaped platten into which the hemispherically ended piston of the loading system was fitted. A similar contact was made at the other end of the loading system.

#### 4.2.2 Instrumentation

A reference beam system was constructed from steel angle sections and was supported at least two times the diameter from the edge of the plate. Deformations were recorded using dial gauges calibrated to 0.001 inch. In the earlier Series 1 tests, only the surface deformation was recorded. In these cases three dial gauges were placed at 120 degree intervals around the top of the 450 mm (18 inch) diameter plate. In addition, for the vertical tests, two gauges were placed at distances  $D/8$  and  $D/4$  from the edge of the plate on the same radial alignment to measure deformation of the surrounding soil. In the first three vertical tests the movement of the surrounding soil was found to be negligible or highly erratic due to fissures and thereafter these gauges were omitted. The settlement gauges which were used for some of the deeper tests were not considered for the upper level of tests as installation was expected to cause too much disturbance in the highly fissured soil.

In some of the tests at the lower levels, settlement gauges were used to observe the deformation with depth under the plate. Four settlement gauges were installed through holes in the plate at 90-degree intervals on a circle of radius  $R/2$ . The tips of the settlement gauges were installed

at depths of  $1R$ ,  $2R$ ,  $3R$ , and  $4R$ , where  $R$  is the radius of the plate. These gauges were specially constructed by brazing extension rods between the auger point and the chuck end of standard 9.5 mm ( $3/8$  inch) diameter wood drill bits as shown in a photograph on Plate 4.9. Installation was achieved by drilling a hole in the soil, through the holes in the plate, by means of a 19 mm ( $3/4$  inch) diameter wood bit, similarly extended. The holes were drilled to within 75 mm (3 inches) of the proposed depth for the tip of the gauge and then a 19 mm O.D. pipe was fitted into each hole. The length of these pipes were designed so that there was a 13 mm ( $1/2$  inch) gap between the base of the plate and the top of the pipe. The settlement gauges were inserted and augered into the soil by hand, ensuring a firm contact with the surrounding soil. The tips of the dial gauges were brought to rest on a specially prepared surface on the top of the settlement gauges. Teflon discs prevented friction between the gauges and the plate. Where the four settlement gauges were used a total of eight dial gauges were required, four for the settlement gauges and another four for measuring the deformation of the plate adjacent to each gauge. Magnetic clamps were used to support all dial gauges. A photograph of a fully instrumented test is shown on Plate 4.9.

Diaphragm-type Weksler pressure gauges were used to control the application of the load with the hydraulic jack. A series of two pre-calibrated gauges were used, one for the high pressure ranges and one, with a lower pressure range, for the lower applied pressures. These pressure gauges were calibrated according to the British system of units, in psi. The high pressure gauge was calibrated from 0 to 10,000 psi with 100 psi divisions, and the low pressure gauge was calibrated from 0 to 3000 psi with 25 psi divisions. The maximum capacity of the jack was about 9000 psi, at a load of 89 kN (10 tons).

#### 4.2.3 Preparation of Test Surfaces

The preparation of good plane surfaces for the tests was a major problem in this fissured soil. At the first level of vertical tests, about 1.0 m (3.3 feet) below the ground surface, the fissure spacing was of the order of 6 to 18 mm (1/4 to 1/2 inch), but the fissure openings were considerably less than in the even drier soils above this level. Clay blocks of this size tended to crumble away from the rest of the soil when attempts were made to prepare a level surface and it was necessary to place a thin layer of fine sand between the plate and the soil. This procedure worked satisfactorily for all the vertical tests at the

first level and also at the second level, about 2.5 m (8.2 feet) below the ground level. Less sand was required at the lower level as the soil was more intact. At the third level, about 4.25 m (14 feet) below the ground level, the fissure spacing was of the order of 250 mm (10 inches) and the preparation of test surfaces was quite simple.

The most difficult surfaces to prepare were the vertical surfaces for the horizontal tests. The problem with the fissures was more acute on the vertical sides of the trench and, in addition, two perfectly parallel surfaces had to be prepared for each test set-up. After the first attempt at this, a special cutting tool was designed. The details of this design are shown on Plate 4.10. Basically, each end of the cutting tool consists of four cutting blades welded on a steel shaft. The shafts could be enclosed inside a split pipe and clamped so that the cutting planes were parallel. A guiding probe 225 mm (9 inches) long, ahead of each cutting plane, was pushed into the side of the excavation. Unfortunately, the apparatus was rather heavy and the total weight being supported by the embedded probes caused an opening of the fissures and the loosening of some blocks of the clay. Later, the weight of the cutting tool was supported by a wooden bench resting on the base of the excavation. There was still a problem with blocks of

fissures clay breaking away and plaster of paris was used to ensure a good seating contact for the plates.

At the first level of horizontal tests, elevation 85.3 m (280 feet), the preparation of the test surfaces was relatively easy because the blocks of clay which broke away were small. Hence it did not require too much trimming to obtain a surface that could be finished off with the plaster. However, at the second level, the blocks were considerably larger and if a large block fell away the whole operation had to be started again. An idea of the problems associated with this fissured soil can be seen in the photographs on Plates 4.5(a) and (b).

Great care was taken in the preparation of all test surfaces to remove all material that had become disturbed in the base of the trench or had dried out on the sides of the trench since the start of the excavation. In the case of the surfaces prepared on the sides of the trench this required the removal of a considerable amount of material, until soil was reached that apparently had not been affected by exposure. For this reason, the width of the trench increased considerably, in stages, during the test program.

#### 4.2.4 Layout of Tests

Of the total of nineteen tests performed, nine were vertical tests and ten (five double sets) horizontal. The basic intention was to perform tests at different levels between the level of the base of the test footing and a depth which was considered to be the base of the crust though this maximum depth was influenced by the reach of conventional excavation equipment. In order to keep the dimensions of the excavation to a minimum and to avoid performing tests on soils which had been previously stressed by tests at upper levels, it was only possible to test three different levels. The location of each test relative to the base of the footing test and the reaction beam is shown in a longitudinal cross section of the test trench on Plate 4.11. On this cross section of the trench, the horizontal lines represent the locations of the vertical plate tests and the circles represent the locations of the horizontal tests. The tests at any particular level are not necessarily at identical depths. This is primarily because at different locations a greater amount of disturbed soil had to be removed or because of difficulties in preparing a test surface at a particular location. However, they are generally within a range of 0.3 m (1 foot) and are considered, for reference purposes, to be at the same level.

#### 4.2.5 Testing Procedures

Three basic testing procedures were employed at each level. One of the procedures was chosen to assimilate the loading pattern of the full-scale footing test, which had been loaded in increments to a maximum load of 300 kPa (3 Tsf). Another was chosen to determine the amounts of recoverable and non-recoverable deformations under a cyclic loading pattern with an increase in bearing pressure for each cycle. The third loading procedure was chosen to obtain the time dependency of deformations under loading. This third procedure was also to provide information on the creep properties of the soil. However, this was only successful for one of the vertical tests (V2/3), primarily because of the strength of the soil in relation to the capacity of the loading system. A more detailed description of each loading procedure is presented below.

##### 4.2.5.1 Procedure 1 Tests

This loading procedure was a direct simulation of the large-scale footing test and consisted of loading up to a bearing pressure of 316 kPa (3.16 Tsf) in increments of 32 kPa (0.32 Tsf), unloading to 0 in increments of 64 kPa (0.64 Tsf) and reloading to failure or the capacity of the loading system in increments of 32 kPa. Where the capacity of the jack was not sufficient to cause failure, the load

was reduced again to 0 in increments of 64 kPa. The criteria for applying any increment of load in this testing procedure was that the rate of deformation should have reduced to 0.025 mm/min (0.001 in/min), under each load increment. The average time taken for a test of this nature was about 3 hours.

#### 4.2.5.2 Procedure 2 Tests

The second loading procedure was designed to obtain the performance of the soil under cyclic loading. The procedure of loading was to apply a load of 32 kPa (0.32 Tsf) and then unload to 0 or as close to 0 as was practical, and then apply successive load cycles in which increments of 32 kPa were applied so that each successive cycle reached a peak load greater than the last by 32 kPa. This procedure of successively increasing the maximum pressure of each cycle was continued until failure or until the capacity of the loading system was reached. Unloading decrements of 64 kPa (0.64 Tsf) were used for each unloading cycle. The criteria for applying an increment or a decrement of load was the same as in Test Procedure 1. The average time required for this type of test was 5 hours.

#### 4.2.5.3 Procedure 3 Tests

The third loading procedure, used for a vertical test at each of the three levels and only one set of horizontal tests at the first level, determined the time dependency of the deformations. The load was applied in increments of 32 kPa and deformation readings were taken every 3 minutes up to 15 minutes under each load increment. The load application was controlled so that the rate of deformation remained less than 0.15 mm/min (0.006 in/min). When it became impossible to control the rate of deformation below this limit the load was applied so as to cause a constant rate of deformation of 0.15 mm/min for 30 minutes. As indicated before, only one of the tests, V2/3, was finished in this proposed fashion. Once this constant rate of strain had been applied for 30 minutes, the hydraulic pump was shut off, and deformation and pressure readings were recorded with time until no more deformation occurred. Then the load was applied so as to cause a constant rate of strain of 1.5 mm/min (0.06 in/min) for another 30 minutes. After this, the hydraulic pump was closed again and pressure and deformation readings were again taken with time until no more deformation occurred. At this stage the test was terminated. The time for this test (V2/3) was 4-3/4 hours. The other Procedure 3 Tests took about 4 hours.

Table 4.2 on Plate 4.12 presents a list of all of the plate tests, indicating the type of test, the elevation, the loading procedure, and the approximate time for each test.

#### 4.2.6 Data Recorded

In all the tests performed, readings were taken of the hydraulic pressure in the loading system and all the dial gauges at certain intervals. In most cases these readings were taken only when the rate of deformation criterion was reached. In the tests following Procedure 3 the readings were taken at regular time intervals as explained above. Table 4.3, Plate 4.13 gives a list of the number of dial gauges used for each test and the performance which they recorded. In all cases, the average deformation of the plate was obtained by taking the mean of all the gauges measuring such deformation.

In addition to these recordings, any information about irregularities in the soil at any particular test set-up, either during the preparation of the test surface, or in the behaviour of the fissures during the test, was noted. In many cases the fissures adjacent to the loading plate were observed to open, and during some of the horizontal tests blocks of clay fell away from the face of the

excavation. The above noted observations are summarized in Table 4.4, Plate 4.14.

### 4.3 FOOTING TEST

#### 4.3.1 Test Set-up

The full-scale footing test had been performed expressly to determine the amount of settlement of such a foundation in the crust of the Leda clay. This test footing consisted of a 3.05 m square (10 foot square) by 0.66 m (26 inch) thick reinforced concrete slab. The maximum reaction of 2.67 MN (300 tons) required for this test was provided by twelve stranded cables anchored through the center of the footing, as shown in the cross section on Plate 4.15, into the underlying bedrock at a depth of about 18 m (59 feet). The base of the anchor was grouted into a rock socket 6.1 m (20 feet) long, with the tip of the anchor at elevation 61.0 m (elevation 200 feet). Loads were applied to the footing by means of a hydraulic jack pulling against the cables which were brought up through the center of the footing and fixed to the jack. The jack rested on a small concrete pedestal centered on the footing.

#### 4.3.2 Instrumentation

The main interest of the foundation consultant was the amount of surface deformation which would occur

under the proposed design load of 300 kPa (3 Tsf). However, several additions were made to the basic instrumentation program by the Civil Engineering Department of the University of Ottawa (Gaumy, 1970).

A plan view of the footing is given in Plate 4.16, and the locations of the various instruments are shown. A total of six dial gauges calibrated to (0.025cm) 0.001 inches recorded the deformation of the surface of the footing. Four gauges were located at the corners, one at the center and one at the midpoint of one side. Contact pressures were measured at five locations with Geonor vibrating wire pressure gauges (Bauer, 1967). These gauges were confined to one quadrant of the footing, as shown on Plate 4.16. The deformation with depth was measured at the center of the footing and also at the edge of one side of the footing. Spiral foot settlement gauges (similar to Bozozuk, 1968) were installed at depths of  $B/4$ ,  $B/2$ ,  $B$ , and  $3B/2$ , where  $B$  is the width of the footing. Finally, two inclinometer tubes were installed: one at a distance of  $B/4$  from the center, towards the midpoint of one of the edges, and the other beside the midpoint of one of the edges, as shown on Plate 4.16.

#### 4.3.3 Loading Procedure

The main purpose of the test was to determine how much immediate deformation and time dependent deformation would occur under a full-size footing loaded to the proposed design pressure of 300 kPa (3 Tsf). Two cycles of load were applied with increments of 50 kPa (0.5 Tsf) and unloading decrements of 100 kPa (1 Tsf). Each increment of load was held for approximately 15 minutes and the full load was held for 19 minutes for each cycle. The zero load at the end of each cycle was held for about 2 hours.

#### 4.3.4 Observations

Vertical deformations of the surface and the various layers under the footing were recorded during and at the completion of each load increment. Observations were made of the contact pressures and the horizontal deformations (i.e. the inclinometers) at the completion of each load increment. All of the observed data has been reported by Gaumy (1970) and only the data pertinent to this study is presented in the next chapter.

## CHAPTER 5

PRESENTATION AND DISCUSSION OF RESULTS5.1 PLATE TESTS5.1.1 Introduction

The results of all of the individual plate bearing tests are given in Plates 5.1 to 5.19. The results are presented in the form of applied bearing pressure,  $q$ , in kPa ( $10^{-2}$  Tsf), versus deformation,  $\rho$ , in centimeters. All the results were actually plotted on large, 25 x 38 cm (11 x 17 inch) paper so that greater accuracy could be obtained for calculations; however, the reduced copies included in this thesis are satisfactory for the purposes of discussion and comparison.

One major problem encountered with virtually all tests was tilting of the plate. The contact between the loading system and the plate was free-jointed so that the loading system would not induce an eccentric load. However, for one of each set of horizontal tests the contact between the loading system and the plate was a rigid coupling. This

coupling was used for the B tests (e.g. H1/2B) with the exception of Test H1/1A. For tests V2/2 and V2/3 the rigid coupling was also used.

The pressure was fairly uniformly distributed and the major cause of the tilting was probably due to the location and orientation of major, slightly inclined fissures (see Plate 4.5(b)). A table presenting the maximum tilt in absolute terms (with reference to the average deformation), and also as a percentage of the total deformation is given for each plate test in Table 5.1, Plate 5.20, for an applied pressure of 316 kPa (3.16 Tsf). The tests which had a rigid coupling to the loading system are indicated by the notation (R) following the test number (e.g. H1/1A (R)).

It can be seen that the tilt, as a percentage of total deformation, varies between 6 and 44% with an average of 22%. There does not appear to be any particular trend to these tilt values except possibly with the test procedure, or duration of test. The average percentage tilt values for each test procedure are set out below:

<u>TEST PROCEDURE</u>	1	2	3
<u>AVERAGE PERCENT TILT</u>	14.2	27.3	26.2
<u>TYPICAL DURATION OF TEST (HOURS)</u>	3	5	4 1/4

While the actual values within each test series are rather erratic there appears to be a definite difference between the average tilt for Test Procedure 1 and Procedures 2 and 3. It is possible that the duration of each test has some influence on the tilt, as the tilt is less for the quicker, Procedure 1 Tests.

It can be seen in Plate 5.20 that the effect of the rigid coupling did not improve the tilt and in fact the tilt for each of the horizontal sets of tests was greater for the rigid case than for the free jointed case. This fact indicates that while the contact between the loading system and the plate may have been rigid for some of the tests the loading system itself may not have been rigid enough to overcome the effect of fissure orientation on the deformation characteristics.

The various additional relevant observations made at the time of each test were made with a view towards assisting in the discussion and comparison between the test results. They were presented in Table 4.4, Plate 4.14. Generally speaking, the majority of the tests were performed without any reason to doubt that they were representative. While some tests tilted more than others, this probably represents a limitation of using relatively small plates

in a fissured soil. The largest percentage of tilt for Test V2/2 (44%) is explained by the definite visible difference in the fissure spacings between one-half of the loaded area and the other, as pointed out in Plate 4.14. Hence, it is assumed that the tilting is primarily influenced by the relative position of major fissures.

#### 5.1.2 Discussion of Plate Test Results

All of the test results follow a typical pattern. With the exception of the initial stages of some tests (Procedure 3 Tests) all tests show an increase in rate of deformation per load increment with increasing pressure. Therefore the soil is obviously not deforming in an ideally linear elastic manner and, in fact, shear strains must be occurring. In most of the tests, the soil was too strong for the loading system to produce failure. Where failure did occur the form of failure was usually a punch type failure that was fairly sudden, but there were some rotation type failures. Some photographs of the failed tests are shown on Plate 5.21(a). Photographs of a portion of a wedge of soil which remained in contact with the plate when a test was dismantled are shown on Plate 5.21(b). This wedge clearly shows the sheared surface.

For the purpose of analysis and comparison it has been necessary to transform the zero point of the pressure versus deformation relationship to account for stress relief in the excavated trench. This transformation has been performed for the vertical tests only and is based on the assumption that the deformation should be zero at a pressure equal to the effective in-situ pressure prior to excavation. These pressures have been estimated for each elevation of test series, as follows:

<u>TEST SERIES</u>	<u>ELEVATION</u>		<u>IN-SITU STRESS</u>	
	m	(feet)	kPa	(Tsf)
VI	85.3	(280)	20	(0.20)
V2	83.8	(275)	35	(0.35)
V3	82.5	(270.5)	45	(0.45)

The transformed origin has been shown on each of the respective pressure-deformation curves. All of the analyses based on these results consider this point the origin of the pressure-deformation curves.

It would probably have been more efficient to have applied the estimated in-situ pressure initially as a seating load; however, this would have resulted in less accuracy since the pressure gauges chosen for the loading

system provided a good range of pressure increments relative to the major divisions on the gauges. Therefore, it was easier and probably more accurate to start each vertical test at a very low nominal seating pressure of about 6.3 kPa (0.063 Tsf).

No such transformation has been presented for the horizontal tests partially due to the difficulty in estimating the effective in-situ horizontal stress. At the upper levels of the soil profile it is considered that the in-situ horizontal stress would approach zero on account of the extreme horizontal shrinkage, with open vertical fissures. At greater depths the in-situ horizontal pressure presumably increases. However, on account of the fissures it is very difficult to represent the in-situ stresses. The effects of different forms of over-consolidation have been discussed in Chapter 3 and will be discussed again later in this chapter.

Another reason for not transforming the origin for the horizontal tests is that a significant load was applied in all these tests primarily to assist in the support for the loading system. These initial pressures are tabulated on the following page and are compared to the estimated vertical in-situ pressures for each test and the values of

$K_0$  measured by Gaumy (1970) for this soil deposit.

<u>TEST</u>	<u>INITIAL PRESSURE (kPa)</u>	<u>EST. VERTICAL IN-SITU PRESS.</u>	<u>INFERRED <math>K_0</math></u>	<u>MEASURED <math>K_0</math> Gaumy 1970 (Approx.)</u>
H1/1A & B	19	20	0.95	0.70
H1/2A & B	13	20	0.65	0.70
H1/3A & B	19	20	0.95	0.70
H2/1A & B	32	35	0.91	0.20
H2/2A & B	32	35	0.91	0.20

The comparison between the "inferred" and the approximate measured values of  $K_0$  (Gaumy, 1970) is interesting. It was pointed out in Chapter 3 that the higher measured values of  $K_0$  in the upper levels of the crust can be misleading and almost meaningless in terms of deformation studies. The actual in-situ horizontal stresses in the macrostructure are probably considerably less than these values of  $K_0$  imply. Therefore, the initial seating pressures for both levels of horizontal tests have applied a pressure significantly greater than the more probable in-situ horizontal pressures. Under these circumstances these initial pressures will have greatly influenced the pressure versus deformation response of these Horizontal tests. This effect will be discussed again later.

### 5.1.3 Comparison of Test Procedures

As was discussed in Chapter 4 there were three main testing procedures used for the plate tests. The chief differences are the pattern of increasing load and the criteria for observing deformation and applying an increment in load. While there do not appear to be any major differences between the results for any particular procedure initially tests using the same procedure will be discussed.

#### 5.1.3.1 Procedure 1 Tests

For the tests following Test Procedure 1 (V1/1, H1/1A, H1/1B, V2/1 etc.), the results show: the pressure versus deformation relationship for the initial loading cycle up to 316 kPa (3.16 Tsf); the unloading cycle to some small pressure; then the reload cycle up to the capacity of the loading system or failure of the soil; and finally where possible, the rebound response, from the maximum pressure to zero pressure. A dashed line has been drawn between the cycles to represent the 'virgin' deformation curve. It can be seen that, at elevation 82.5 m (270.5 feet), the V3 Series tests failed during the initial cycle.

The rebound curves indicate the amount of recoverable and non-recoverable deformation for each test. A 'chord' (or secant) has been drawn for each rebound curve. In the case of the horizontal tests, it was not practical to

unload to zero pressure and hence the rebound curves have been projected to zero pressure so that the chord could be drawn. Where results are available for two complete cycles, chords have been drawn for each rebound curve.

These chords represent the recoverable deformation for each cycle of each test. Parallel lines have been drawn at the top of each pressure-deformation curve to represent the 'elastic' component of the total deformation. Where two complete cycles were performed there are two such elastic deformation lines. The slope of the elastic deformation line is greater for the cycle at the higher stress level. It will be shown from the Procedure 2 Tests that this so-called elastic deformation varies significantly for cycles at different pressure levels.

The 'elastic' deformation line occasionally indicates a greater deformation than was actually observed. This again is because of the stress dependency of the 'elastic' deformation, based on the rebound chord. (It will be shown later that the slope of the rebound chord increases for cycles at increasing pressure levels.) Hence, it can be seen that comparison between recoverable and non-recoverable deformation must take into consideration the pressure level.

### 5.1.3.2 Procedure 2 Tests

For tests following Procedure 2, the pressure versus deformation relationship is shown for all cycles. For each cycle the successive increment in pressure was 31.6 kPa (0.316 Tsf). As before the pressure was increased to the capacity of the loading system or failure of the soil. A dashed line has been drawn to join up the maximum points for each cycle to represent the 'virgin' deformation curve.

Once again it was not practical to reduce the pressure to zero in the horizontal tests. In addition the pressure was not reduced to zero for the vertical tests V2/2 and V3/2 because the loading system may have become unstable. Hence, the only test which shows the complete cycles is Test V1/2 (Plate 5.2).

Although the rebound chords have not been drawn, the recoverable 'elastic' deformation has been calculated for each cycle for Test V1/2. The net recoverable deformation has been plotted above the total deformation curve to represent each cycle and these have been joined by a solid line. It can be seen for the case of Test V1/2 this incremental 'elastic' deformation line is rather erratic; however, the general trend is to increase with increasing pressure.

With the exception of Test V2/2 (Plate 5.11) all other Procedure 2 Tests were cycled to increasing increments and unloaded to the same constant minimum load, although not to zero. Therefore, while these tests do not represent the complete cycle they can still serve as a means of comparing the recoverable deformation for successive increments. The corresponding recoverable deformation for each of the cycles is shown above the total deformation curve and in order to illustrate that these values do not represent the complete recoverable deformation the points have been joined by a dotted line. The recoverable deformation is still rather erratic but the trend to increase with increasing stress is further illustrated. Hence, it has been shown that the recoverable, so-called 'elastic' deformation varies significantly with increase in pressure. This variation is more pronounced at lower levels of pressure. In addition, it can be seen that at greater levels of applied pressure the variation in the recoverable deformation tends towards linearity; however, it does not approach a line passing through the origin.

#### 5.1.3.3 Procedure 3 Tests

The tests performed using this third procedure were an attempt to study the time dependency of deformation under each increment of pressure and also to measure the creep

properties of the soil. The results plotted in this series of plates (5.1 to 5.19) are the final deformation under each load increment versus the pressure. At the upper levels in the test trench the strength of the soil was too high for the creep tests. At elevation 83.8 m, Test V2/3 was the only test which was successfully completed as intended. At elevation 82.5 m the soil was so soft that failure occurred before the creep portion of Test V3/3 was completed. Hence only one test (V2/3) provided any such information and it is not proposed to analyse this single test for creep properties. However, the deformation with time results for each increment can be studied. The deformation versus time results have been plotted for each pressure increment for each test in Plates 5.22 to 5.26. Also shown on these plates are the step-wise pressure versus deformation curves.

In order to compare these Procedure 3 Tests with tests using the other two procedures it is necessary to study the time dependency of the deformations. For the two previous test procedures it will be remembered that the criterion for increasing the load (Procedures 1 and 2) or for observing the maximum deformation under each pressure cycle (Procedure 2) was the same, at less than 0.003 cm/min of deformation. A review of the rates of deformation for the Procedure 3 Tests shows that for the given 15-minute period under each increment of pressure the rate of deformation

at the end of the 15 minutes can be related to the shape of the total pressure-deformation curve. There are three separate conditions;

(1) For the lower pressure levels, when the deformation has terminated in less than 15 minutes;

(2) For intermediate pressure levels (with the exception of Test V3/3, Plate 5.26), when the rate of deformation at the end of the 15-minute interval corresponds with the same criteria for Test Procedures 1 and 2; and

(3) For higher pressure levels, when (with the exception of Test V1/3, Plate 5.22) the rate of deformation is greater than the criteria for Procedures 1 and 2.

These three conditions have been indicated on Plates 5.22 to 5.26 and also on Plates 5.3, 5.8, 5.9, 5.12 and 5.19. The pressure levels which separate these conditions are tabulated in Table 5.2, Plate 5.27 for each of the respective tests. The pressure levels are quite inconsistent and difficult to interpret.

An examination of the pressure-deformation curves with respect to these conditions shows that there is an almost linear to even concave upwards form to the pressure-deformation curves where the deformation has terminated in

less than 15 minutes. This is more apparent in the curves showing the variation in the function of modulus  $f(M)$ , plotted below each of the pressure-deformation curves on Plates 5.1 to 5.19. This function of modulus  $f(M)$  has been defined in Chapter 2 and will be discussed in detail in Chapter 6.

The linear to concave form of the pressure-deformation curves is particularly evident in Tests V1/3, H1/3A and V3/3 (Plates 5.3, 5.8, and 5.19). This linear to concave shape appears to be unique to this first, rate of deformation condition for these Procedure 3 Tests. The deformation under each increment at the lower pressure levels appears to be greater than in the other tests which were loaded at a faster rate. It is not immediately apparent why this is the case, since the deformation had actually terminated under each increment before the full 15-minute interval.

At the higher pressure levels, where the criteria for increasing the pressure either corresponds to or is greater than the other test procedures, there does not appear to be any significant difference in the pressure-deformation curves.

#### 5.1.4 Estimation of Failure Pressure

Much of the analysis of the results of these tests will be presented with respect to a non-dimensional pressure ratio. Pressure ratio is defined as bearing pressure expressed as a ratio of the ultimate failure pressure,  $q_u$ . Since many of the tests did not reach failure, it was necessary to estimate the value of  $q_u$ . This estimated failure pressure is based on one or a combination of three methods: the shape of the pressure-deformation curve; the bearing capacity theory for the Leda Clay crust as proposed by Mitchell, Sangrey and Webb (1972); and a graphical method proposed by Kondner and Krizek (1962).

The values obtained for each test, for each method are presented in Table 5.3, Plate 5.28. Where a plate test obviously approached failure the best estimation of  $q_u$  could be observed from the bearing pressure versus deformation curve. It will be seen that for the vertical tests the failure theory of Mitchell et al., overestimates the failure pressure for the V1 series of tests and underestimates the failure for the V2 and V3 series. The shear strength properties shown on Plate 4.4 have been used for this analysis.

The method presented by Kondner and Krizek is explained graphically on Plate 5.29 illustrating some

typical examples from Table 5.3, Plate 5.28. Almost all of the tests showed a good linear relationship between  $p/q$  and  $p$ ; however, for some tests (eg: H1/1A, see Plate 5.29) it was rather difficult to 'fit' a representative line. Since the failure pressure is equal to  $1/b$ , where  $b$  is the slope of this line, the degree of 'fit' of the line is rather critical. However, except for some debatable situations this graphical method generally overestimates the failure pressure. This method would possibly be more successful for a more intact, homogeneous soil deposit. Hence, in almost all the cases the chosen failure pressure, for the purposes of all future analyses, was based on the shape of the pressure deformation curve. This chosen estimate of the ultimate failure pressure is shown on all of the individual bearing pressure versus deformation Plates 5.1 to 5.19.

The same comparison of the methods used to estimate the failure pressure of the test footing is also shown on Table 5.3, Plate 5.28. Kondner and Krizek's method seems to underestimate the failure pressure. It is quite difficult to estimate failure from the pressure-deformation curve (Plate 5.44) and hence in the absence of any other guidelines the method of Mitchell et al., has been chosen as the representative failure pressure.

### 5.1.5 Relationship Between Recoverable and Non-Recoverable Deformations

In order to study the inelastic behaviour of the soil and to determine whether there is any characteristic trend to the variation between the recoverable deformation,  $\rho_R$  and the total deformation,  $\rho_T$ , it is of interest to plot the values of the deformation ratio of  $\rho_R/\rho_T$  against bearing pressure ratio. This presentation is made in Plate 5.30. The curves on this plate represent the Procedure 2 Tests (except V2/2) and the individual points represent the deformation ratios for some of the other tests where the recoverable deformations were observed. It should be remembered, that with the exception of Test V1/2, the unloading cycles in the Procedure 2 tests were not unloaded to zero pressure; however, for the purposes of characteristic trends this should not be too significant.

As can be seen, there is a considerable scatter between the different tests. The only consistency appears in the deformation ratios for the set of horizontal tests, H1/2A and H1/2B. Apart from this there appear to be two different trends in the deformation ratio versus pressure ratio. Most of the tests tend to exhibit a decrease in the deformation ratio for the range of pressure ratios presented; however, there are three tests, V3/2, H1/2A and H1/2B which

show considerably lower deformation ratios at lower pressure ratios. (The results of the horizontal tests may not be representative in view of the earlier discussion on initial seating pressures.) For most of the test results there is too much scatter to enable any meaningful discussion or interpretation. This scatter can probably be attributed to the effects of the fissures and the sensitivity of the initial loading conditions on such a fissured soil.

#### 5.1.6 Deformation at Depth

A total of six tests were performed with settlement gauges below or behind the plate (V2/1, V2/2, H2/1A, H2/2A, V3/1 and V3/2). The deformations were observed at four points, at depths or distances from the loaded surface of  $z = 1R, 2R, 3R$  and  $4R$  (where  $R$  is the radius of the plate). The four separate gauges were located at 90-degree spacings on a circle of radius  $R/2$ . The results are compared to the surface deformation and bearing pressure for each of the respective tests in Plates 5.31 and 5.36. In some cases the gauges were either broken or the results were undecipherable, as noted on the respective plates.

As was mentioned earlier, the plates tilted quite severely during some tests. This tilting obviously affects

the deformation distribution below the plate, particularly at shallow depths. Hence, for most of these tests some correction has been applied to the results to account for tilting. Fortunately, the axis of tilt generally passed through the center of the plate.

The results for the vertical tests appear more representative than those for the horizontal tests. For the vertical tests the curves representing the deformation at each of the points below the plate follow the same form as the total deformation curves. In addition, there appears to be a reasonable proportionality to the deformation at different depths with increase in pressure.

The curves further indicate that a large portion (approximately 86 percent) of the total deformation occurs within a depth of 2 radii and in the case of Test V3/1 (Plate 5.35), virtually all of the deformation occurs within a depth of 4 radii, especially at the lower levels of pressure. These results of the distribution of deformation with depth will be discussed in considerable detail in Chapter 6.

For the Horizontal Tests H2/1A and H2/2A (Plates 5.33 and 5.34) the greater frequency of vertical fissures,

discussed in Chapter 3, is probably the major cause for the erratic results. In practise, the vertical fissures closest to the plate have to close before pressure is transmitted to deeper blocks of intact clay and this would account for the smaller deformations of the deeper gauges. In addition, these settlement gauges were in a horizontal position and were probably less stable in this position than the vertical, even though the gauges were supported by teflon discs attached to the plate.

#### 5.1.7 Comparison Between Tests Within Each Test Series

A comparison is made between the pressure versus total deformation curves (or the virgin deformation curves where applicable) for each of the tests in a series. The discussion in Section 5.1.3 has established that there were no major differences in the deformation responses attributable to the different loading procedures except that the Procedure 3 tests did exhibit a slightly different characteristic response at low pressure levels. All of the deformation curves have been plotted for each respective series on Plates 5.37 to 5.41. The average deformation curve for each series has also been drawn on these plates.

##### 5.1.7.1 V1 Series Tests

For the V1 Series, Plate 5.37, there is an excellent comparison between Tests V1/1 and V1/2. Test V1/3 shows

less deformation at the higher pressure levels. With reference to the observations set out in Table 4.4, Plate 4.14, the soil was significantly stiffer and less fissured at the location of Test V1/3. Therefore, the difference in the deformation curves represents the non-homogeneity of the soil deposit.

#### 5.1.7.2 H1 Series Tests

For the H1 Series, Plate 5.38, there is a much greater variation between the test results. Test H1/2A shows considerable deformation at all pressure levels though more pronounced at the lower pressures. Test H1/3A shows the lowest deformations, especially at the higher pressure levels. The remaining tests in this series compare more favourably.

Considerable care was taken to remove all loosened and dried out soil on the sides of the excavation while setting up these horizontal tests. Therefore, the difference between these horizontal deformation curves should represent the different configuration of major fissures. However, these tests are probably not representative due to the relatively high initial seating pressures.

### 5.1.7.3 V2 Series Tests

For the V2 Series Tests, Plate 5.39, there is again a considerable difference between the pressure-deformation curves. While this difference is less pronounced at lower levels of pressure, no specific observations, with the exception of tilting, were made for these tests to indicate the reason for the difference. Once again, the difference is attributed to non-homogeneity of the soil and also the size of plate with respect to the position and orientation of major fissures.

Test V2/3 (Plate 5.12) does not show a linear or concave form at the lower pressure level, in spite of the relatively large range of pressure increments which were applied under conditions where deformations had terminated within the 15-minute interval. This has been discussed above.

### 5.1.7.4 H2 Series Tests

For the H2 Series Tests, Plate 5.40, there is a very good comparison between Tests H2/1A and H2/2B and also between Tests H2/1B and H2/2A. With reference to Table 4.4, Plate 4.14, none of the observations can explain why the individual sets of horizontal tests do not compare better. Once again the difference is attributed to non-homogeneity.

Considerable deformation may have occurred under the initial seating load, so these tests are probably not representative either.

For Tests H2/1A and H2/2B the deformation under any given pressure is significantly greater than for any other test discussed so far.

#### 5.1.7.5 V3 Series Tests

For the V3 Series Tests, Plate 5.41, there is a reasonable comparison between each test, especially with regard to the pressure at failure. For Test V3/3 the initial portion of the curve is virtually linear. This portion of the curve corresponds to the range of pressures where the deformation had terminated for the 15-minute interval.

#### 5.1.8 Comparisons Between Vertical and Horizontal Tests

A comparison is made between the vertical and horizontal series at the two elevations where both series were performed. That is, a comparison between the V1 and H1 Series and the V2 and H2 Series. This comparison is based on the average deformation curve for each series and is shown on Plates 5.42 and 5.43.

#### 5.1.8.1 V1 Series Versus H1 Series

A comparison between the vertical and horizontal test series at Elevation 85.3 m (280 feet), on Plate 5.42, shows that the horizontal deformations under the same pressures are slightly greater than the vertical deformations. Some considerable deformation may have occurred under the initial seating pressure. If this deformation had been measured the total horizontal deformations would have been significantly greater.

With reference to the discussion on the effect of fissures and desiccation in Chapter 3, this comparison is all the more interesting. The effect of desiccation is to cause fissures. Fissures will develop easier in the vertical direction, due to the lack of sufficient in-situ horizontal stresses to compensate for shrinkage. On the other hand, while desiccation also causes fissures on a horizontal plane, these fissures are less frequent, and due to the ever present weight of the soil, these fissures do not open as much. The individual blocks of intact soil are not only columnar but the actual fissure openings are greater for vertical fissures than for horizontal fissures. Hence, when a pressure is applied in the horizontal direction the percentage of the total deformation which is attributable to the closing of fissures is much greater than for any vertical

application of pressure. However, the soil will behave in a truly over-consolidated manner once the fissures are compressed. This suggests that the desiccated crust exhibits a variable degree of anisotropy with pressure level. At low levels of applied pressure the anisotropy ( $E_H/E_V$ ) would be less than one. At higher pressures the compressed macrostructure would exhibit anisotropy greater than one. Hence, in terms of isotropy the type of over-consolidation must be considered. As discussed earlier, the over-consolidating effect of desiccation actually causes an effective "under-consolidation."

#### 5.1.8.2 V2 Series Versus H2 Series

The comparison between these two series, on Plate 5.43, is remarkably close. Once again the horizontal deformations may have been greater if the deformations under the initial seating pressure had been observed. Therefore, this comparison is not considered valid with regard to anisotropy.

With reference to the discussion in Chapter 3 and above on the effect of fissures this comparison is also interesting. In Chapter 4, it was stated that the fissure spacing at the elevation of the V2 and H2 Series Tests was considerably larger than at higher elevations. Also, the fissure openings are less at this lower level. Therefore,

the effect of the fissures will be less significant at this level though a variable degree of anisotropy with pressure levels would still be expected.

In summary, the comparison between vertical and horizontal test results in Plates 5.42 and 5.43 is not considered valid. The effect of the fissures in the crust of the clay would appear to cause a varying degree of anisotropy with pressure level. It would be difficult to relate horizontal deformation data to vertical deformation response. These horizontal tests would not provide readily useable data for foundation design.

## 5.2 FULL-SCALE FOOTING TEST

The results of this full-scale footing test have been fully discussed by Gaumy (1970). Only the results pertinent to this study are presented here.

### 5.2.1 Pressure Versus Total Deformation

The results of the pressure versus total deformation response for each pressure cycle of the footing test are shown for the center and the edge of the footing, on Plates 5.44 and 5.45 respectively. The shape of these curves is similar to the plate tests but the deformation under similar applied bearing pressures is considerably greater than in the plate tests. A comparison is made between the deformations

of the footing test and the average deformations for the plate tests (V1 Test Series) for three different pressures, in Table 5.4, Plate 5.46.

Some comparison of the loading procedures of the plate tests and the footing test should be made. The pattern of loading for the footing test is identical to Procedure 1 for the plate tests except that the footing test was not loaded towards failure during the second cycle. However, the criteria for incrementing the load or recording deformations are slightly different. For the footing test, the final deformation under each level of applied pressure was recorded after a specific time interval and this interval was not constant. Load increments were applied after 12 to 18 minutes and the rate of deformation at that time was not necessarily considered. Therefore, the footing test appears to compare more with the Procedure 3 Plate Tests in this respect. As in the case of the plate tests this factor may not be very significant and certainly is not the major explanation for the considerably greater deformations for a given surface pressure. Hence, the greater deformations under the test footing are primarily related to the greater size of loaded area.

Obtaining a general relationship between deformation response and the size of the loaded area is beyond the scope of this study and is not possible with only two sizes of tests. However, the deformations presented in Table 5.4, Plate 5.46, have been expressed as a function of the radius of the loaded area. It is interesting that the values of  $p/R$ , for the footing test (center) and the plate tests, at a bearing pressure of 300 kPa are quite close. At lower pressure levels, this comparison is poor.

Another point which has to be considered for the footing test is the difference between the center and edge deformations. At the maximum applied pressure of 300 kPa (3 Tsf) the respective surface deformations (first cycle) were 2.16 cm and 1.76 cm. Therefore, the footing is clearly not perfectly rigid and this may have some significance on the analysis to be presented in Chapter 6.

### 5.2.2 Deformation At Depth

The deformation at the depths of the settlement gauges under the center and edge of the footing test are compared with the surface deformation on Plates 5.47 and 5.48, respectively. These results of the deformations at specific depths are considerably more erratic than the

results from the plate tests. However, there is a reasonably consistent proportionality to the deformations at depth for each pressure level.

The depths,  $z$ , of the settlement gauges under the footing test were chosen to represent ratios of  $z/B = 0.25$ ,  $0.5$ ,  $1.0$  and  $1.5$  (where  $B =$  the width of the square footing). In order to compare these results with the plate test it will be necessary to use the equivalent radius  $R'$  (Equation 3.2). Therefore, the depth ratios mentioned above with respect to  $B$  have been transformed into the following ratios with respect to  $R'$ :

$z/B$	$z/R'$
0.25	0.44
0.50	0.89
1.0	1.78
1.5	2.66

In Plates 5.47 and 5.48 at the maximum pressure, the deformation within a depth,  $z/B = 1.5$  ( $z/R' = 2.66$ ) is about 92% of the total deformation for the center of the footing, and 96% for the edge of the footing. While these percentages cannot be readily compared with the plate tests, the results are similar (average of 93% to  $z/R = 3$  for vertical plate

tests). Hence a large proportion of the total deformation occurs within a relatively shallow depth and this will be discussed in considerable detail in Chapter 6.

## CHAPTER 6

ANALYSIS AND INTERPRETATION OF RESULTS6.1 PRESSURE VERSUS SURFACE DEFORMATION6.1.1 Introduction

As discussed in Chapter 2, the results of the applied bearing pressure versus surface deformation relationships will be analysed and interpreted in the form of a function of modulus,  $f(M)$  rather than an actual deformation modulus. The main reason for such a presentation is to illustrate that the results presented in the previous chapter (and in the literature) do not represent the reactions of a linear elastic medium. Therefore, instead of analysing the deformations according to the linear elastic theory, but presenting the results in a form for discussion and interpretation, the basic test results are analysed in the form:

$$f(M) = \frac{\pi Rq}{\rho} \quad (2.7)$$

Values of  $f(M)$  have been calculated for various levels of applied bearing pressure for all of the plate

tests and the footing test (1st cycle only, center and edge), and the results have been plotted against bearing pressure below the pressure versus surface deformation curves for each individual test in Plates 5.1 to 5.19 and Plates 5.44 and 5.45.

For all of the vertical plate tests the effect of stress release due to excavation has been considered and all calculations for  $f(M)$  are relative to the transformed origin shown on the plates for each individual vertical test, as discussed in Chapter 5. No such transformation of the origin was performed for the horizontal tests due to the difficulty in estimating the stress release and the fact that the initial seating pressures were probably greater than the in-situ pressures. Also, no transformation was considered for the footing test since the difference between the weight of the footing and the weight of removed soil was considered to be negligible.

The  $f(M)$  versus pressure curves are directly related to the shape of the pressure-deformation curves. However, since this  $f(M)$  comprises the data for any analysis of deformation modulus, it is more meaningful to analyse and interpret the results in this form.

All of the  $f(M)$  versus bearing pressure relationships including the footing test, have been plotted on Plate 6.1. Apart from the considerable scatter between these curves, there is a definite trend to the shape of the curves, just as there is a typical trend to the pressure-deformation curves. However, the  $f(M)$  curves accentuate the variation in the pressure-deformation response, especially at the lower bearing pressure levels for the Procedure 3 tests.

Within the scatter of these results, there is a general difference between the values of  $f(M)$  for each of the test series (V1, V2 and V3). This will be discussed in more detail later. Also, while the general shape of most  $f(M)$  curves is similar, the variation of  $f(M)$  with pressure is more pronounced for the V1 and the V3 Series than for the V2 Series. This factor is primarily related to the difference in physical properties of the soil at the levels of the different test series and will be discussed in more detail at a later stage.

On the function  $f(M)$  versus pressure curves for the Procedure 3 Tests, the characteristic lower values of  $f(M)$  at the lowest levels of pressure reflect the concave shape of the pressure versus deformation curves for these tests.

Since these  $f(M)$  curves directly represent the results of the tests which have been discussed and compared in some detail in Chapter 5, only the vertical tests in the form of the  $f(M)$  curves will be discussed in further detail as only the vertical tests are relevant for the purposes of design and comparison with the footing test. The horizontal test results were discussed with respect to anisotropy in Chapter 5. Horizontal tests are usually cheaper to perform, but the degree of anisotropy would have to be established for a given soil deposit before horizontal moduli could be used for design.

#### 6.1.2 Variation of the Average $f(M)$ with Applied Bearing Pressure for the Vertical Tests

The variation of  $f(M)$  with pressure for each of the average pressure-deformation results for the three vertical test series has been calculated and the results plotted on Plate 6.2. This combination of the three plate test series illustrates the variation of  $f(M)$  with bearing pressure and with depth through the crust of the Leda clay at this site. The values of  $f(M)$  for the V2 series are generally higher than for the V1 and the V3 series.

Also shown on this Plate 6.2 is the variation of  $f(M)$  with bearing pressure for the center and edge deformations for the first cycle of the footing test. With the exception of the lower pressure levels these values of  $f(M)$  are within the same range as the plate bearing tests. However, the values of  $f(M)$  for the footing test are higher than for the VI Series plate tests, performed at approximately the same elevation, due to the difference in size of the loaded areas (compare with Table 5.4, Plate 5.46). At a pressure of 300 kPa values of  $f(M)$  for the footing test and plate test Series VI are reasonably close.

### 6.1.3 Variation of $f(M)$ with Applied Bearing Pressure and Depth

In order to illustrate the variation of  $f(M)$  with depth the average values for the plate tests, shown on Plate 6.2, have been plotted with respect to depth, for various bearing pressure levels, in Plate 6.3. In addition to the depth scale (elevation), the depth is also shown with respect to the footing test in the form of  $z/R'$ , where  $R' = \sqrt{\frac{A}{\pi}}$  (Schleicher, 1926), the equivalent radius of the full-scale square footing. The values of  $f(M)$  at the same bearing pressure levels, for the center of the footing test are shown at  $z/R' = 0$ .

Between the V1 and V2 Series  $f(M)$  increases for each individual pressure level, and between the V2 and V3 Series  $f(M)$  decreases. These curves represent the variation of  $f(M)$  with depth as measured by similarly loaded plate tests at each level of test. Hence, these curves represent the non-homogeneity with depth with regard to the deformation response.

It is interesting to compare this particular variation of deformation response with the shear strength of the soil, as shown on Plate 4.4. Normally the deformation response would vary with depth in much the same manner as the strength varies with depth; in fact, several authors have shown that for many soil deposits there is a reasonably consistent relationship between deformation modulus and undrained shear strength,  $E/c$  (e.g. D'Appolonia, Poulos and Ladd, 1971). This relationship implies that the modulus values would be considerably greater than the observed moduli, in the upper layers of the crust. However, the observed variation of deformation response with depth can be explained in terms of the varying degree of fissuring with depth through the crust.

At the first level of tests (V1 Series), the strength of the individual blocks of clay is very high; however, the

frequency of fissures is also high. Therefore the deformations are quite large. At the second level of tests (V2 Series), the strength of the soil is still relatively high due to the effects of desiccation; and the frequency of fissures is lower. Therefore, the deformations are not as large. At the third level of tests (V3 Series) the frequency of fissures is considerably less but the strength of the soil is significantly lower. Therefore, the deformations are again quite large due primarily to the softer soil.

#### 6.1.4 Variation of $f(M)$ for the Vertical Plate Tests with Bearing Pressure Ratio

With reference to the variation of  $f(M)$  with pressure for each test as shown on Plate 6.1 and also Plate 6.2, the rate of change in  $f(M)$  varies for each test even though there is a typical trend. The main reason for the difference between the  $f(M)$  versus pressure curves, for tests within a specific series, is due to the non-homogeneity of the soil, as discussed in Chapter 5. A better comparison of the deformation characteristics can be achieved if the variation in  $f(M)$  is presented with respect to the ultimate failure pressure for each test or, more specifically, bearing pressures which are ratios of the ultimate failure pressure. This dimensional presentation of the variation of  $f(M)$  with bearing pressure should show a characteristic pressure-deformation response for the soil.

The  $f(M)$  versus bearing pressure results for the vertical tests (except the Procedure 3 Tests) have been re-analysed with respect to bearing pressure ratios between 0.0 and 0.5. This upper limit to the range of pressure ratios has been chosen because it more than adequately covers the range of bearing pressure ratios encountered in foundation engineering.

The plate tests performed at the upper test levels did not reach failure, and for these tests the ultimate failure pressure has been estimated, as discussed in Chapter 5 (see Plate 5.28). The estimated or predicted ultimate failure pressure for each test is shown on each of the respective pressure-deformation plates (Plates 5.1 to 5.19).

The results of this  $f(M)$  versus bearing pressure ratio analysis are shown, for each of the respective vertical tests, on Plate 6.4. While there is still some scatter due to the difference in elevation of the different test series, and probably non-homogeneity at each elevation, the rate of variation of  $f(M)$  with bearing pressure ratio is more consistent. The variation of  $f(M)$  is relatively small between pressure ratios of 0.1 to 0.5, but at the lowest pressure ratios, between 0.0 and 0.1, the variation of  $f(M)$  is more significant. This indication of higher modulus values at the

lowest pressure levels represents an interesting aspect of the non-linearity of soil deformation response.

## 6.2 DISTRIBUTION OF DEFORMATION WITH DEPTH BELOW THE LOADED SURFACE

### 6.2.1 Distribution of Deformation for the Plate Tests

#### 6.2.1.1 Observed Results from Plate Tests

In order to study the vertical distribution of deformation with depth for the plate tests which were performed with settlement gauges, the results are presented in non-dimensional form. Once again, to obtain a deformation characteristic, the deformations with depth are analysed at various bearing pressure ratios of the ultimate failure pressure. The deformations are expressed as percentages of the total deformation. More specifically, the analysis presents the deformation which occurs between the surface and the respective depths of each settlement gauge (i.e.  $z/R = 1, 2, 3$  and  $4$ ) as a percentage of the total deformation. The results of this analysis are presented on Plates 6.5 to 6.9, for bearing pressure ratios of 0.1 to 0.5 respectively. On each of these plates, the results from the four vertical plate tests, V2/1, V2/2, V3/1, and V3/2, are shown.

Also shown on each of these plates is the average distribution of deformation curve which has been calculated, taking into consideration the degree of tilting and the reproducibility of the results for each test. While there is some scatter to either side of this average curve, the scatter is generally less than  $\pm 10\%$  of the average.

When the bearing pressure ratio is taken into account, the distribution of deformation appears to be independent of test elevation. In fact, the maximum scatter can be observed between tests performed at the same elevation. Also, there does not appear to be any influence from the method of testing (i.e. between Procedures 1 and 2). Hence, the scatter at any depth,  $z/R$ , should be attributed to non-homogeneity of the soil deposit rather than testing method.

#### 6.2.1.2 Comparison Between Observed and Theoretical Distribution of Deformation with Depth for the Plate Bearing Tests

As discussed in Chapter 3, the most comprehensive analysis, based on the linear elastic theory, is presented by Giroud (1972). This analysis permits the calculation of the deformation at any point within a homogeneous, infinite, elastic medium. Giroud's analysis is particularly useful for this study since the theoretical deformations under the point  $r/R = 0.5$  are compared with the observed plate deformations.

and under the points  $r/R = 0$  and  $r/R = 1.0$  with the observed footing deformations. Other solutions published by Fischer (1965) and Jumikis (1973) only consider the case where  $r/R = 0$ , and all three solutions are identical for this case.

For the plate bearing tests, the comparison between the observed and theoretical distribution of deformation with depth is shown on Plate 6.10. For the observed distribution the results are given for bearing pressure ratios of 0.1 and 0.5, illustrating the range between these values. The results for bearing pressure ratios of 0.2, 0.3 and 0.4 fall within this range. Also shown is the arithmetic average for this range, which incidentally coincides very closely with an interpolated value for a bearing pressure ratio of 0.33 (a common design pressure ratio). For the theoretical distribution, the curve is drawn for the case where  $r/R = 0.5$ , (for a Poisson's Ratio of 0.33) as presented by Giroud (1972).

In spite of the range of values for the observed case there is a marked disparity between the observed and the theoretical distribution of deformation. Further, this disparity is greatest at the lowest pressure level ( $0.1 q_u$ ). The general disparity between the observed and the

theoretical distribution of deformation will be discussed in more detail later.

### 6.2.2 Distribution of Deformation for the Footing Test

#### 6.2.2.1 Observed Results from Footing Test

The same analysis has been performed with the results of the footing test for the deformations under both the center and the edge. Only the initial loading cycle has been considered. The ultimate failure pressure was estimated, as discussed in Chapter 5 (see Plate 5.28).

The results of this analysis are presented in the form of the percentage of the total deformation occurring within certain depths on Plate 6.11 for different bearing pressure ratios of 0.1 and 0.4. The results for both the center and edge deformations are presented. Also the average pressure with respect to distribution of deformation is shown.

The deformations appear to be more concentrated within a shallower depth at higher pressure levels but the reason is not clear. However, it is possible that at lower pressure levels the load is being transmitted to a greater depth by "columns" of intact blocks of hard clay, while at higher pressures these columns are buckling and breaking up,

causing greater amounts of deformation in the upper levels.

Σ

6.2.2.2 Comparison Between Observed and Theoretical Distribution of Deformation with Depth for the Footing Test

In order to compare the observed results for the footing test with the theoretical solution for the distribution of deformation under the center and edge of the footing, the theoretical cases presented by Giroud, for  $r/R = 0$  and  $r/R = 1.0$  are required. This comparison is also made on Plate 6.11. For the theoretical case the distribution of deformation has been given for the center of the test,  $r/R = 0$ , for values of Poisson's Ratio of 0.33 and 0.50, thus illustrating the theoretical effect of Poisson's Ratio. The main point to be observed is that the difference between the observed results and the theoretical solution is considerable, and of the same order of magnitude as the difference for the plate tests. The effect of Poisson's Ratio appears to be quite significant on the theoretical solution.

6.2.3 Comparison Between Plate Tests and the Footing Test

Direct comparison of the actual distributions of deformation with depth for the plate tests with those for the footing test is not feasible because of the different

locations at which the deformations were observed. However, in order to show how the characteristic deformation of this soil deviates from the linear elastic theory, the average distribution of deformation curves for the plate tests and the center and edge deformations of the footing can be combined with the theoretical solutions for the respective situations. This comparison is shown on Plate 6.12; in the same form as the previous comparisons. The relationship between the three situations ( $r/R = 0, 0.5$  and  $1.0$ ) is similar for the observed and theoretical cases but there is the definite disparity between the observed results and the theoretical solutions.

The same comparison between the observed and theoretical results is presented in tabular form in Table 6.1, Plate 6.13, for the plate tests and the footing test. Also shown in this table is the ratio of observed deformation to the theoretical deformations. This ratio between observed and theoretical deformations is presented with respect to depth,  $z/R$ , on Plate 6.14. The ratio between observed and theoretical deformations decreases significantly with depth, as can be observed on Plate 6.12. The disparity between observed and theoretical deformations is very similar for the plate tests and the center line deformations of the footing test. The

results for the edge of the footing follow the same pattern but are not consistent with the center results at the upper levels and this probably reflects the non-rigidity of the footing.

It was pointed out earlier in this chapter that, for the plate tests, the elevation at which different plate tests were performed did not appear to influence the deformation characteristics. For this soil, the size of the loaded area (i.e. plate vs. full size footing) does not appear to significantly influence the distribution of deformation either, based on the comparison made in Plate 6.14. The difference between the distribution of deformation with depth for the center and edge of the footing and that for the plate tests is not very great and they show the same trend as the linear theoretical solution. Therefore it is concluded that the distribution of deformation under the footing is not simply a characteristic related to the thickness of the fissured crust relative to the size of loaded area.

### 6.3 COMPARISON WITH OTHER WORK

The results of similar observations, of deformations with depth by Shvets et al., (1970) Marsland and Eason (1973) and Bauer, Scott and Shields (1973) were presented in Chapter 2 (see Plate 2.2). A comparison between these results and the results of the plate tests are all combined

in Plate 6.15. Also shown are the various theoretical solutions which have been used in the above references..

This combination of all the available observed data clearly indicates a characteristic distribution of deformation with depth which is significantly different from the linear elastic distribution. The fact that the data for the plate and footing tests is close to an average for all observed data indicates that the data obtained in this study is quite representative and is not peculiar to fissured soils.

The Russian, SNIIP (1963) solution represents the in-situ deformation characteristics more realistically. However, the excellent agreement between the SNIIP solution and Marsland and Eason's observations is probably not representative due to the depth of embedment factor involved in the latter's tests.

In order to compare the accuracy of the various solutions for predicting deformation characteristics it is interesting to compare the ratio of the observed to the theoretical deformations versus depth ratio,  $z/R$ . This comparison is made on Plate 6.16. Once again it can clearly be seen that the Russian SNIIP solution is the better solution.

This is presumably due to the consideration of the depth of soil being deformed. The results presented by Marsland and Eason (1973) have also been compared to the theoretical solution presented by Giroud (1972) and it is interesting to note the improvement. Even though the depth of embedment factor is not considered in Giroud's solution it is still difficult to understand the results of the finite element solution presented by Marsland and Eason, especially for the case where  $z/b = 0$  (i.e. a load applied at the surface), as discussed in Chapters 2 and 3.

#### 6.4 DISCUSSION OF THE DEFORMATION CHARACTERISTICS

##### 6.4.1 General

The most interesting observations to be made from the foregoing presentation are that:

- (1) in practice, deformations under loaded surfaces occur within a much shallower depth than the linear elastic theory predicts,
- (2) this phenomenon appears to be characteristic of all cohesive soils and is not peculiar to fissured soils; and
- (3) the SNiP solution, more accurately predicts the deformation characteristics of the soil.

The limiting depth of deformation is a characteristic of all soils. An approximation of the maximum depth of deformation, based on the observations presented in Plate 6.15, would be between depth ratios,  $z/R = 5$  and  $6$ . This limiting depth and the distribution of deformation can primarily be explained in terms of the non-linearity of the deformation response of the soil. The effects of anisotropy and non-homogeneity are considered insignificant for the data being discussed here. }

#### 6.4.2 Effect of Non-Linear Deformation Response

With regard to the deformation response of this soil, it has been established that the deformation characteristics do not represent a medium with linear elastic modulus. The presentation of the function of modulus,  $f(M)$ , for certain vertical plate tests in relation to bearing pressure ratio in Plate 6.4 illustrates the variation in deformation response with bearing pressure ratio. The significant observation from these curves is that at lower pressure levels, between zero and  $0.1q_u$ , the value of  $f(M)$  decreases significantly with increasing bearing pressure ratio. At higher pressure ratios, between  $0.1$  and  $0.5$ , the reduction in  $f(M)$  with increasing pressure appears less significant.

To analyse the effect of this non-linearity of  $f(M)$  it is interesting to study the distribution of the resultant vertical stress, with depth, below a loaded surface. As discussed in Chapter 3, the vertical stress distribution is not significantly affected by non-linearity (Morgenstern and Tamuly Phukan, 1968; and Huang, (1968)). However, Morgenstern et al., indicated that the horizontal stresses are significantly affected, as will be discussed later.

The resultant vertical stress is defined by Jumikis (1973) as:

$$\bar{\sigma}_v = \sigma_z - \frac{2}{m} \sigma_{x=y} \quad (6.1)$$

Where:

$\sigma_z$  = the vertical stress

\*  $\sigma_{x=y}$  = the horizontal stress

and  $m$  = Poisson's No.

Hence, the distribution of both the vertical and the horizontal stresses with depth must be known. The resultant vertical stress can be considered to represent the effective vertical stress which produces a deformation in the soil. This resultant vertical stress, which incorporates the Poisson's effect, should always be considered in analysing in-situ deformations.

The distribution of the resultant vertical stress with depth in a linear elastic medium is presented in Plate 6.17 for values of Poisson's No. of 2, 2.5, and 3 (i.e.,  $\mu = 0.5, 0.4,$  and  $0.33$  respectively). This resultant vertical stress increases considerably, especially for the case where Poisson's No. is 2 ( $\mu = 0.5$ ), to a depth of about  $1R$  and then decreases gradually to zero at  $z/R = \infty$ . While this solution by Jumikis (1973) is based on linear elastic theory, it can provide an insight into the variation of deformation modulus with depth in a non-linear soil.

The effect of non-linearity on the distribution of center-line stresses below a loaded surface, as presented by Morgenstern and Tamuly Phukan (1968), should be considered at this stage. Although this reference considers a strip load, the effect of non-linearity on the stresses is illustrative. The vertical stresses were shown to be affected negligibly but the horizontal stresses were significantly affected. For the bi-linear form of deformation response considered, the horizontal stresses were lower (about 85%) than the linear solution between depths of zero and  $1B$  (where  $B$  is the width of the strip footing). At a depth of  $2B$ , the horizontal stress is very much greater (208%) than for the linear solution. With reference to Equation 6.1 it is obvious that the effect on the horizontal stresses will

influence the value of the resultant vertical stress, as given by Jumikis (1973), in the following manner:

- When the horizontal stresses are less than that for the linear solution the value of  $\bar{\sigma}_v$  will be greater, and
- When the horizontal stresses are greater than the linear solution the value of  $\bar{\sigma}_v$  will be less.

#### 6.4.3 Distribution of Modulus of Deformation with Depth in a Non-Linear Soil

The variation of  $f(M)$  with applied bearing pressure ratio, as presented in Plate 6.4, represents the non-linearity of the soil at the site being studied. In order to illustrate how this non-linearity affects the distribution of the modulus of deformation with depth below the loaded surface, the form of the non-linear response of Test V2/2, has been chosen as typical for this soil. The non-linearity exhibited by this test can be used to determine the distribution of modulus with depth for the case of a rigid circular load equal to one-third of the ultimate strength of the soil. The linear elastic solution (Jumikis, 1973) is used. A value for Poisson's No. of 2.5 (i.e.  $\mu = 0.4$ ) has been chosen as representative for this soil, as suggested by Bozozuk (1963).

The values of  $f(M)$  presented for Test V2/2 in Plate 6.4 are by definition given as:

$$f(M) = \frac{\pi R q}{\rho} \quad (2.7)$$

The presentation of Equation 2.7 in terms of  $q$ , is primarily to make the solution more readily useable. The solutions for the modulus of deformation, as presented by Fischer (1965) and Jumikis (1973), actually consider the contact pressures at the surface of a linear elastic medium. The theoretical vertical center-line contact stress is, for instance, equal to  $0.5q$  and the horizontal stress at the surface is  $0.45q$  (for  $m = 2.5$ ). From Equation 6.1, the resultant vertical stress at the surface is equal to  $0.14q$ .

The presentation of  $f(M)$  versus applied bearing pressure ratio on Plate 6.4 can be transformed into a presentation of the function of modulus versus the resultant vertical stress ratio by the following conversions:

$$f(M)' = \frac{\pi R \bar{\sigma}_v}{\rho} = 0.14 f(M) \quad (6.2)$$

and  $\bar{\sigma}_v = 0.14 q$

The results of Test V2/2 have been replotted in this form in Plate 6.18. This variation of  $f(M)$  with the resultant vertical stress ratio can now be directly related to the variation of  $\bar{\sigma}_v$  with depth below the surface. Using linear elastic distribution of  $\bar{\sigma}_v$  with depth, the distribution of  $f(M)$  with depth, is presented in Plate 6.19 for a Poisson's No. of 2.5 ( $\nu = 0.4$ ). This distribution of  $f(M)$  with depth represents the distribution of the modulus of deformation with depth.

This distribution of  $f(M)$  with depth can be used to determine the distribution of deformation with depth. The linear elastic solution for deformations (Jumikis, 1973):

$$\rho = \frac{\pi Rq}{E} \frac{1}{2\pi} \left(\frac{1+m}{m}\right) \left[ 2 \left(\frac{m-1}{m}\right) \left(\frac{\pi}{2} - \alpha\right) - \sin\alpha \cos\alpha \right] \quad (3.4b)$$

is used. This equation can be rewritten as:

$$\rho = \frac{\pi Rq}{E} x f(\alpha) \quad (3.4a)$$

$$\text{where: } f(\alpha) = \frac{1}{2\pi} \left(\frac{1+m}{m}\right) \left[ 2 \left(\frac{m-1}{m}\right) \left(\frac{\pi}{2} - \alpha\right) - \sin\alpha \cos\alpha \right] \quad (6.3)$$

This  $f(\alpha)$  is the deformation influence value.

Values of  $f(\alpha)$  are given in tables for several values of Poisson's No.,  $m$ , in Jumikis (1973). These tables permit the calculation of deformations of a layered system by means of the following expressions:

$$\rho = \Delta\rho_1 + \Delta\rho_2 + \Delta\rho_3 + \dots + \Delta\rho_n \quad (6.4a)$$

$$= \pi Rq \left[ \frac{f(\alpha)_1}{E_1} + \frac{f(\alpha)_2 - f(\alpha)_1}{E_2} + \frac{f(\alpha)_3 - f(\alpha)_2}{E_3} + \dots + \frac{f(\alpha)_n - f(\alpha)_{n-1}}{E_n} \right] \quad (6.4b)$$

$$= \sum_1^n (\Delta\rho) = \sum_1^n \left[ (\pi Rq) \cdot \frac{\Delta(f\alpha)}{E} \right] \quad (6.4)$$

where:  $n$  = the number of layers.

By calculating the deformations in each layer of a multilayer system the distribution of deformation can be obtained by summation. The distribution of deformation with depth has been calculated for the chosen non-linear example using a 25-linear system to represent the non-linearity, as shown on Plate 6.19. The calculated distribution of deformation for a Poisson's No. of 2.5 has been plotted on Plate 6.20.

Also shown on Plate 6.20 are the observed distribution of deformation for Test V2/2 (for  $q/q_u = 0.3$ ) and the averages for all the plate tests and the footing test. The calculated distribution of deformation is in close agreement with the observed results and actually overestimates the deformation at the shallower depths. However, the main point to be observed is that this analysis, based on the non-linear deformation response predicts the observed deformations much more accurately than the linear elastic theory.

This distribution of deformation with depth has been obtained by means of the linear elastic solutions for both the distribution of the resultant vertical stress and the deformation influence values. Referring to the effect of non-linearity on the horizontal stresses, presented by Morgenstern and Tamuly Phukan (1968), the value of  $\bar{\sigma}_v$  appears to be slightly greater between depths of zero to  $2R$ , (due to the lower horizontal stresses) while at greater depths the value of  $\bar{\sigma}_v$  would be considerably reduced (due to the greater horizontal stresses). It can be assumed that the effect of these changes in  $\bar{\sigma}_v$  would decrease the modulus of deformation within the shallower depths and increase the modulus at greater depths.

Therefore, the variation in the modulus of deformation with depth would probably be even more significant than

that shown in Plate 6.19. As a result, the distribution of deformation would likely be more concentrated within shallower depths. Since the calculated deformations, based on linear elastic theory seem to over-estimate the deformations at shallower depths a higher value of Poisson's No. (i.e. lower  $\mu$ ) might be more representative for this soil.

The same analysis has been carried out for a value of Poisson's No. = 3 ( $\mu = 0.33$ ). The resulting distribution of deformation for this analysis is also shown on Plate 6.20. In this case the effect of the non-linearity is less significant (compare with Plate 6.17). However, when the possible effect of non-linearity on the resultant vertical stress is considered the calculated distribution of deformation might be closer to the observed case. At any rate it appears that non-linearity can explain the deformation characteristics, although a theoretical solution is required to establish the effect of non-linearity on the resultant vertical stress and deformations.

#### 6.5 OTHER FACTORS INFLUENCING DEFORMATION CHARACTERISTICS

While the effect of non-linearity of soil deformation response can explain the observed deformation characteristics of soil two other common properties of soil could have some influence in specific extreme cases.

### 6.5.1 Effect of Non-Homogeneity on the Distribution of Deformation with Depth

Most soil deposits exhibit some degree of non-homogeneity with depth. However, it can be shown from Carrier and Christian (1973) and Brown and Gibson (1972) that except for soils with extreme non-homogeneity the effect on deformations is negligible. Carrier and Christian show that for quite extreme cases of increasing modulus with depth the vertical and horizontal stresses are significantly increased; however, such cases of non-homogeneity are not common (at least relative to increasing strength with depth) and are beyond the scope of this thesis. Therefore the conclusion is that non-homogeneity, of the order shown on Plate 6.3 for example has no significance on the distribution of deformation with depth observed in this study or published in the literature.

### 6.5.2 Effect of Anisotropy on the Distribution of Deformation with Depth

Unfortunately there is no solution available in the literature which presents the distribution of the stresses within an anisotropic half space. However, the analysis presented by Milovic (1970) for an anisotropic medium underlain by a rigid base, indicates that for anisotropy ( $E_H/E_V$ ) greater than unity, the resultant vertical stresses would generally be less than the isotropic case and vice versa.

However, the effects of anisotropy on the distribution of the resultant vertical stress with depth is not significant, and hence anisotropy should not influence the distribution of deformation with depth.

## 6.6 MODELLING A NON-LINEAR MEDIUM FOR ANALYTICAL SOLUTION

This section summarises some of the pertinent discussions and contributions in this thesis and makes some suggestions for measuring and representing the non-linearity of soils.

### 6.6.1 Measurement of Modulus and Its Non-Linearity

The measurement of the modulus of deformation of soil and its non-linearity with respect to stress level is in itself a relatively simple task. The major problem is to decide what type of test will best represent the required foundation performance. In any tests on soil the stress-strain or the pressure-deformation response is dependent on the test type (i.e. stress or strain controlled; drained or undrained; etc.). The discussion in Section 2.2 was intended to provoke some serious thought on the effectiveness of any particular test type to represent the real "immediate" or end of construction deformation. In many cases it has been considered that the immediate deformation is the same as the end of construction deformation. Since immediate

deformation is, by definition, due to undrained displacement, predictions are generally based on undrained tests. Hence, they can not properly represent most actual foundation deformations at the end of construction. In most building foundation situations the actual load is applied so slowly that the soil behaves in a drained manner. Therefore, even for foundations which apply a pressure less than the preconsolidation pressure, a drained modulus test is more representative.

The use of laboratory tests has been discredited in Section 2.2, primarily from the point of view of sample disturbance; definition and reproduction of in-situ stresses; representativeness of test methods and representativeness of such small scale tests. However, if good samples can be obtained it is probably worth the effort to carry out drained tests. It should be remembered that the in-situ horizontal stresses will vary with the level of applied vertical stress and also the value of Poisson's ratio. Hence, a constant cell pressure is probably not valid.

Drained tests on clay soils take a considerable length of time to perform; but for realistic representation of the actual foundation situation they should be given serious consideration. These tests should be strained at

a sufficiently slow rate so that no excess pore pressures are developed. Even this type of test will load the soil much faster than in the real foundation case but it would be much more representative.

A drained test performed in this manner would provide both the modulus of deformation and the degree of non-linearity of the modulus, suitable for a non-linear analytical solution for soil deformations. This analysis would represent the end of construction deformation. For an indication of long term, time dependent deformations the maximum design stresses should be maintained on the sample until a long term deformation pattern is established.

Until a non-linear solution is available, a solution can be approximated by a method similar to that presented in Section 6.4.3. Alternatively, and as a minimum, the prediction of foundation deformations should consider the finite depth of deformation according to the method summarised later.

With reference to the common practise of using cyclic undrained tests to determine the modulus of deformation of the soil this method has to be discredited on the grounds of

incompatible drainage conditions. However, if this method is to be used to predict end of construction deformation predictions can be significantly improved by considering the actual depth of soil being deformed, as presented below. No representation of non-linearity can be incorporated in these predictions.

The measurement of the modulus of deformation and its non-linearity by in-situ load bearing tests is to be preferred over all types of laboratory tests. In-situ tests should also be drained tests and as such could take quite long to perform and be expensive. While it may not be possible to carry out such a test for a particular engineering problem, it should be seriously considered as a research topic. Ideally an in-situ test should be loaded, sufficiently slowly to prevent excess pore pressures, to a realistic bearing pressure (say  $1/3 q_u$ ) and this maximum pressure should be maintained for a sufficient length of time to establish the long term dependent response. The initial portion of this test will provide the non-linear pressure versus deformation response from which the non-linear modulus variation can be obtained.

Any in-situ test should also measure the distribution of deformation with depth at points equidistant from and close to the centre of the loaded area. The depth range

of measurement should extend to at least 3 times the width of the loaded area. The modulus should be calculated from the observed data by taking into consideration the actual depth of soil being deformed using the expression:

$$E = \frac{\pi Rq}{\rho} \times f(\alpha)_H \quad (6.5)$$

where  $f(\alpha)_H$  = the deformation factor, equals the value of  $f(\alpha)$  (Fischer, 1965) at the limiting depth of deformation (= S, in Jumikis, 1973).

This method of calculating the modulus from in-situ plate on footing tests should be used in all cases. Even if the finite depth of deformation is not observed it should be estimated. A method for estimating the limiting depth of deformation was presented in Section 2.3 and is given as:

$$\sigma_{z=H} = \alpha \gamma H \quad (2.4)$$

The value of  $\alpha$  used in Russian practise varies between 0.1 and 0.5 (Stefanoff and Krastilov, 1973). More field observations are required to relate this to soil type and some suggested values are presented in Section 2.3, and on Page 3.14.

As an example, the above expression is presented graphically in Plate 6.21, for the case of the test footing and with values of  $\alpha$  ranging from 0.1 to 0.5. The vertical stress distribution shown is given by Jumikis (1973). It can be seen that the prediction of the limiting depth of deformation varies considerably with the choice of  $\alpha$ . The position of the water table and the density of the soil is also important.

Extrapolation of the observed distribution of deformation with depth for the test footing indicates the limiting depth of deformation is  $5.4R'$ . This depth coincides with an  $\alpha$ -value of 0.1 in Plate 6.21. While the purpose of presenting Plate 6.21 is simply to illustrate the use of Equation 2.4 it is interesting to note that the test footing results indicate the maximum depth of deformation (i.e. lowest  $\alpha$ ) suggested by Stefanoff and Krastilov (1973).

If the limiting depth is not observed or there is no rational basis for the estimation of this depth (Equation 2.4) it is proposed that a general limiting depth of 3 times the width of the loaded area be used in all foundation analyses. Hence, the value of the deformation factor,

$f(\alpha)_{H=6}$  (Eqn. 6.5) should be the maximum value used in all analyses whether for obtaining the modulus from in-situ tests or for predicting in-situ deformations using laboratory moduli.

As an illustration of the effect of the limiting depth of deformation the values of the deformation factor,  $f(\alpha)_H$  (Fischer, 1965) (=S, Jumikis, 1973) are presented for depths of deformation of 4R, 5R and 6R and for various values of Poisson's Ratio in Plate 6.22. The values for an infinite depth of deformation (classic elastic theory) are also shown. It is interesting to compare, for example, the modulus for a limiting depth of deformation of 5R to that for the infinite depth of deformation (for  $\mu = 0.33$ ). It is found that for the limited case the modulus is 78% of that for the infinite case.

The implication here is that if the laboratory measured moduli, presented in the literature and discussed in Section 2.2, had been analysed by Equation 6.5 (with the maximum value of  $f(\alpha)_{H=6}$ ) the resulting predicted deformations might not have over-estimated the observed deformations by so much. This observation supports the use of Equation 6.5 for all foundation analysis.

The above discussion has presented suggestions for measuring the modulus of deformation in the laboratory and by in-situ load bearing tests. The results of these tests should provide the necessary input for any non-linear analytical solution for soil deformations. Some alternative improvements to existing practise are suggested for use in foundation analysis until a non-linear solution is available.

#### 6.6.2 Representation of Non-Linearity

It is expected that the simplest approach to a non-linear solution is to use the method of successive approximations (as in Huang, 1968) though a two dimensional finite element solution would be more desirable. Whatever the form of the solution it should be possible to represent the non-linearity of soil deformation response by either stress-strain, pressure-deformation or pressure-modulus relationships. If the limiting depth of deformation is observed or reasonably estimated for in-situ tests the non-linearity can be represented as a pressure versus strain relationship (as in Soderman, Kim and Milligan, 1968).

Although the tests presented in this thesis do not indicate that a hyperbolic relationship between pressure and deformation (Kondner and Krizek, 1962) is really valid for this fissured soil, it is likely that for intact, homogeneous and isotropic soils this relationship would be more

valid. It is suggested that this two-constant hyperbolic relationship proposed by Kondner and Krizek could be used in a non-linear analysis. Some other representations are discussed by Chin (1969) and Huang (1968). Hence, once the degree of non-linearity has been established, representation does not appear to be a problem for the purposes of analysis.

The value of Poisson's Ratio will have to be considered as this affects the horizontal stresses and possibly even the vertical stresses. In the ideal elastic theory the vertical stresses are independent of  $\mu$  but in the non-homogeneous elastic solution by Carrier and Christian (1973) the vertical stress are dependent on  $\mu$ . In view of the effect of  $\mu$  on some stresses and the deformation, at least a realistic constant value for  $\mu$  should be used though it is not necessarily true that  $\mu$  remains constant. More research is required into this parameter and its value under different conditons.

## CHAPTER 7

CONCLUSIONS AND RECOMMENDATIONS7.1 CONCLUSIONS7.1.1 Variation of Modulus of Deformation with Depth

The vertical modulus of deformation varies with depth through the crust but not very significantly. The variation of modulus with depth can be related to the effects of desiccation. Closest to the surface the extreme fissuring results in a relatively low modulus; at intermediate depth (in the crust) the soil is more intact and still quite hard due to desiccation resulting in a relatively higher modulus; and at the base of the crust the soil is quite intact but significantly softer resulting in a lower modulus.

It is not considered that the variation in modulus with depth is significant enough to explain the observed distribution of deformation under the test footing and certainly under the plate tests with their smaller depth of influence.

The observed variation of deformation with depth is interesting when considered with regard to the concept of a constant relationship between modulus and shear strength ( $E/c$ ). Due to the effects of desiccation the strength of the soil is considerably higher in the upper levels of the crust suggesting a considerably higher modulus but because of extreme desiccation (fissuring) the modulus is in fact much lower than expected by the constant  $E/c$  concept.

At greater depth in the crust the observed modulus does increase but is still partially affected by fissuring. The concept of a constraint  $E/c$  relationship is probably only valid for an intact, homogeneous clay deposit. This concept is based on continuum mechanics and is therefore invalidated by the occurrence of fissures.

#### 7.1.2 Distribution of Deformation Below the Loaded Surface

The observed distribution of deformation below the vertical plate tests is confined within a finite depth and is in close agreement with the footing test results. The effects of desiccation and fissuring does not appear to influence the distribution of deformation for these tests.

The observed distributions of deformation at this site are also in close agreement with other reported results in the literature. Deformations in soils are generally confined within a finite depth relative to the infinite depth assumed in the classic, ideal elastic theory. Deformations in clay soils are confined within a depth of 4 to 6 Radii, depending on applied pressure, strength and density. This fact has been recognised in Russian practice and is considered in their foundation analyses and designs.

The results of this study, combined with other published data, discredits the classic, ideal elastic theory sufficiently to suggest the necessity to reconsider its use in foundation analyses.

#### 7.1.3 Explanation of Deformation Characteristics

It is clearly evident that soil does not behave according to the classic, linear elastic theory. While this has been recognised as a problem for some time, the results of this study illustrating a finite depth of deformation, indicate a more important limitation to the linear elastic theory. A theoretical review of some of the major factors influencing soil deformation indicates that the non-linearity of soil deformation response can explain the finite

depth within which deformation occurs.

Soil deformation response is non-linear. Consideration of the non-linearity of soil deformation response with respect to the distribution of stress with depth below a loaded surface provides an explanation for the distribution of deformation with depth below the surface.

The distribution of the resultant vertical stress (the stress responsible for deformations) with depth is such that it increases significantly to a maximum value between the surface and a depth of about 1 Radii and below that level it decreases gradually. The non-linearity of soil deformation response is such that soil is more deformable at greater stress levels. Therefore, the fact that the stresses below a loaded surface are considerably greater at a relatively shallow depth (one Radii) than at the surface and at much greater depth, suggests that a large percentage of the deformation will occur at this relatively shallow depth. It is therefore concluded that all of the distributions of deformation presented in this thesis can be explained in terms of the non-linearity of soil deformation response.

The theoretical effect of other major influences on soil deformation response have been reviewed and it is concluded that non-homogeneity (except in extreme cases) should not significantly affect the distribution of deformation. Similarly the effect of anisotropy should not affect the distribution of deformation though the total deformations may be affected significantly.

It is evident that a general solution for rigid loads applied to a non-linear medium is required and this thesis should suggest a possible approach to such a solution.

#### 7.1.4 Suggestions for Measuring and Representing Non-Linearity

It is evident that the end of construction deformation of actual foundations can not be represented by undrained tests due to incompatible drainage situations. Therefore, drained tests should be used to measure the modulus of deformation and its non-linearity whether in the laboratory by in-situ load bearing tests. An improved method for obtaining the modulus of deformation from in-situ tests, which considers the depth of soil being deformed, is suggested. This method is also recommended for predicting deformations from laboratory moduli until a non-linear solution is available.

Actual representation of the non-linearity of soil deformation response can probably be expressed in terms of stress-strain or pressure-modulus relationships. The proposed two constant hyperbolic relationship (Kondner and Krizek, 1962) between stress and strain or pressure and deformation may be suitable. The value of Poisson's Ratio is likely to have a considerable effect on the solution of non-linear deformation response.

#### 7.1.5 Some Conclusions Specifically Relevant to This Study

Based on the actual test results and the analysis and interpretation of these results the following conclusions are made in order of consideration:

The distribution of fissures relative to the size of loaded area and the position and orientation of major fissure surfaces is considered to be the cause of tilting of the plates.

The use of a rigid connection between the loading system and the plate did not effectively reduce the degree of tilting.

Estimation of the undisturbed in-situ horizontal stresses is difficult in a fissured soil.  $K_0$  values

for the intact blocks of clay are misleading and almost meaningless in a deformation study.

Initial seating pressures for horizontal plate tests in the fissured crust should consider the effects of desiccation and the fissures. The soil macrostructure is probably "under-consolidated" due to the effects of shrinkage. Only the microstructure (i.e. the intact blocks of clay) is over-consolidated due to desiccation.

The horizontal plate tests performed in this study are not representative due to the high initial seating pressures applied.

No major differences were observed in the soil deformation response for the three loading procedures used. The Procedure 3 tests exhibited a linear to concave pressure-deformation response at the low pressure levels.

The most reliable method for estimating the ultimate failure pressure for the plate tests is by extrapolation of the pressure-deformation response. Methods proposed by Mitchell, Sangrey and Webb, (1972) and Kondner and Krizek (1962) were not successful.

The ratio of recoverable deformation to total deformation varies erratically with pressure level and interpretation is difficult. The values for the horizontal tests are not representative.

The variation in the pressure-deformation response for tests performed at the same depth is attributed to non-homogeneity (varying degrees of fissuring and orientation of fissure surfaces).

The close agreement between the vertical and horizontal pressure-deformation responses at the two depths of comparison is not representative. Considerable deformations would have occurred under the high seating pressures applied in the horizontal tests.

The effect of the fissures, primarily on horizontal tests, is expected to cause a varying degree of anisotropy with pressure level. Horizontal tests would be difficult to relate to vertical loading situations for foundation design purposes.

## 7.2 RECOMMENDATIONS

The following are some topics recommended for study and analysis:

A non-linear elastic solution for soil deformation response is required for rigid loads.

The use of drained stress-strain and pressure-deformation tests for modulus determination should be studied with regard to end of construction deformation predictions. The limiting depth of deformation should be considered.

A study of different rates of loading of in-situ load bearing tests should be undertaken with measurement of pore pressures. This could result in a relationship which permitted extrapolation to the fully drained situation.

More information is required on the effect of size of loaded area. A relationship between deformation and size of loaded area, for a given pressure, is required to permit extrapolation to a full scale foundation.

In-situ observations are required of the distribution of stresses within a soil medium. Studies observing stress distributions should be supported

by in-situ measurements of non-homogeneity, anisotropy and non-linearity.

Detailed observations of the distribution of deformation with depth are required for all soil types. These observations should be made for in-situ tests and also under actual foundations. Observations should be made to a depth of at least 6 Radii (or three widths). All studies of deformation characteristics should be supported by measurements of non-homogeneity, anisotropy and non-linearity.

## LIST OF REFERENCES

- Alderman, J.K. (1957)  
Discussion. Proc. 4th ICSMFE, 3:5:16
- Barden, L. (1963)  
"Stresses and Displacements in a Cross-Anisotropic Soil." Geotechnique 13:3:198-210.
- Bauer, G.E. (1967)  
"A Critical Evaluation of a Vibrating-Wire Pressure Transducer." Bautechnik 8:12:19.
- Bauer, G.E. Scott, J.D. and Shields, D.H. (1973)  
"The Deformation Properties of a Clay Crust."  
Proc. 8th ICSMFE. 1:31-38.
- Bauer, G.E. Shields, D.H. McRostie, G.C. and Scott, J.D. (1976)  
"Predicted and Observed Footing Settlements in a Fissured Clay" (In Press).
- Borowicka, H. (1936)  
"Influence of Rigidity of a Circular Foundation Slab on the Distribution of Pressures Over the Contact Surface". Proc. 1st ICSMFE, 2:144-149.
- Bozozuk, M. (1963)  
"The Modulus of Elasticity of Leda Clay from Field Measurements." Can. Geot. Journal 1:1:43-51.

Bozozuk, M. (1968)

"The Spiral Foot Settlement Gauge". Can. Geot. Journal 5:2:123-125.

Brown, P.T. and Gibson, R.E. (1972)

"Surface Settlements of a Deep Elastic Stratum Whose Modulus Increases Linearly with Depth." Can. Geot. Journal, 9:4:467-476.

Burmister, D.M. (1956)

"Stress and Displacement Characteristics of a Two-Layer Rigid Base Soil System: Influence Diagrams and Practical Applications". Proc. Hwy. Res. Bd. (35) 773-814.

Burmister, D.M. (1962)

"Prototype Load-Bearing Tests for Foundations of Structures and Pavements." Proc. ASTM, STP 322, 98-119.

Carrier III, W.D. and Christian, J.T. (1973)

"Rigid Circular Plate Resting on a Non-homogeneous Elastic Half-Space." Geotechnique 23:1:67-84.

Chin, F.K. (1969)

"Size and Load Effect on Settlement of Footings in Clay." Proc. 7th ICSMFE, 53-57.

Coates, D.F. and McRostie, G.C. (1963)

"Some Deficiencies in Testing Leda Clay." Proc.  
ASTM, STP 361, 459-470.

Crawford, C.B. (1963)

"Cohesion in an Undisturbed Sensitive Clay."  
Geotechnique 13:132-146.

Crawford, C.B. and Burn, K.N. (1962)

"Settlement Studies on the Mt. Sinai Hospital,  
Toronto." The Engineering Journal, December, 1962.

Crawford, C.B. and Eden, W.J. (1965)

"A Comparison of Laboratory Results with In-situ  
Properties of Leda Clay." Proc. 6th ICSMFE 1:31-35.

D'Appolonia, D.J. and Lambe, T.W. (1970)

"Method for Predicting Initial Settlement." ASCE,  
JSMFD 96:SM2:523-544.

D'Appolonia, D.J., Poulos, H.G. and Ladd, C.C. (1970)

"Initial Settlement of Structures on Clay." ASCE,  
JSMFD 97:SM10:1359-1377.

Dawson, J.W. (1893)

The Canadian Ice Age. Geological Survey of Canada.

DeJong, J. and Harris, M.C. (1971)

"Settlements of Two Multistory Buildings in Edmonton."  
Can. Geot. Journal 8:2:217-235.

Eden, W.J. (1960)

"Field Studies on the Consolidation Properties of  
Leda Clay." Proc. Fourteenth Canadian Soil Mechanics  
Conference, 107.

Egorov, K.E., Kuzmin, P.G. and Popov, B.P. (1957)

"The Observed Settlements of Buildings as Compared with Preliminary Calculation."

Fischer, K. (1965)

Beispiele zur Bodenmechanik. Aufsätze mit Formeln, Tafeln und Schaubildern. Verlag von Wilhelm Ernst and Sohn, Berlin.

Gadd, N.R. (1962)

"Surficial Geology of Ottawa Map-Area, Ottawa and Quebec." Paper 62-16, Geological Survey of Canada.

Gaury, Y. (1970)

"Etude du Tassement Immédiat d'une Semelle Carree Reposant sur une Argile Sensible." M.A.Sc. Thesis, University of Ottawa, Ottawa (unpublished).

Giroud, J.P. (1972)

Mécanique des Sols: Tables pour le Calcul des Fondations. Tome 1. Tassement. Dunod, Paris.

Hanna, T.H. (1965)

Discussion. Can. Geot. Journal 11:2:129-131.

Huang, Y.H. (1968)

"Stresses and Displacements in Nonlinear Soil Media." ASCE, JSMFD, 94:SM1:1-19.

Johnston, W.A. (1917)

"Pleistocene and Recent Deposits in the Vicinity of Ottawa, with a Description of the Soils." Geological Survey of Canada, Mem. 101.

Jumikis, A.R. (1973)

Settlement Tables for Centrally Loaded, Rigid  
Circular Footings on Multilayered Systems. Eng.  
Res. Bull. No. 54, Rutgers University, New Jersey.

Karrow, P.F. (1961)

The Champlain Sea and Its Sediments. in: Soils in  
Canada, Edited by R.F. Leggett; University of  
Toronto Press; Royal Society of Canada.

Kenney, T.C. (1964)

"Sea Level Movements and Geological Histories of  
the Post-Glacial Marine Soils at Boston, Nicolet,  
Ottawa and Oslo." Geotechnique 14:3:203.

Klohn, E.J. (1965)

"The Elastic Properties of a Dense Glacial Till  
Deposit." Can. Geot. Journal 11:2:116-128.

Kondner, R.L. and Krizek, R.J. (1962)

"Correlation of Load Bearing Tests on Soils." Hwy.  
Res. Bd. Proc. 41, 557-584.

Krizek, R.J. and Corotis, R.B. (1973)

"Synthesis of Soil Moduli Determined from Different  
Types of Laboratory and Field Tests." ASCE Specialty  
Conference on In Situ Measurement of Soil Properties,  
North Carolina State University, Raleigh, N.C.  
1:225-240.

Ladd, C.C. (1964)

"Stress-Strain Modulus of Clay in Undisturbed Shear." ASCE, JSMFD, 90:SM5:103-132.

Lambe, T.W. (1964)

"Methods of Estimating Settlement." ASCE, JSMFD, 90:SM5:43-66.

Lo, K.Y., Seychuk, J.L. and Adams, J.I. (1971)

"A Study of the Deformation Characteristics of a Stiff Fissured Clay." ASTM, STP 483, 60-76.

LaRochelle, P. and Lefebvre, G. (1970)

"Sampling Disturbance in Champlain Clays." ASTM, STP 483, 143-163.

Malikova, T.A. (1972)

"Analysis of Natural Settlements of Slab and Box Foundations of Multistory Buildings." Soils and Foundations, No. 2 (Translated from Osnov. Fund. Mekh. Grunt. No. 2)

Marsland, A. and Eason, B.J. (1973)

"Measurement of Displacements in the Ground below Loaded Plates in Deep Boreholes." Soil Mech. Conf. on instrumentation, London, England, 304-317.

Milovic, D.M. (1970)

"Stresses and Displacements in an Anisotropic Medium due to a Circular Load." Proc. 2nd. Cong. Int. Soc. R.M., Belgrade, Theme 8, No. 11, 479-482.

Mitchell, R.J., Sangrey, D.A. and ~~Webb~~, G.S. (1972)

"Foundations in the Crust of Sensitive Clay Deposits." ASCE Conf. on Performance of Earth and Earth Supported Structures, Vol. 1, Pt. 2, 1051-1072.

Morgenstern, N.R. and Tamuly Phukan, A.L. (1968)

"Stresses and Displacements in a Homogeneous Non-Linear Foundation." Int. Symp. on R.M., Madrid, III: 7:313-320.

Poulos, H.G. and Davis, E.H. (1974)

Elastic Solutions for Soil and Rock Mechanics  
*John Wiley & Sons Inc.*, New York.

Raymond, G.P., Townsend, D.L. and Lojkasek, M.J. (1971)

"The Effect of Sampling on the Undrained Soil Properties of a Leda Soil." Can. Geot. Journal, 8:4:546-557.

Sangrey, D.A. and Townsend, D.L. (1969)

"Characteristics of Three Sensitive Canadian Clays." C.E. Research Report #63, Queen's University, Kingston, Canada.

Seed, H.B. (1965)

"Settlement Analyses, a Review of Theory and Testing Procedures." ASCE, JSMFD, 91:SM2: 39-48.

Shvets, V.B. and Kul'chitskii, G.B. (1970)

"Experimental Investigation of the Depth of Compressed Soil Foundation Stratum under a Plate." Soils and Foundations, No. 1 (Translated from Osnov. Fund. Mekh. Grunt. No. 1).

Skempton, A.W. (1954)

"The Pore Pressure Coefficients A and B." Geotechnique, 4:143-147.

Skempton, A.W. and Bjerrum, L. (1957)

"A Contribution to the Settlement Analysis of Foundations on Clay." Geotechnique, 7:4:168-178.

SNiP II-B.1-62

Bases of Buildings and Structures (in Russian), Gosstroizdat.

SNiP II-B.3-62

Bases of Hydraulic Structures (in Russian), Gosstroizdat.

Soderman, L.G., Kim, Y.D. and Milligan, V. (1968)

"Field and Laboratory Studies of Modulus of Elasticity of a Clay Till." Hwy. Res. Record, No. 243:1-11.

Stefanoff, G. and Krastilov, G. (1973)

"Evaluation of the Active Zone of Settlement." Proc. 8th ICSMFE, 2:4:249-251.

Sudhindra, R. and Khanfa, S.K. (1969)

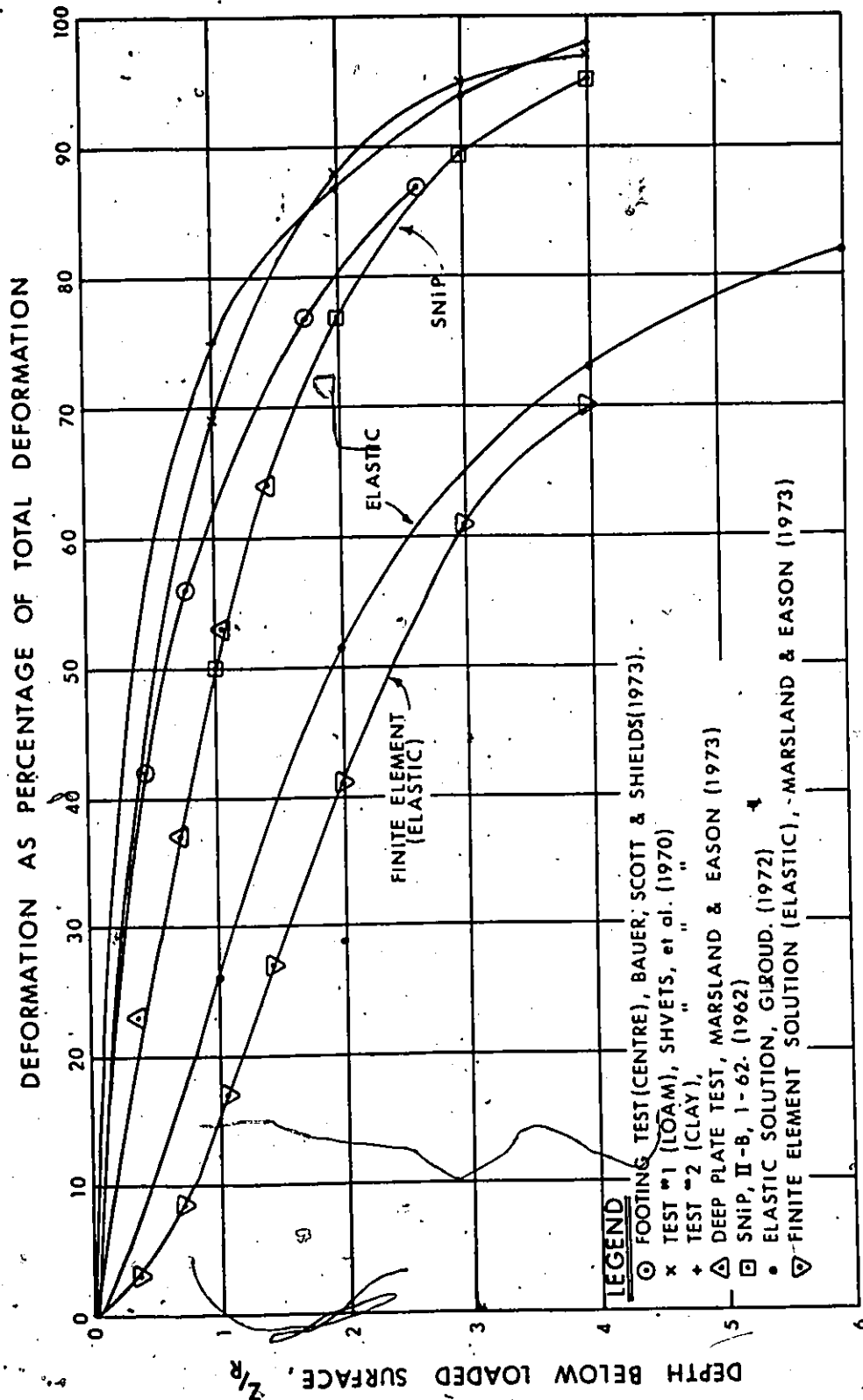
"Load Displacement Characteristics of Subgrade  
Soil." Journ. Indian Roads Congress, 32:2:241-259.

Townsend, D.L., Sangrey, D.A. and Walker, L.K. (1969)

"The Brittle Behavior of Naturally Cemented  
Soils." Proc. 7th ICSMFE, 1:411-417.

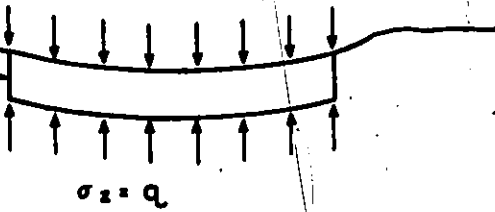
FOUNDATION SETTLEMENTS							
CASE No.	OBSERVED (cm)	THEORETICAL					
		SNIP II - B.1a - 62.		SNIP II - B.3 - 62.		Egorov (1958)	
		Predicted (cm)	Ratio Obs/Theor.	Predicted (cm)	Ratio Obs/Theor.	Predicted (cm)	
1	5.9	4.6	1.28	7.4	0.80	5.8	1.02
2	5.7	5.7	1.0	9.0	0.63	5.7	1.0
3	6.6	4.6	1.43	10.0	0.66	6.9	0.96
4	7.2	3.4	2.12	9.4	0.77	7.5	0.96
5	10.7	6.0	1.78	10.6	1.01	10.8	0.99
6	11.7	7.6	1.54	12.7	0.92	11.8	0.99
7	7.7	5.2	1.48	9.7	0.79	7.9	0.97
8	7.0	6.3	1.11	11.0	0.64	7.5	0.93
9	4.5	4.7	0.96	7.4	0.61	4.6	0.98
10	4.7	3.6	1.31	6.4	0.73	4.8	0.98
11	4.3	4.4	0.98	7.3	0.59	5.1	0.84
12	3.8	6.1	0.62	8.8	0.43	4.2	0.90
13	5.9	6.8	0.87	9.7	0.61	6.3	0.94
14	6.7	8.6	0.78	9.8	0.68	6.9	0.97
15	6.5	10.4	0.63	13.5	0.48	12.0	0.54
16	5.5	6.7	0.82	9.2	0.60	6.0	0.92
17	13.5	12.4	1.09	15.5	0.87	18.0	0.75
18	15.4	26.0	0.59	34.0	0.45	29.0	0.53
19	10.8	6.7	1.61	11.9	0.91	10.0	1.08
20	6.5	3.9	1.67	8.3	0.78	9.0	0.72
21	5.7	1.8	3.17	5.5	1.04	6.0	0.95
		Average	1.28	Average	0.71	Average	0.90
		Std. Deviation	0.59	Std. Deviation	0.17	Std. Deviation	0.14

TABLE 2.1 COMPARISON BETWEEN OBSERVED AND PREDICTED SETTLEMENTS FOR THREE RUSSIAN SOLUTIONS (compiled from: Malikova, 1972)

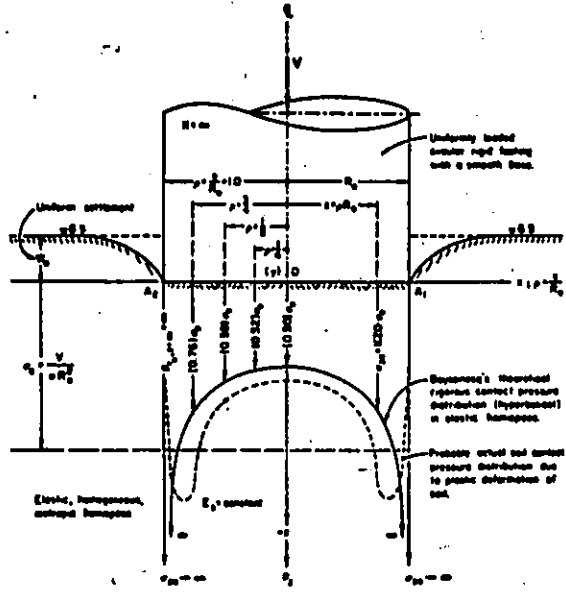


COMPARISON BETWEEN REPORTED DEFORMATION DISTRIBUTIONS AND: AN EMPIRICAL SOLUTION (SNIP); AN ELASTIC SOLUTION (GIROUD, 1972) AND A FINITE ELEMENT (ELASTIC) SOLUTION (MARSLAND & EASON, 1973).

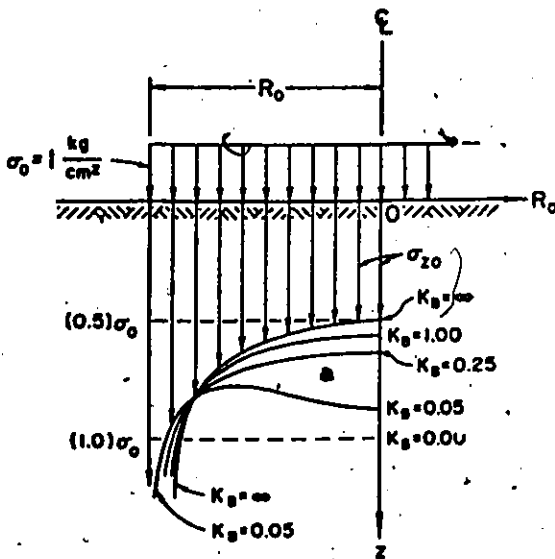
UNIFORMLY LOADED FLEXIBLE FOUNDATION



(a) Contact Pressure Under a Flexible Load



(b) Contact Pressure Under a Rigid Circle (Jumikis, 1973)



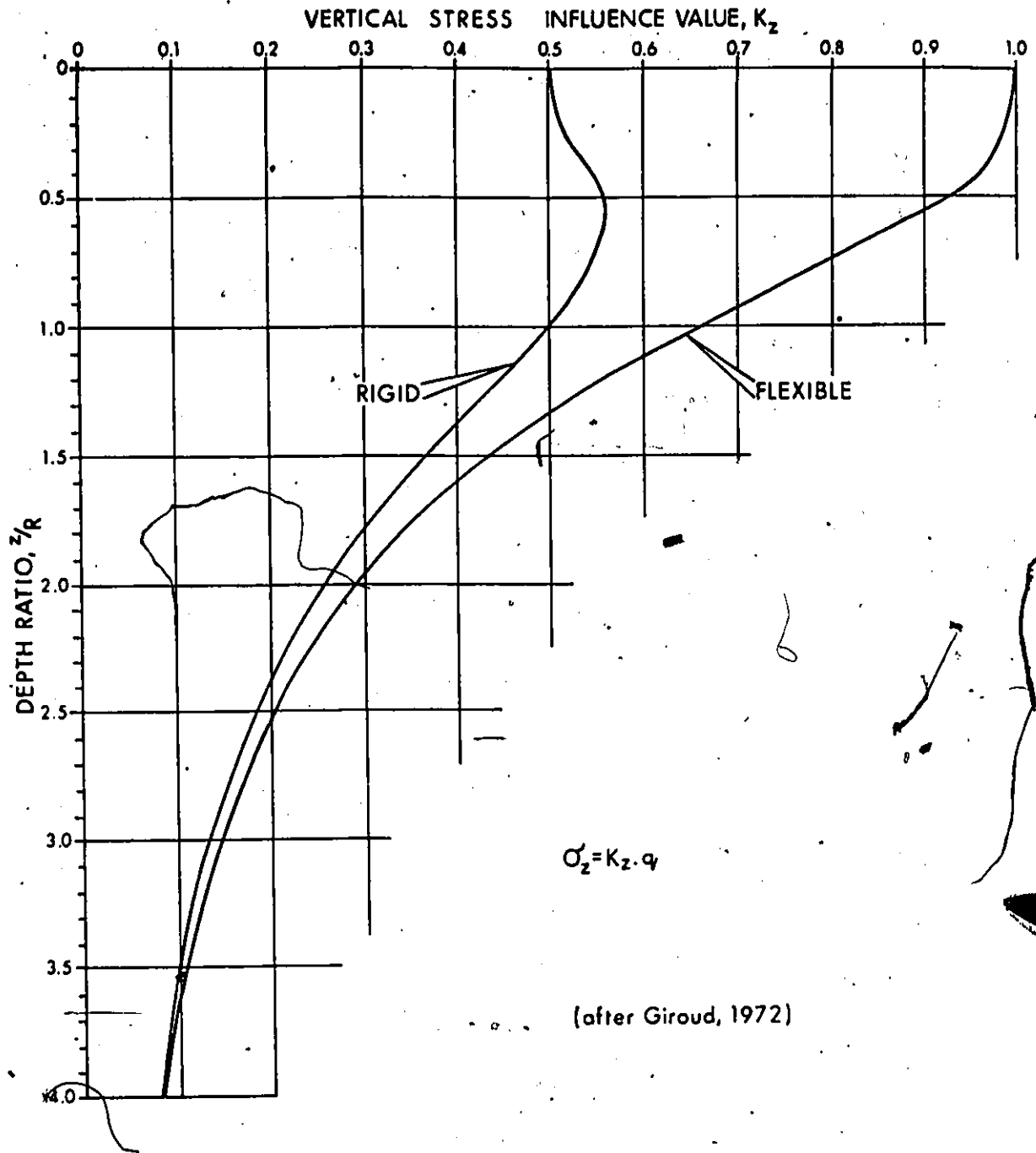
$$K_B = \left(\frac{1}{6}\right) \left(\frac{m_s^2 - 1}{m_f^2 - 1}\right) \left(\frac{m_f^2}{m_s^2}\right) \left(\frac{E_f}{E_s}\right) \left(\frac{d}{R_0}\right)^3$$

where

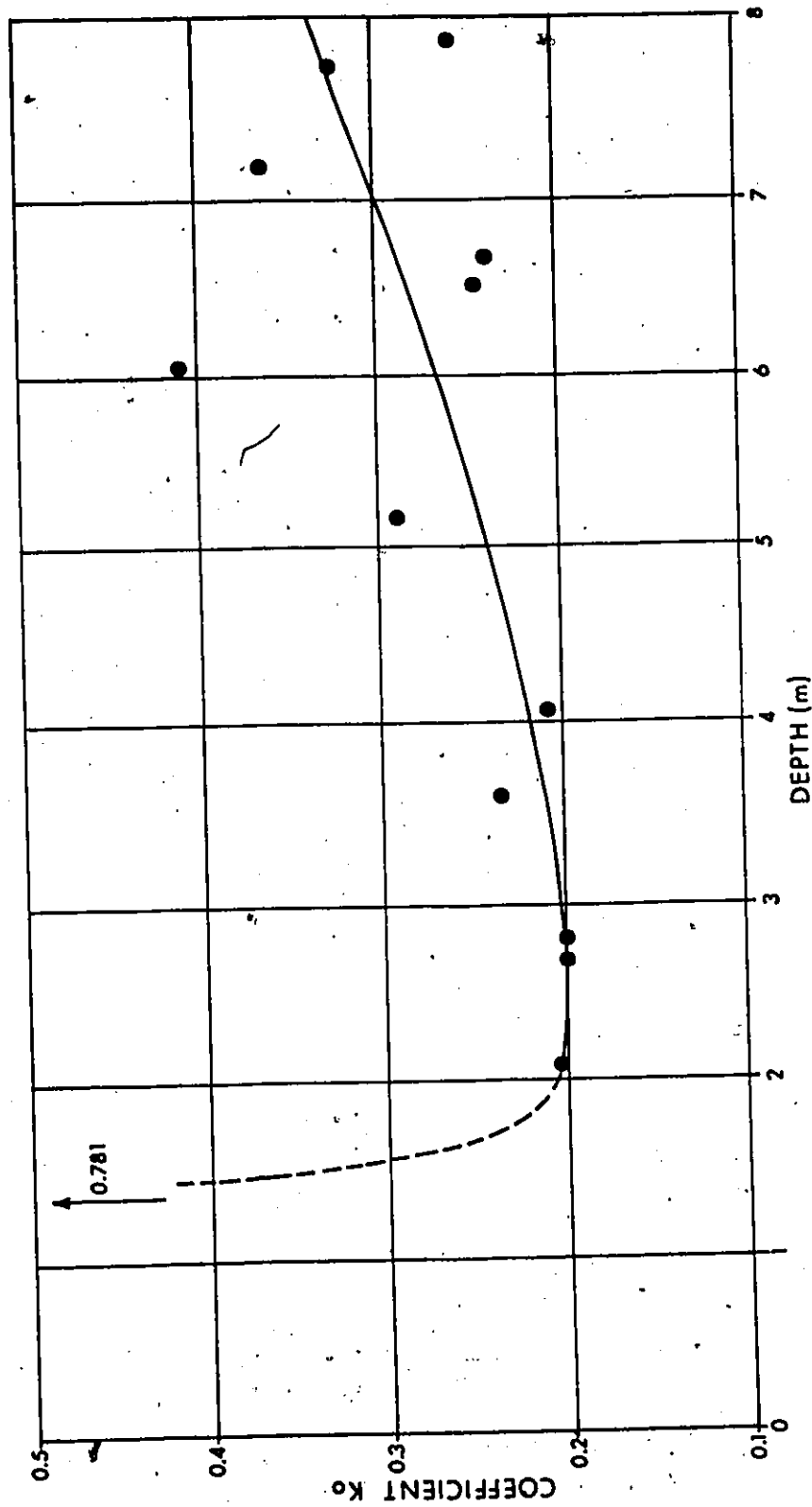
- $E_f, m_f = 1/\mu_f =$  elasticity coefficients of foundation;
- $E_s, m_s = 1/\mu_s =$  elasticity coefficients of the soil;
- $d =$  thickness of the foundation slab, and
- $R_0 =$  radius of the slab.

(c) Contact Pressure Distribution from a Circular Footing with Varying Degrees of Rigidity (Borowicka, 1936)

Effect of Rigidity of a Foundation on Contact Pressure Distributions

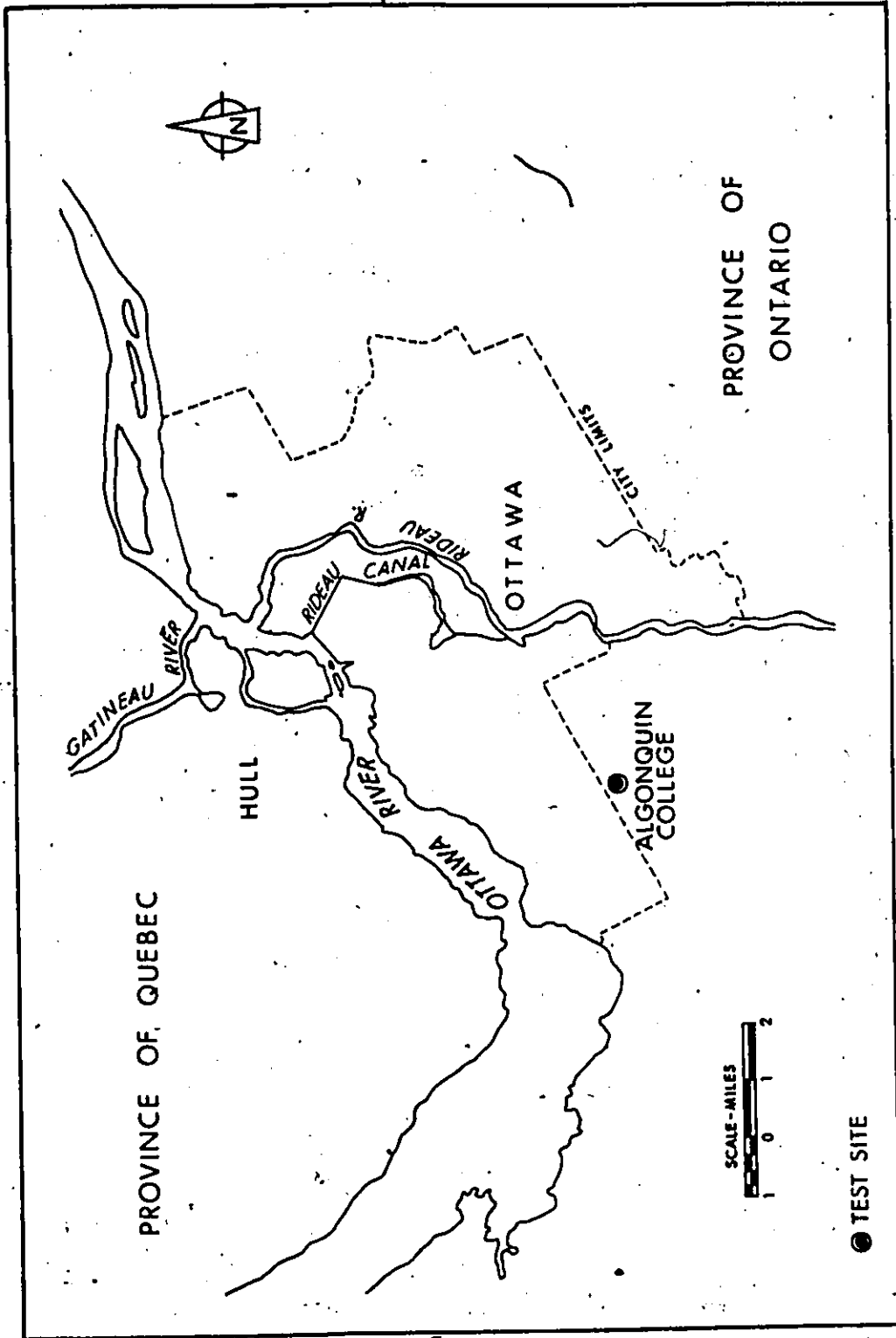


DISTRIBUTION OF VERTICAL STRESS,  $\sigma_z$ , WITH DEPTH. COMPARISON BETWEEN CENTRE-LINE STRESSES FOR RIGID AND FLEXIBLE LOADS.

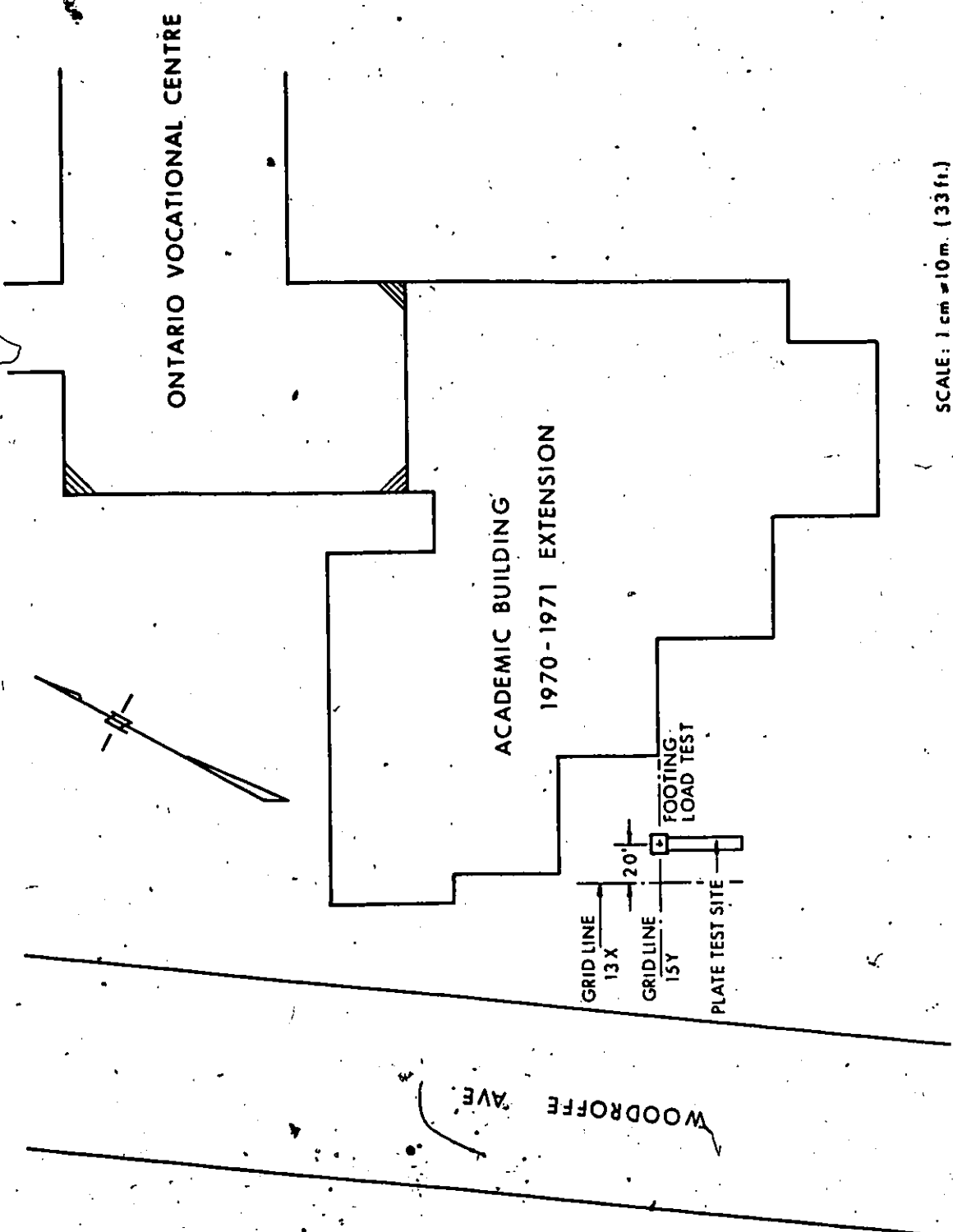


(AFTER GAUMY, 1970)

VARIATION OF  $K_0$  WITH DEPTH



MAP OF OTTAWA REGION SHOWING LOCATION OF TEST SITE

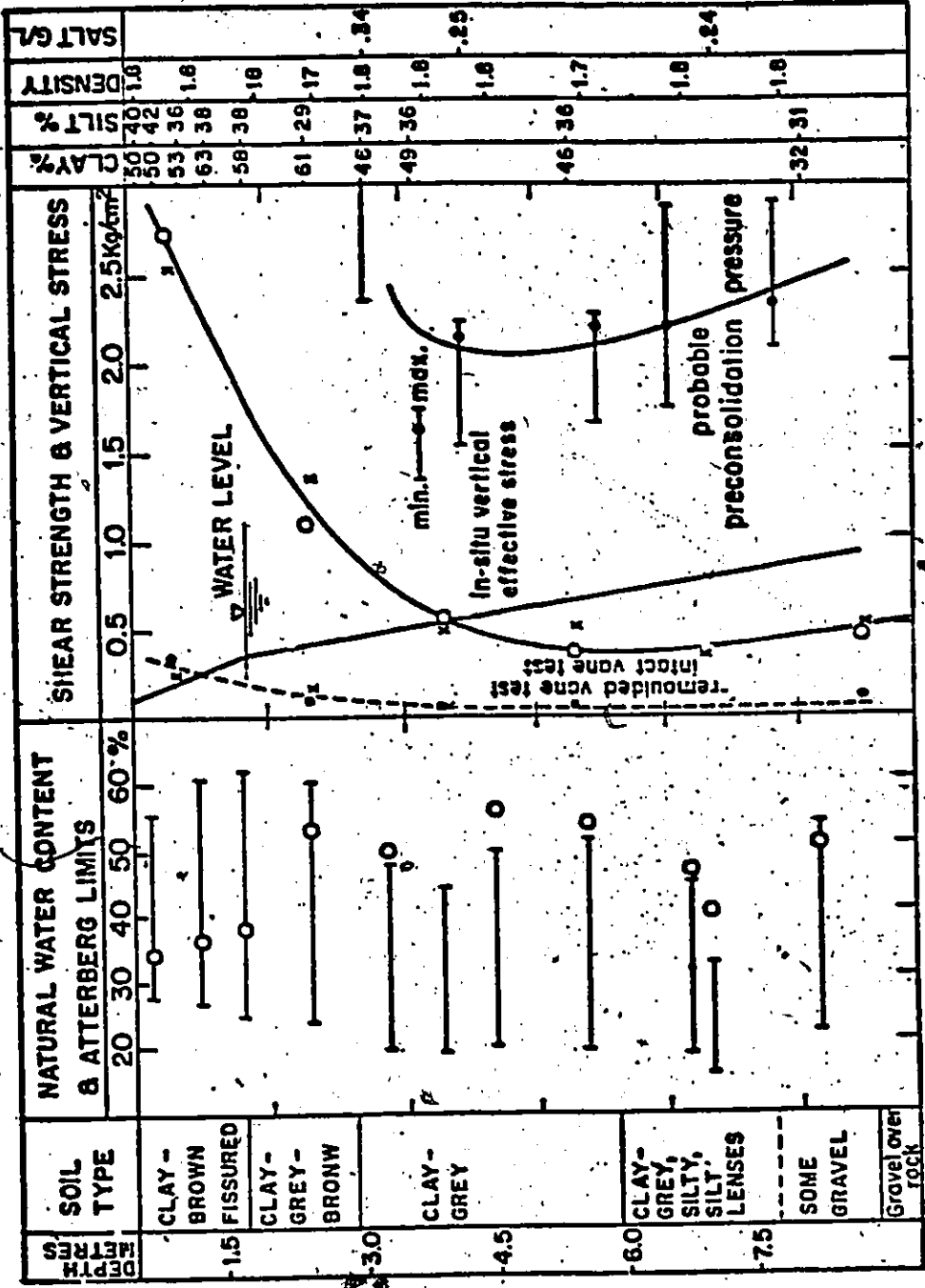


SITE PLAN

Location	Approx. Elevation (ft.)	Natural Water Content (w/c %)	Liquid Limit (LL %)	Plastic Limit (PL %)	Liquid Index (LI)	Shrinkage (%)	Clay Size (%)	Activity	Salt Content (gram/litre)	Undrained Shear Strength (tons/sq. ft.)	Reference
QNSLR	+250 -125	38 (20-70)	34	19	1.3	-	(40-65)	0.5	(0.5-5)	1.1 (0.5-2)	Pryor and Woods (1956)
St. Thauribe	+175	44	33	21	1.9	-	36	0.3	-	0.8	Perc. Ireland and Fry, (1951)
Nicolet	(Upper) +50 20 (Lower) +20 -30	65	55	23	-	9	73	0.4	0.5	0.3	Hurtubise and Rochette (1950) and Crawford and Edén (1960)
Beauharnois	+140 100	68 (50-80)	50 (44-68)	24 (22-20)	1.3	12 (7-23)	64 (47-72)	0.5	0.4	0.5	Edén and Hamilton (1957)
Mascena	+215 200	60 (50-75)	50 (35-60)	27 (20-35)	1.5	7 (7-)	45 (30-55)	0.5	(0.0-2)	0.3	Burke and Davis (1957) Hazelt, Adams and Mayras (1960) DBR unpublished
Hawkesbury	+225	80 (61-90)	64 (53-72)	20 (25-28)	1.4	27 (9-)	74 (65-88)	0.5	0.3	0.4	Edén and Hamilton (1957)
Ottawa	(Upper) +310 200 (Middle) +200 170 (Lower) +170 100	80 (60-90)	60 (50-75)	25 (20-30)	1.6	24 (6-)	70 (55-80)	0.4	1.0	0.7 (0.3-1.0)	Edén and Crawford (1957) and DBR (unpublished)
		45 (35-60)	32 (20-50)	21 (14-27)	3.0	-	64 (60-75)	0.4	1.5	0.7 (0.6-1.0)	
		65 (50-70)	65 (60-75)	28 (27-30)	1.2	5 (5-)	73 (60-75)	0.6	(0.5-15)	1.2 (0.5-1.5)	

Notes: LI = (w/c - PL)/(LL - PL). Activity = (LL - PL)/(% clay size). Clay size = finer than 0.002 mm.

Table 4.1 Typical Geotechnical Properties and Index Values for Leda Clay



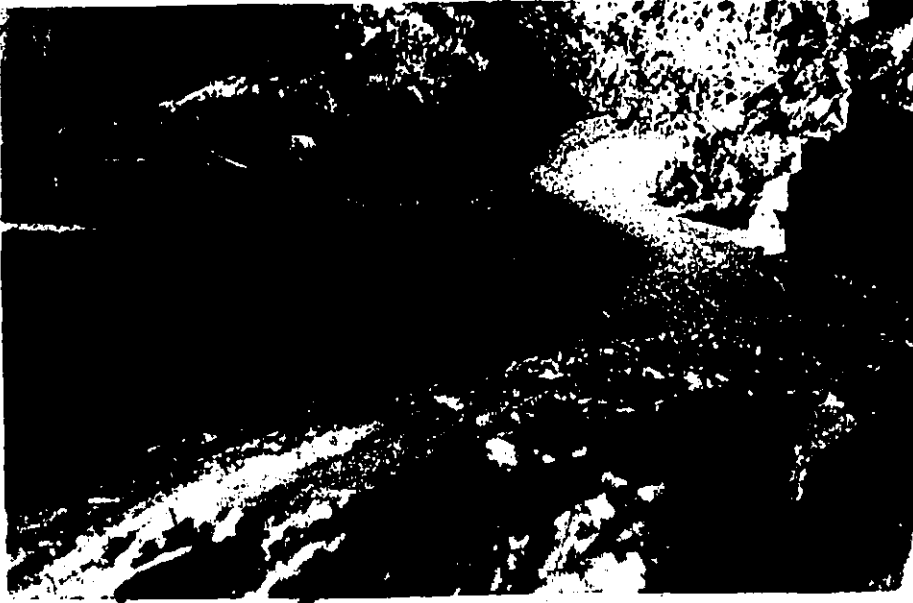
Log of Soil Profile at the Site



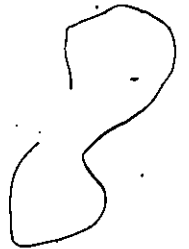
TYPICAL PHOTOGRAPHS OF FISSURES

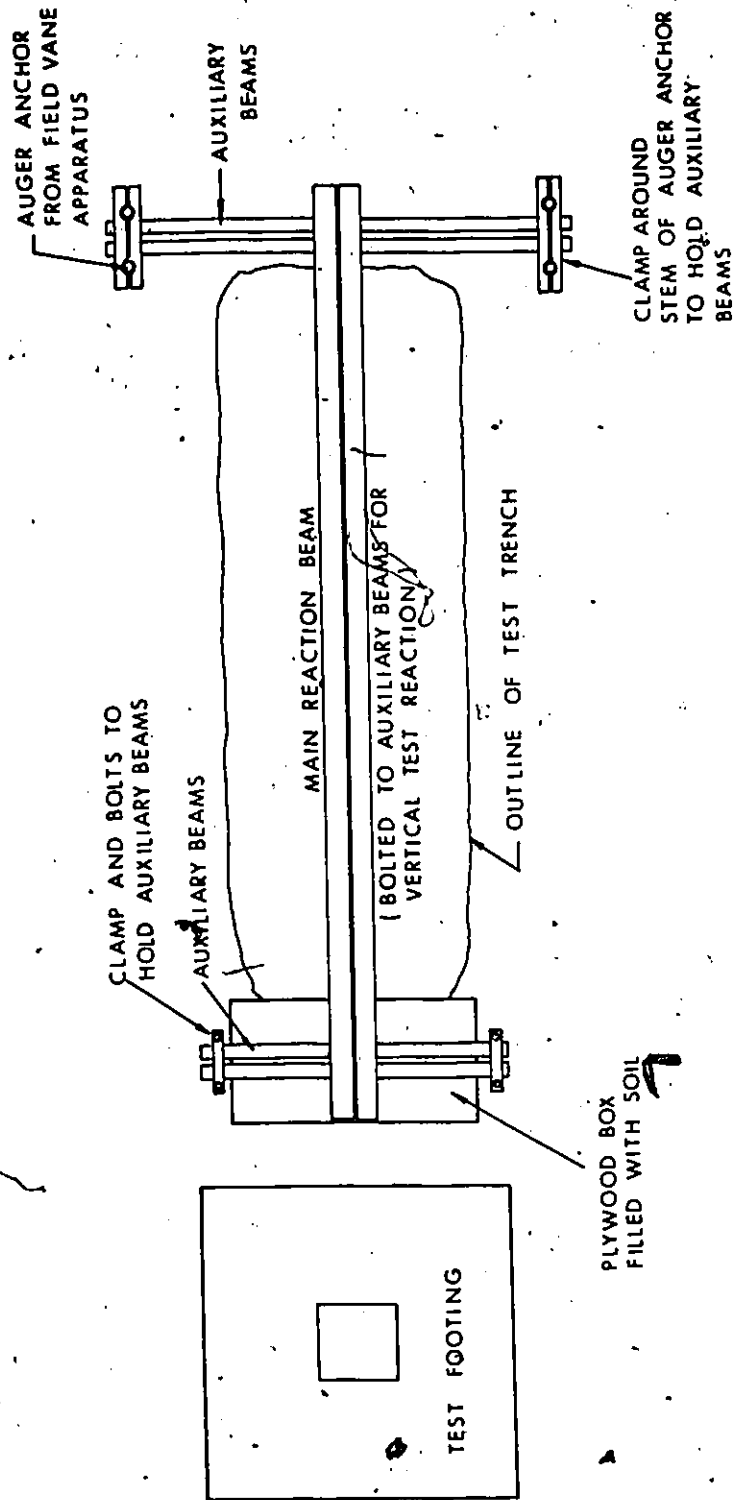
ON THE SIDE OF THE TRENCH AT A

DEPTH OF ABOUT 1.5m (5 FEET)



TYPICAL PHOTOGRAPHS OF MAJOR  
FISSURE SURFACES AT  
A DEPTH OF ABOUT 3m (10 FEET)





PLAN OF TEST AREA

0 1  
SCALE - METER



1. Typical view of trench and bracing. 'Box' reaction system can be seen at the end of the trench.



2. Typical view of Reaction beam and loading system can be seen at end of trench. Maximum load is being applied to Test V1/3. Observe deflection of beams.

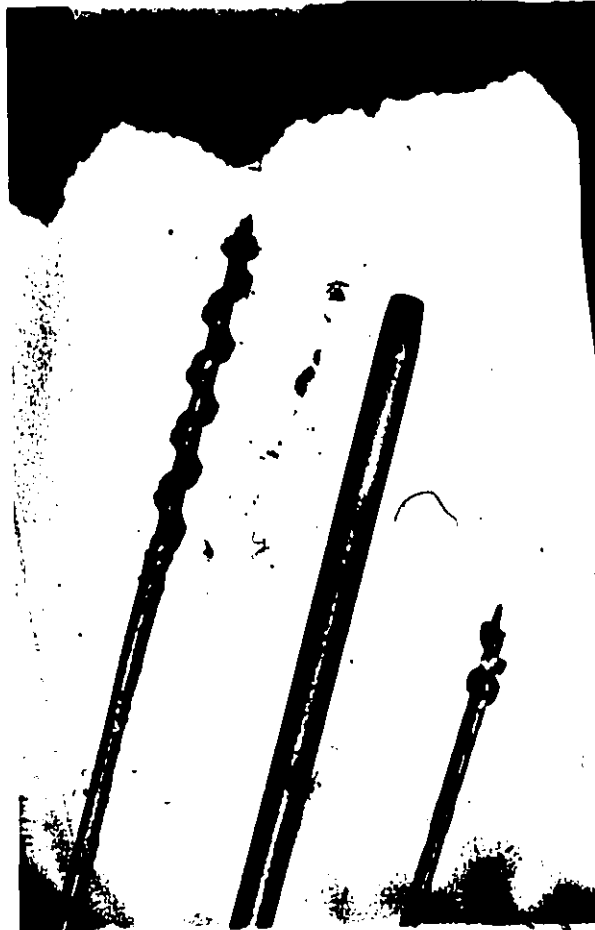


1. TYPICAL VERTICAL LOAD  
TEST, AFTER FAILURE.



2. TYPICAL HORIZONTAL LOAD TEST.

TYPICAL PHOTOGRAPHS OF TEST AND LOADING SYSTEMS

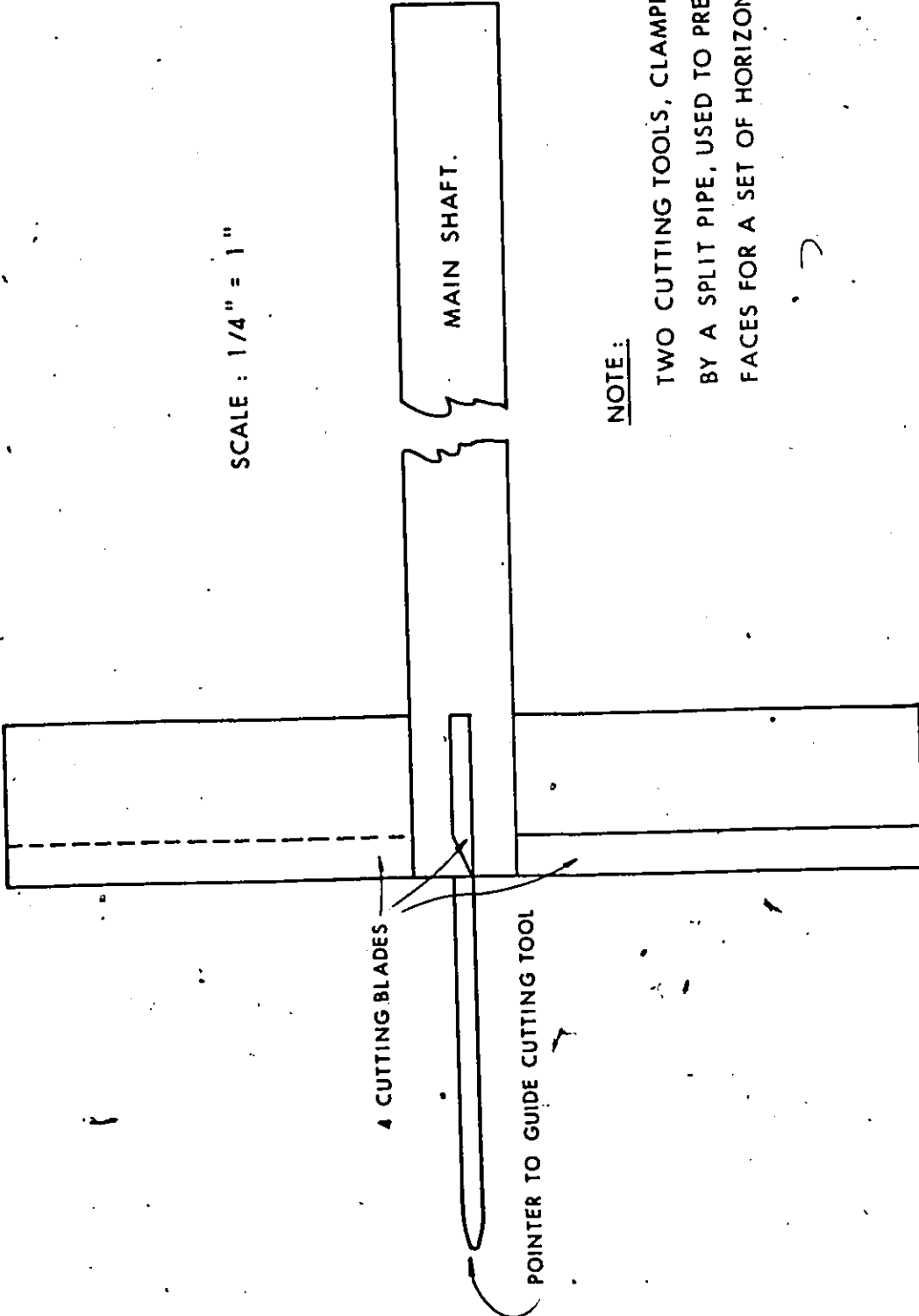


1. Tip of settlement gauge, pipe liner and bit used to form hole for liner and gauge.

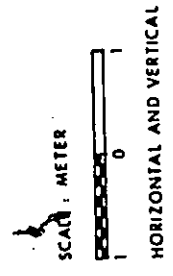
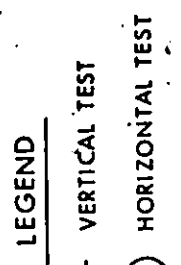
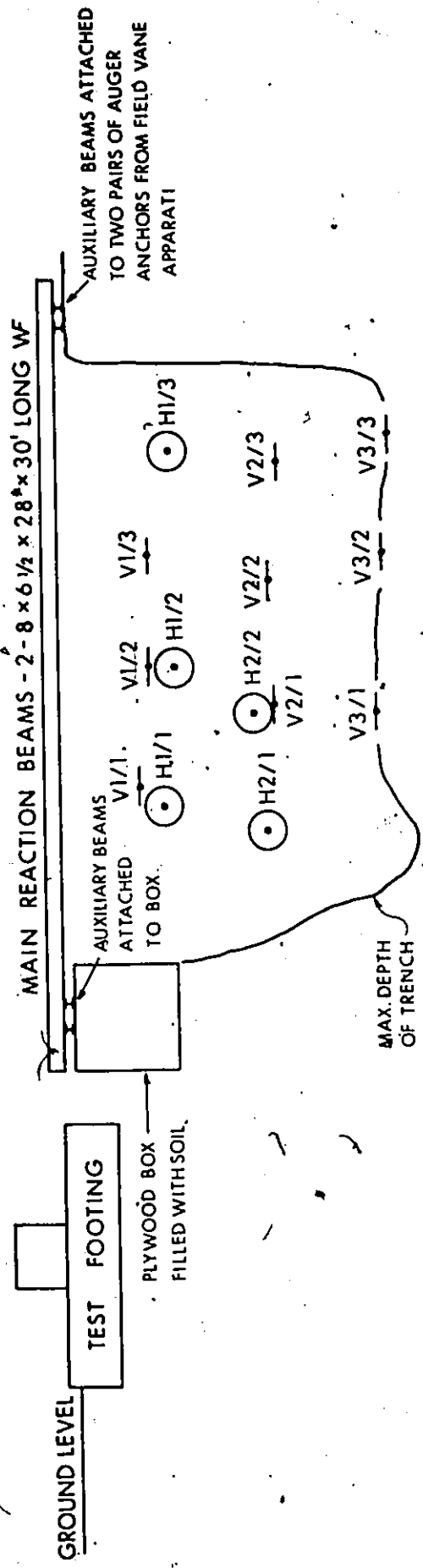


2. Fully instrumented vertical test. Main reference beam is the angle iron. Dexion sections are auxiliary.

TYPICAL PHOTOGRAPHS OF THE INSTRUMENTATION



SKETCH OF CUTTING TOOL USED TO PREPARE PARALLEL  
VERTICAL FACES ON SIDES OF TRENCH.



LONGITUDINAL SECTION TROUGH TEST TRENCH AND THE TEST FOOTING

<u>TEST NO.</u>	<u>LEVEL</u>	<u>ELEVATION m (ft.)</u>	<u>TEST TYPE</u>	<u>LOADING PROCEDURE</u>	<u>DURATION OF TEST (hours)</u>
V1/1	1	85.4 (280.1)	Vert.	1	3.5
V1/2	1	85.2 (279.6)	"	2	5.5
V1/3	1	85.2 (279.6)	"	3	4.0
H1/1A	1	85.0 (278.9)	Hor.	1	3.75
H1/1B	1	85.0 (278.9)	"	1	3.75
H1/2A	1	84.9 (278.6)	"	2	7.5
H1/2B	1	84.9 (278.6)	"	2	7.5
H1/3A	1	85.0 (278.9)	"	3	4.5
H1/3B	1	85.0 (278.9)	"	3	4.5
V2/1	2	83.8 (274.9)	Vert.	1	3.0
V2/2	2	83.9 (275.1)	"	2	6.5
V2/3	2	86.7 (274.6)	"	3	4.75
H2/1A	2	83.9 (275.1)	Hor.	1	3.25
H2/1B	2	83.9 (275.1)	"	1	3.25
H2/2A	2	84.0 (275.6)	"	2	6.0
H2/2B	2	84.0 (275.6)	"	2	6.0
V3/1	3	82.6 (270.9)	Vert.	1	1.75
V3/2	3	82.5 (270.6)	"	2	2.75
V3/3	3	82.4 (270.3)	"	3	2.75

NOTE: Test No. indicates test-type (i.e. Vertical or Horizontal, level of test by V1 or H2 and loading procedure by V1/2 or H2/1B. The A and B for the horizontal tests signifies the simultaneous pair of tests performed for each horizontal set-up.

TABLE 4.2

LIST OF ALL TESTS INDICATING THE LEVEL,  
TEST TYPE, LOADING PROCEDURE AND  
DURATION OF EACH TEST

TEST NO.	GROUND MOVE- MENT ADJACENT TO PLATE	DEFORMATION OF PLATE	DEFORMATION AT DEPTHS			
			R	2R	3R	4R
V1/1	2	3	-	-	-	-
V1/2	2	3	-	-	-	-
V1/3	2	3	-	-	-	-
H1/1A	-	3	-	-	-	-
H1/1B	-	3	-	-	-	-
H1/2A	-	3	-	-	-	-
H1/2B	-	3	-	-	-	-
H1/3A	-	3	-	-	-	-
H1/3B	-	3	-	-	-	-
V2/1	-	1 central	1	1	1	1
V2/2	-	4	1	1	1	u/s
V2/3	-	4	-	-	-	-
H2/1A	-	4	1	1	1	u/s
H2/1B	-	1 central	-	-	-	-
H2/2A	-	4	1	1	1	1
H2/2B	-	3	-	-	-	-
V3/1	-	4	1	1	1	1
V3/2	-	4	1	1	1	1
V3/3	-	3	-	-	-	-

TABLE 4.3

LIST OF ALL PLATE TESTS INDICATING  
THE NUMBER OF DIAL GUAGES USED  
AND THE PERFORMANCE RECORDED

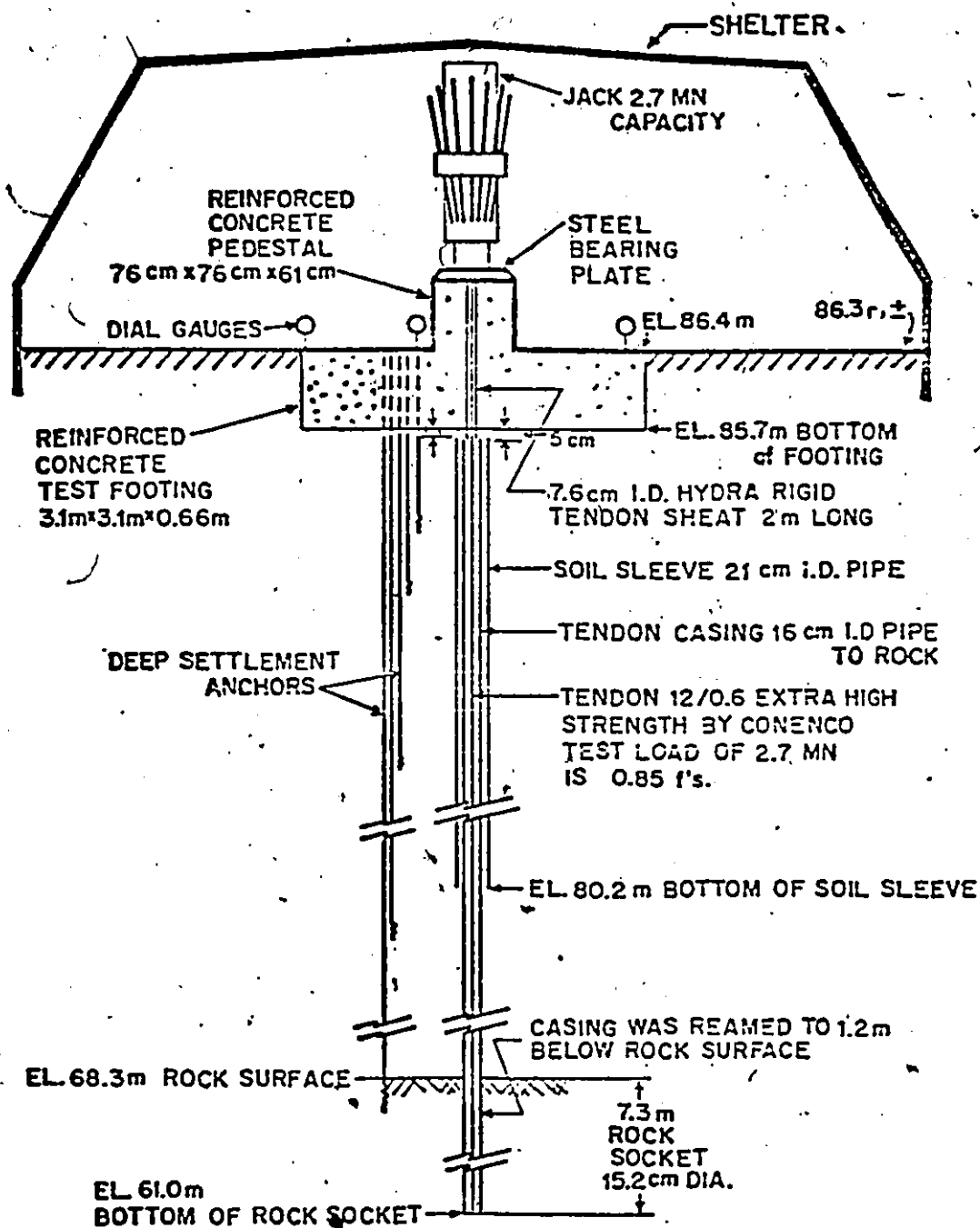
TEST NO.                      SUMMARY OF PERTINENT FIELD OBSERVATIONS

REMARKS

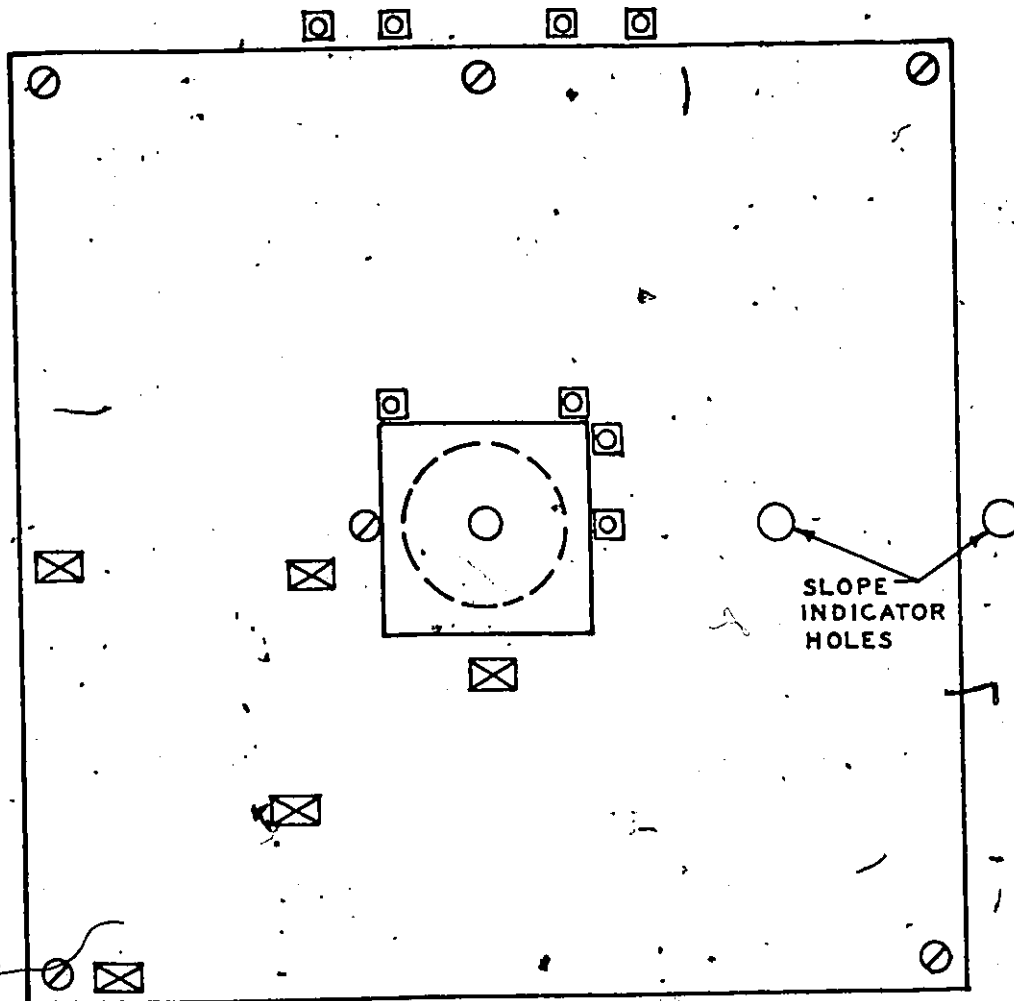
V1/1	Reference beam jolted during final unloading	Results O.K.
V1/2	No comments	Results O.K.
V1/3	Soil appeared more stiff and intact	Results O.K.
H1/1A	Poor contact between plate and soil at top of plate	Probably O.K.
H1/1B	Fairly large surface area of soil adjacent to plate appeared to deform with the plate	Effect of fissures
H1/2A	Falling block of soil disturbed some gauges during final unloading	Results O.K.
H1/2B	No comments	Results O.K.
H1/3A	Soil appeared more intact at this side than other side of trench (H1/3B)	Results O.K. Non-homogeneity
V2/1	Plate tilted badly. Some dial gauges had to be reset during second cycle. Second cycle interrupted by bad weather.	First cycle O.K. Effect of fissures
V2/2	Plate tilted quite badly. After test some digging showed south side more intact than north side	Results O.K.
V2/3	No comments	
H2/1A	Reference beam and dial gauges disturbed by falling block of soil during final unloading cycle	Results O.K.
H2/1B	Block of soil fell away from beside the plate just as test started	Results O.K.
H2/2A	Gauge disturbed by falling block of soil during cycle to 316 kPa. Reset with minimal interruption	Results O.K.
H2/2B	No comments	Results O.K.
V3/1	No comments	Results O.K.
V3/2	Use of rigid connection between loading system and plate did not significantly reduce tilting	Results O.K.
H2/1B	Block of soil fell away from beside the plate just as test started	Results O.K.

TABLE 4.4

ADDITIONAL OBSERVATIONS PERTAINING TO THE PERFORMANCE OF INDIVIDUAL TESTS



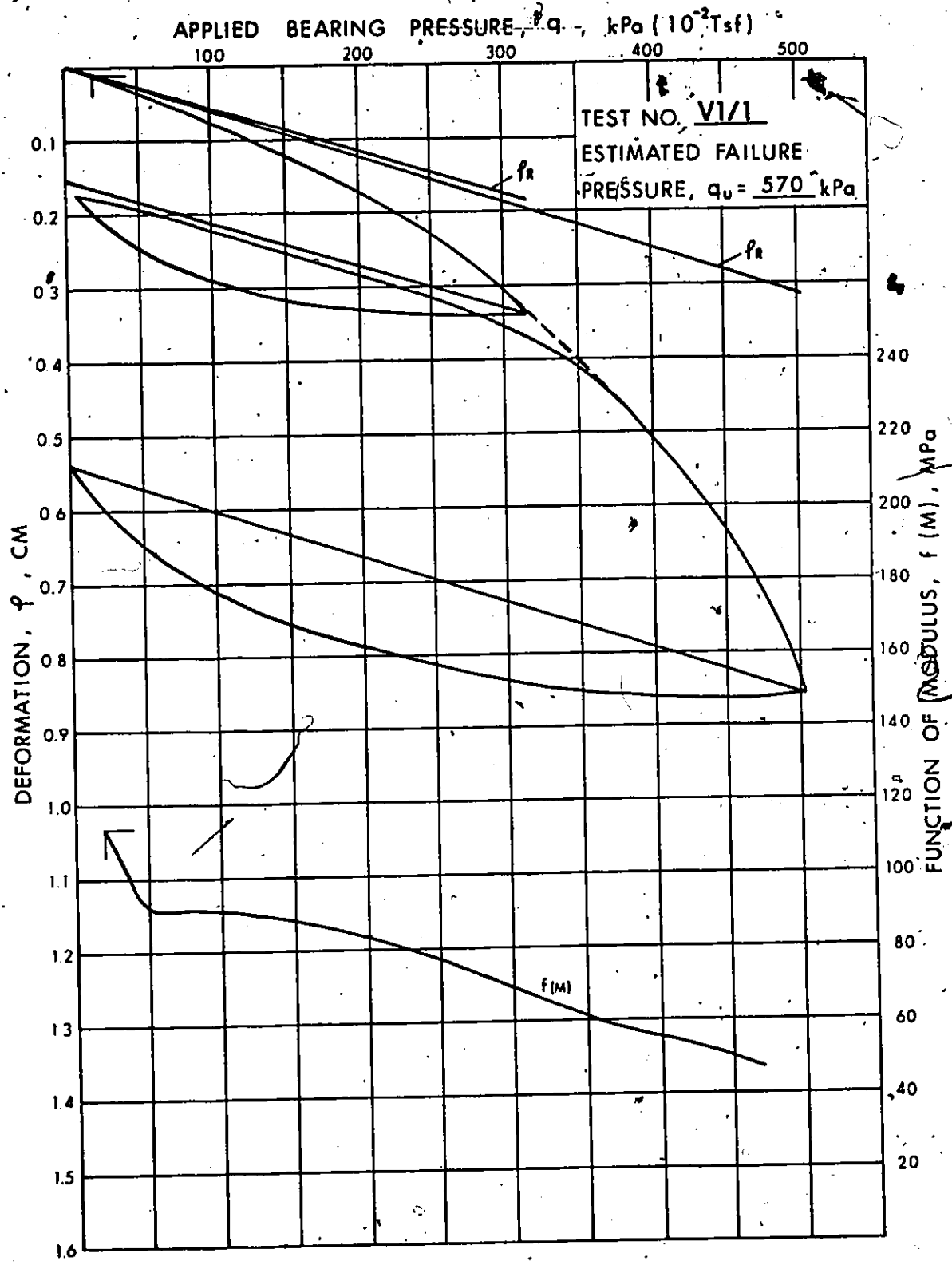
Section through Test Footing  
and Reaction System



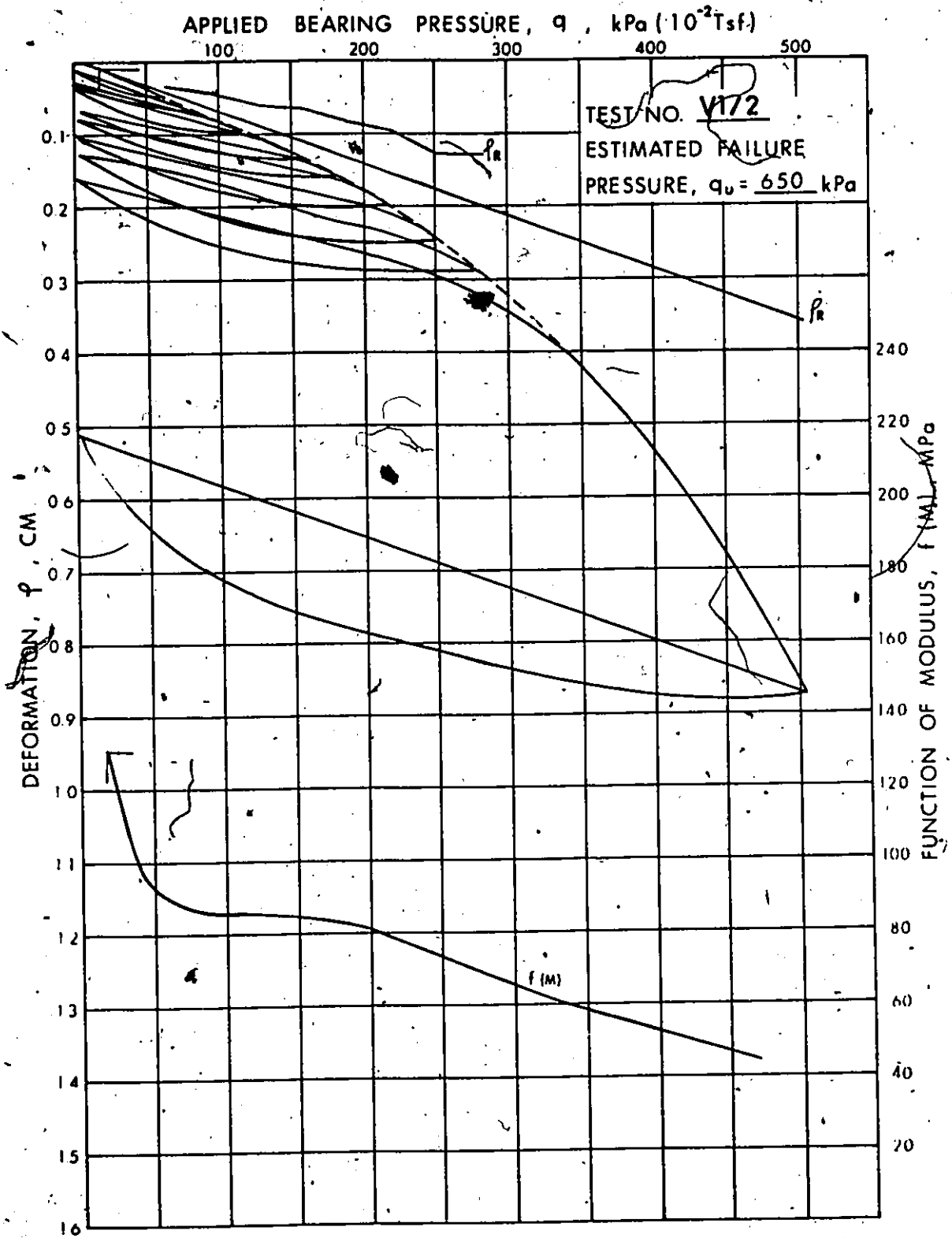
LEGEND

- ⊘ DIAL GAUGE ON TOP OF FOOTING.
- ⊙ DIAL GAUGE ABOVE REFERENCE POINTS AT DEPTH.
- ⊗ CONTACT PRESSURE CELLS.

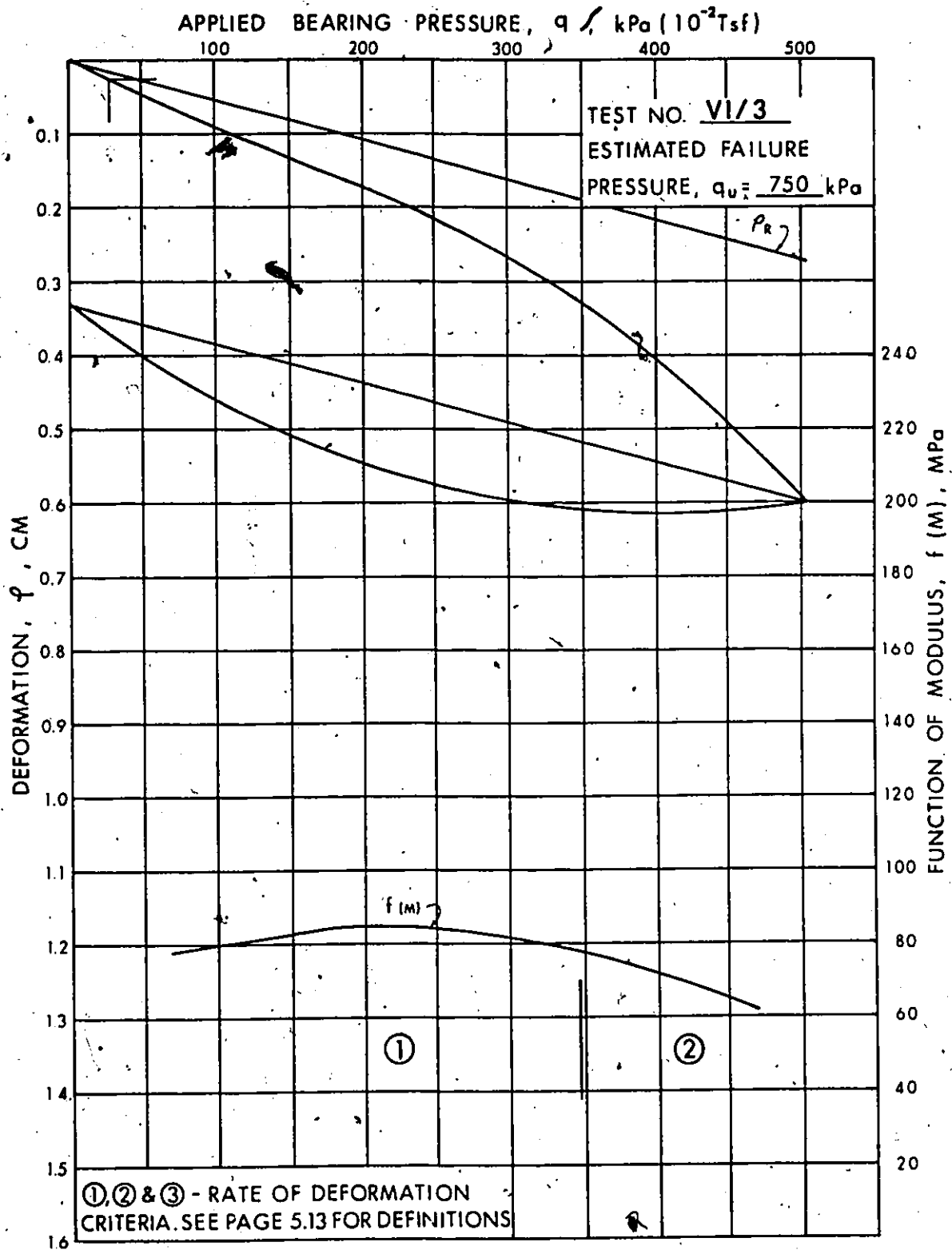
Plan View of Test Footing - Instrument Locations



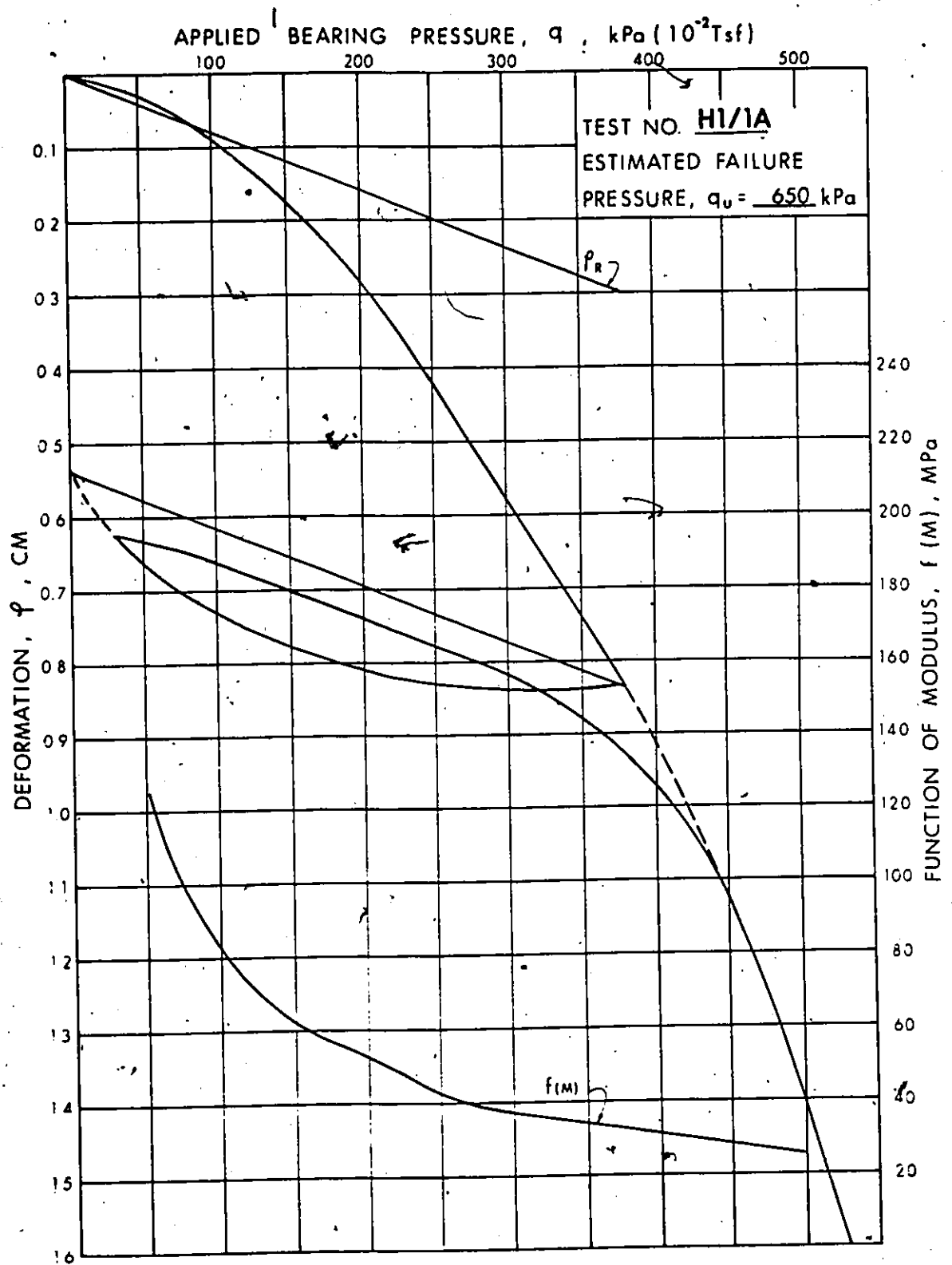
PRESENTATION OF : TOTAL DEFORMATION ; RECOVERABLE DEFORMATION AND FUNCTION OF MODULUS VERSUS APPLIED BEARING PRESSURE.



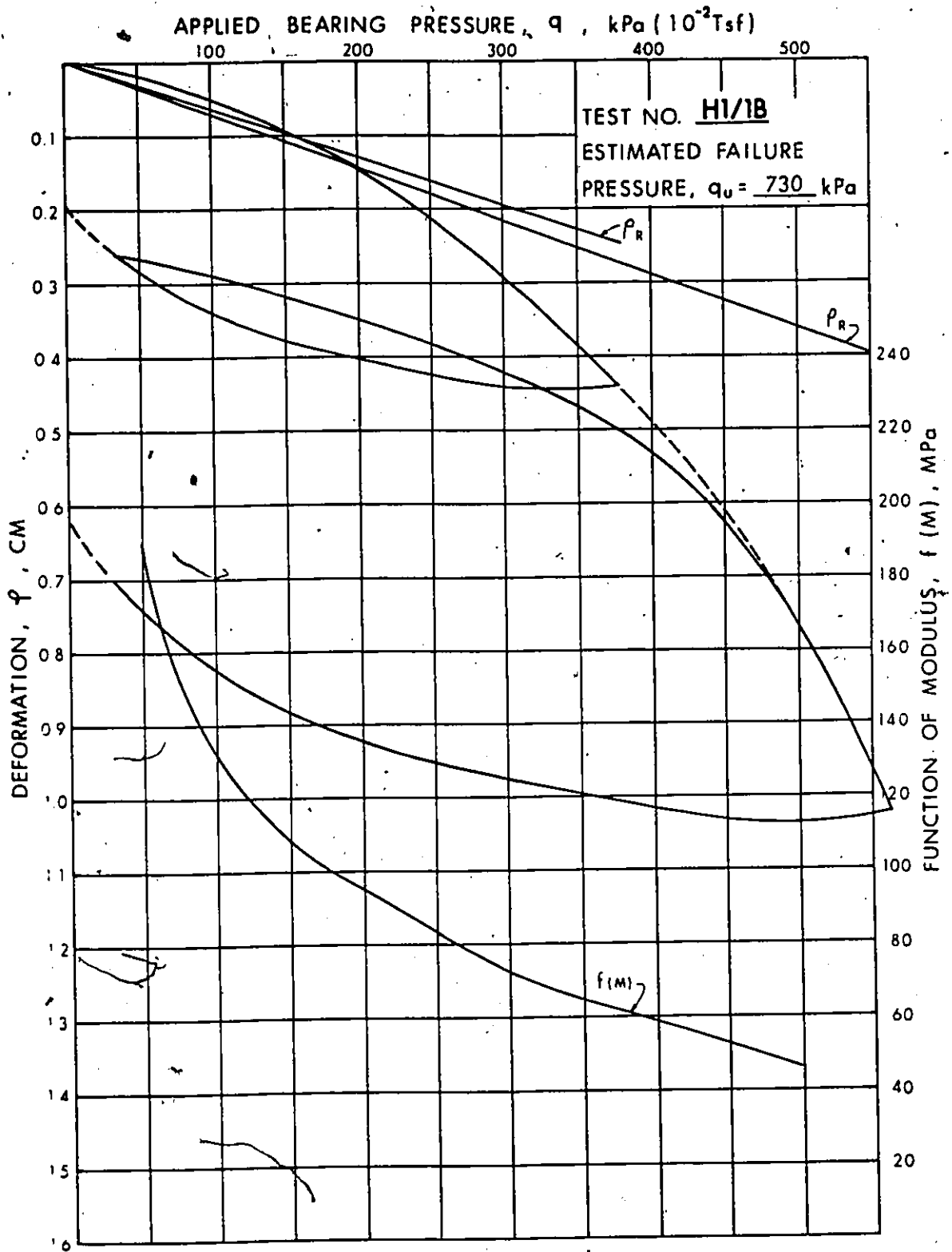
PRESENTATION OF: TOTAL DEFORMATION; RECOVERABLE DEFORMATION AND FUNCTION OF MODULUS VERSUS APPLIED BEARING PRESSURE.



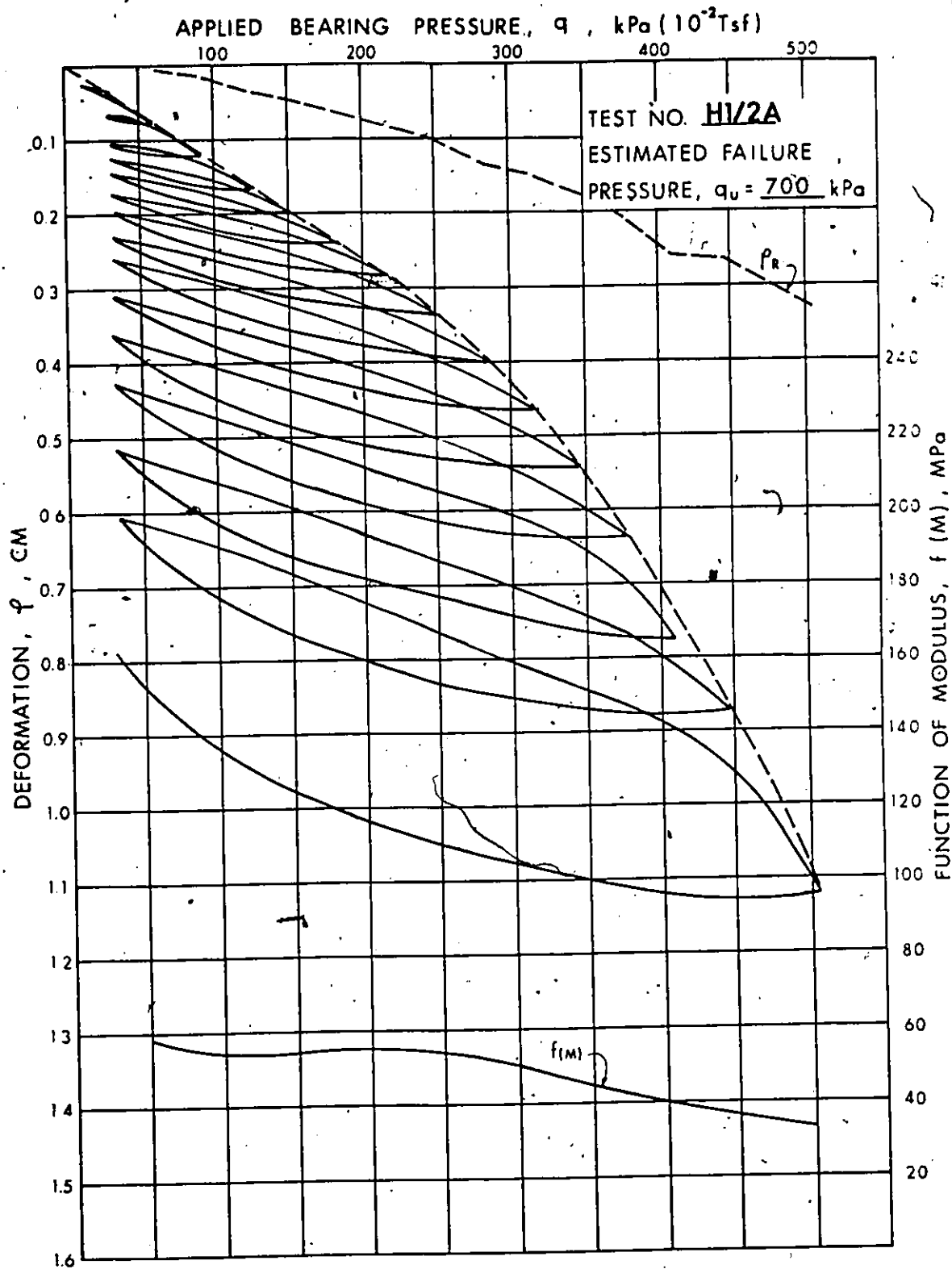
PRESENTATION OF: TOTAL DEFORMATION, RECOVERABLE DEFORMATION AND FUNCTION OF MODULUS VERSUS APPLIED BEARING PRESSURE.



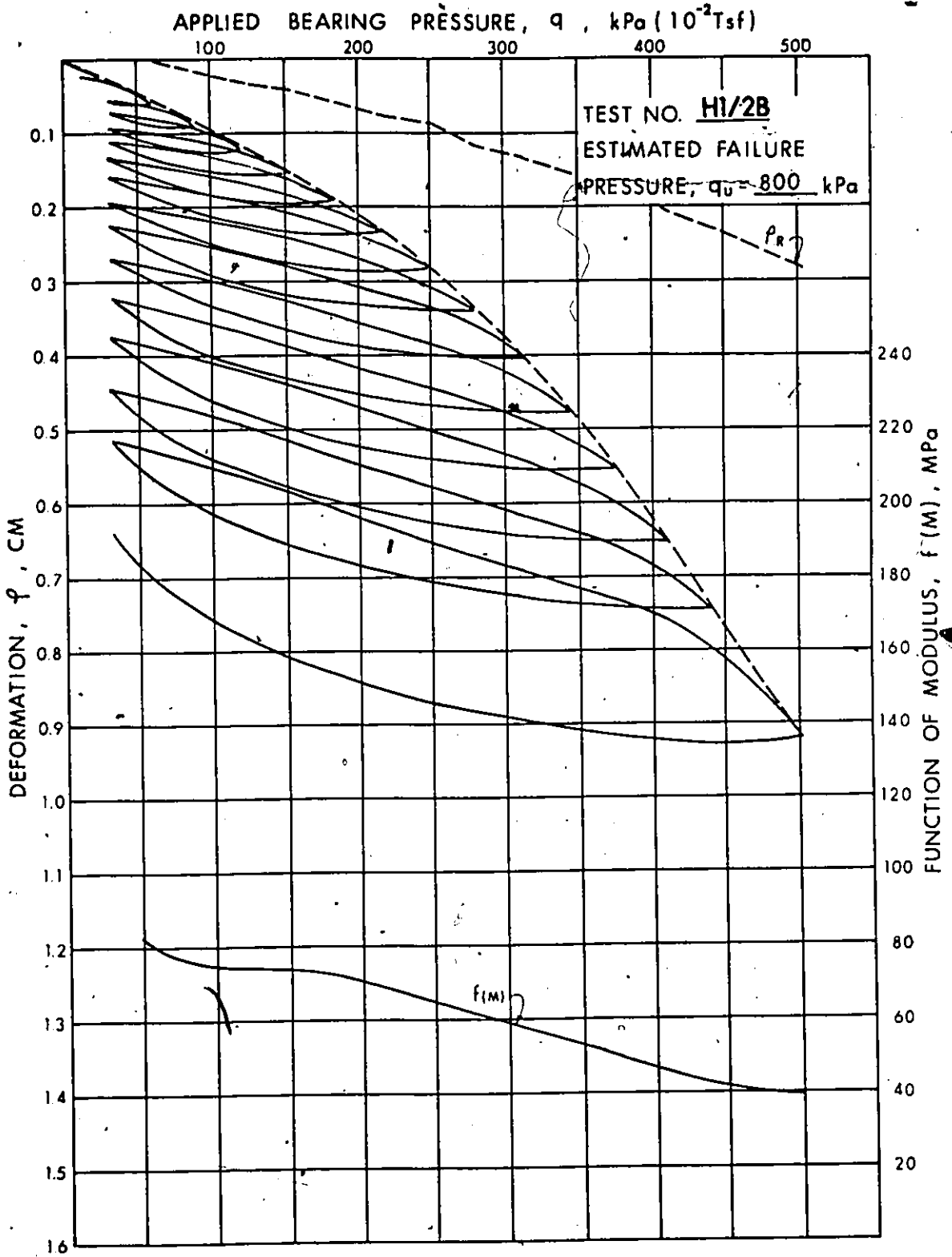
PRESENTATION OF TOTAL DEFORMATION, RECOVERABLE DEFORMATION AND FUNCTION OF MODULUS VERSUS APPLIED BEARING PRESSURE.



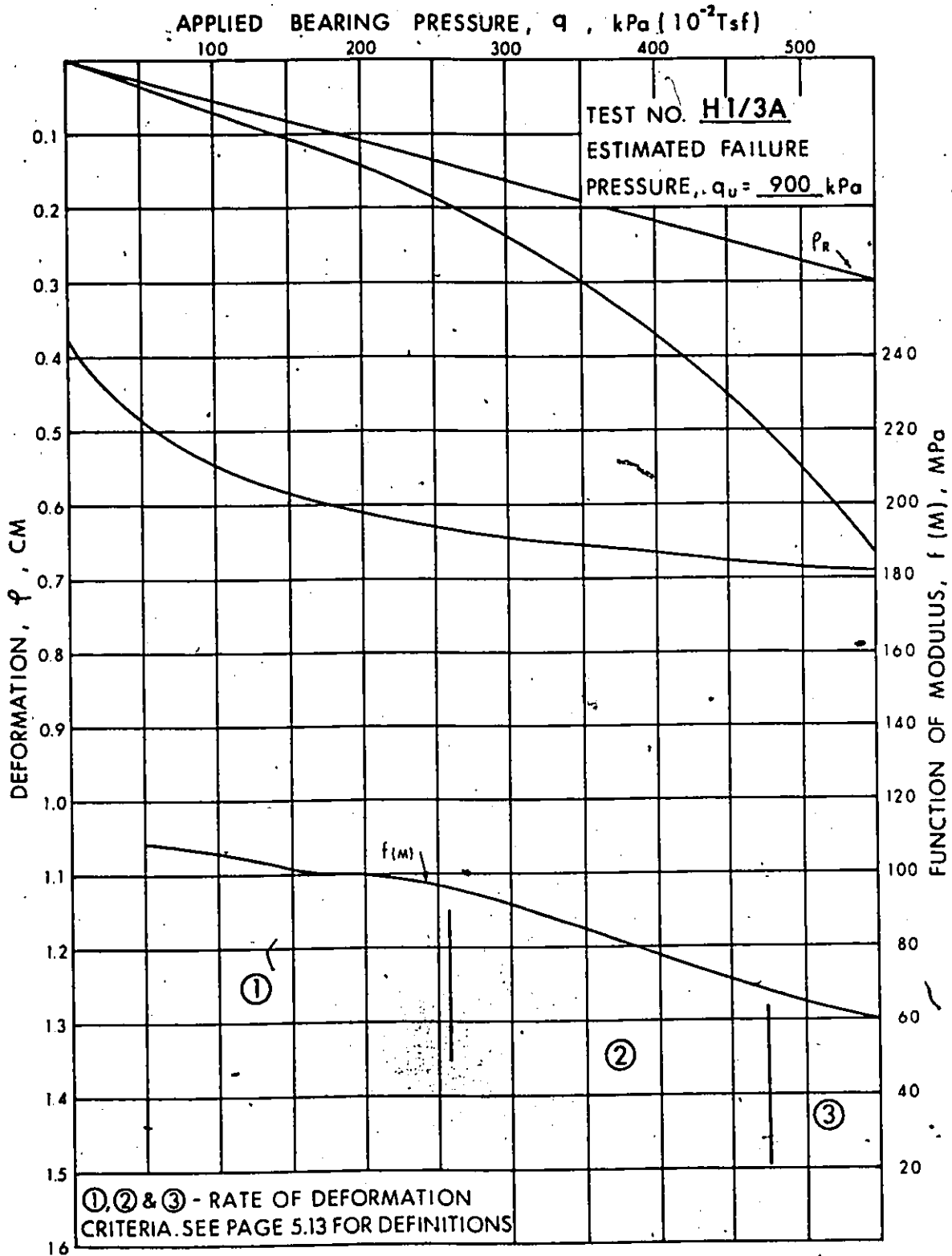
PRESENTATION OF TOTAL DEFORMATION, RECOVERABLE DEFORMATION AND FUNCTION OF MODULUS VERSUS APPLIED BEARING PRESSURE.



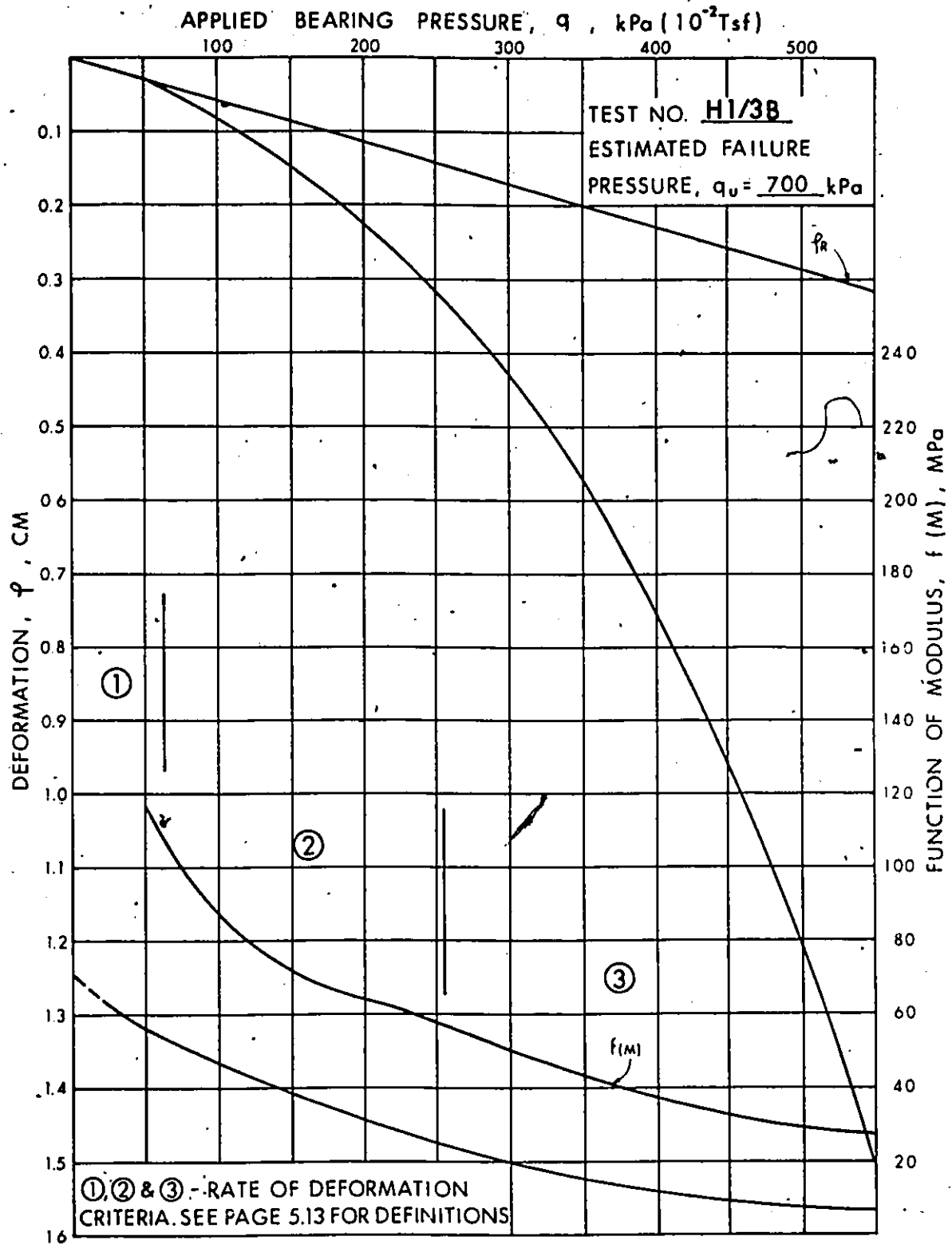
PRESENTATION OF: TOTAL DEFORMATION; RECOVERABLE DEFORMATION AND FUNCTION OF MODULUS VERSUS APPLIED BEARING PRESSURE.



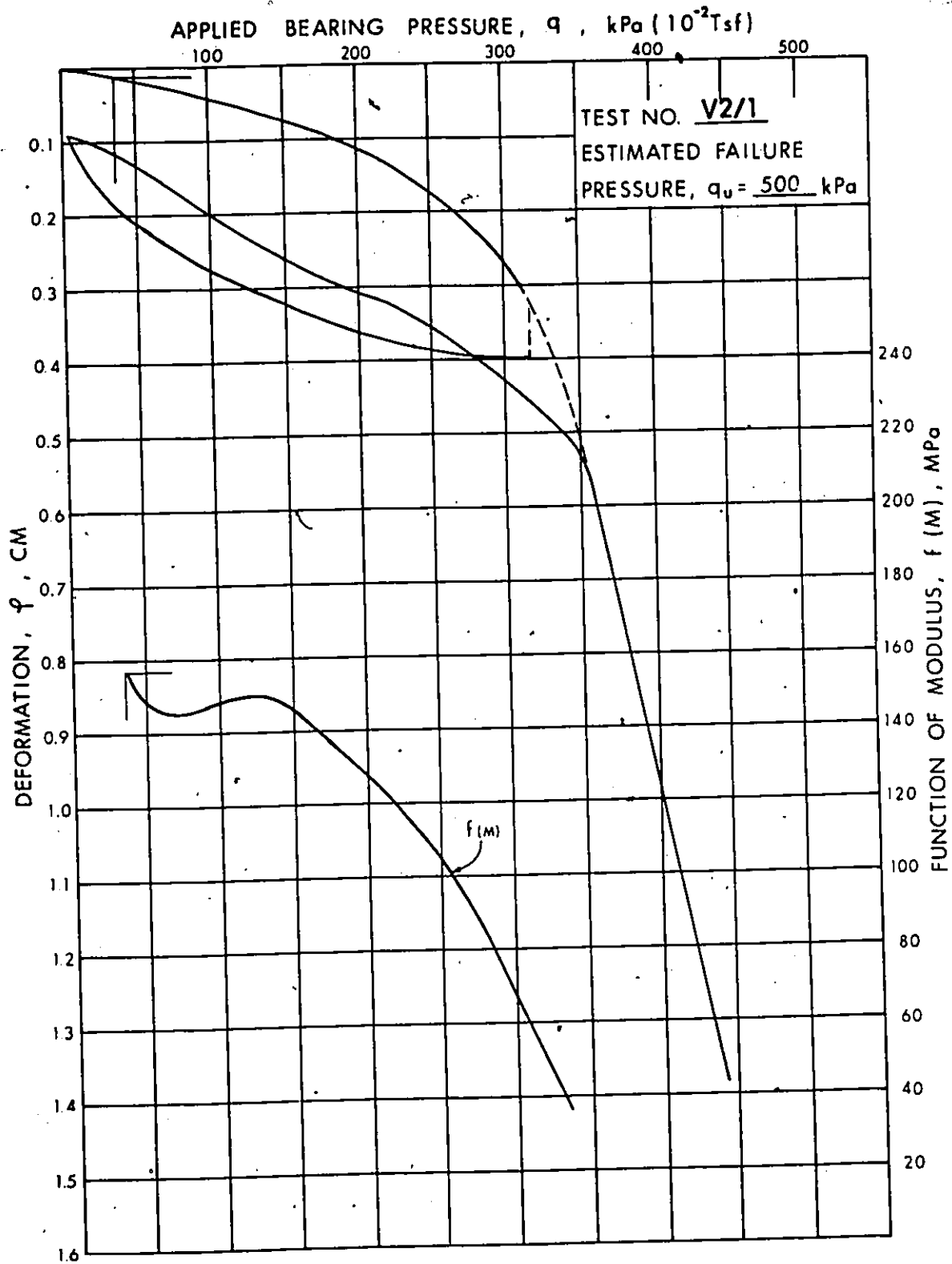
PRESENTATION OF: TOTAL DEFORMATION; RECOVERABLE DEFORMATION AND FUNCTION OF MODULUS VERSUS APPLIED BEARING PRESSURE.



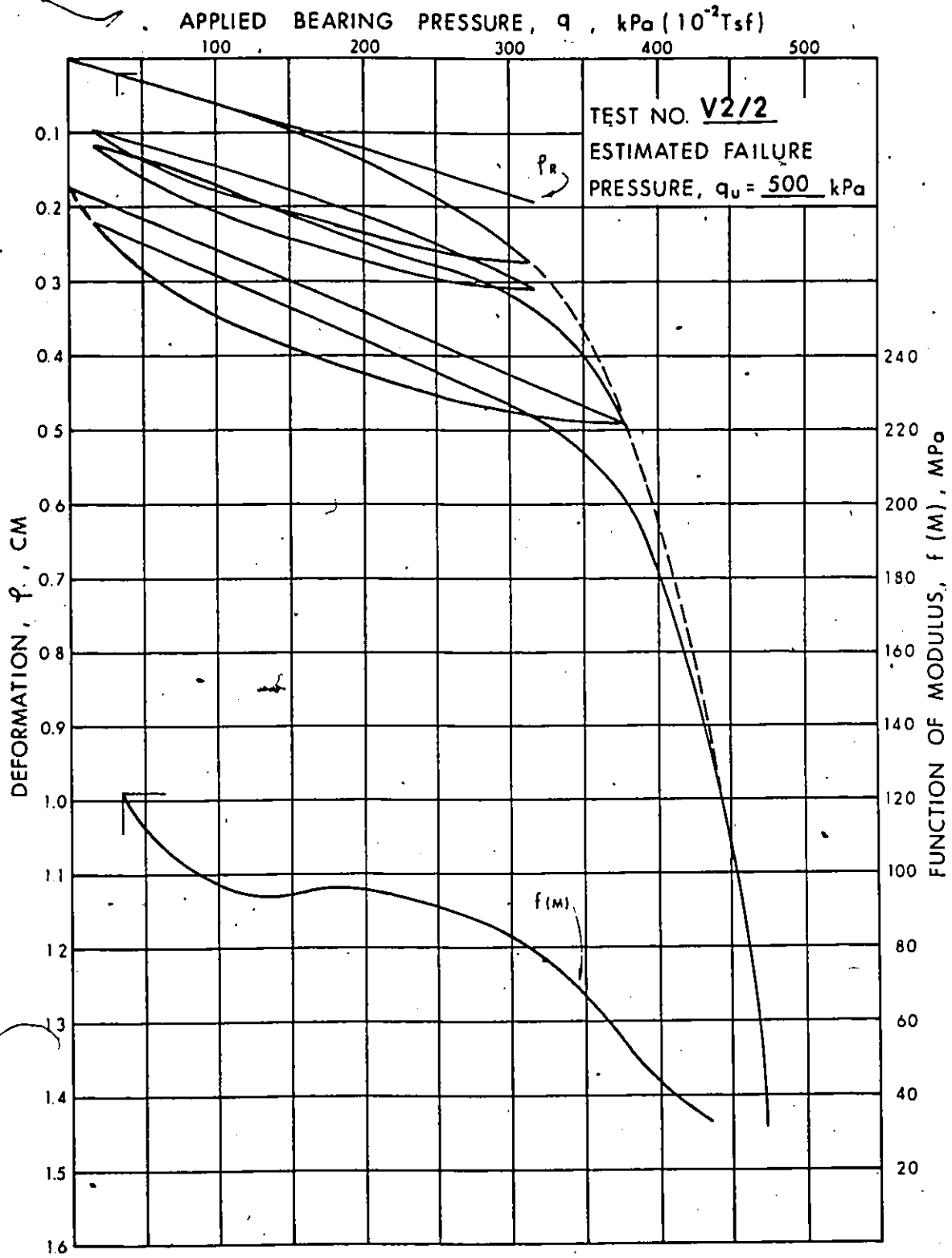
PRESENTATION OF: TOTAL DEFORMATION; RECOVERABLE DEFORMATION AND FUNCTION OF MODULUS VERSUS APPLIED BEARING PRESSURE.



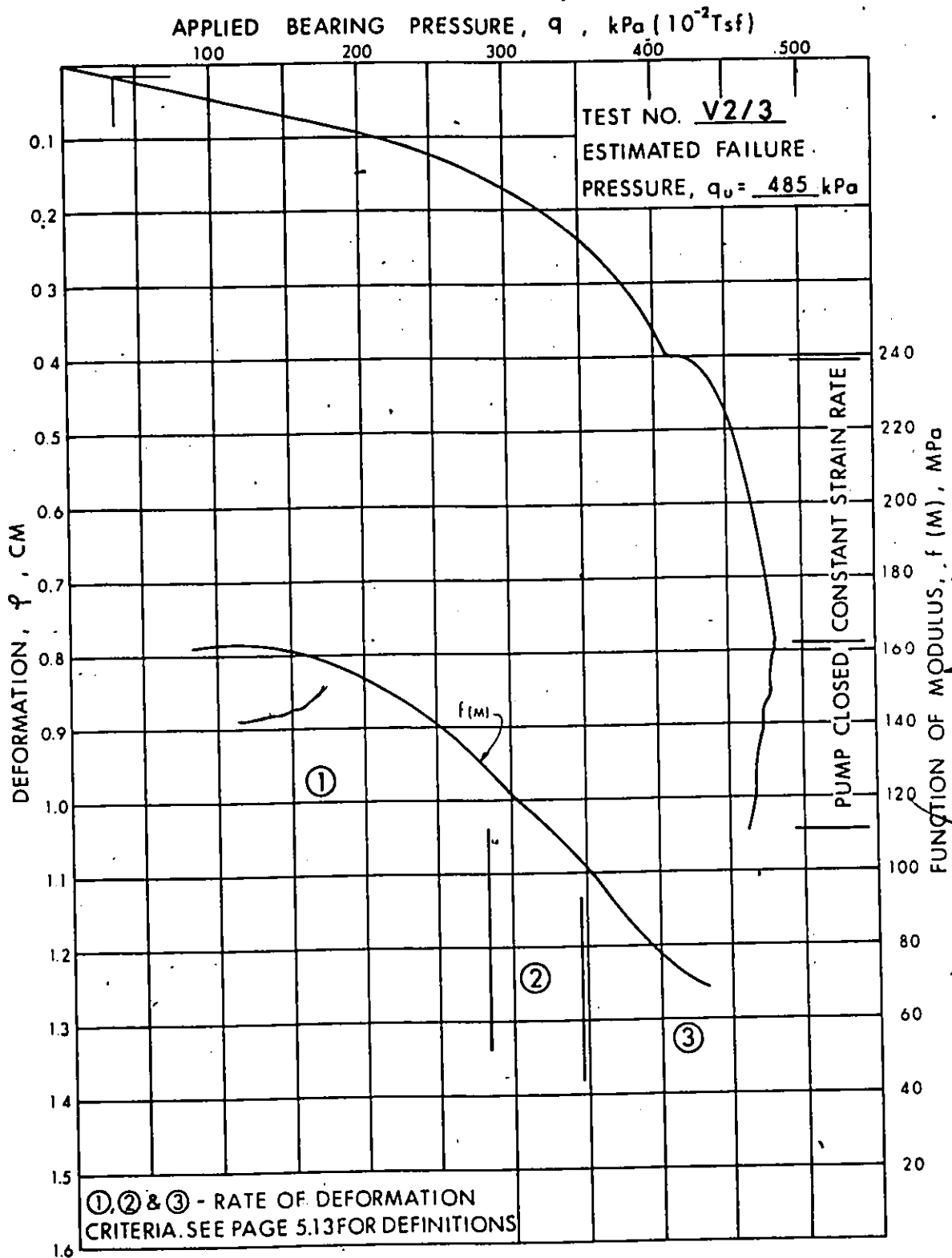
PRESENTATION OF : TOTAL DEFORMATION ; RECOVERABLE DEFORMATION AND FUNCTION OF MODULUS VERSUS APPLIED BEARING PRESSURE.



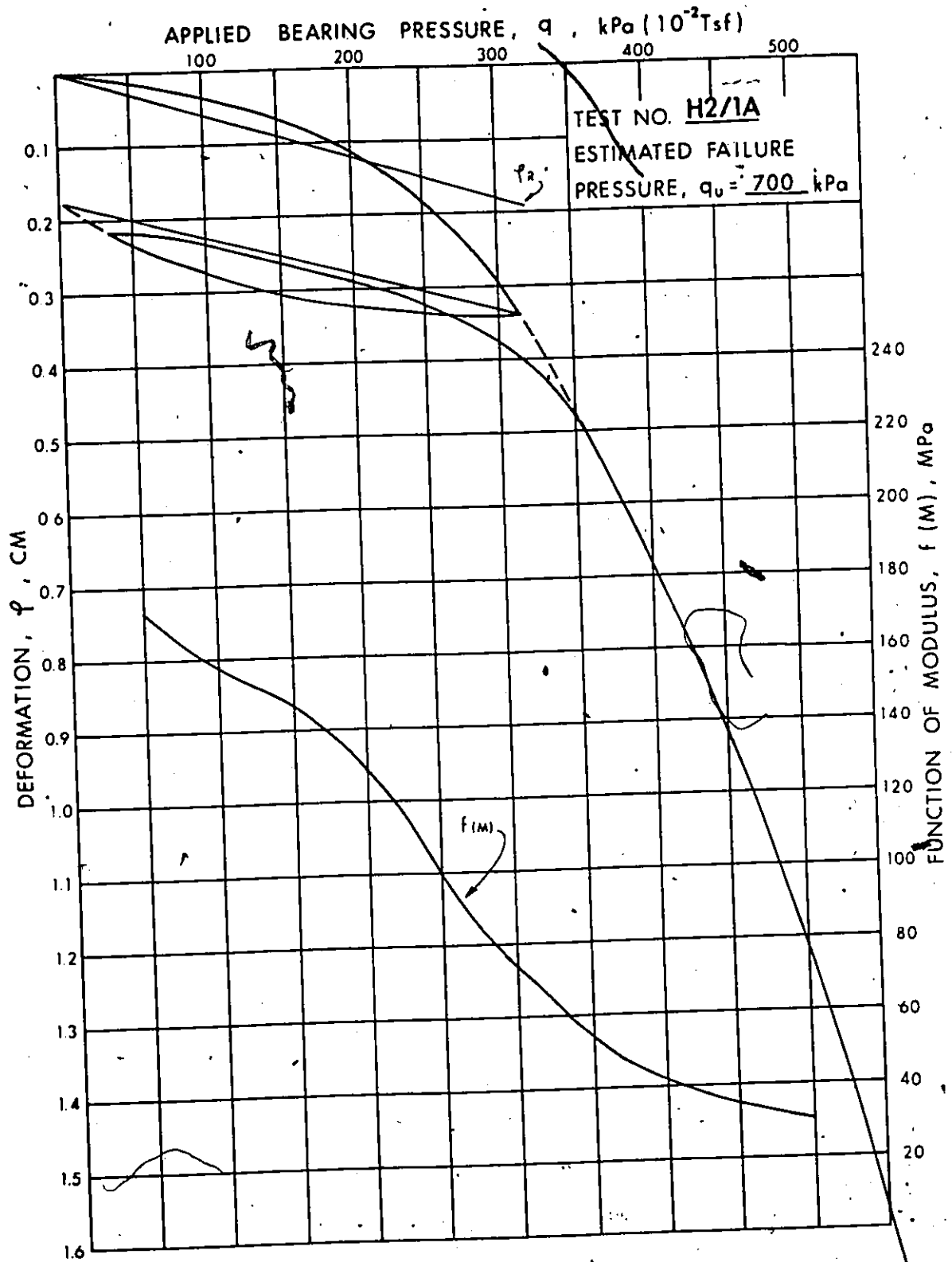
PRESENTATION OF: TOTAL DEFORMATION; RECOVERABLE DEFORMATION AND FUNCTION OF MODULUS VERSUS APPLIED BEARING PRESSURE.



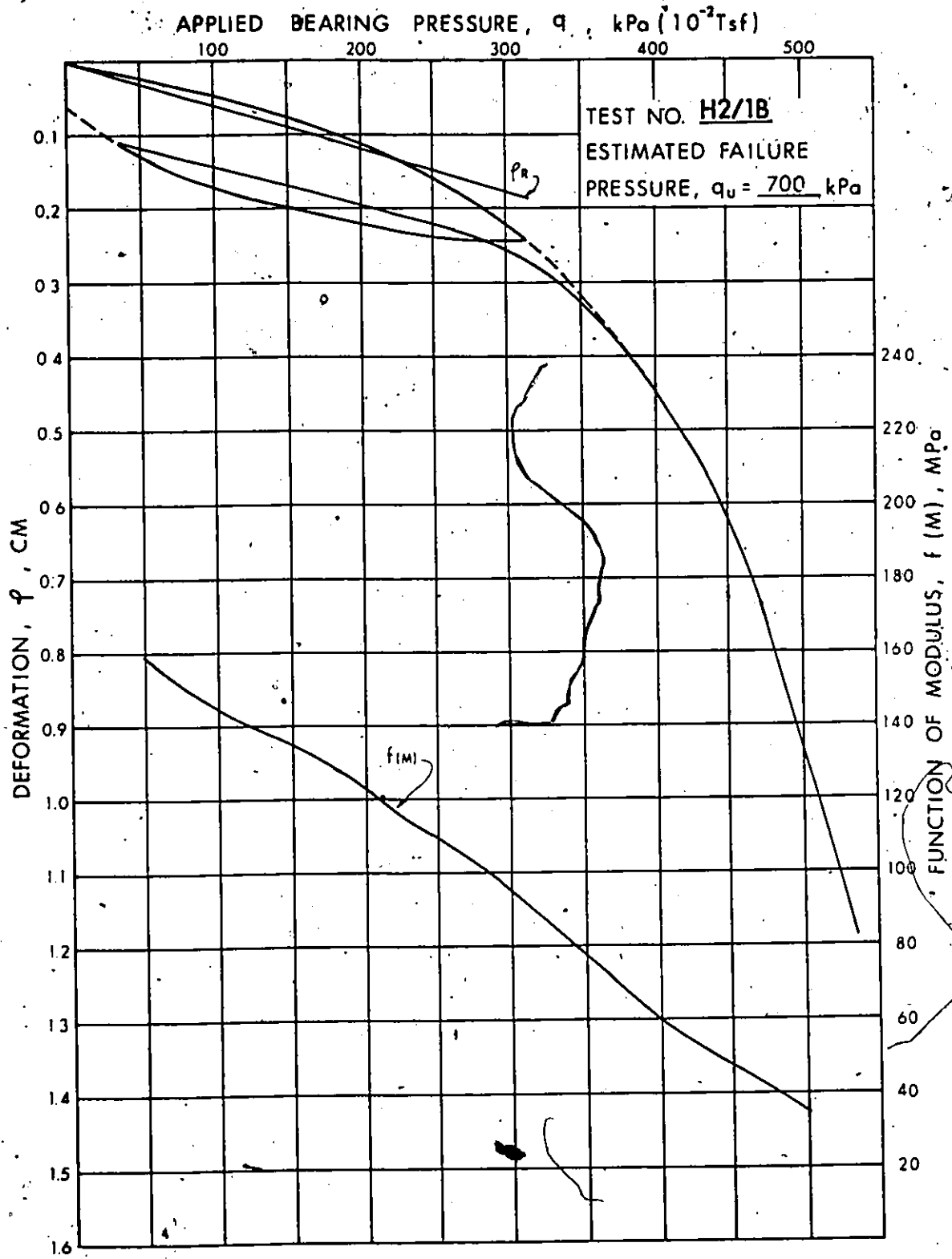
PRESENTATION OF: TOTAL DEFORMATION; RECOVERABLE DEFORMATION AND FUNCTION OF MODULUS VERSUS APPLIED BEARING PRESSURE.



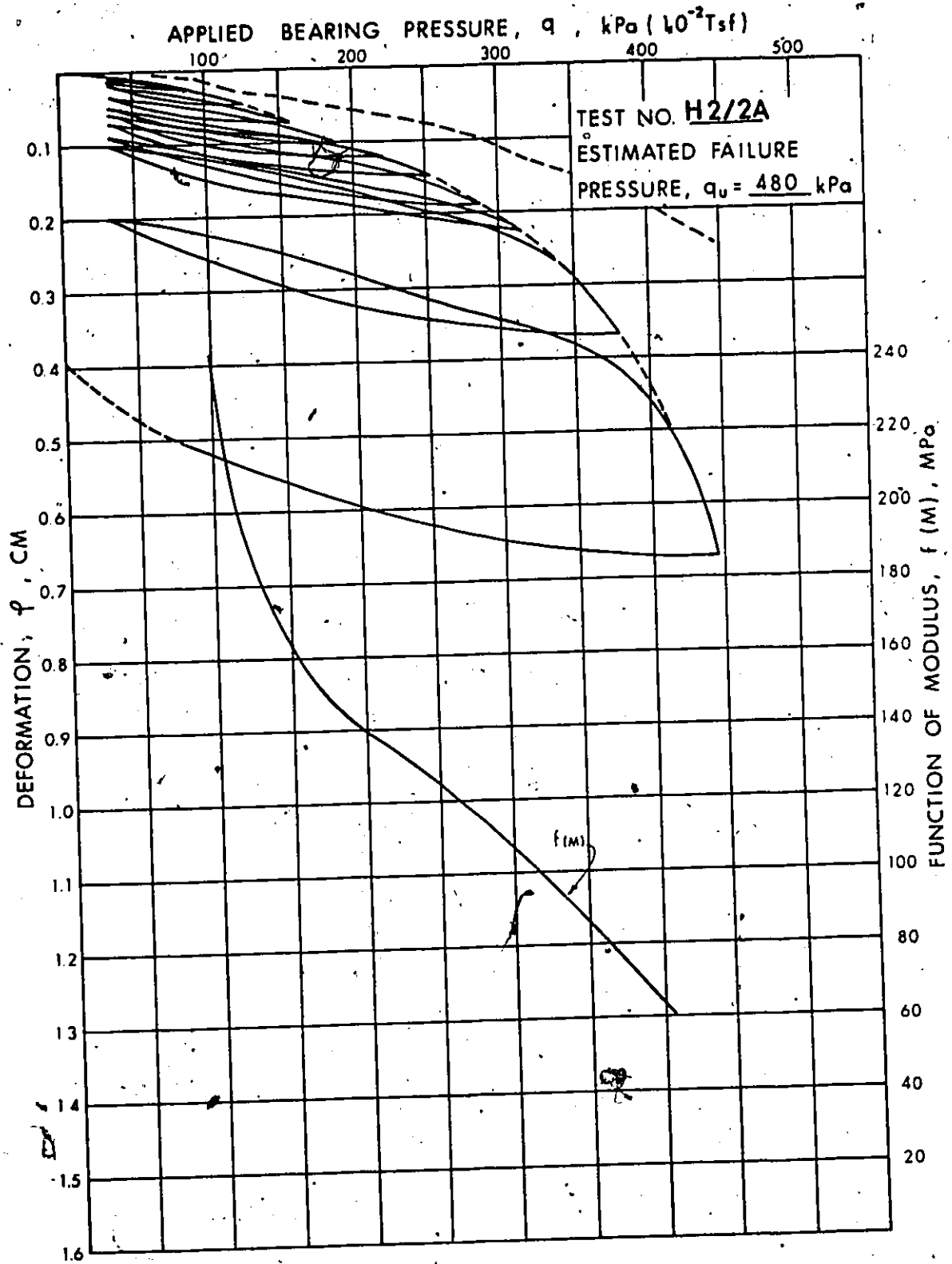
PRESENTATION OF: TOTAL DEFORMATION; RECOVERABLE DEFORMATION AND FUNCTION OF MODULUS VERSUS APPLIED BEARING PRESSURE.



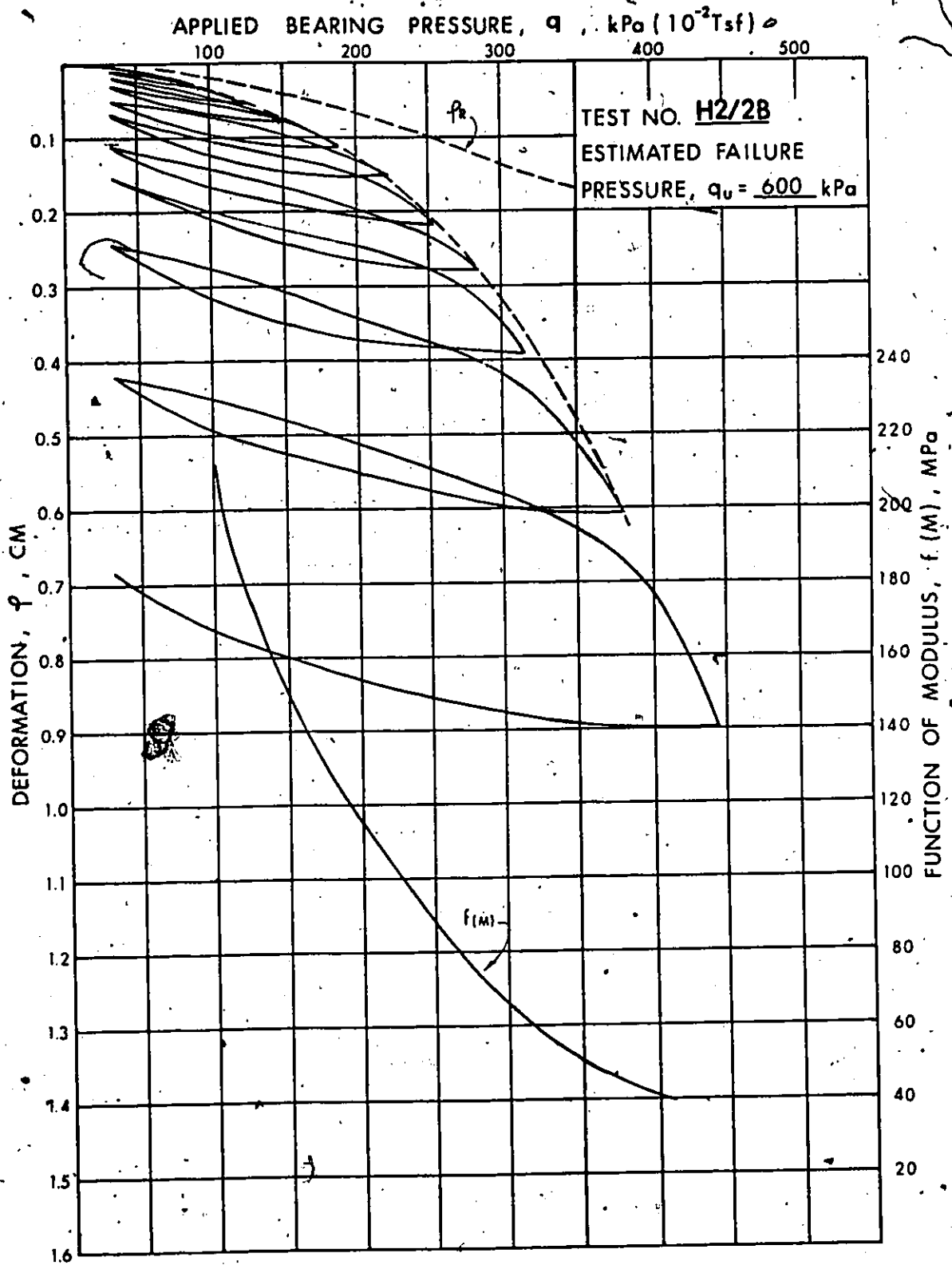
PRESENTATION OF: TOTAL DEFORMATION; RECOVERABLE DEFORMATION AND FUNCTION OF MODULUS VERSUS APPLIED BEARING PRESSURE.



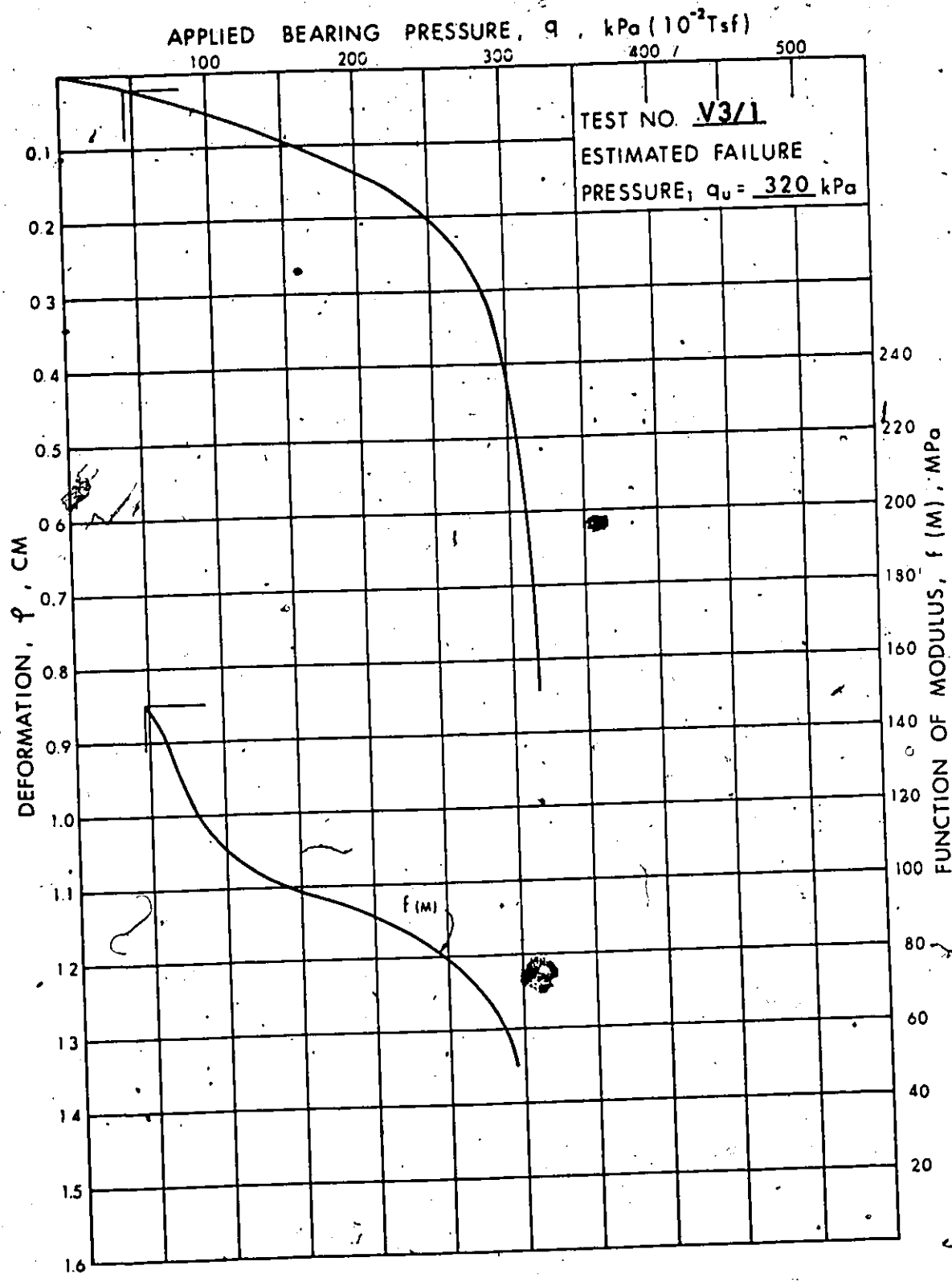
PRESENTATION OF: TOTAL DEFORMATION, RECOVERABLE DEFORMATION, AND FUNCTION OF MODULUS VERSUS APPLIED BEARING PRESSURE.



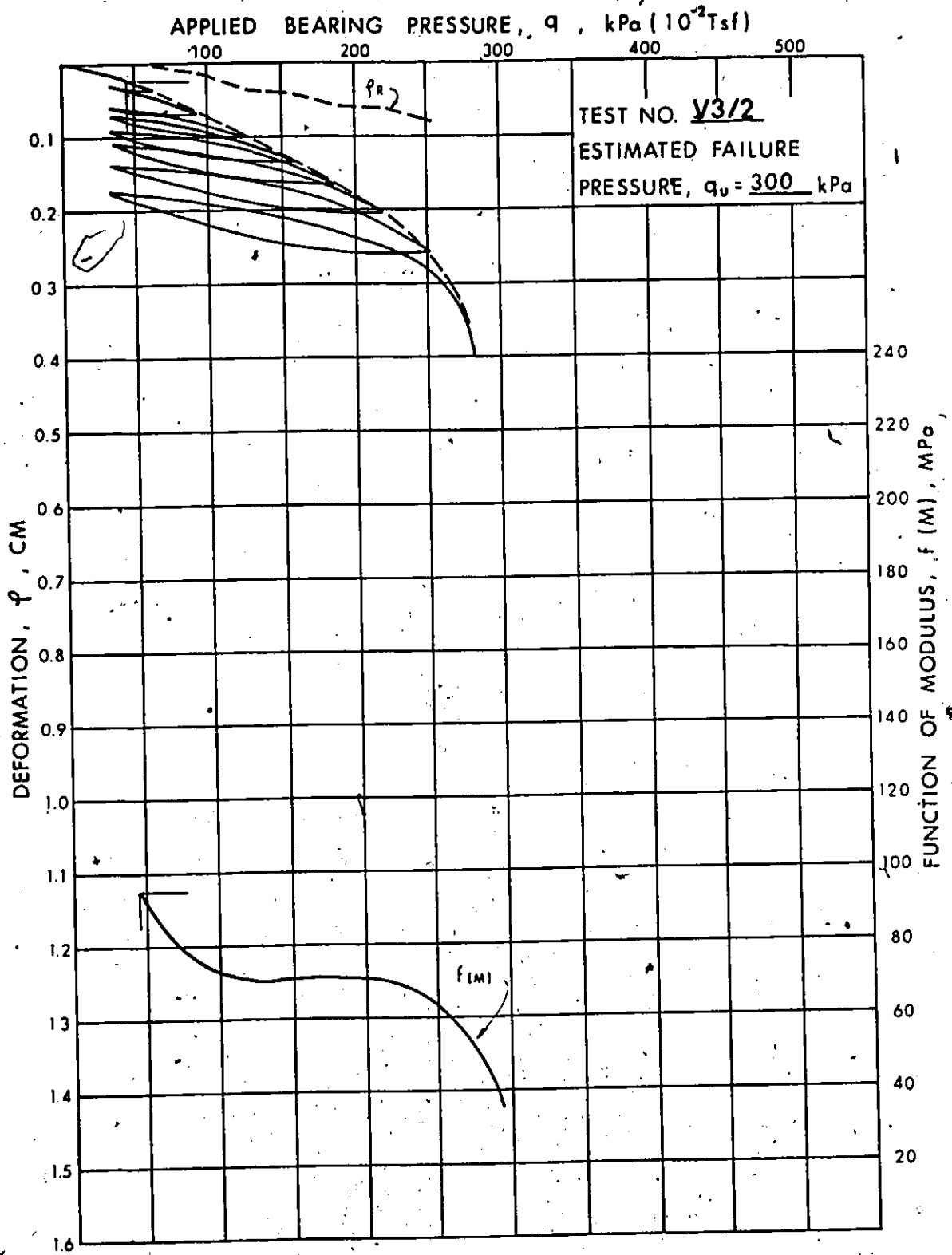
PRESENTATION OF: TOTAL DEFORMATION, RECOVERABLE DEFORMATION AND FUNCTION OF MODULUS VERSUS APPLIED BEARING PRESSURE.



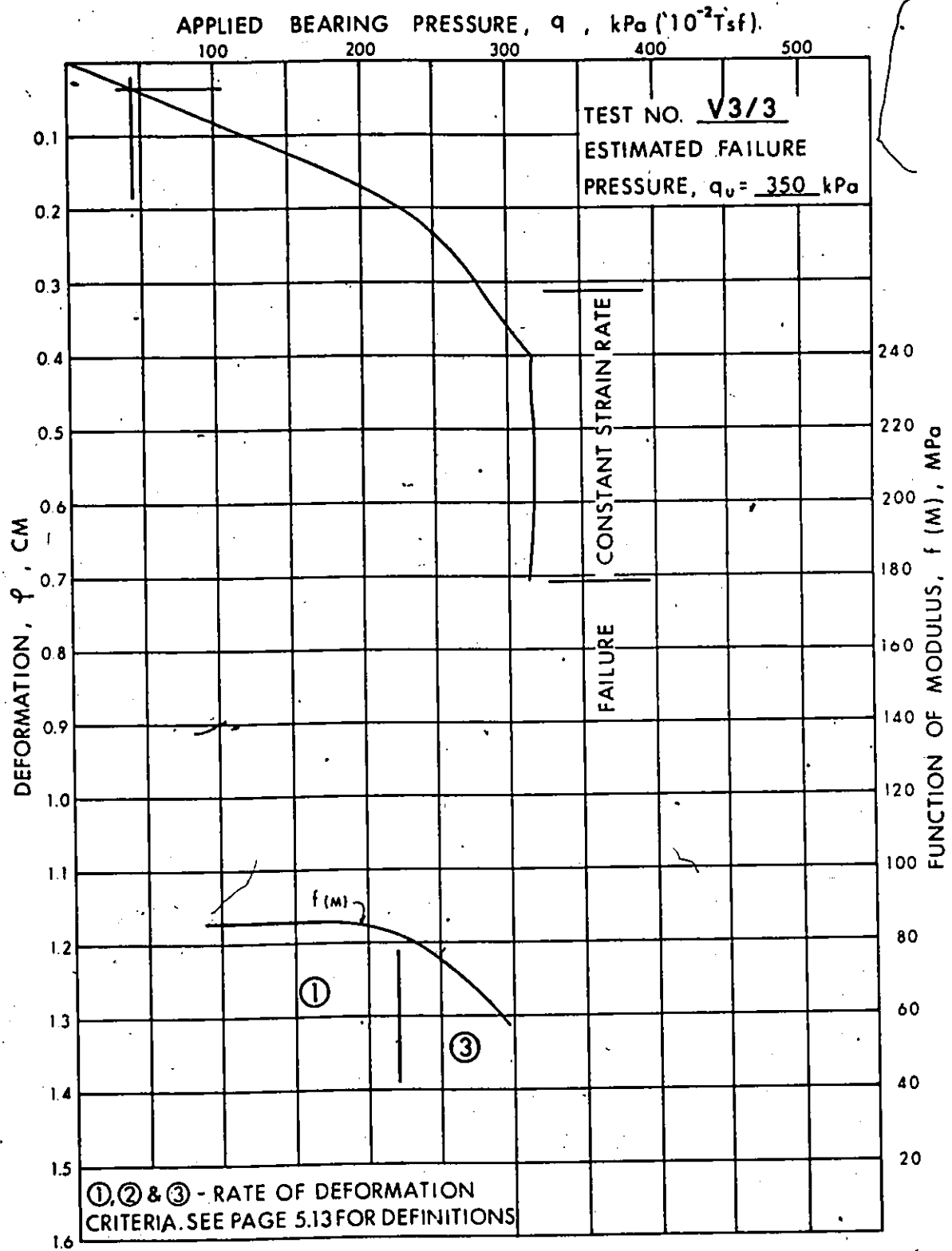
PRESENTATION OF: TOTAL DEFORMATION; RECOVERABLE DEFORMATION AND FUNCTION OF MODULUS VERSUS APPLIED BEARING PRESSURE.



PRESENTATION OF: TOTAL DEFORMATION ; RECOVERABLE DEFORMATION AND FUNCTION OF MODULUS VERSUS APPLIED BEARING PRESSURE.



PRESENTATION OF: TOTAL DEFORMATION, RECOVERABLE DEFORMATION AND FUNCTION OF MODULUS VERSUS APPLIED BEARING PRESSURE.



PRESENTATION OF : TOTAL DEFORMATION ; RECOVERABLE DEFORMATION AND FUNCTION OF MODULUS VERSUS APPLIED BEARING PRESSURE.

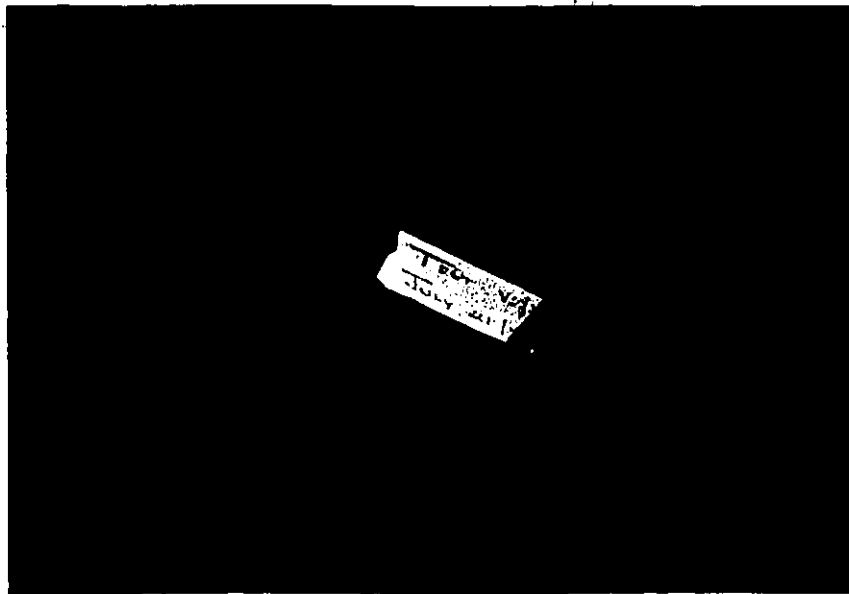
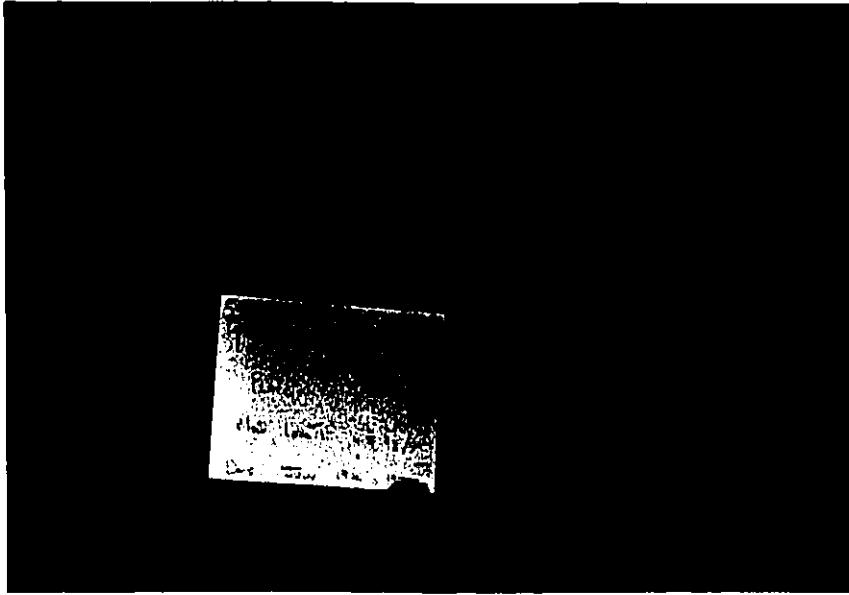
TEST NO.	AVERAGE TOTAL DEFORMATION		TILT - w.r.t. AVERAGE DEFORMATION		TILT - AS PERCENTAGE OF TOTAL DEFORMATION (a)
	(cm)	(a)	(cm)	(a)	
V1/1	0.322		0.053		16
V1/2	0.389		0.091		23
V1/3	0.269		0.030		28
H1/1A (R)	0.830		0.178		21
H1/1B	0.432		0.053		13
H1/2A	0.462		0.069		15
H1/2B (R)	0.401		0.104		26
H1/3A	0.233		0.053		23
H1/3B (R)	0.420		0.117		28
V2/1	0.305	Only one gauge used, but considerable tilting observed			
V2/2	0.274		0.119		44
V2/3	0.168		0.023		14
H2/1A	0.393		0.058		15
H2/1B (R)	0.266	Only one gauge used			-
H2/2A	0.221		0.066		30
H2/2B (R)	0.394		0.152		39
V3/1	0.838		0.051		6
V3/2 (R)	0.401 (b)		0.056 (b)		14 (b)
V3/3 (R)	0.389		0.074		19

**NOTES:**

- (a) At pressure 316 kPa (3.16 Tsf) - first cycle only
- (b) At pressure 284 kPa (2.84 Tsf)
- (R) eg: H1/1A (R) denotes rigid coupling between loading system and plate

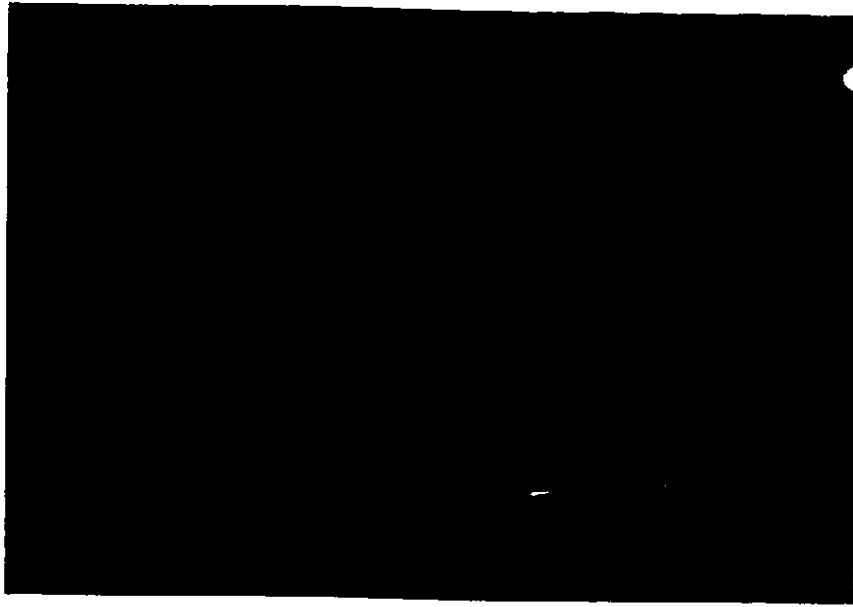
TABLE 5.1

PRESENTATION OF DEGREE OF TILT OF PLATE TESTS WITH RESPECT TO THE AVERAGE TOTAL DEFORMATION AND AS A PERCENTAGE OF AVERAGE TOTAL DEFORMATION



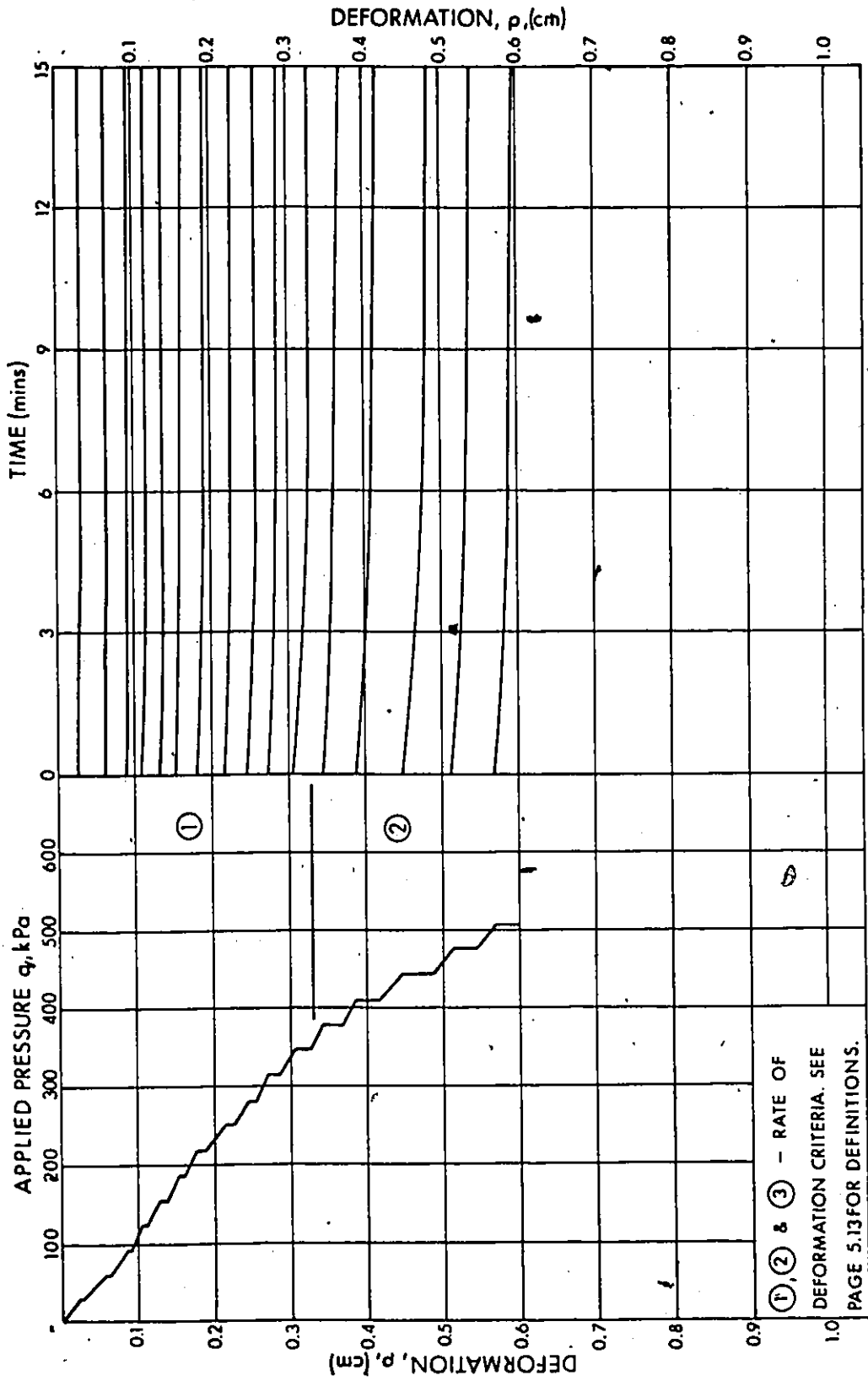
TYPICAL PHOTOGRAPHS  
OF SOME TEST FAILURES

PLATE 5.21(a)

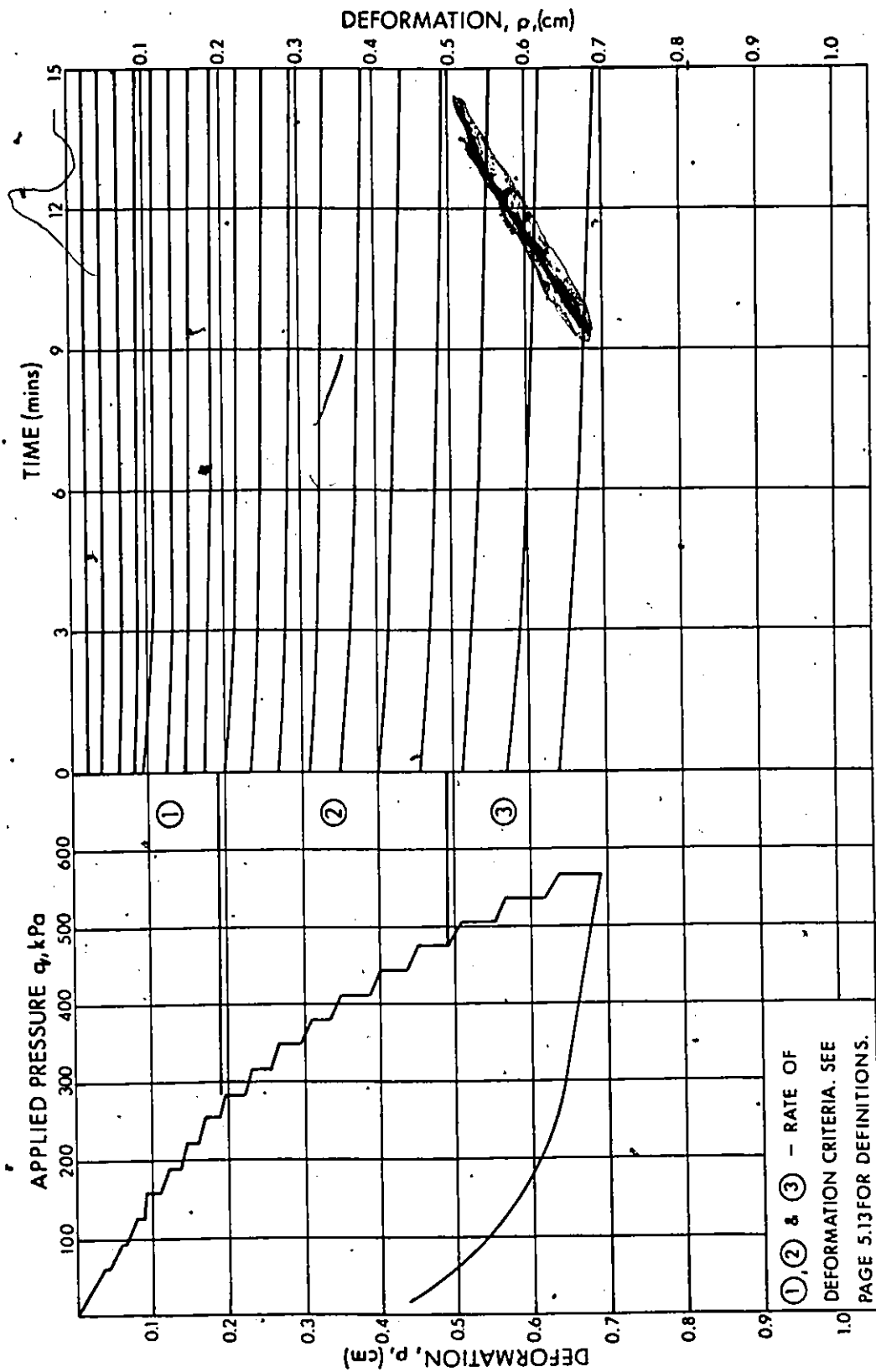


PHOTOGRAPHS OF  
A FAILURE WEDGE.

PLATE 5.21(b)

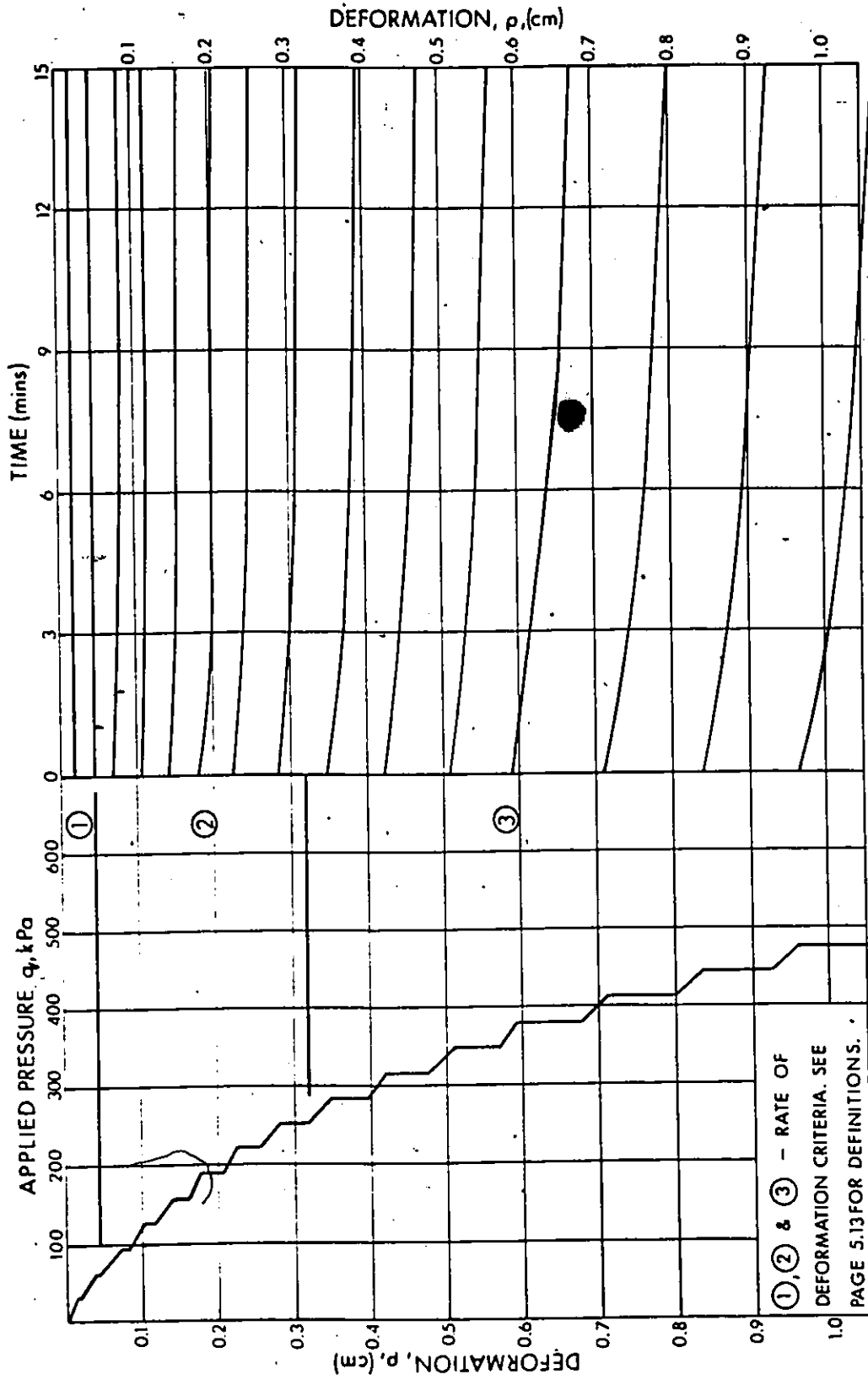


STEPWISE PRESSURE - DEFORMATION RESPONSE AND TIME - DEFORMATION RESPONSE. TEST NO. Y1/3

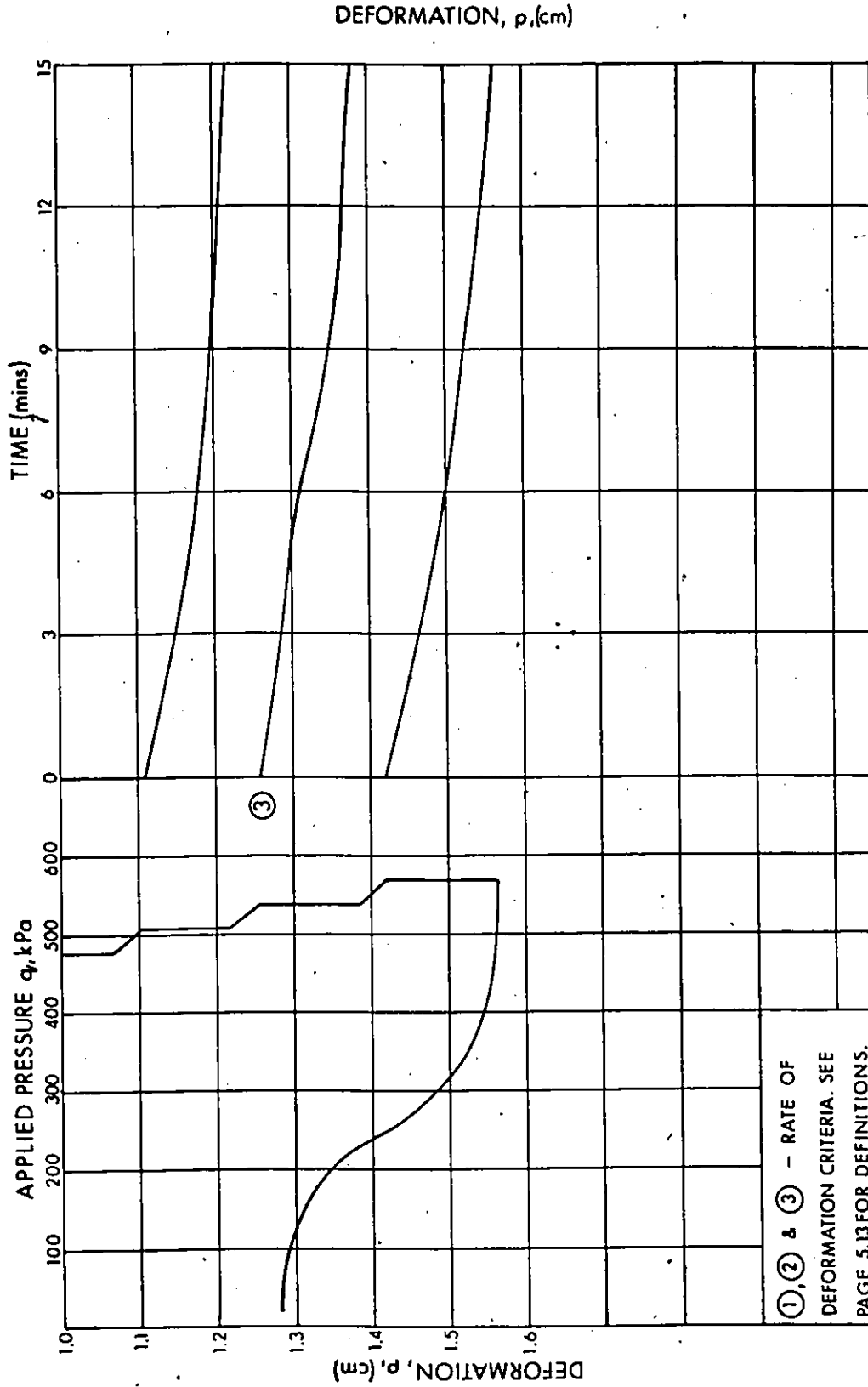


①, ② & ③ - RATE OF DEFORMATION CRITERIA. SEE PAGE 5.13 FOR DEFINITIONS.

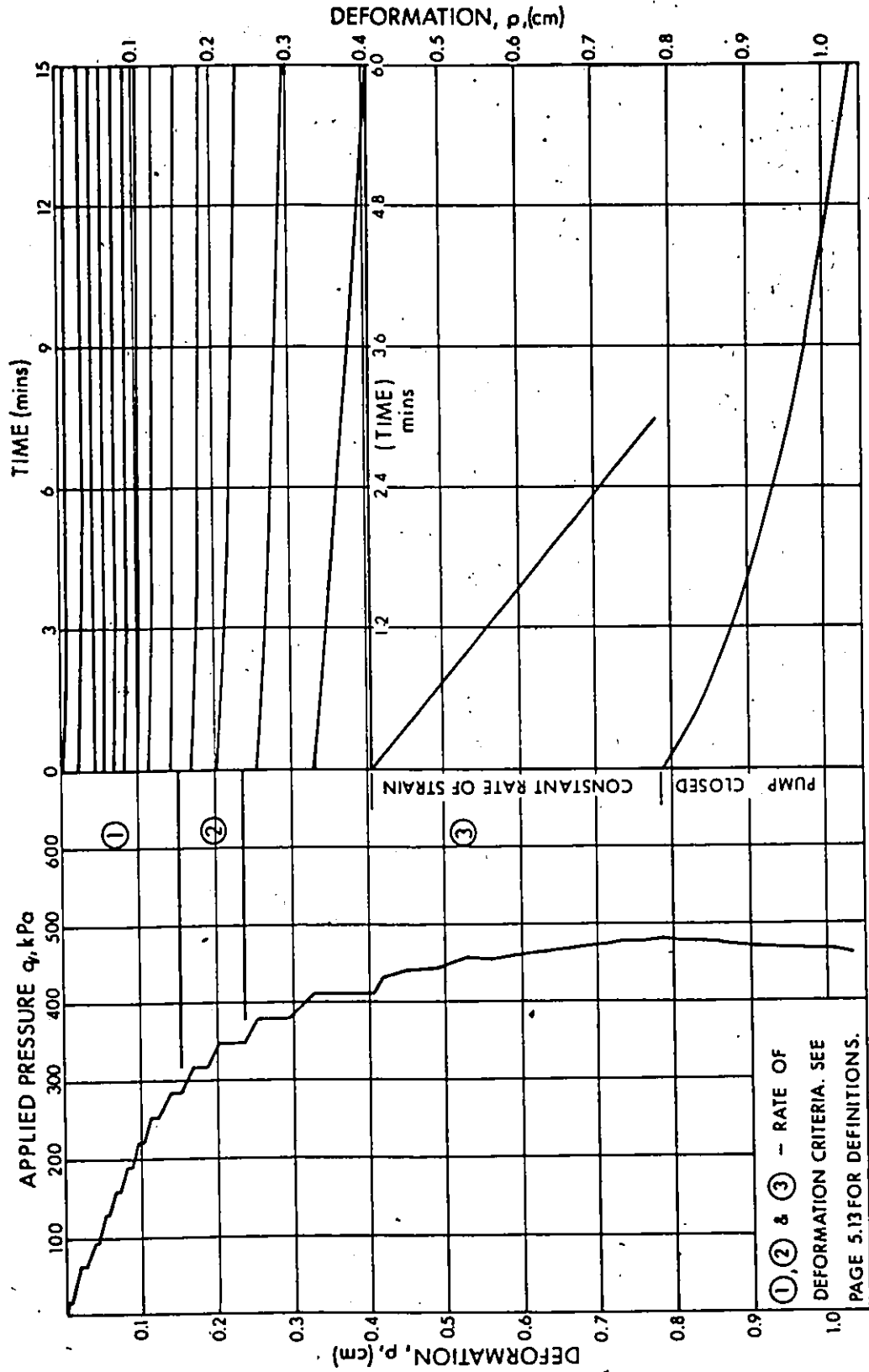
STEPWISE PRESSURE - DEFORMATION RESPONSE AND TIME - DEFORMATION RESPONSE. TEST NO. H1/3A



STEPWISE PRESSURE - DEFORMATION RESPONSE AND TIME - DEFORMATION RESPONSE. TEST NO. H1/3B

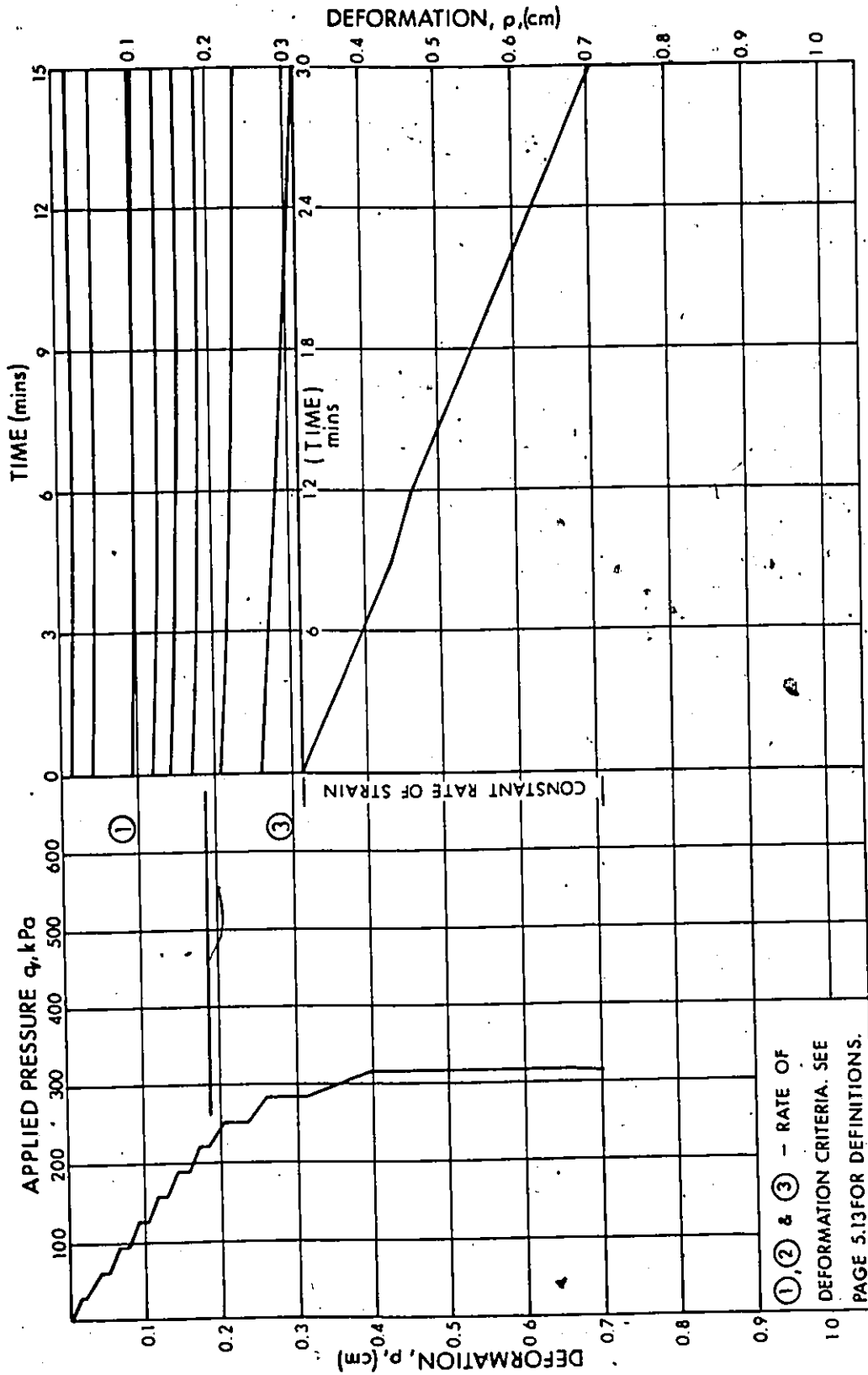


STEPWISE PRESSURE - DEFORMATION RESPONSE AND TIME - DEFORMATION RESPONSE. TEST NO. HI/3B



①, ② & ③ - RATE OF DEFORMATION CRITERIA. SEE PAGE 5.13 FOR DEFINITIONS.

STEPWISE PRESSURE - DEFORMATION RESPONSE AND TIME - DEFORMATION RESPONSE. TEST NO. Y2/3



STEPWISE PRESSURE - DEFORMATION RESPONSE AND TIME - DEFORMATION RESPONSE. TEST NO. V3/3

RATE OF DEFORMATION CRITERIA TEST NO.	① / ②		② / ③	
	$q_{act}$ (kPa)	$q_{act}/q_u$	$q_{act}$ (kPa)	$q_{act}/q_u$
V1/3	3.48	0.46	-	-
H1/3A	2.57	0.29	4.75	0.53
H1/3B	0.64	0.09	2.53	0.36
V2/3	2.86	0.59	3.48	0.72
V3/3	① / ③			
	$q_{act}$ (kPa)		$q_{act}/q_u$	
	2.20		0.63	

TABLE 5.2

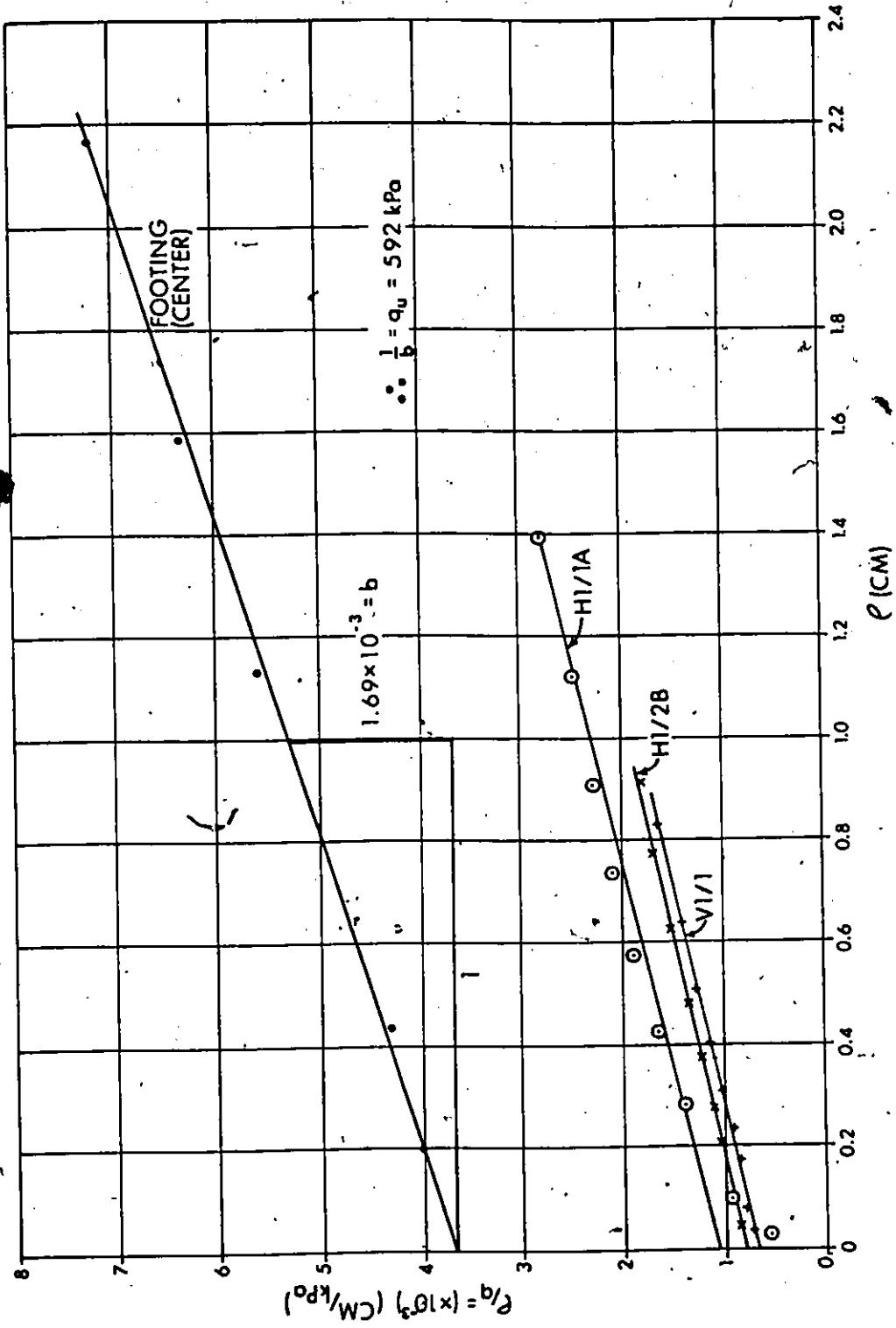
ACTUAL BEARING PRESSURES AND BEARING PRESSURE RATIOS SEPARATING  
DIFFERENT RATE OF DEFORMATION CRITERIA  
(As Defined On Page 5-13)

FAILURE PRESSURE FROM VARIOUS METHODS

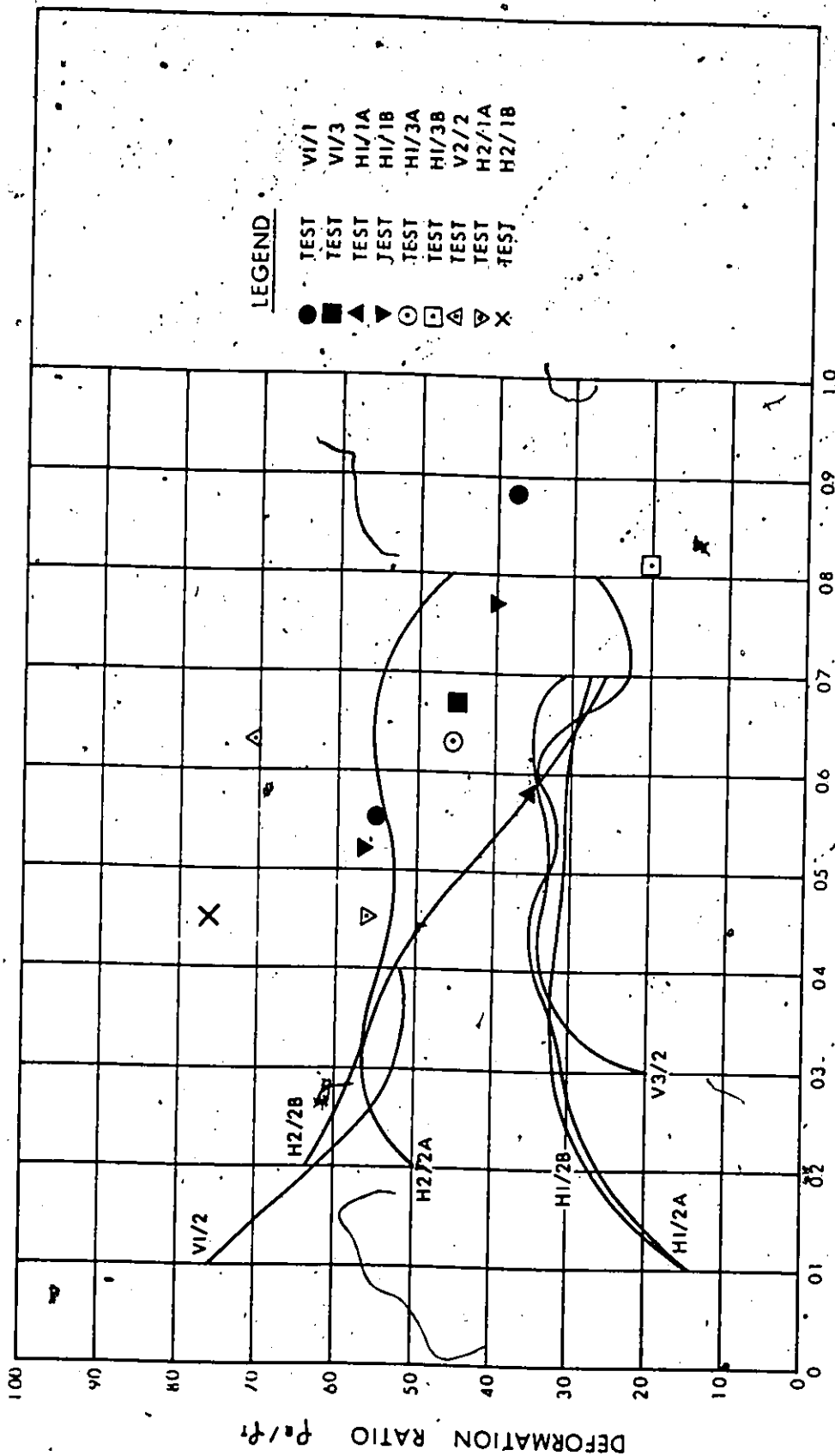
<u>TEST NO.</u>	<u>SHAPE OF q VERSUS <math>\rho</math> CURVE</u>	<u>MITCHEL ET AL. (1973)</u>	<u>KONDNER &amp; KRIZEK (1962)</u>	<u>CHOSEN FOR ANALYSIS</u>
		(kPa)		
V1/1	570	900	840	570
V1/2	650	900	885	650
V1/3	700+	900	847	750
H1/1A	-700	-	645	650
H1/1B	700+	-	730	730
H1/2A	-700	-	926	700
H1/2B	-800	-	943	800
H1/3A	700+	-	1163	900
H1/3B	-700	-	546	700
V2/1	500	260	463	500
V2/2	500	260	629	500
V2/3	485	260	719	485
H2/1A	-700	-	513	700
H2/1B	-700	-	617	700
H2/2A	480	-	543	480
H2/2B	600	-	518	600
V3/1	320	206	431	320
V3/2	300	206	735	300
V3/3	350	206	578	350
Footing Test	600+	783	592	780

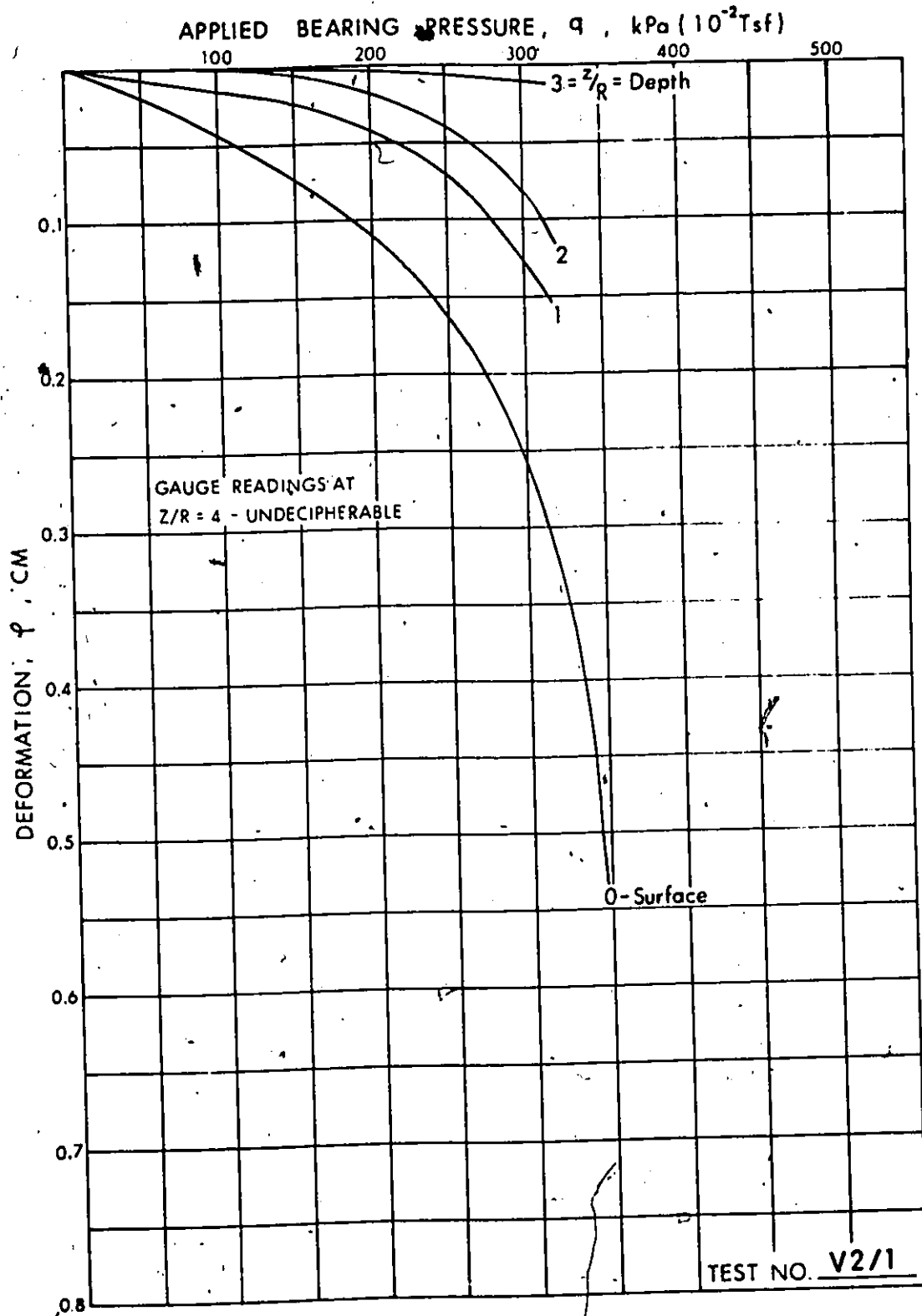
TABLE 5.3

COMPARISON OF METHODS OF ESTIMATING FAILURE PRESSURE

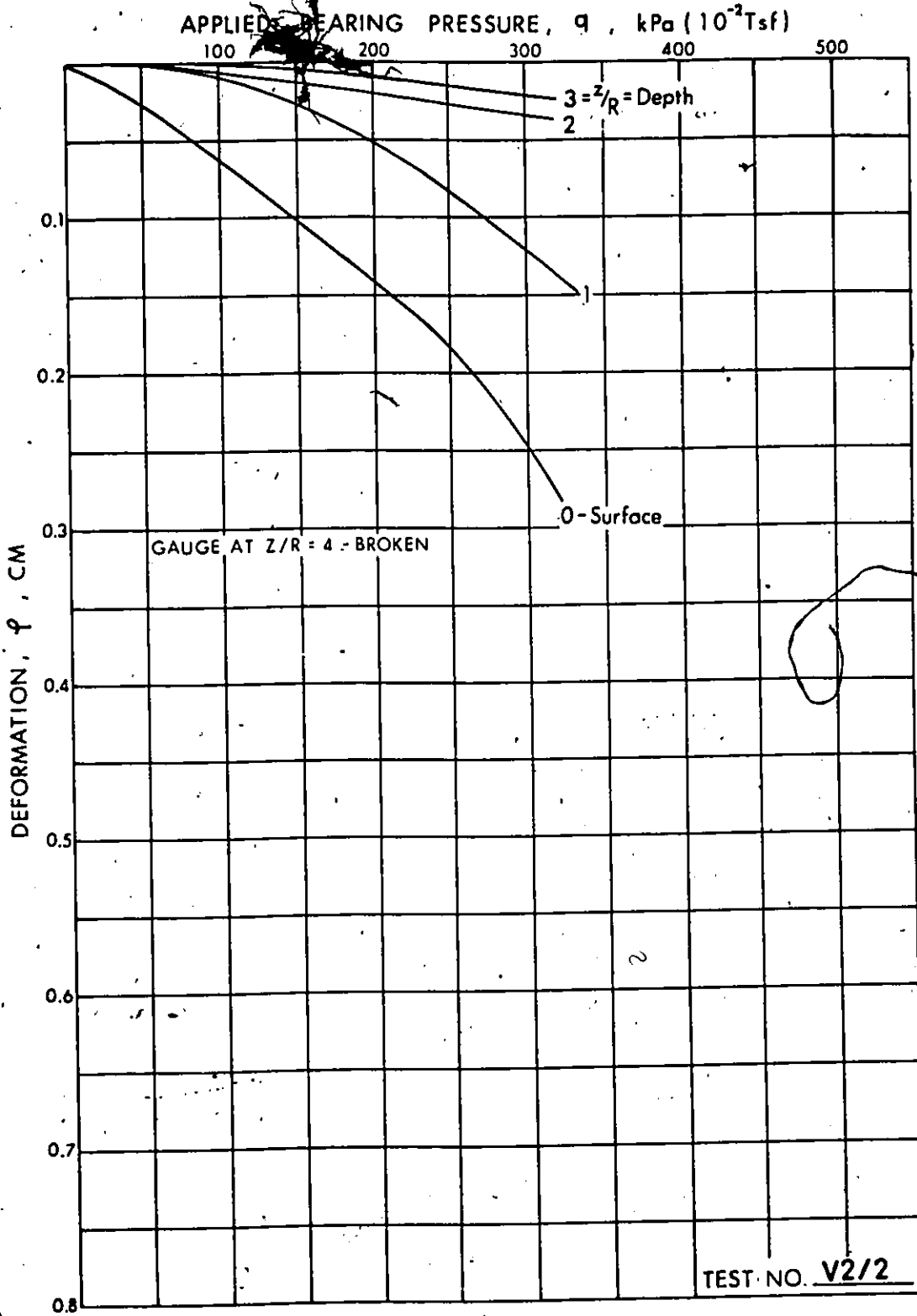


GRAPHICAL METHOD OF DETERMINING ULTIMATE FAILURE PRESSURE  
(KONDNER AND KRIZEK, 1962)

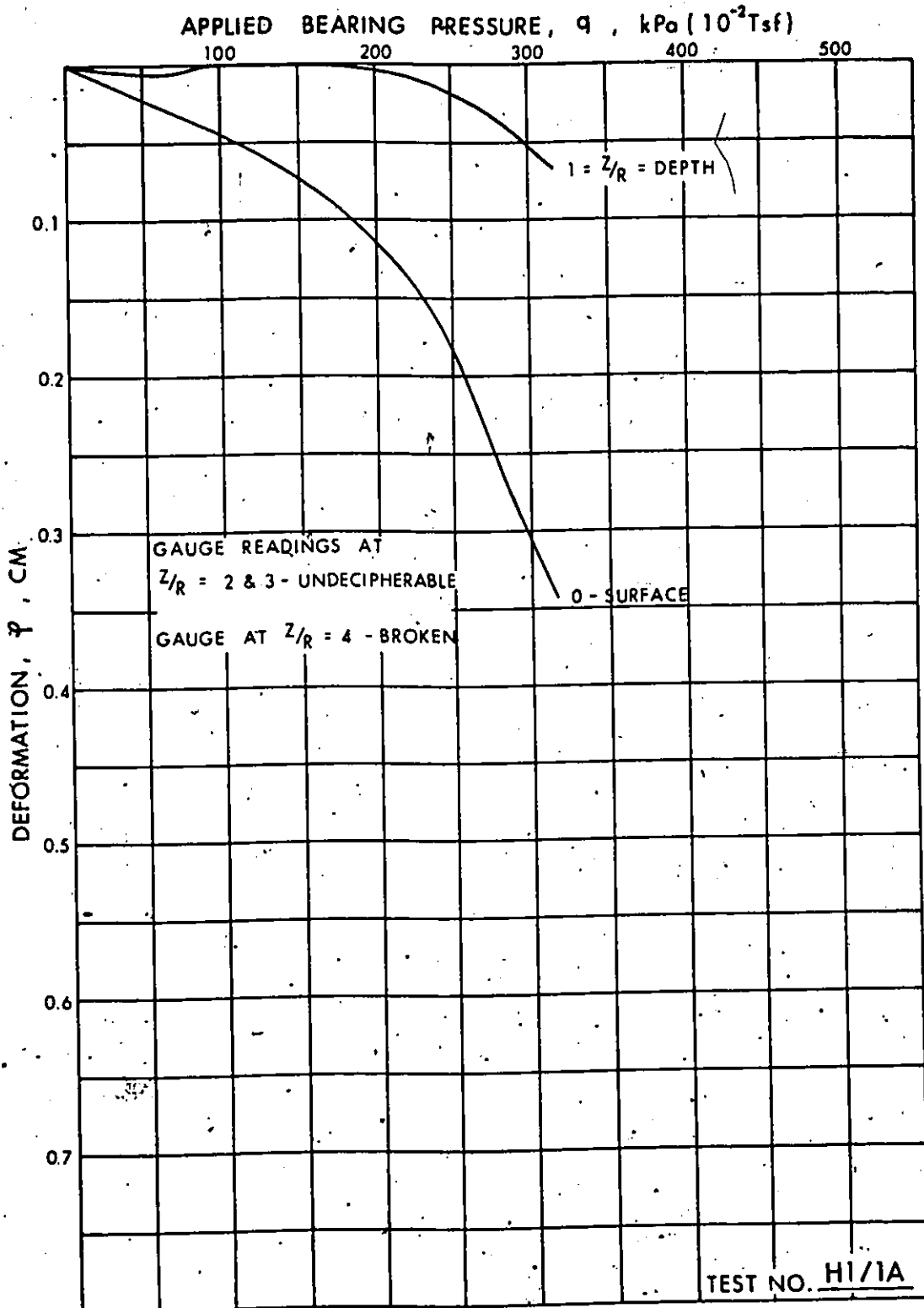




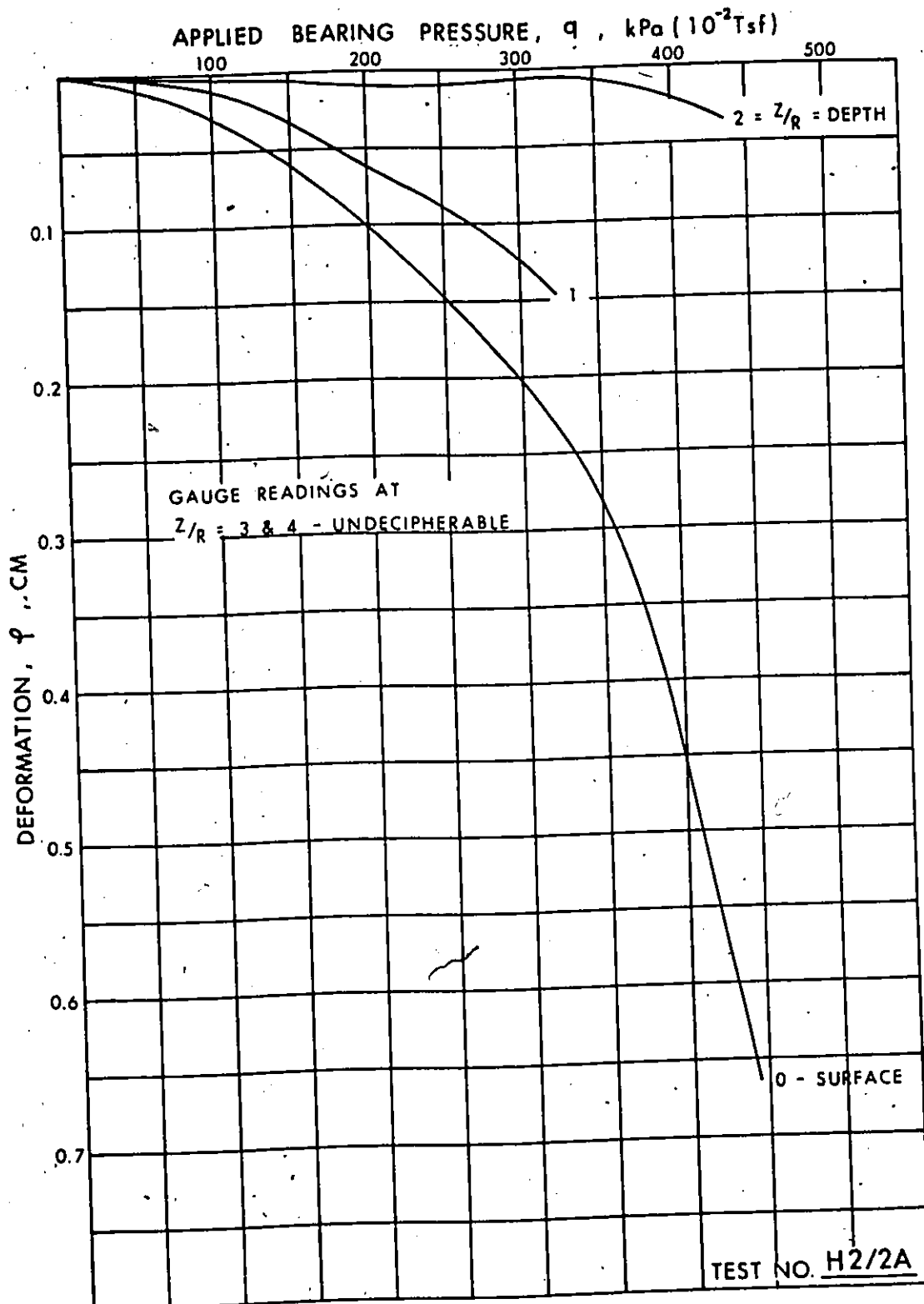
TOTAL DEFORMATION AND DEFORMATION AT VARIOUS DEPTHS BELOW LOADED SURFACE.



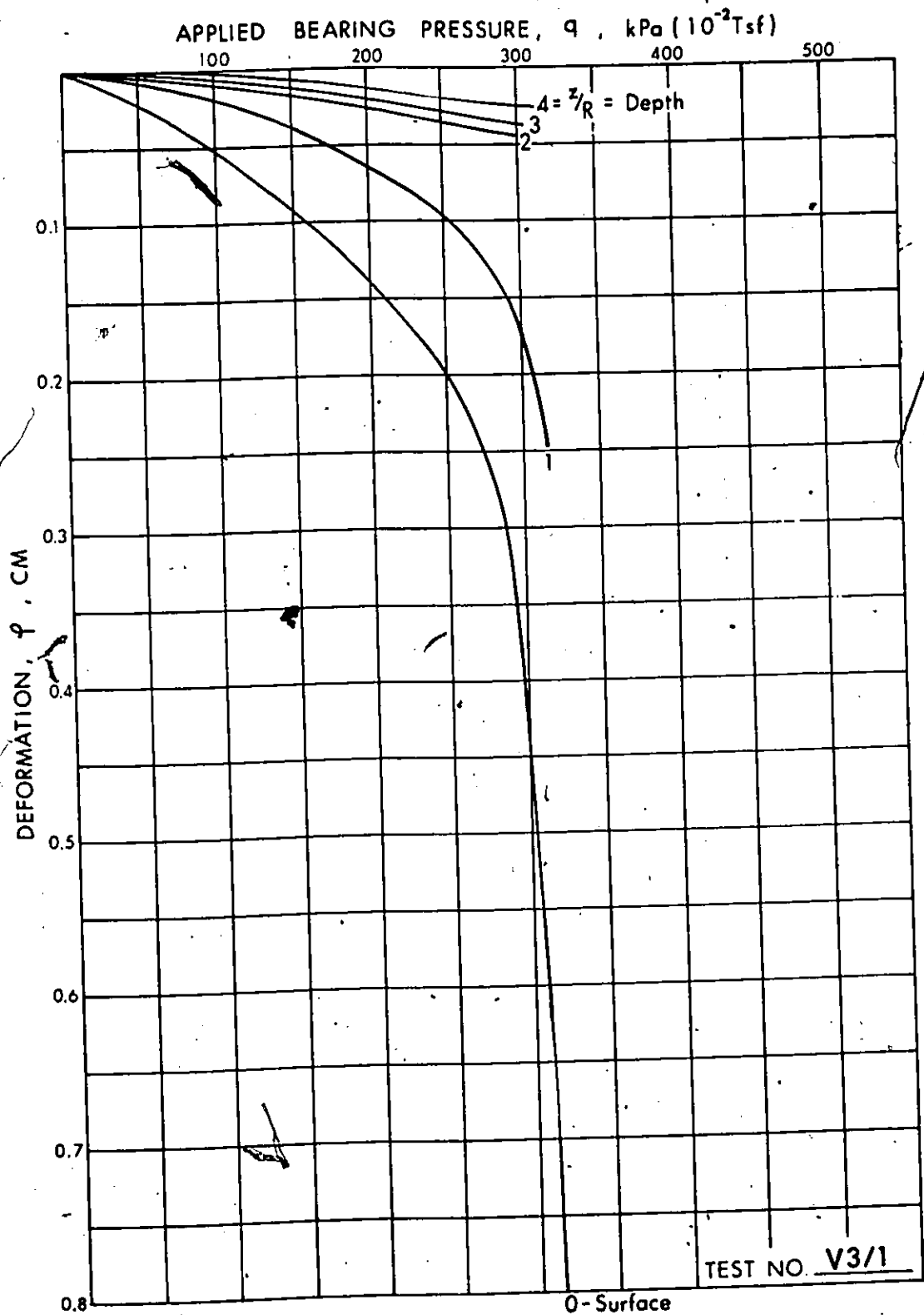
TOTAL DEFORMATION AND DEFORMATION AT VARIOUS DEPTHS BELOW LOADED SURFACE:



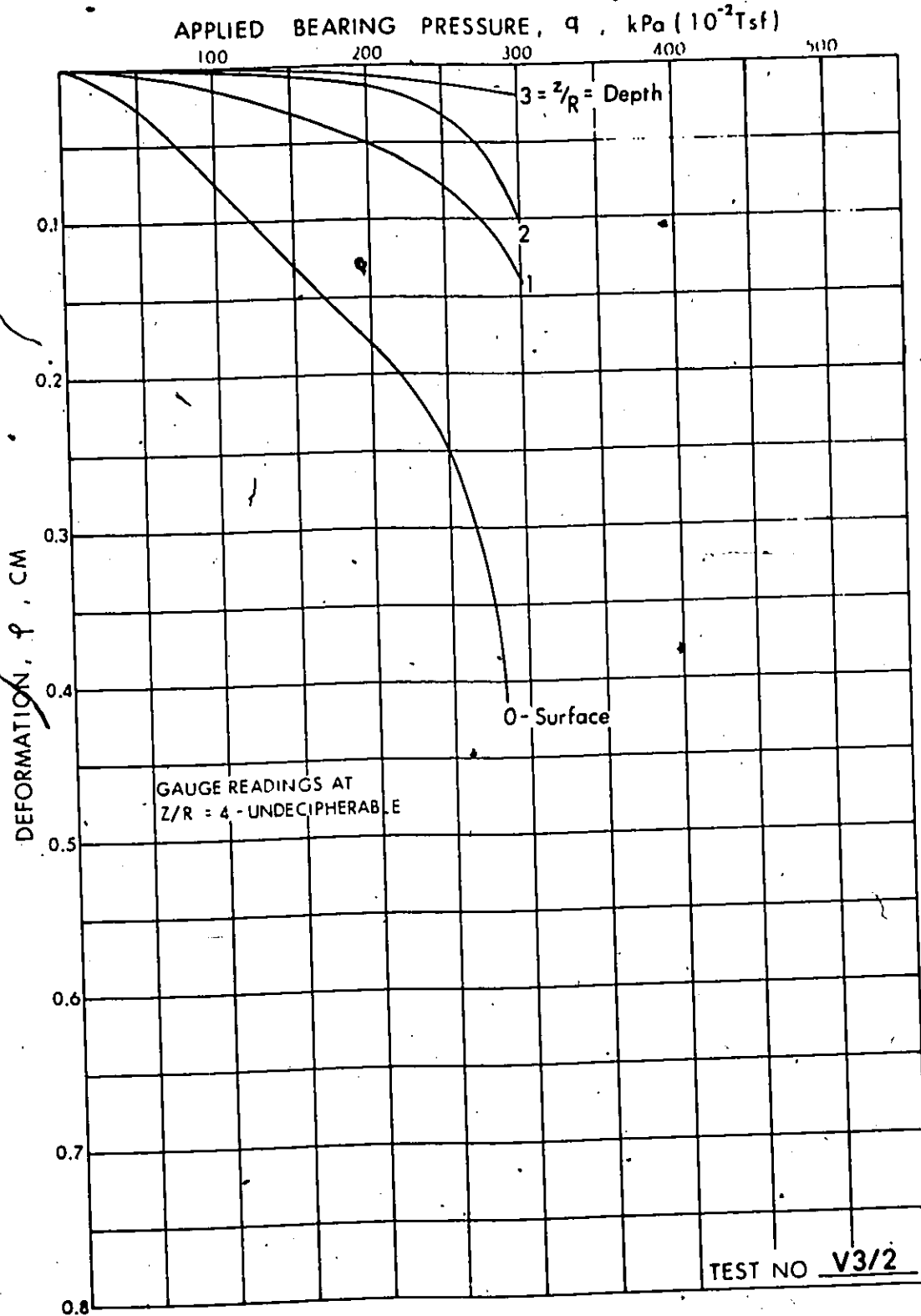
TOTAL DEFORMATION AND DEFORMATION AT VARIOUS DEPTHS BELOW LOADED SURFACE.



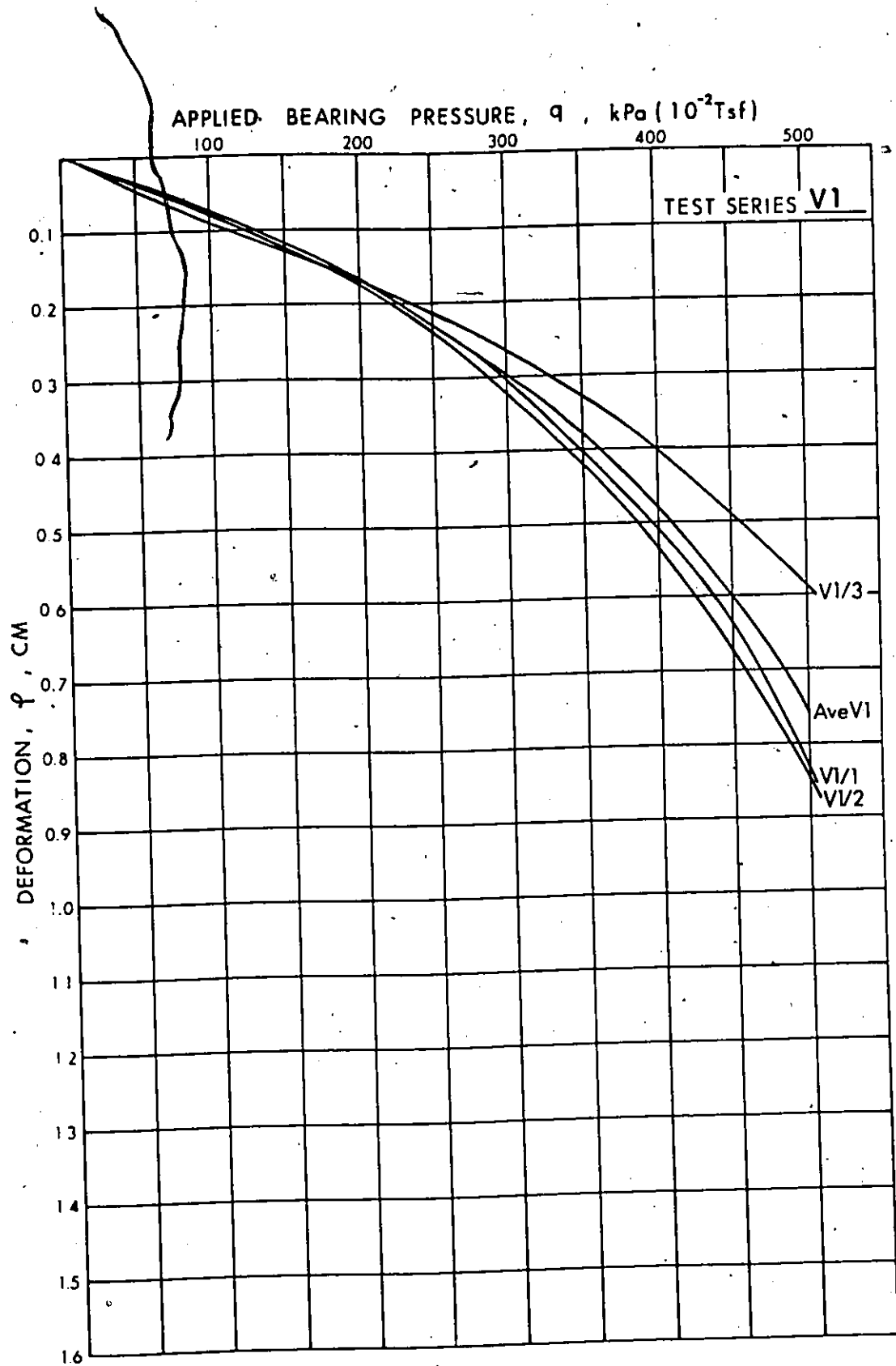
TOTAL DEFORMATION AND DEFORMATION AT VARIOUS DEPTHS BELOW LOADED SURFACE.



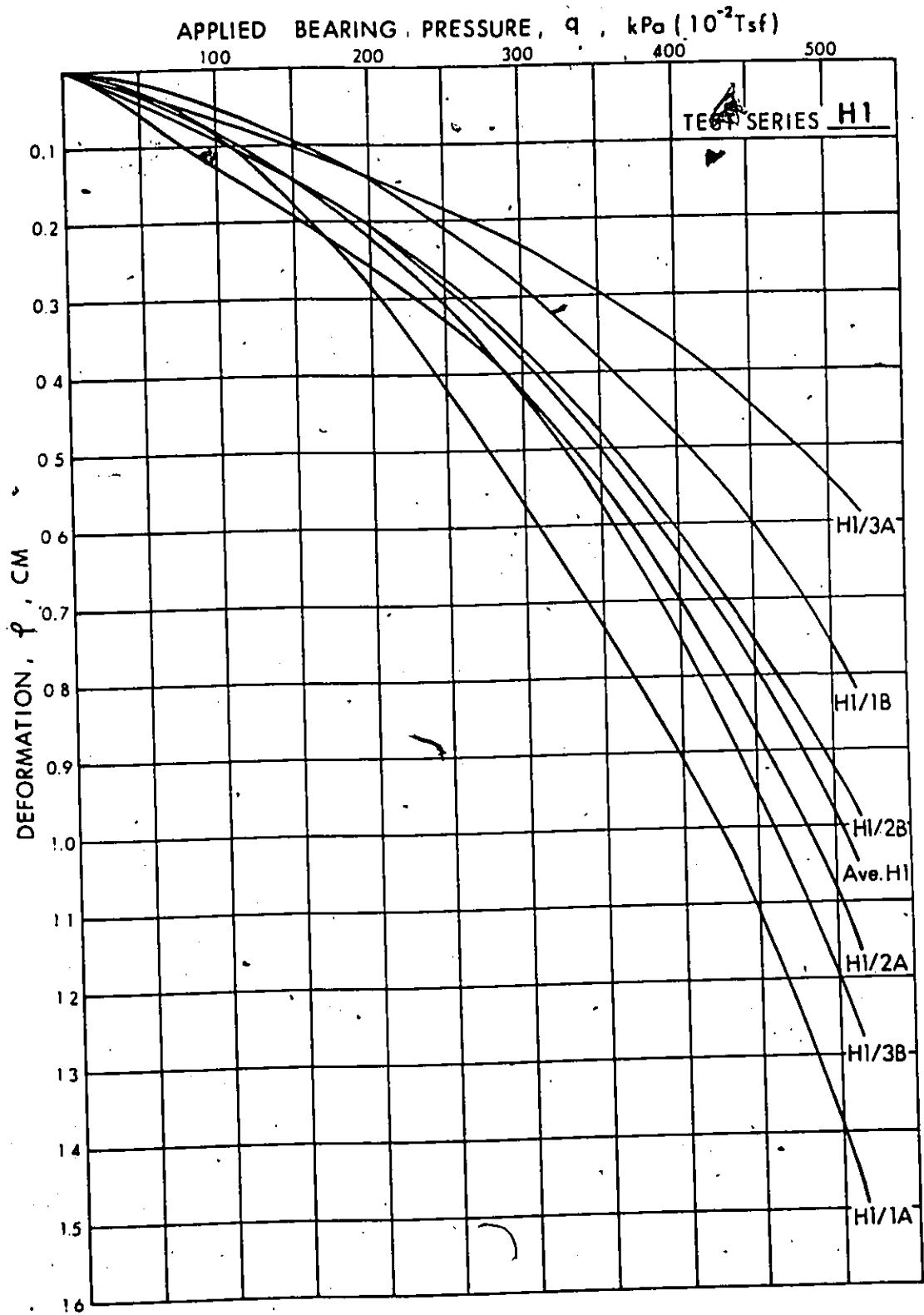
TOTAL DEFORMATION AND DEFORMATION AT VARIOUS DEPTHS BELOW LOADED SURFACE.



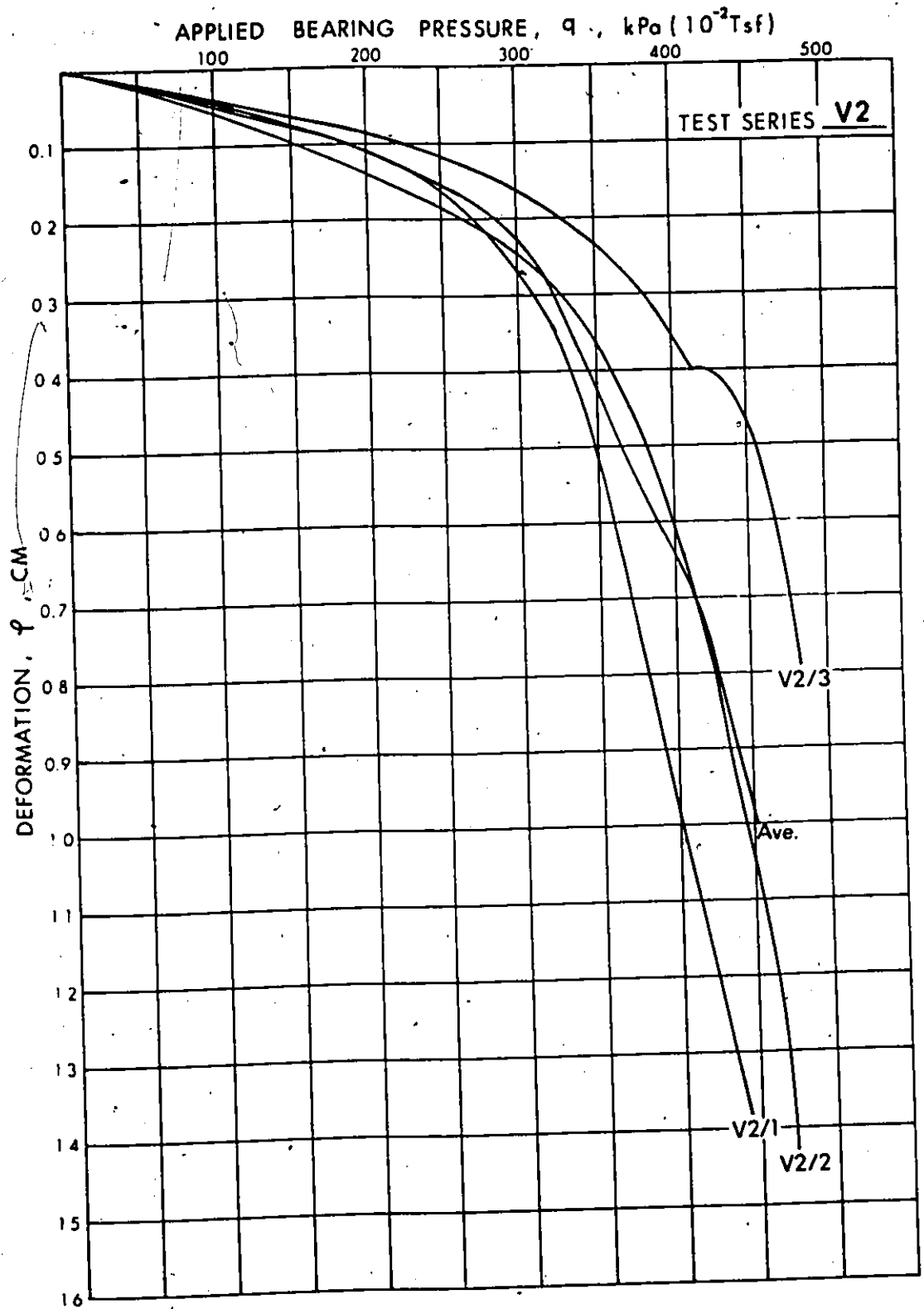
TOTAL DEFORMATION AND DEFORMATION AT VARIOUS DEPTHS BELOW LOADED SURFACE.



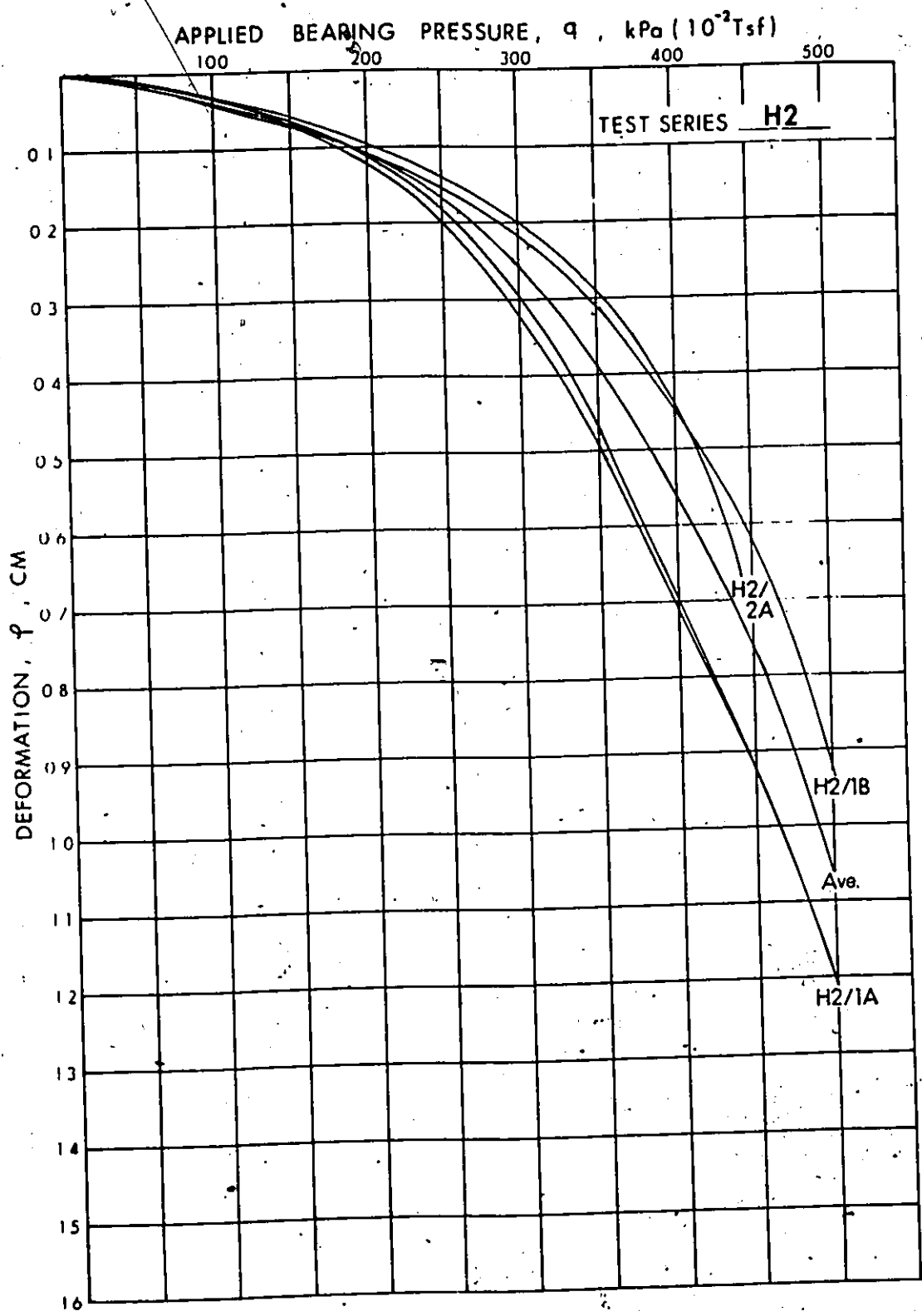
COMPARISON BETWEEN PRESSURE - DEFORMATION RESPONSE FOR TESTS WITHIN A TEST SERIES.



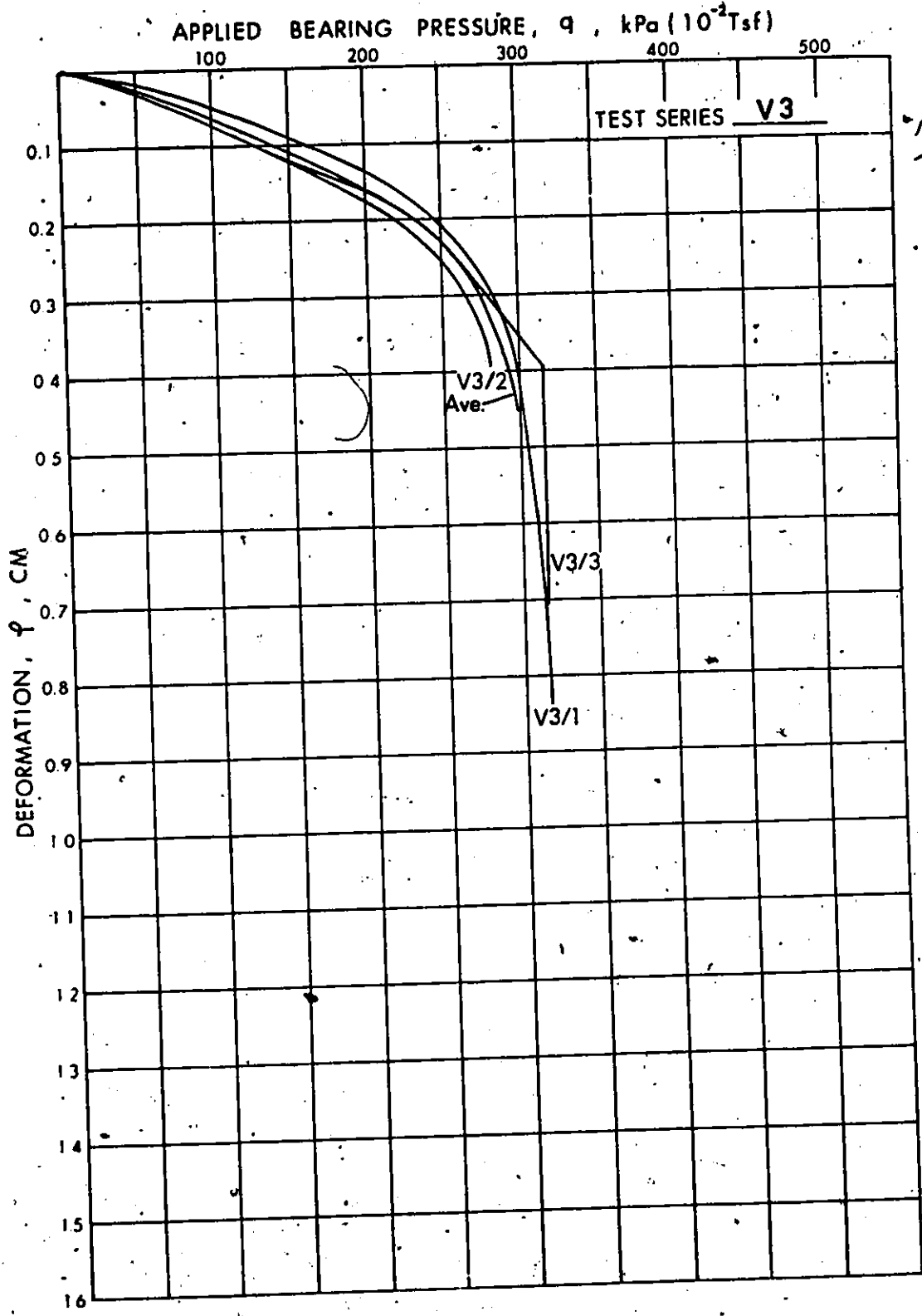
COMPARISON BETWEEN PRESSURE - DEFORMATION RESPONSE  
FOR TESTS WITHIN A TEST SERIES.



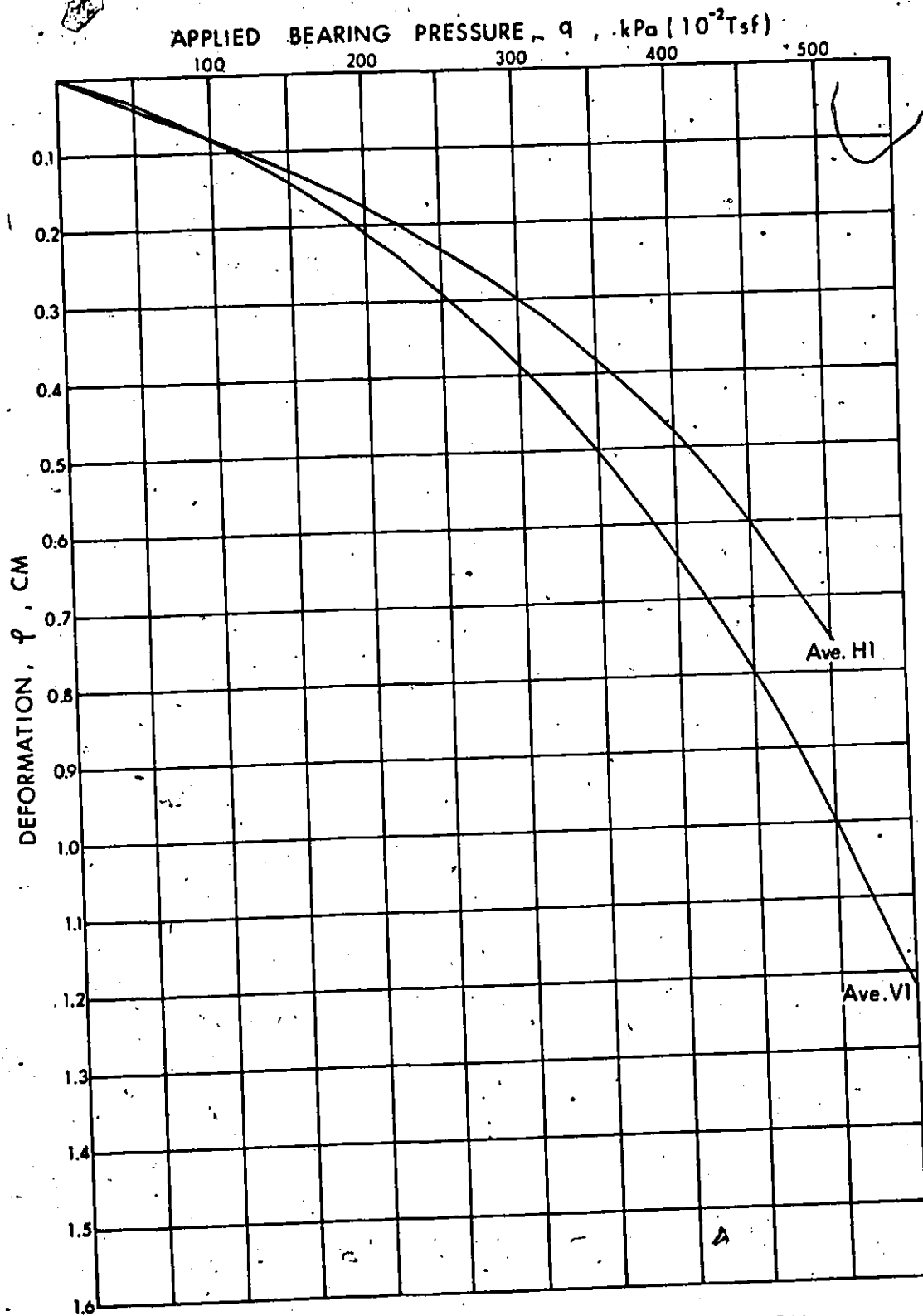
COMPARISON BETWEEN PRESSURE - DEFORMATION RESPONSE  
FOR TESTS WITHIN A TEST SERIES.



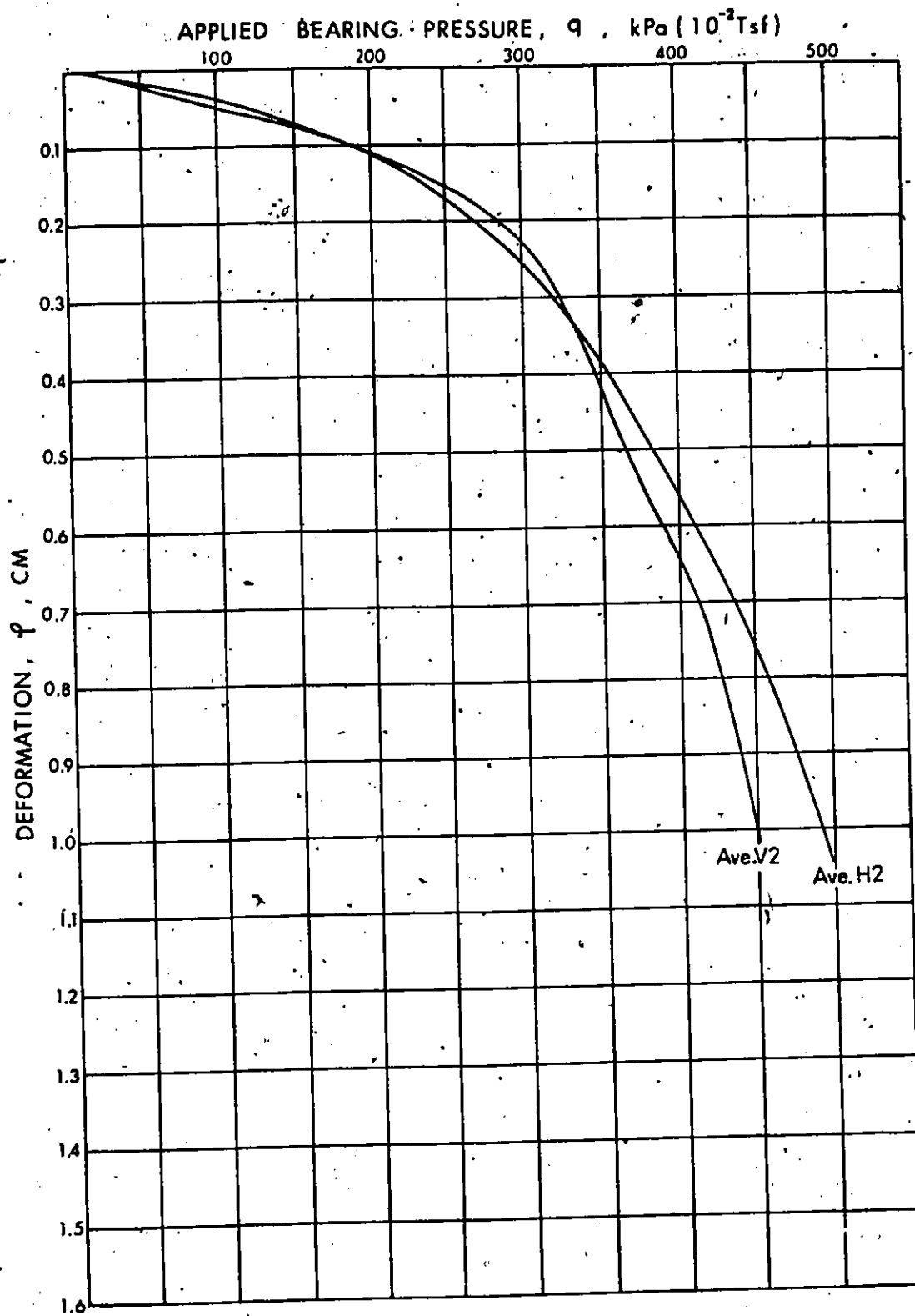
COMPARISON BETWEEN PRESSURE - DEFORMATION RESPONSE  
FOR TESTS WITHIN A TEST SERIES.



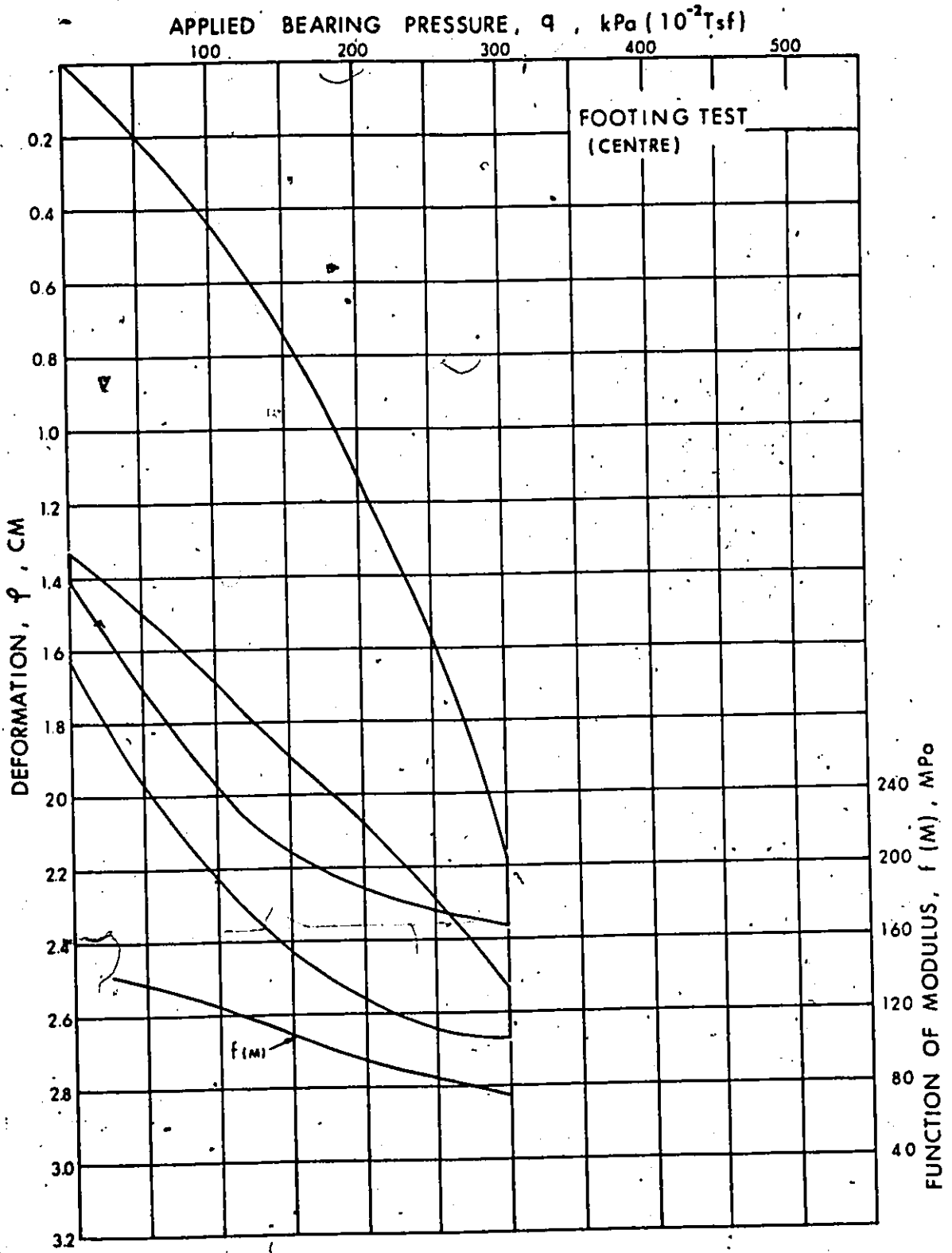
COMPARISON BETWEEN PRESSURE - DEFORMATION RESPONSE FOR TESTS WITHIN A TEST SERIES.



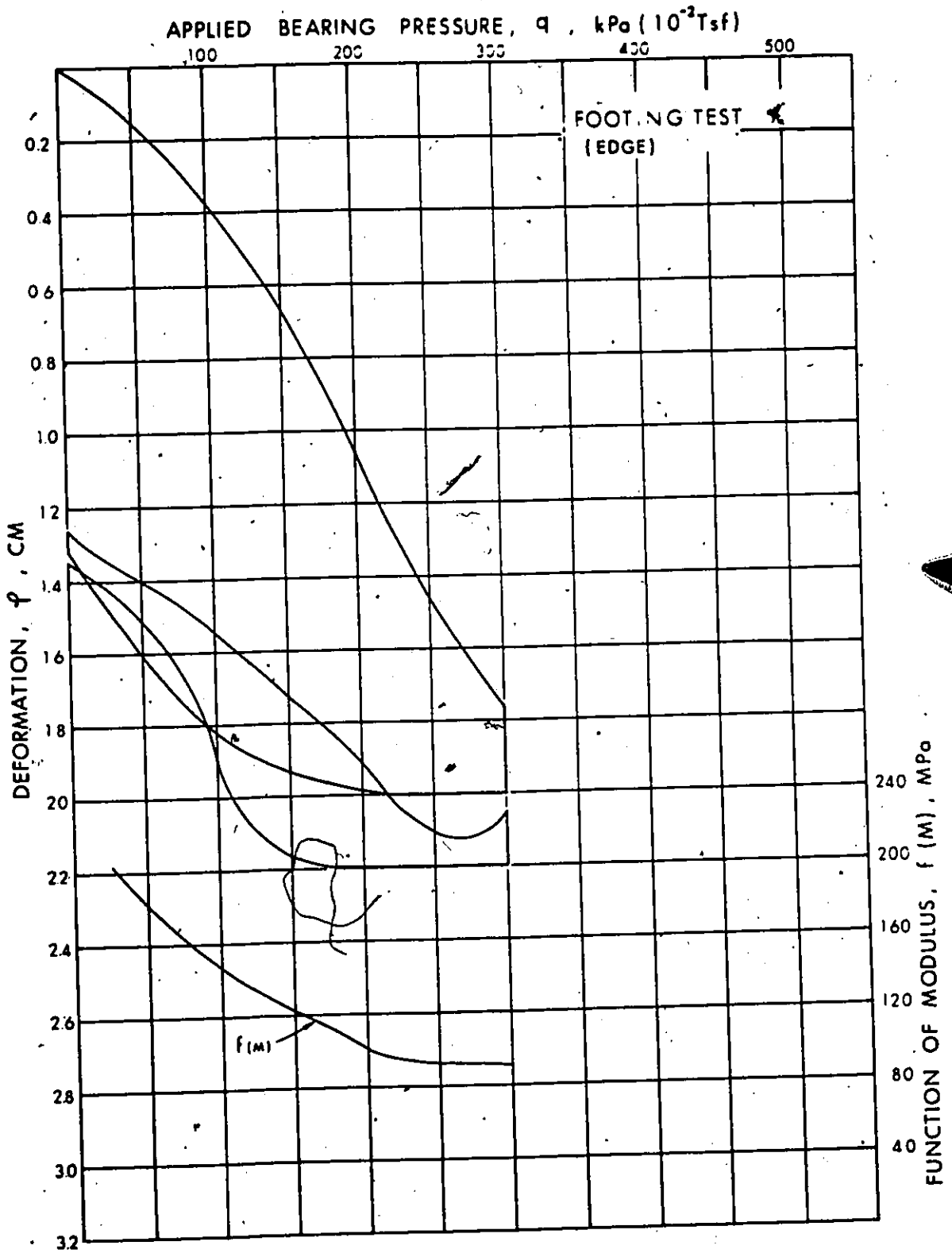
COMPARISON BETWEEN THE AVERAGE DEFORMATION RESPONSES FOR VERTICAL AND HORIZONTAL PLATE TEST AT THE SAME DEPT.



COMPARISON BETWEEN THE AVERAGE DEFORMATION RESPONSES FOR VERTICAL AND HORIZONTAL PLATE TEST AT THE SAME DEPT.



TOTAL DEFORMATION AND FUNCTION OF MODULUS VERSUS  
APPLIED BEARING PRESSURE.

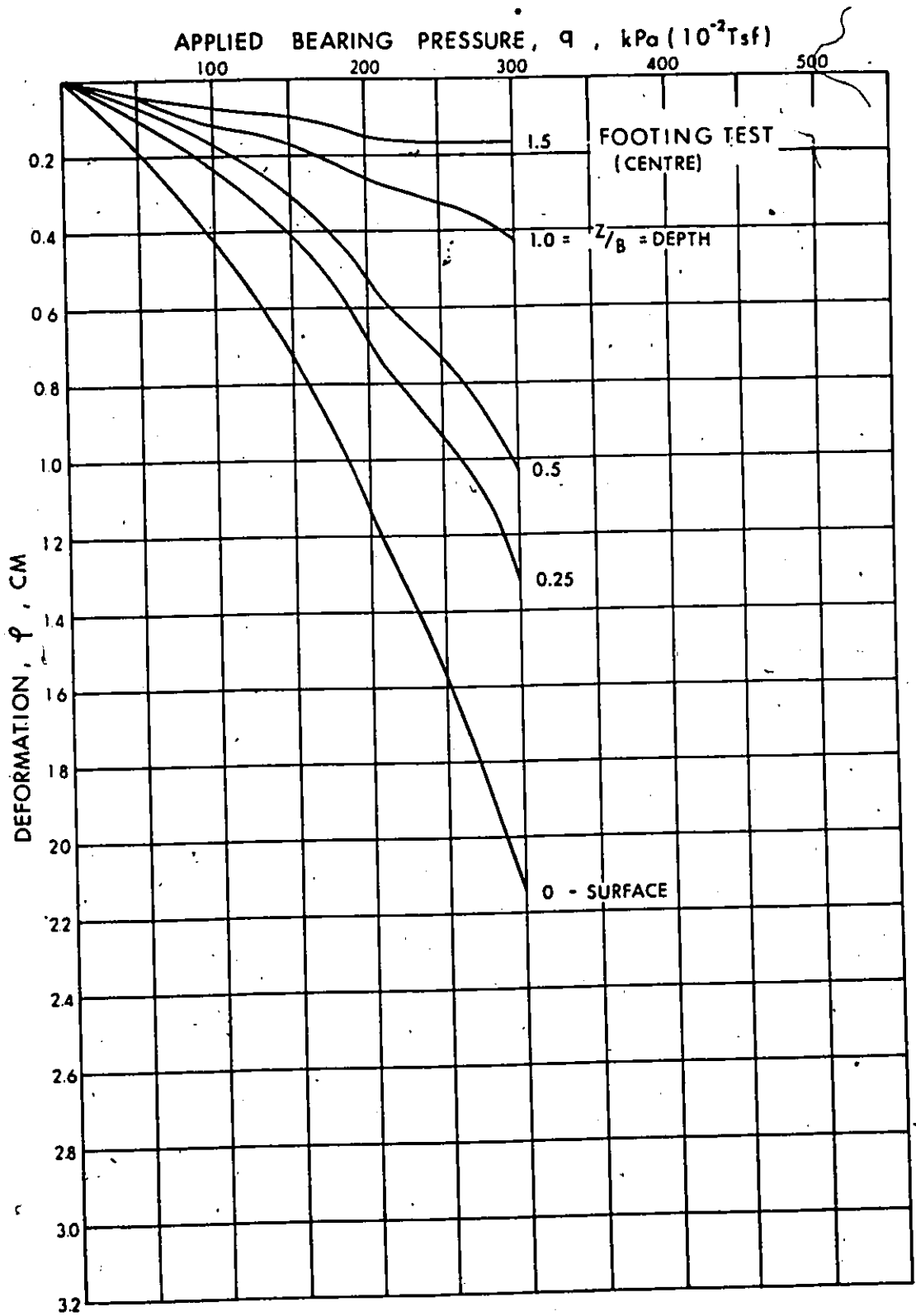


TOTAL DEFORMATION AND FUNCTION OF MODULUS VERSUS APPLIED BEARING PRESSURE.

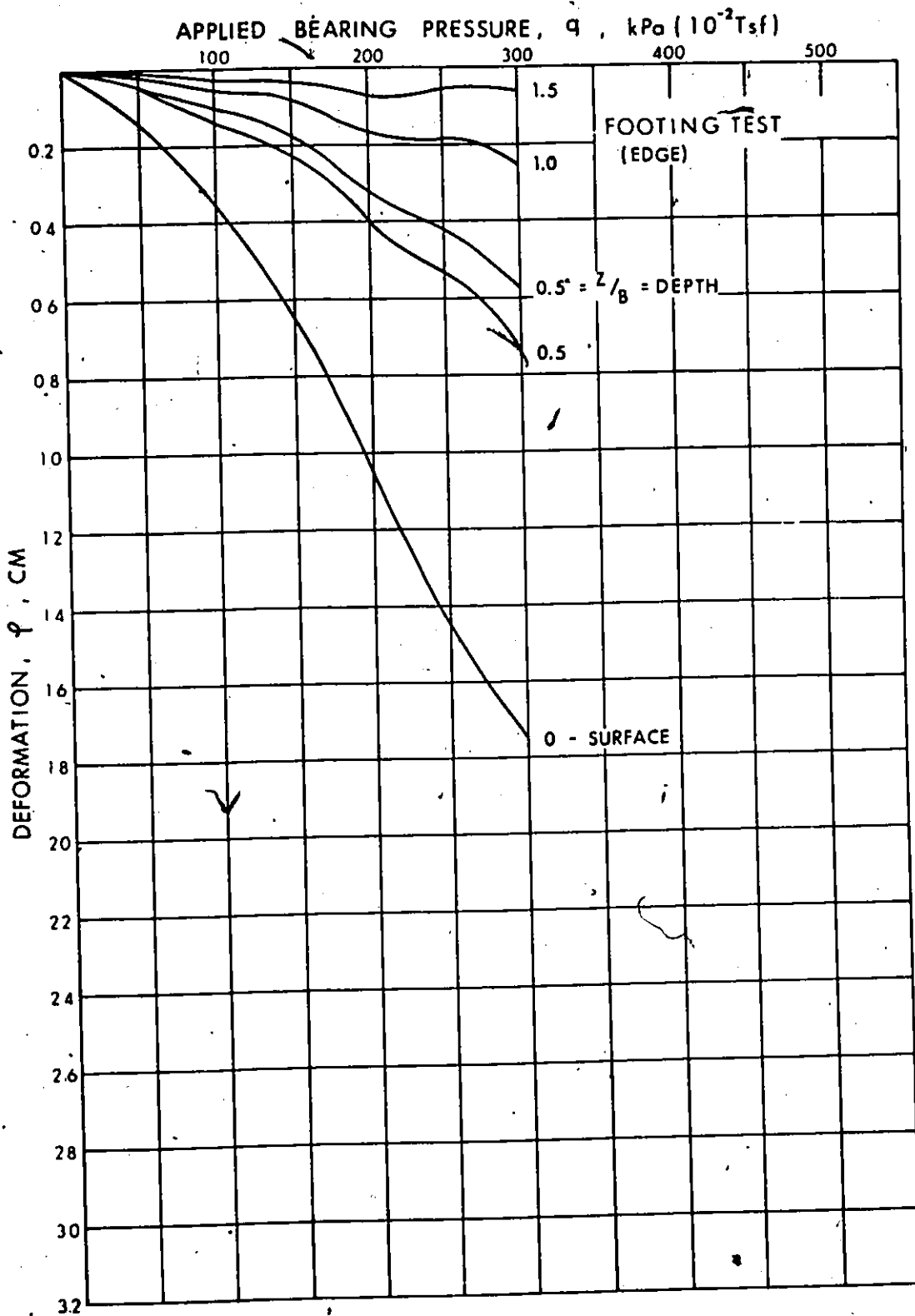
APPLIED BEARING PRESSURE (kPa)		100		200		300	
		DEFORMATION, ( $\rho$ )					
TEST	Radius (cm)	(cm)	$\rho/R$	(cm)	$\rho/R$	(cm)	$\rho/R$
	Footing (centre)	172	0.433	.00252	1.130	.00657	2.160
Footing (edge)	172	0.368	.00214	1.048	.00609	2.755	.0102
Plate - Ave. VI. Series	23	0.084	.00365	0.174	.00757	0.299	.013

TABLE 5.

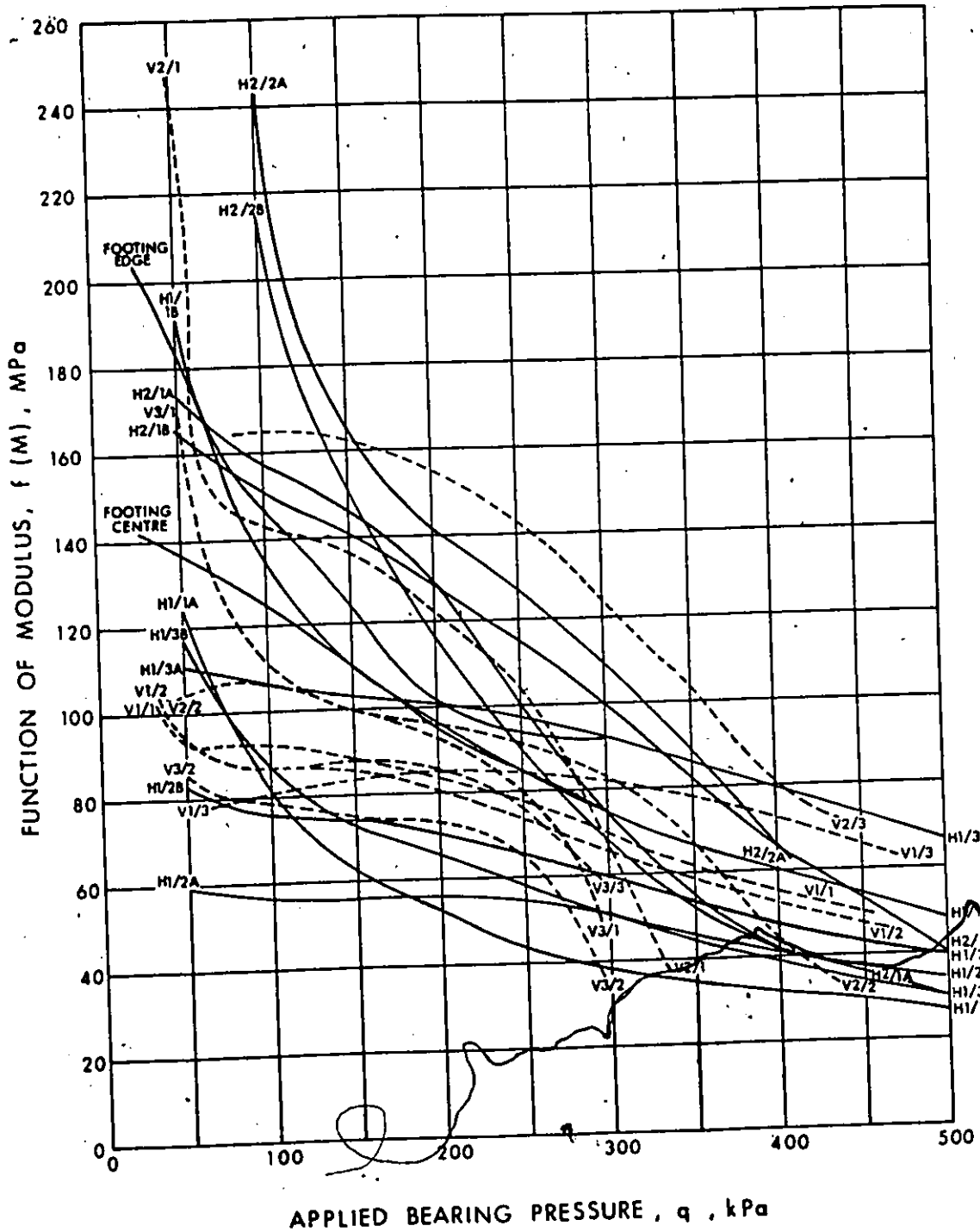
COMPARISON OF TOTAL DEFORMATIONS AND RATIOS OF DEFORMATION TO RADIUS OF LOADED AREA FOR THE FOOTING TEST AND THE AVERAGE DEFORMATIONS OF THE VI SERIES PLATE TESTS



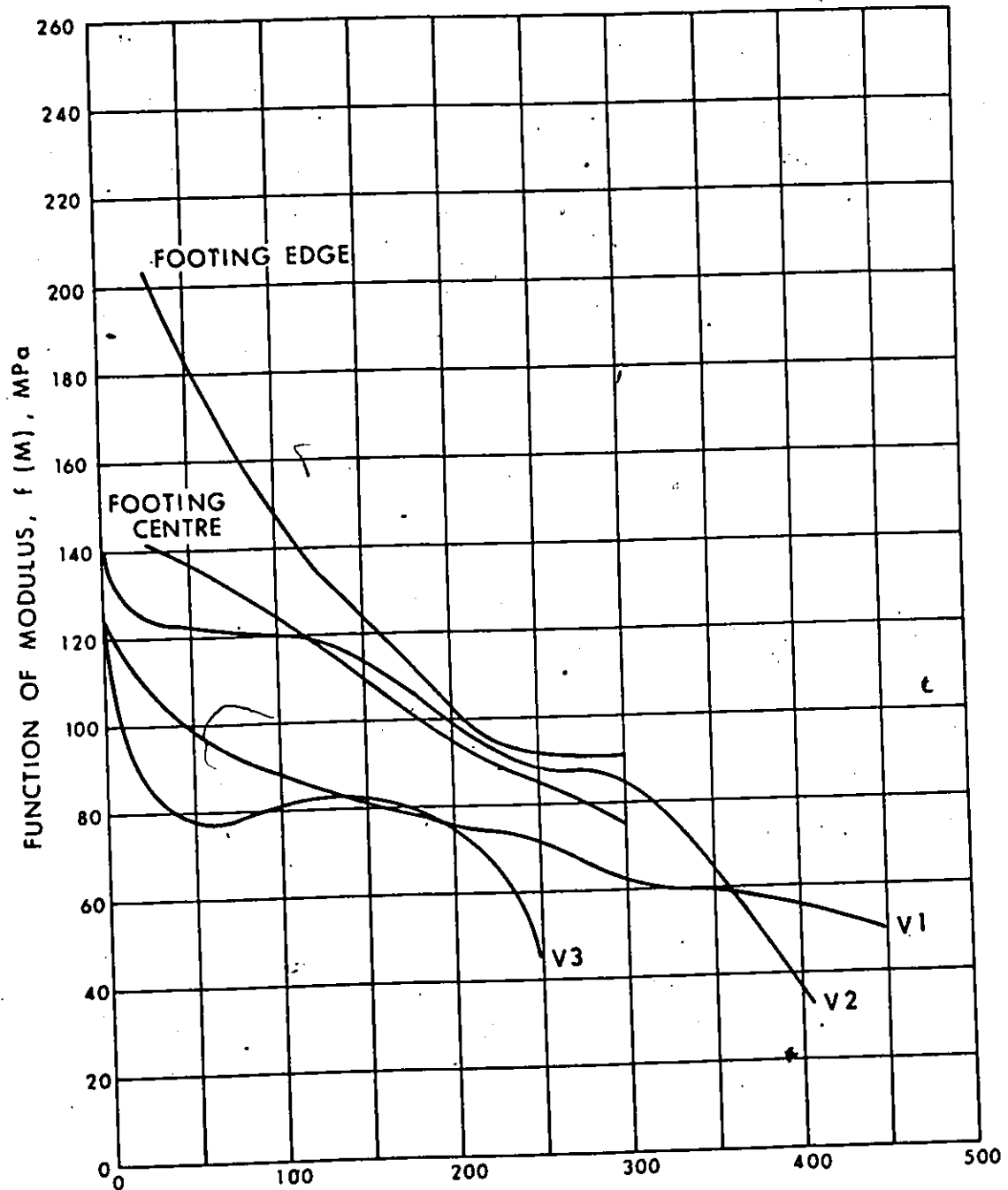
TOTAL DEFORMATION AND DEFORMATION AT VARIOUS DEPTHS BELOW LOADED SURFACE.



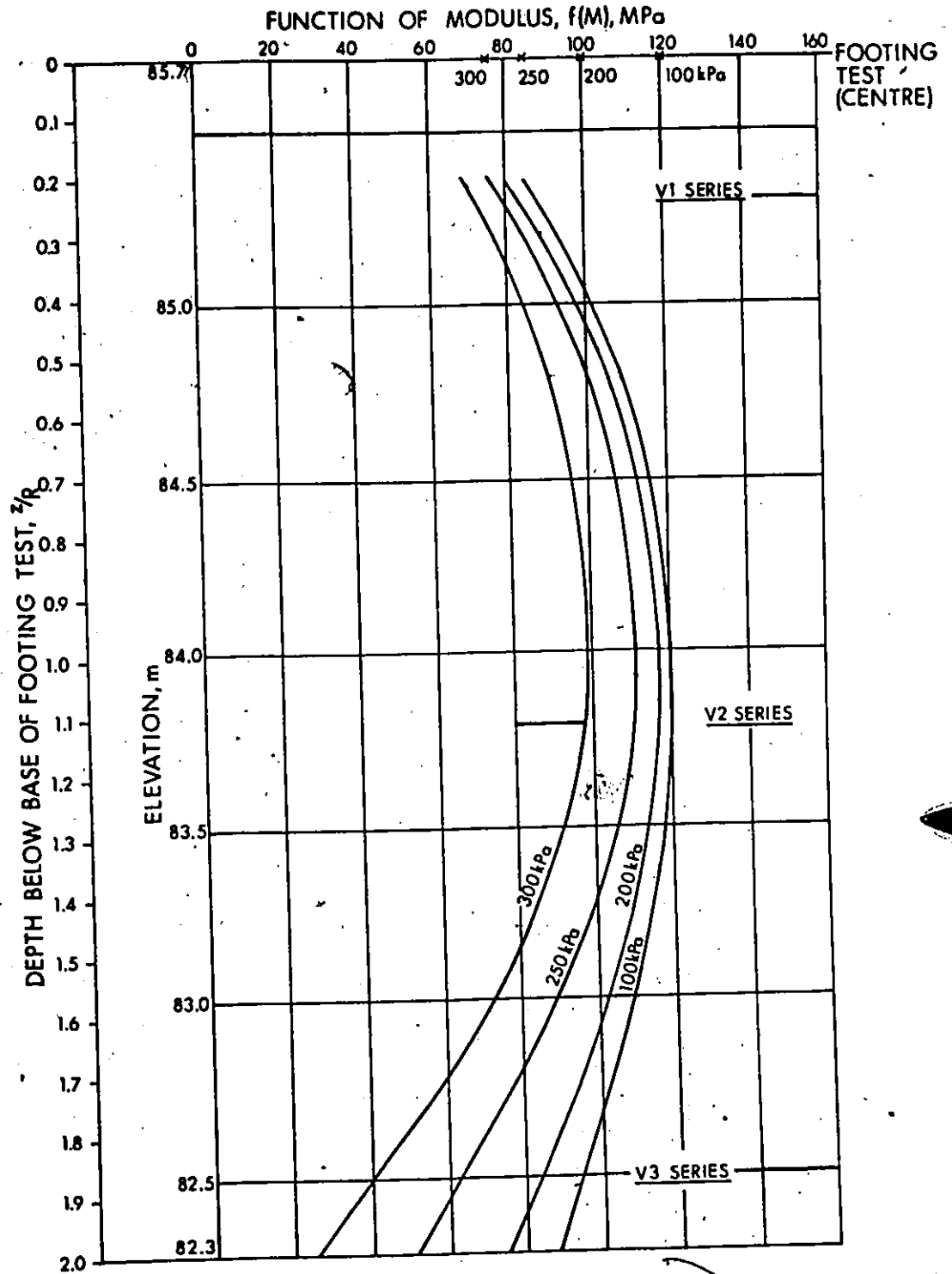
TOTAL DEFORMATION AND DEFORMATION AT VARIOUS DEPTHS BELOW LOADED SURFACE.



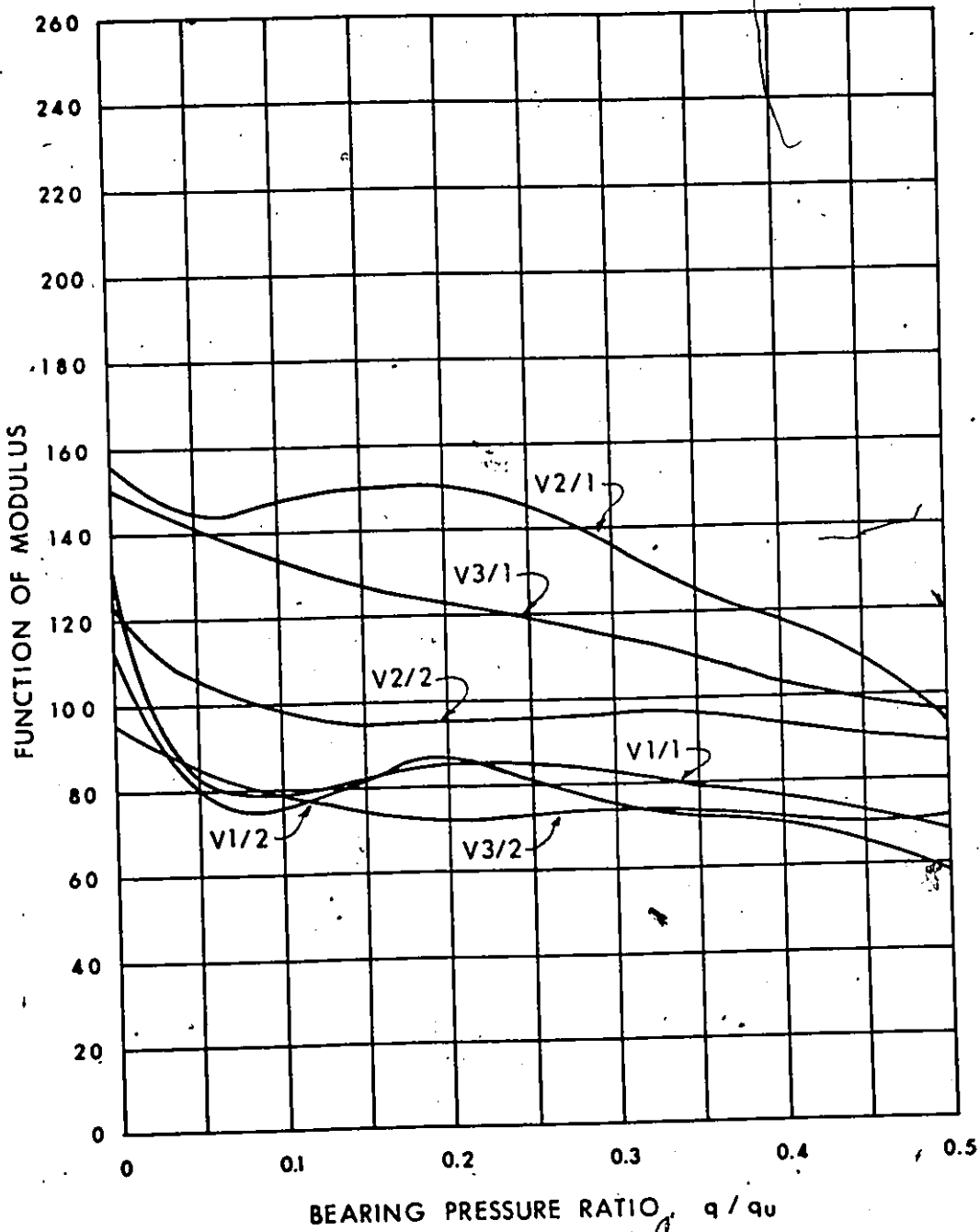
FUNCTION OF MODULUS VERSUS APPLIED BEARING PRESSURE FOR ALL  
 PLATE TESTS AND THE FOOTING TEST. PLATE NO. 6.1



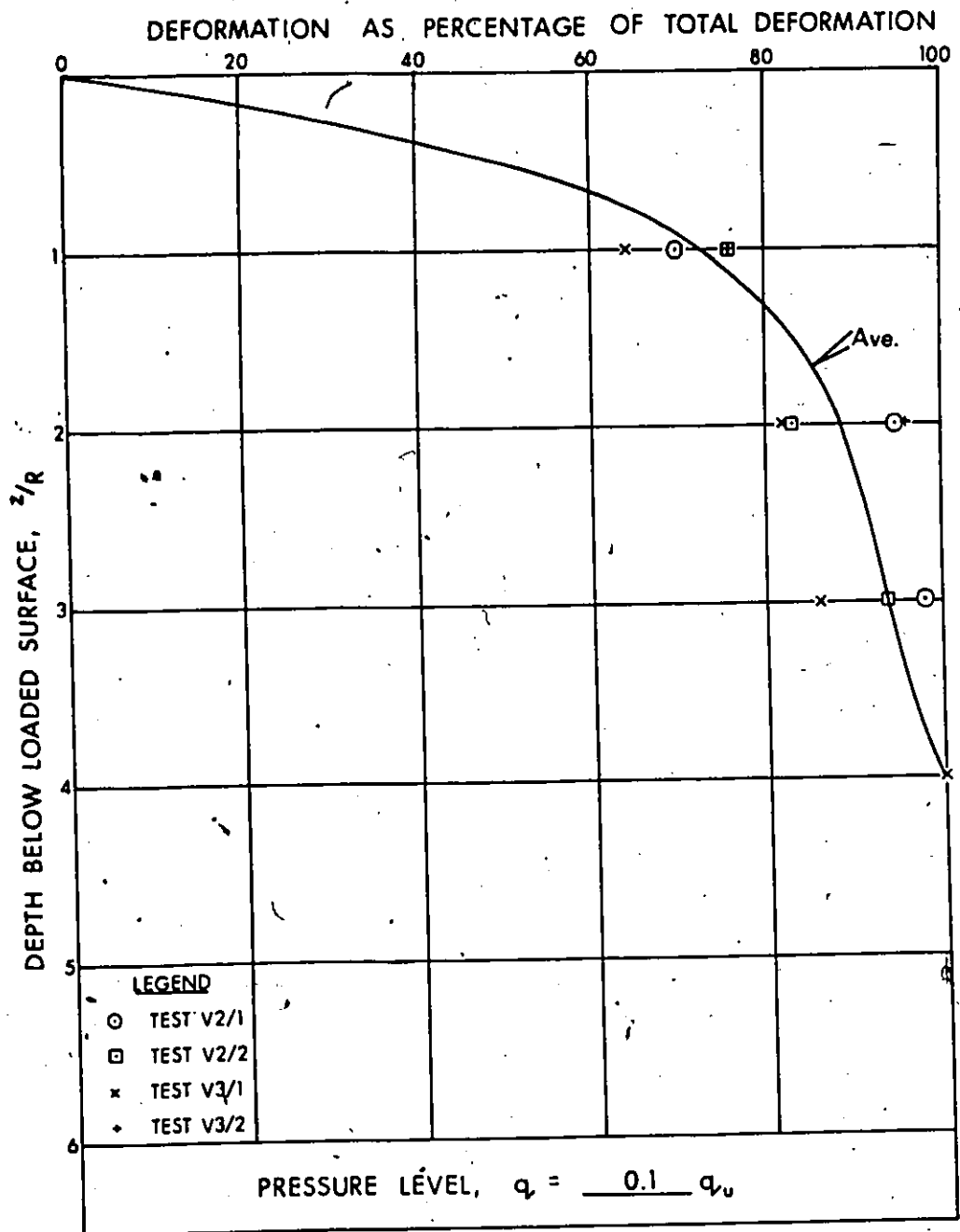
APPLIED BEARING PRESSURE,  $q$ , kPa  
 FUNCTION OF MODULUS FOR THE AVERAGE OF EACH VERTICAL TEST SERIES AND THE FOOTING TEST VERSUS APPLIED BEARING PRESSURE.



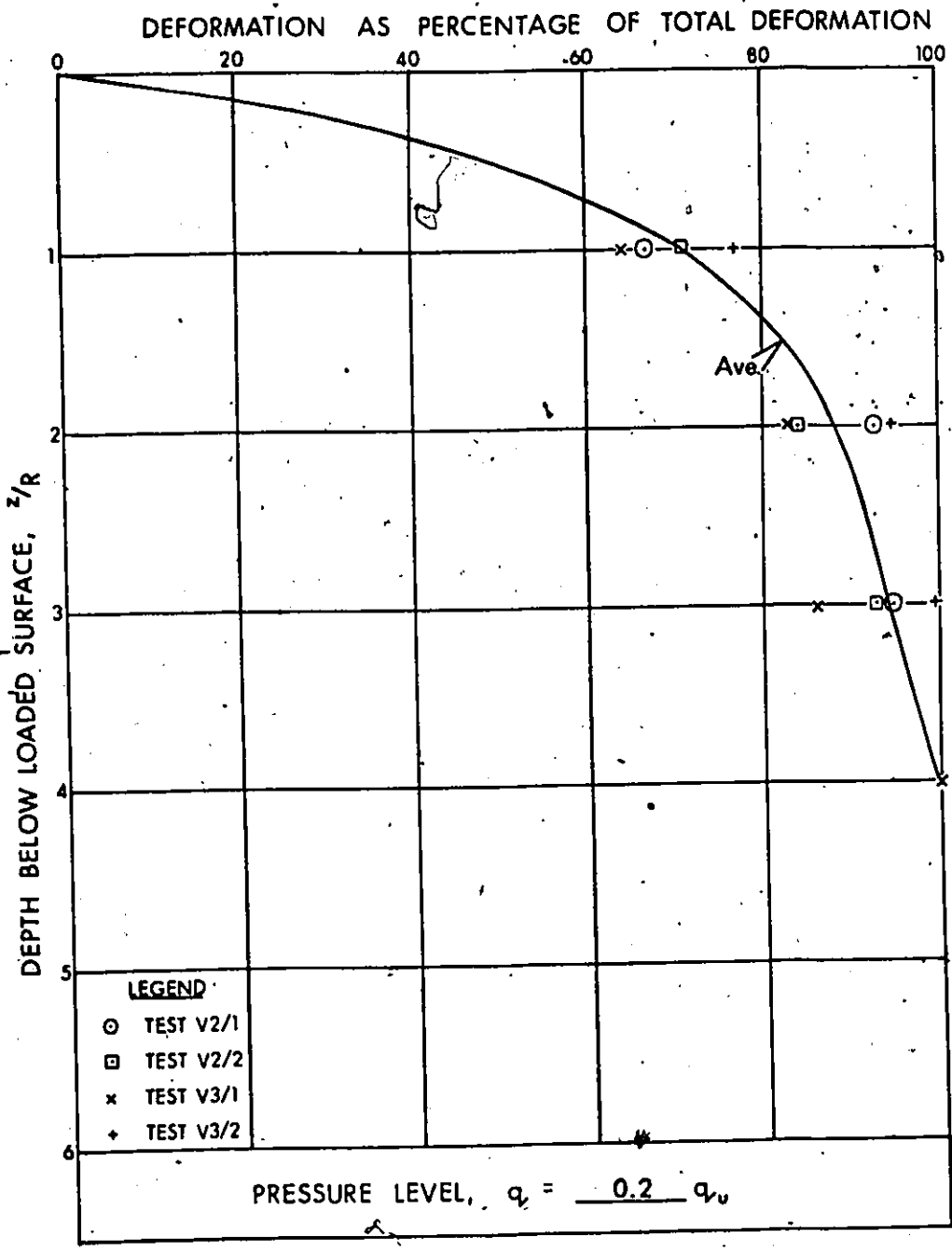
VARIATION OF FUNCTION OF MODULUS WITH DEPTH FOR DIFFERENT PRESSURES FROM THE PLATE TESTS. FUNCTION MODULUS FOR FOOTING TEST (CENTRE) ALSO SHOWN.



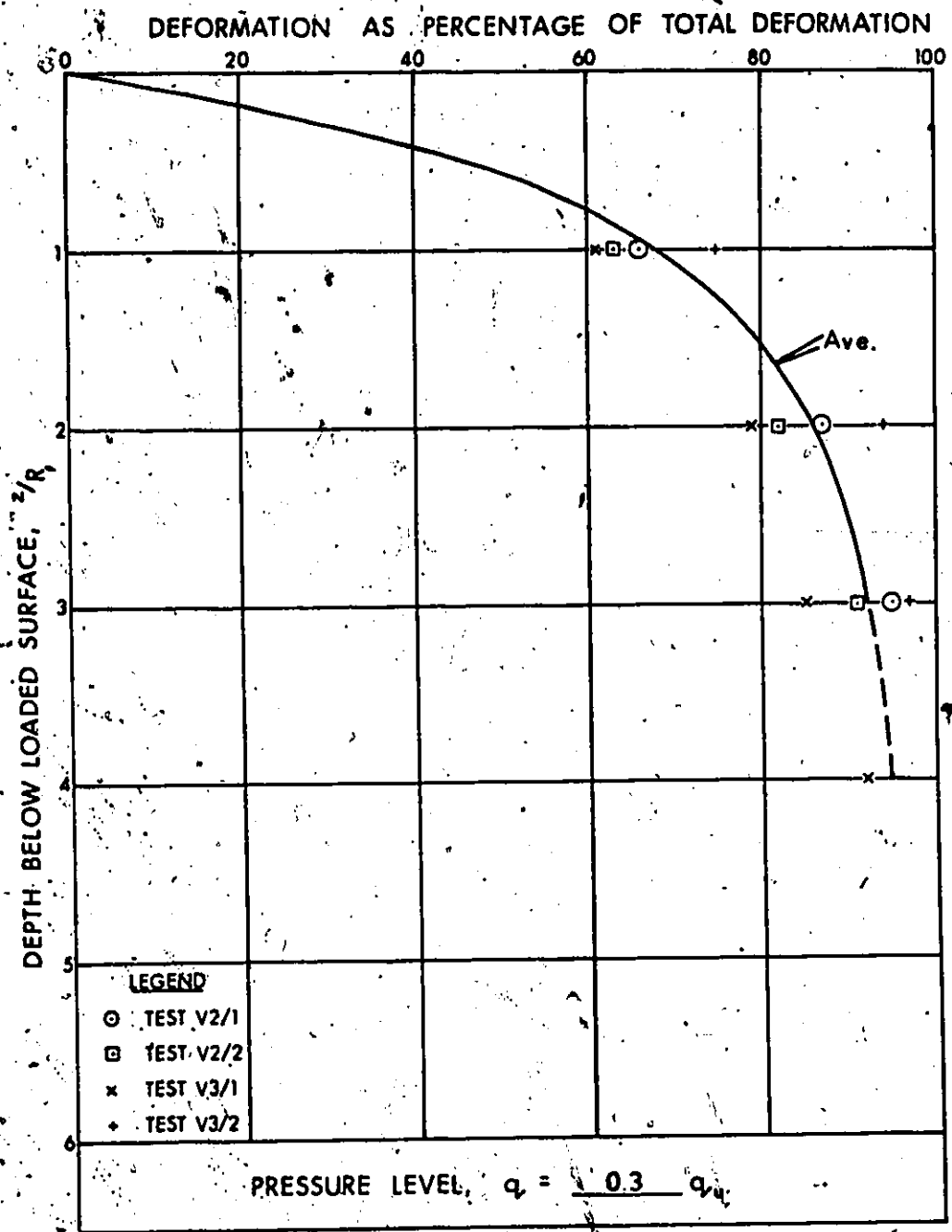
VARIATION OF FUNCTION OF MODULUS WITH APPLIED BEARING PRESSURE RATIO FOR SOME VERTICAL PLATE TESTS.



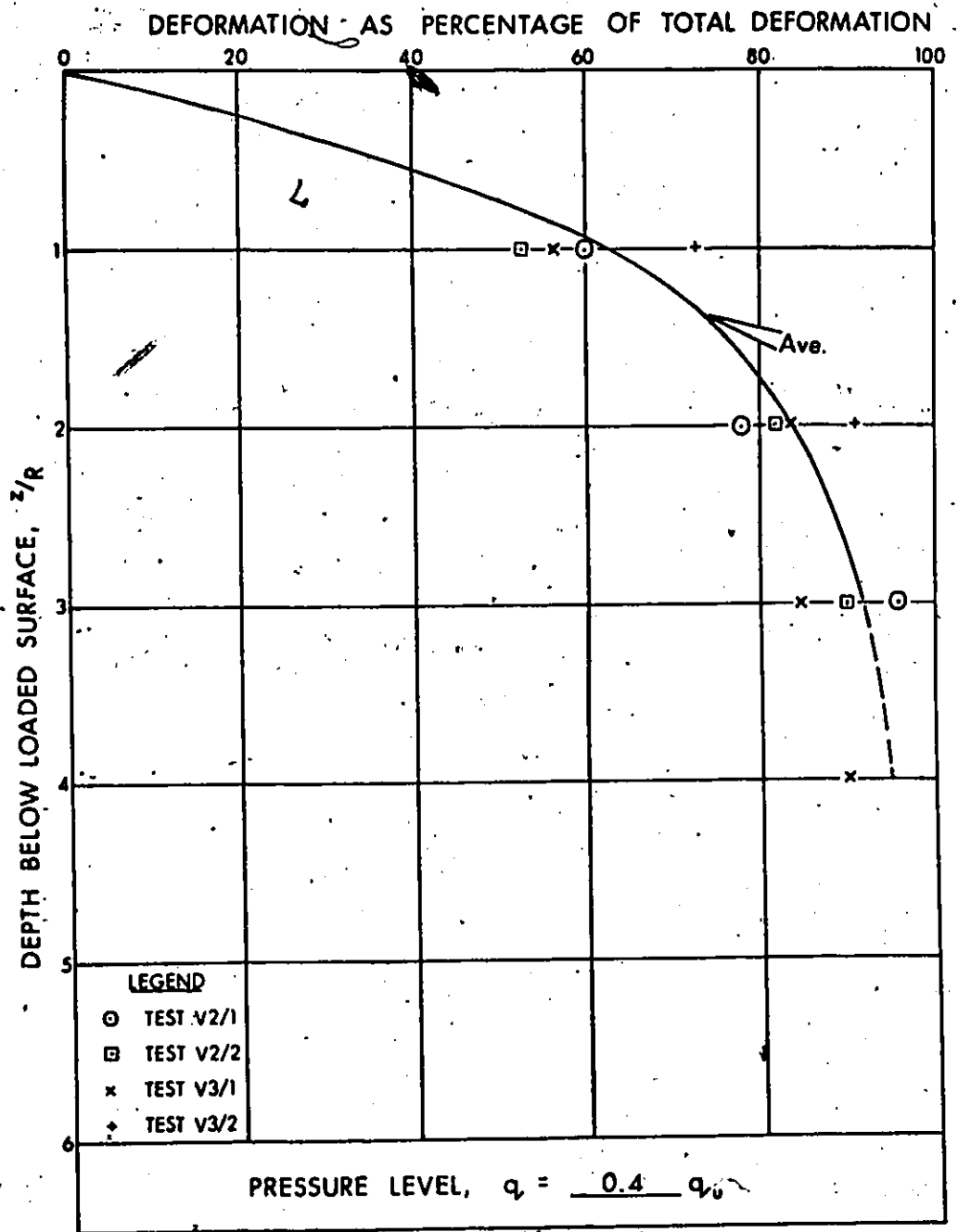
PERCENTAGE OF THE TOTAL DEFORMATION WHICH OCCURS WITHIN A CERTAIN DEPTH RATIO FOR SOME VERTICAL PLATE TESTS.



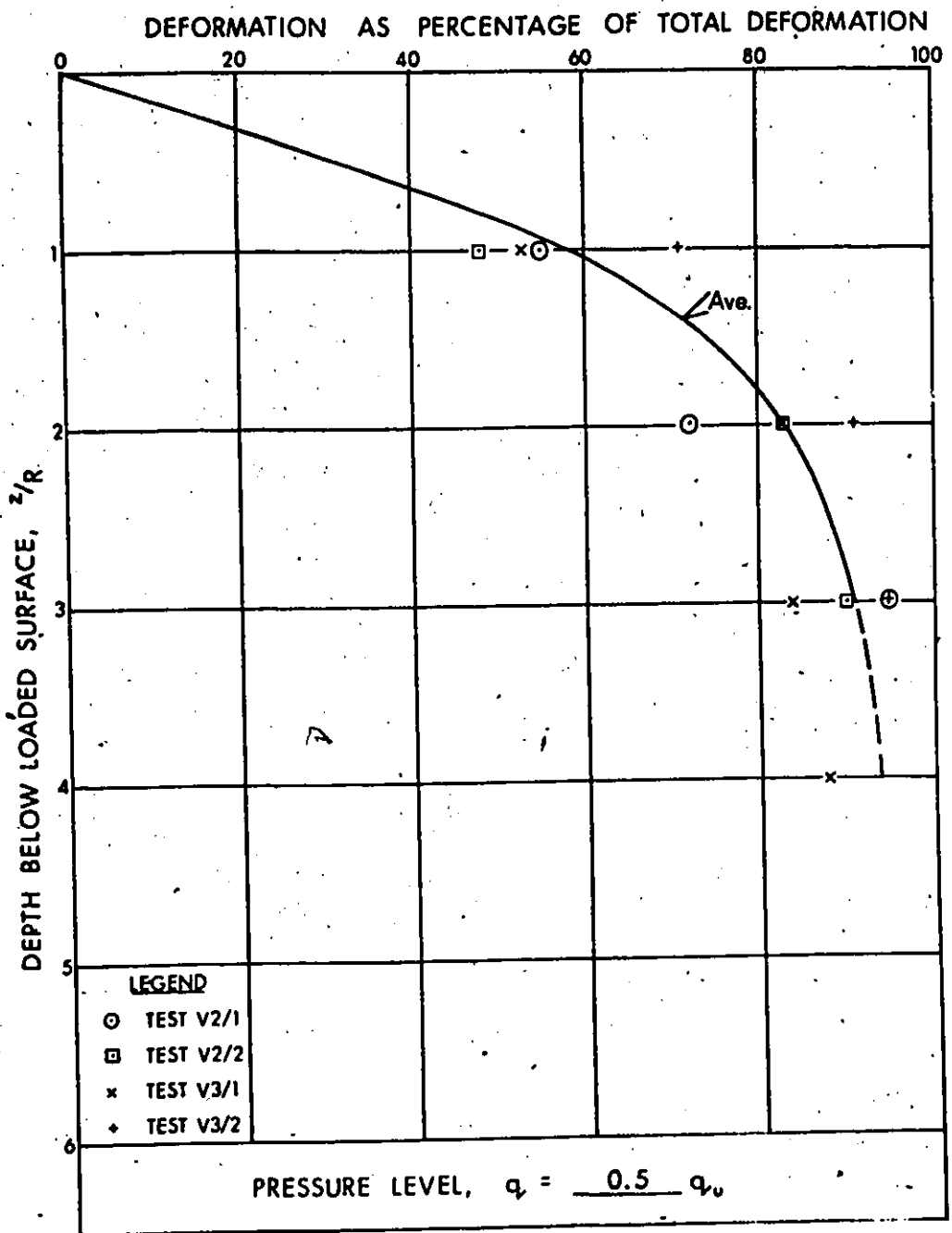
PERCENTAGE OF THE TOTAL DEFORMATION WHICH OCCURS WITHIN A CERTAIN DEPTH RATIO FOR SOME VERTICAL PLATE TESTS.



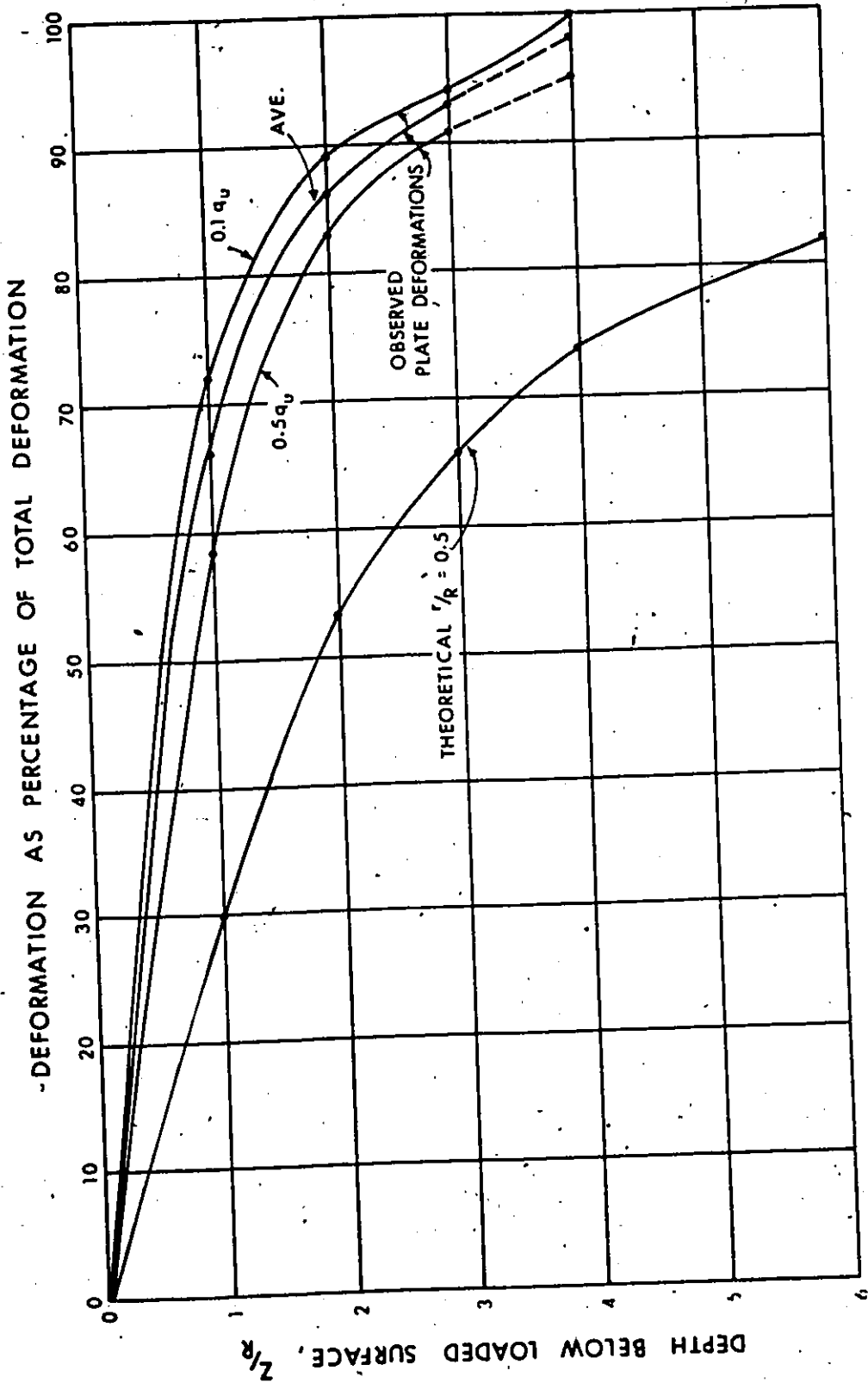
PERCENTAGE OF THE TOTAL DEFORMATION WHICH OCCURS WITHIN A CERTAIN DEPTH RATIO FOR SOME VERTICAL PLATE TESTS.



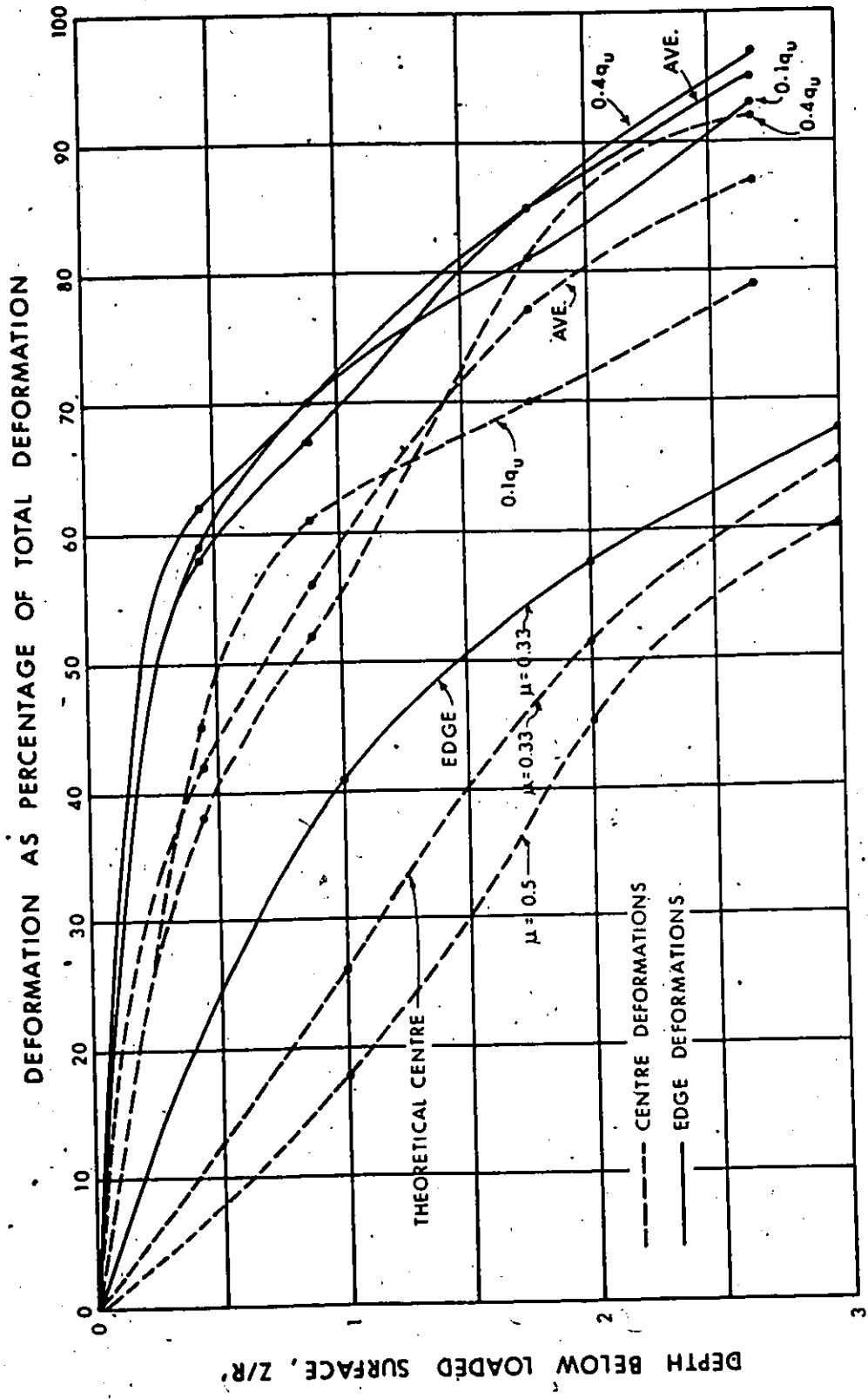
PERCENTAGE OF THE TOTAL DEFORMATION WHICH OCCURS WITHIN A CERTAIN DEPTH RATIO FOR SOME VERTICAL PLATE TESTS.



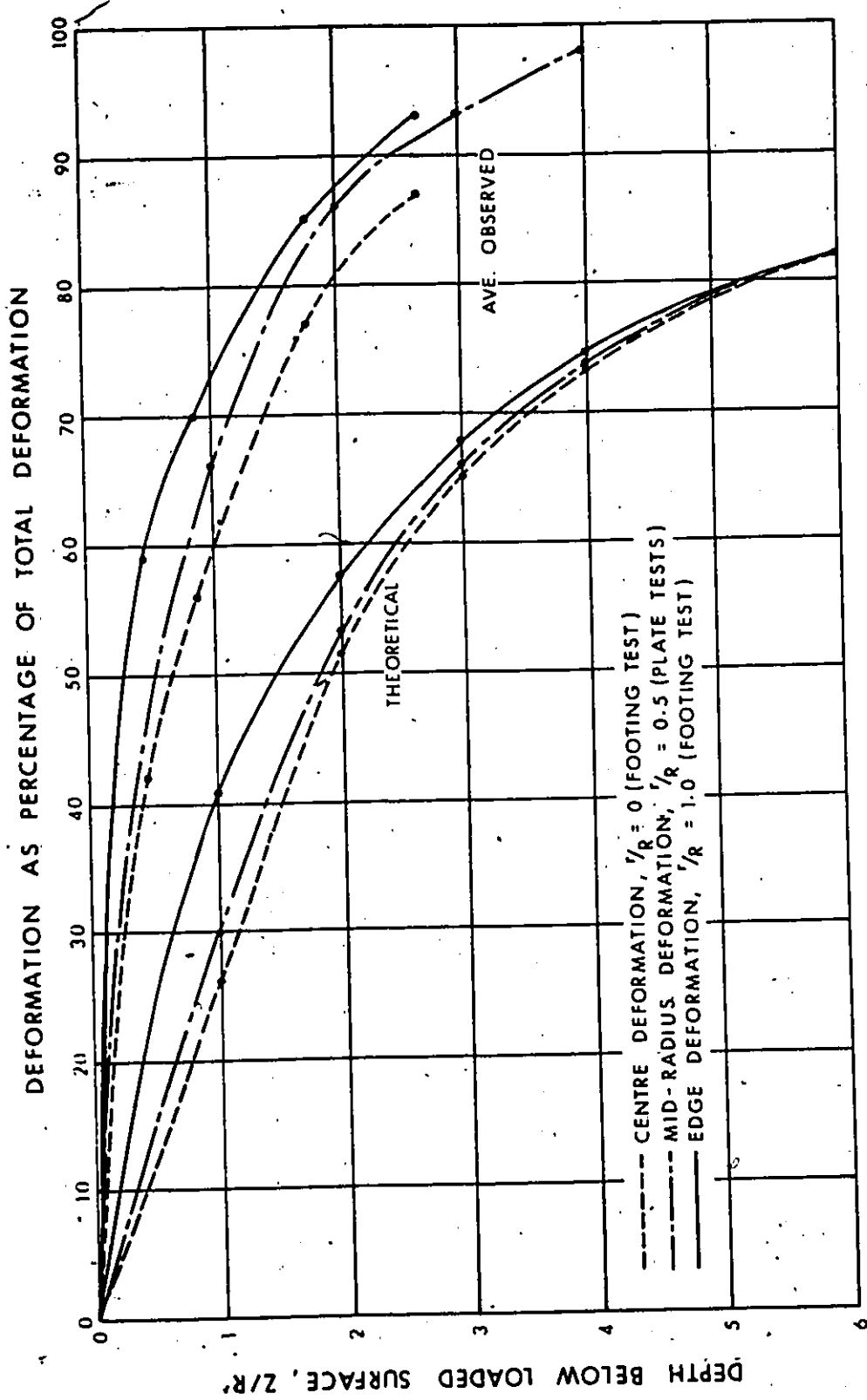
PERCENTAGE OF THE TOTAL DEFORMATION WHICH OCCURS WITHIN A CERTAIN DEPTH RATIO FOR SOME VERTICAL PLATE TESTS.



COMPARISON BETWEEN OBSERVED AND THEORETICAL (GIROUD, 1972) DEFORMATIONS OCCURRING WITHIN CERTAIN DEPTH RATIOS FOR THE PLATE TESTS.



COMPARISON BETWEEN OBSERVED AND THEORETICAL (GIROUD, 1972) DEFORMATIONS OCCURRING WITHIN CERTAIN DEPTH RATIOS FOR THE FOOTING TEST.



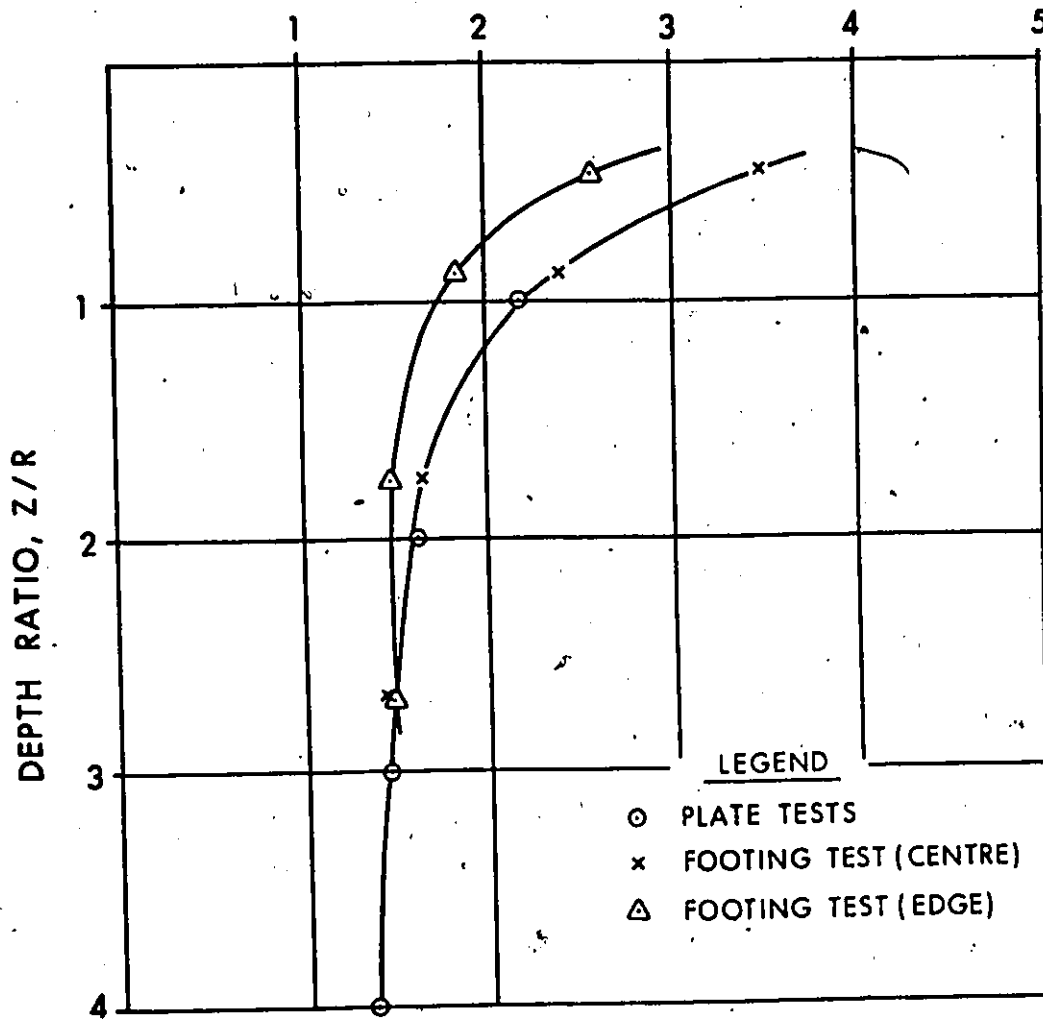
COMPARISON BETWEEN OBSERVED AND THEORETICAL (GIROUD, 1972) DEFORMATIONS OCCURRING WITHIN CERTAIN DEPTH RATIOS FOR THE PLATE TESTS AND THE FOOTING TEST.

PERCENT DEFORMATION WITHIN DEPTH, z/R										
DEPTH z/R	PLATE TESTS			FOOTING TEST (CENTRE)			FOOTING TEST (EDGE)			RATIO OBS/THEOR
	OBSERVED	THEORETICAL	RATIO OBS/THEOR	OBSERVED	THEORETICAL	RATIO OBS/THEOR	OBSERVED	THEORETICAL	RATIO OBS/THEOR	
0.44	-	-	-	42	12	3.50	62	24	2.58	
0.89	-	-	-	56	23.5	2.38	70	38	1.84	
1.0	66	30	2.20	-	-	-	-	-	-	
1.78	-	-	-	77	46	1.67	80	54.5	1.47	
2.0	86	53	1.62	-	-	-	-	-	-	
2.66	-	-	-	87	61	1.43	95	65	1.46	
3.0	93	66	1.41	-	-	-	-	-	-	
4.0	98	73.5	1.33	-	-	-	-	-	-	

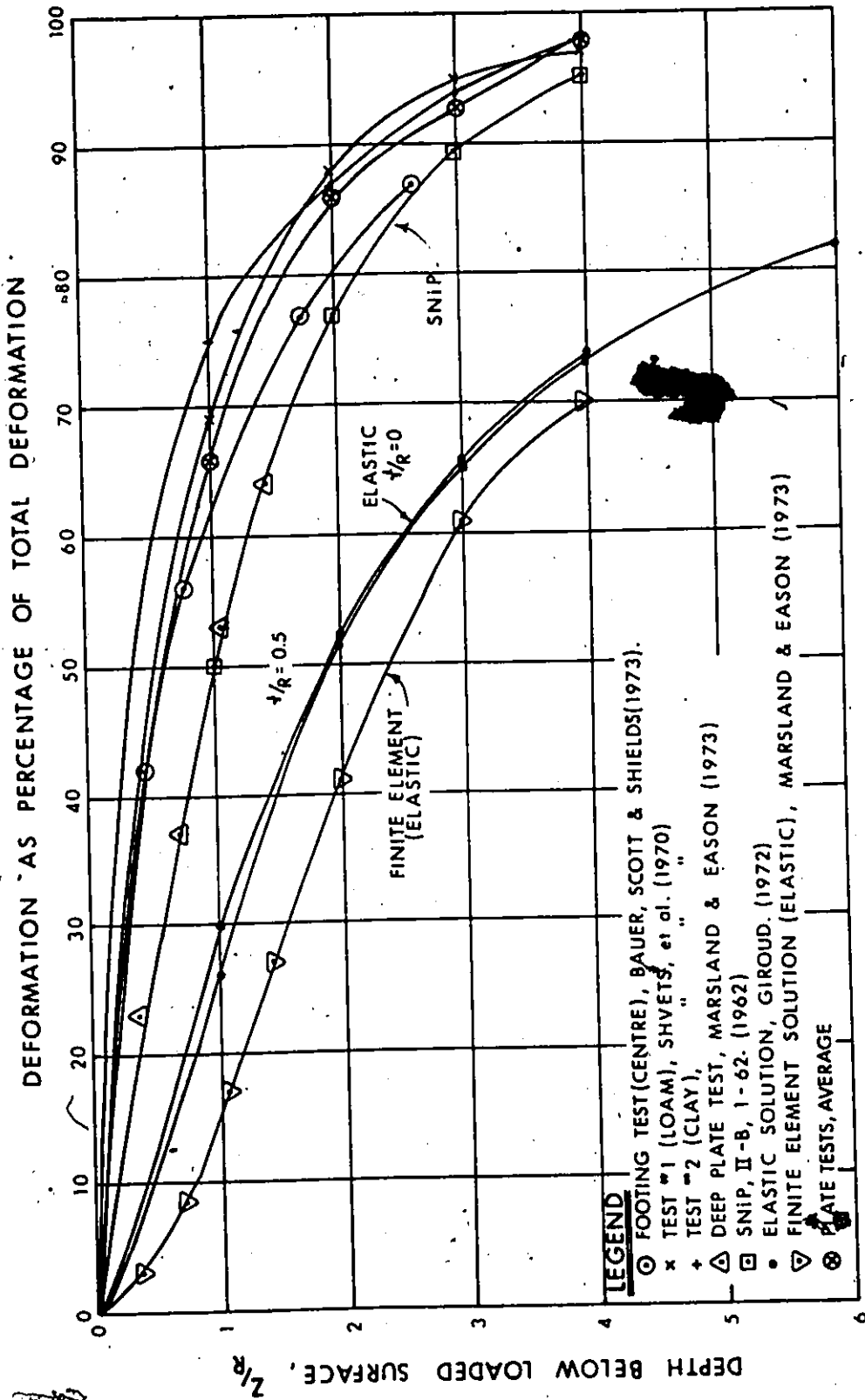
TABLE 6.1

COMPARISON BETWEEN OBSERVED AND THEORETICAL (GIROUD, 1972) DEFORMATIONS OCCURRING WITHIN CERTAIN DEPTH RATIOS FOR THE PLATE TESTS AND THE FOOTING TEST

RATIO OF OBS/THEOR, % OF DEFORMATION WITHIN  
A DEPTH RATIO Z/R.

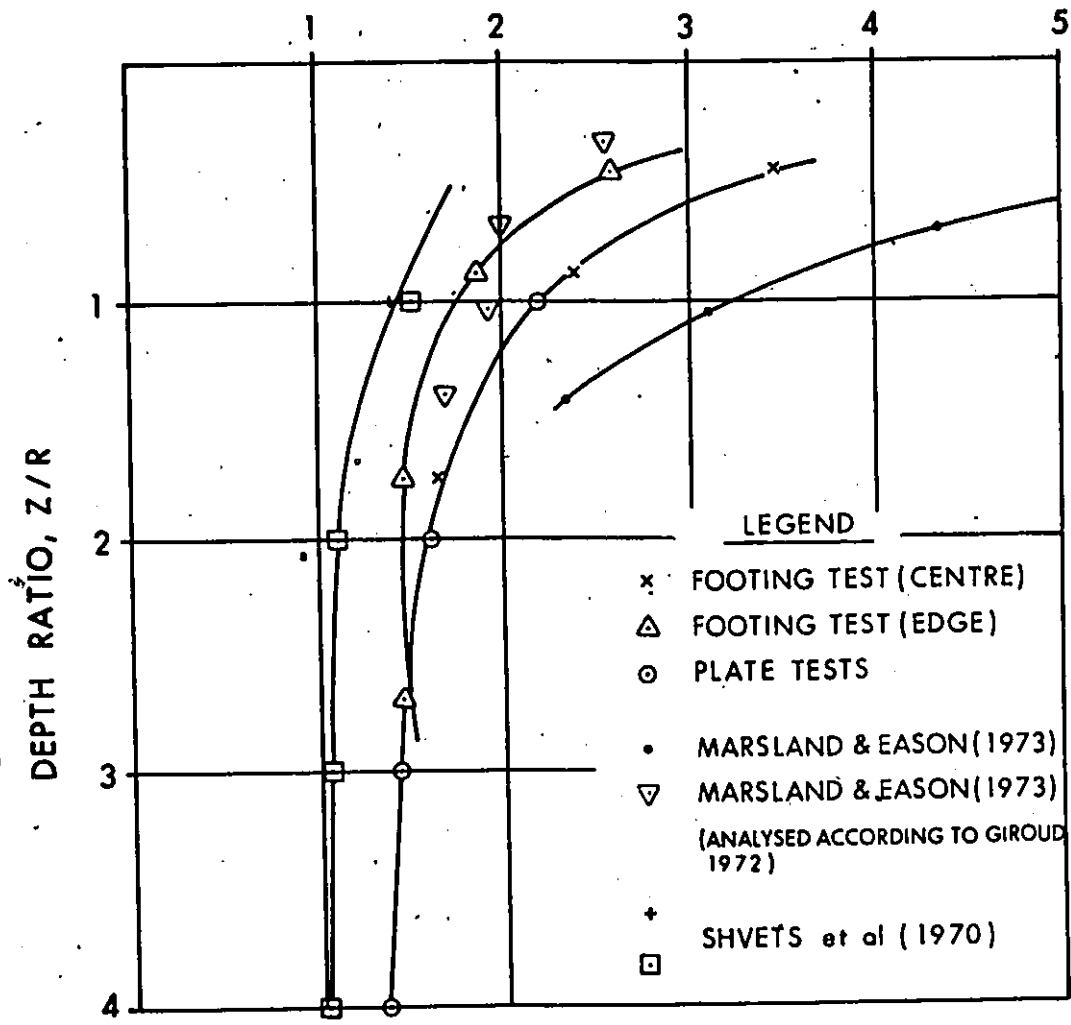


PRESENTATION OF RATIO OF OBSERVED TO THEORETICAL DEFORMATIONS OCCURRING WITHIN CERTAIN DEPTH RATIOS FOR THE PLATE TESTS AND THE FOOTING TEST.

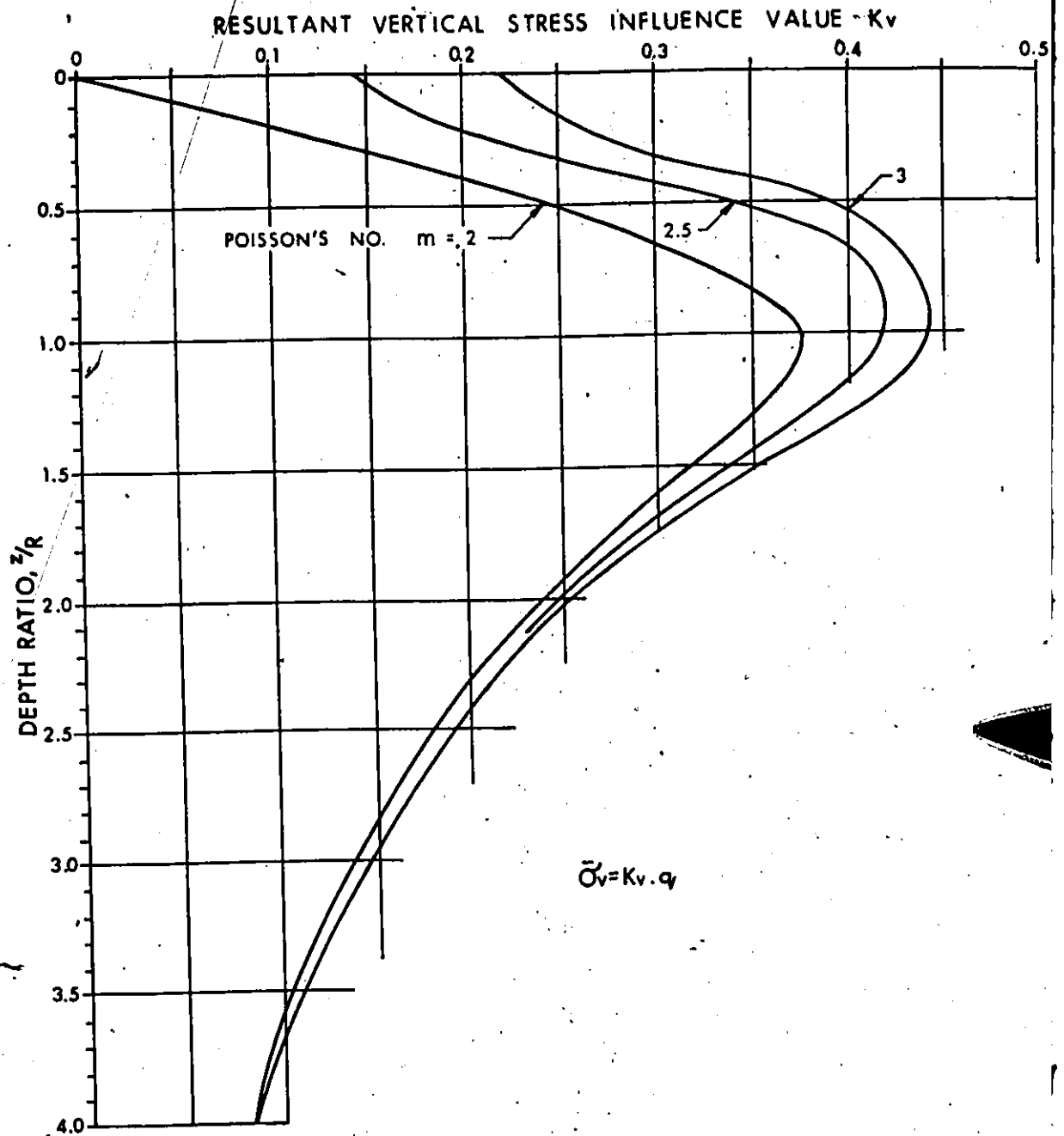


COMPARISON BETWEEN DEFORMATION DISTRIBUTIONS FOR THE PLATE TEST AND OTHER REPORTED DATA AND: AN EMPIRICAL SOLUTION (SNIP); AN ELASTIC SOLUTION (GIROUD, 1972) AND A FINITE ELEMENT (ELASTIC) SOLUTION (MARSLAND & EASON, 1973).

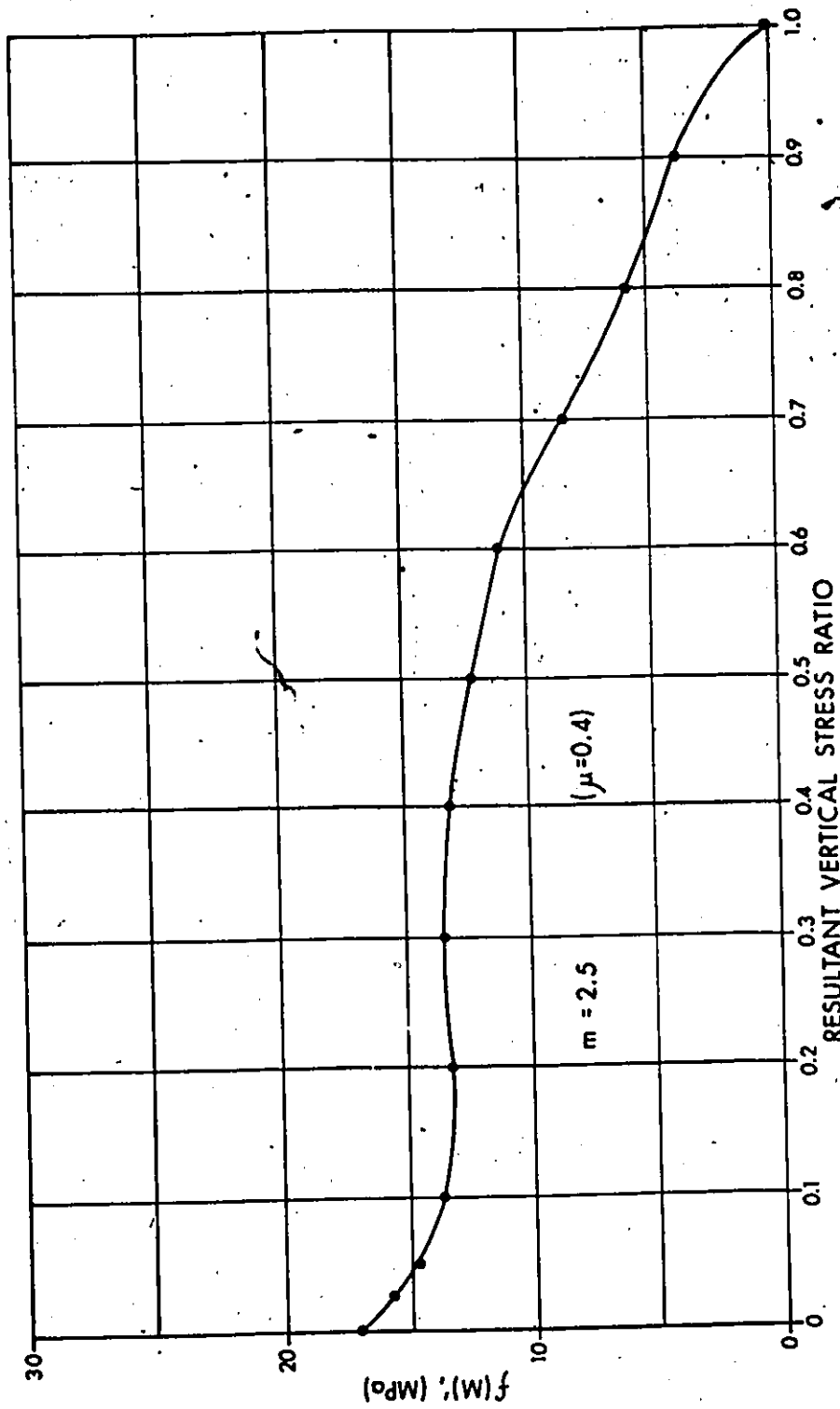
RATIO OF OBS/THEOR, % OF DEFORMATION WITHIN  
A DEPTH RATIO, Z/R



COMPARISON BETWEEN OBSERVED AND THEORETICAL  
DISTRIBUTIONS OF DEFORMATION WITH DEPTH FROM  
VARIOUS SOURCES.

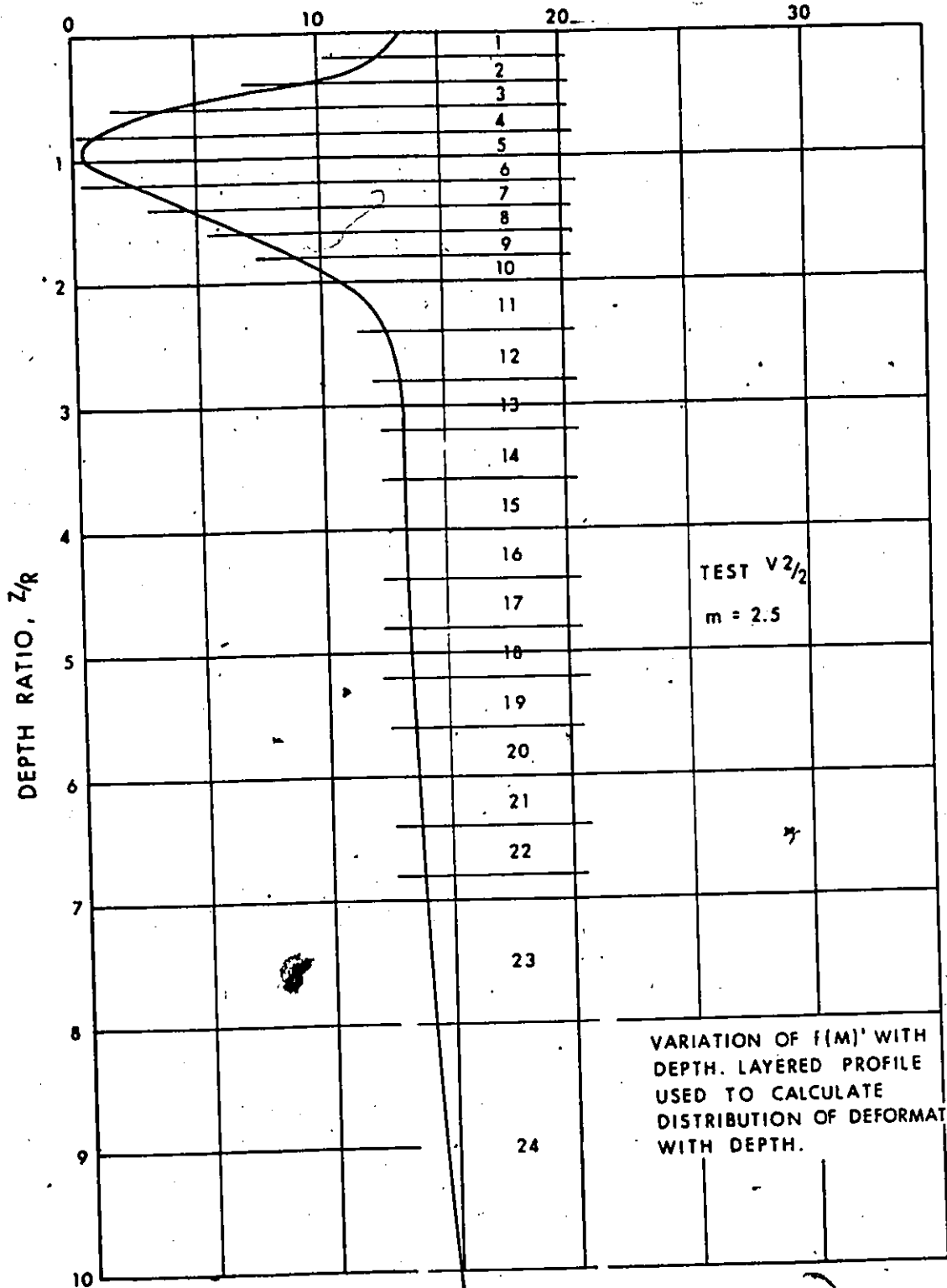


DISTRIBUTION OF RESULTANT VERTICAL STRESS  $\bar{\sigma}_v$  WITH DEPTH

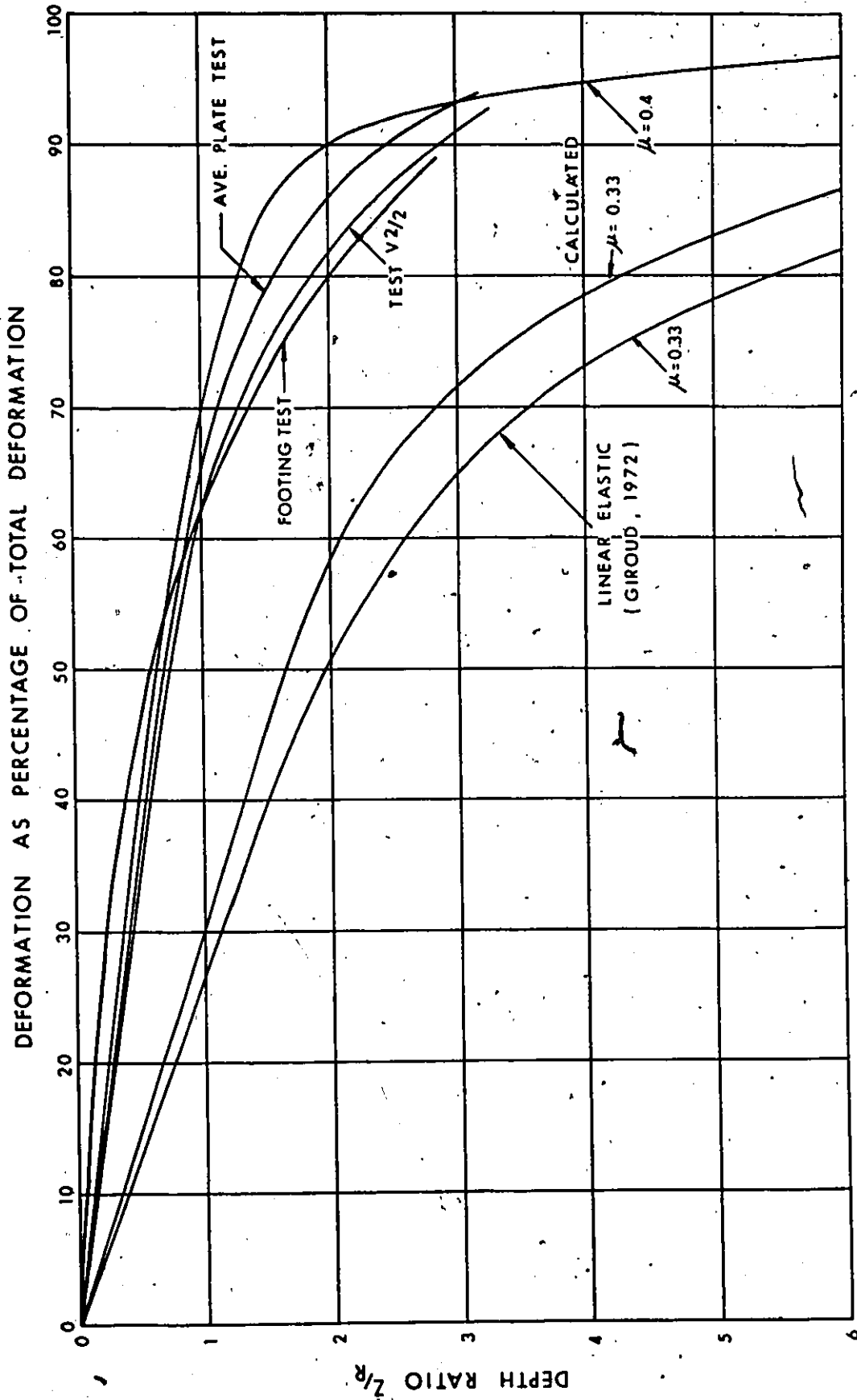


VARIATION OF  $f$  (M) WITH RESULTANT VERTICAL STRESS RATIO FOR TEST V2/2  
 (CONSIDERED TYPICAL FOR THIS SOIL)

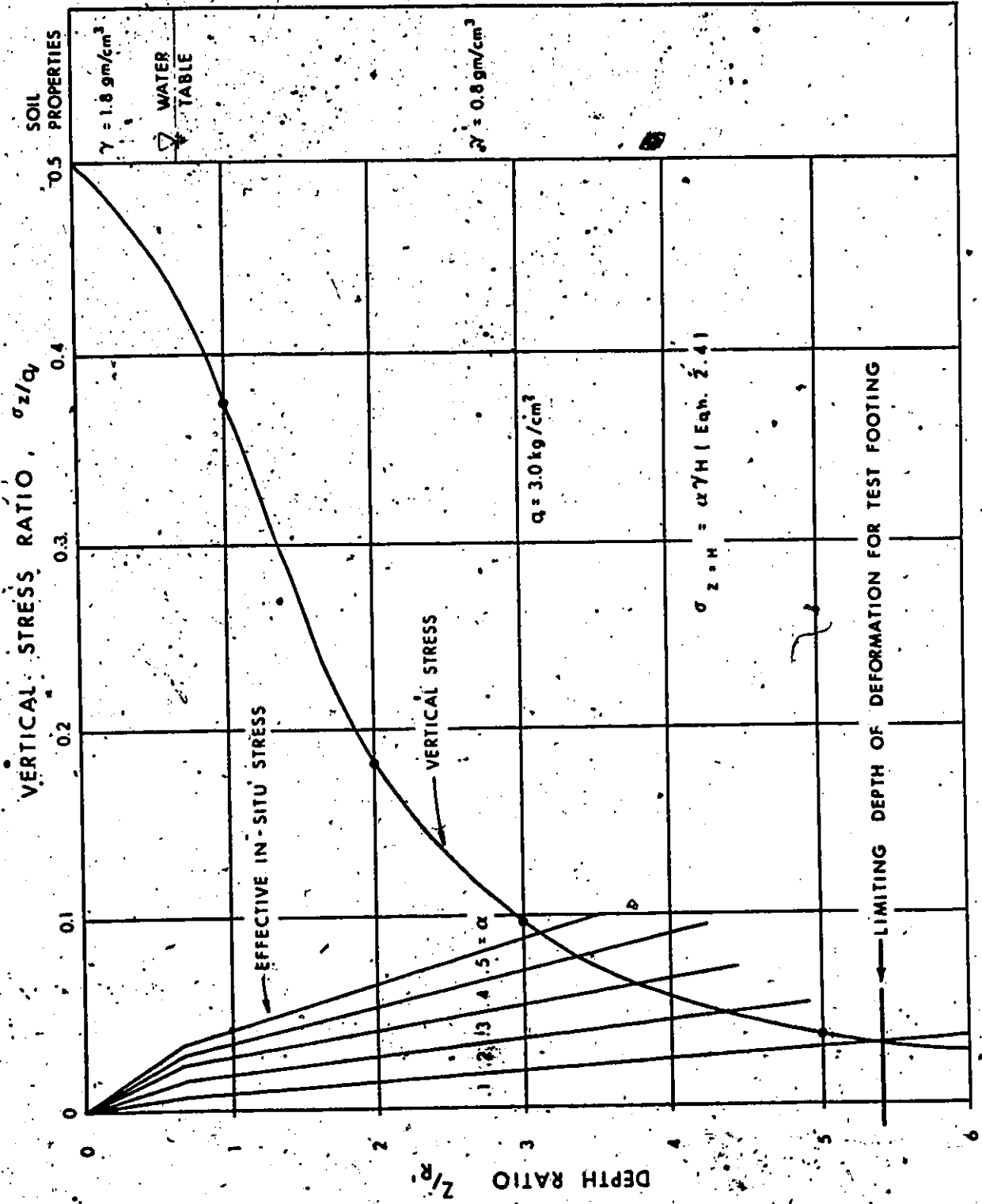
$f(M)'$  (MPa)



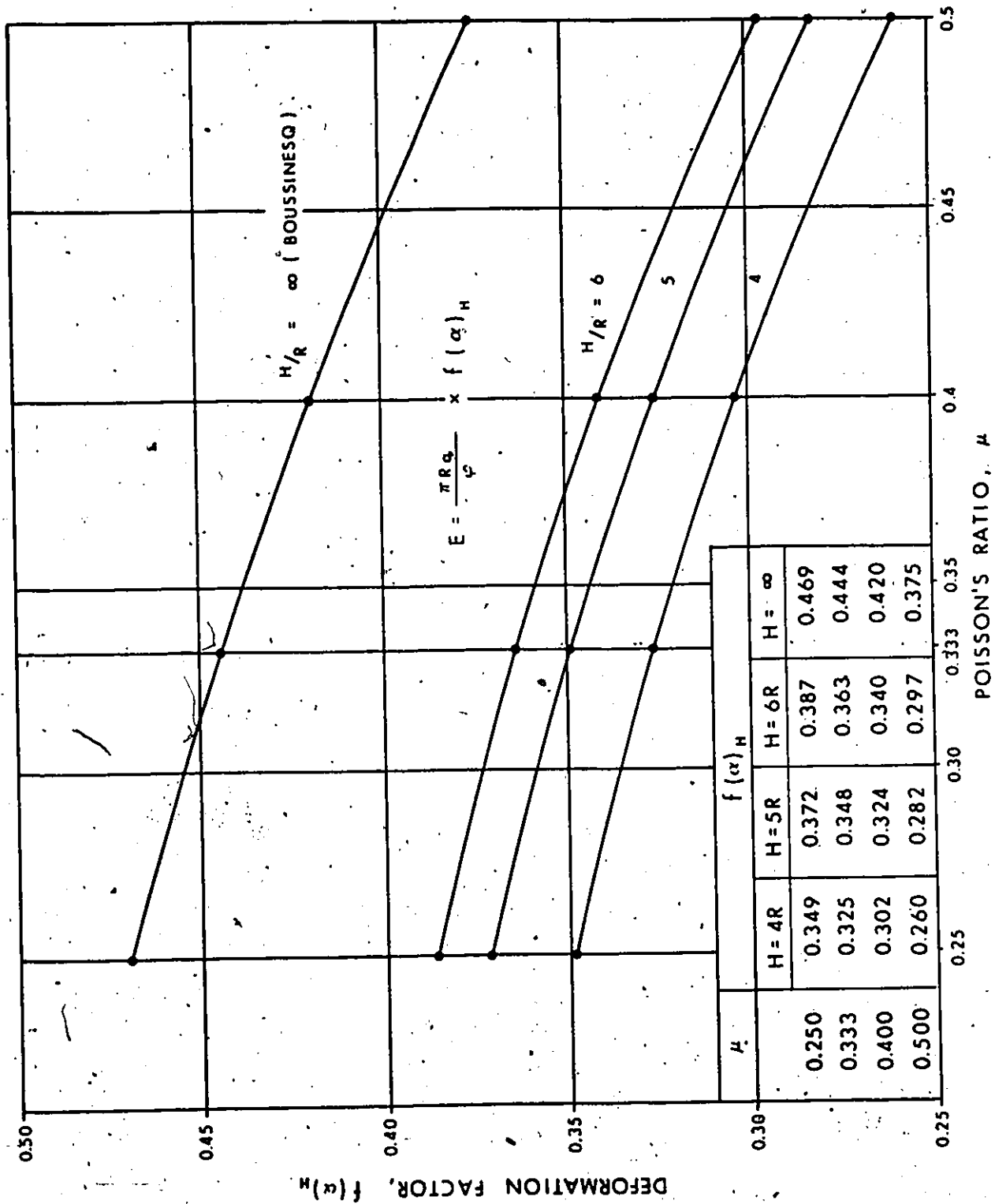
25



COMPARISON BETWEEN OBSERVED, LINEAR ELASTIC AND CALCULATED, DISTRIBUTIONS OF DEFORMATION WITH DEPTH.



GRAPHICAL METHOD OF ESTIMATING THE LIMITING DEPTH OF DEFORMATION, H.



DEFORMATION FACTOR FOR DIFFERENT VALUES OF POISSON'S RATIO, AND LIMITING DEPTH OF DEFORMATION,  $H$ .